THERMAL COMFORT AND INDOOR AIR QUALITY EVALUATION OF A CEILING MOUNTED PERSONALIZED VENTILATION SYSTEM INTEGRATED WITH AN AMBIENT MIXING VENTILATION SYSTEM

YANG BIN

NATIONAL UNIVERSITY OF SINGAPORE

2009

THERMAL COMFORT AND INDOOR AIR QUALITY EVALUATION OF A CEILING MOUNTED PERSONALIZED VENTILATION SYSTEM INTEGRATED WITH AN AMBIENT MIXING VENTILATION SYSTEM

YANG BIN

(B. Eng. Tianjin Univ., China;
M. Sc. Eng., Tianjin Univ., China)

A THESIS SUBMITTED

FOR THE DEGREE OF DOCTOR OF PHILOSOPHY

DEPARTMENT OF BUILDING, NATIONAL UNIVERSITY OF SINGAPORE
DEPARTMENT OF CIVIL ENGINEERING，TECHNICAL UNIVERSITY OF DENMARK

2009

Acknowledgements

I would like to express my sincere gratitude to my supervisor A/P Sekhar, Sitaraman Chandra of the National University of Singapore for his enlightening supervision, valuable advices, constructive suggestions and fruitful discussions throughout my Ph.D. journey from year 2004 to 2009. Being his student has been an enjoyable and memorable experience. I am extremely appreciative to him for being always friendly and available whenever he is approached for solving problems.

I would like to express my deepest acknowledgement to my supervisor A/P Melikov, Arsen Krikor of the Technical University of Denmark. I am so fortunate working with him, famous expert in personalized ventilation system. I learned his strictness to research, his leniency to other person's mistakes and his patience to young researchers. I especially appreciate his valuable suggestions on my experimental design, data analysis and thesis writing.

I am also grateful to my thesis committee members: A/P Tham Kwok Wai and A/P Cheong Kok Wai, David, whose doors are always open, for freely sharing with me their valuable knowledge, experience and expertise on any issues related to personalized ventilation system.

I would like to thank Professor Olesen, Bjarne W. for inviting me to the International

Center for Indoor Environment and Energy, Technical University of Denmark to be a joint Ph.D. student under NUS-DTU joint Ph.D. program. I specially thank A/P Fang Lei for his guidance of developing control system of personalized ventilation system. I am also appreciative to Dr. Zhu Shengwei for optimizing my simulation model, A/P Wargocki, Pawl and guest professor Zhang Yinping from Tsinghua University for their instructive suggestion of experimental design, A/P Toftum, Jørn for his suggestion of my subjective response tests.

I am appreciated to my thesis examiners, Professor Edward Arens from U. C. Berkeley, A/P Toftum, Jørn from Danish Technical University and A/P Wong Nyuk Hien from National University of Singapore.

Warmest thanks to my colleagues with whom I have had the privilege to work: Ms. Li Ruixin for her selfless help in renovating Field Environmental Chamber, Dr. Henry Cahyadi Willem for his suggestion about questionnaire survey.

Many people have assisted to my work generously:

In National University of Singapore: A/P Lee Siew Eang, A/P Wong Nyuk Hien, Dr. Gong Nan, Dr Yu Weijiang, Sun Weimeng Daniel, Jovan Pantelic, Tan Seng Tee, Tan Cheow Beng and Zuraimi Bin Mohd Sultan.

In Technical University of Denmark: Professor Sundell Jan, A/P Clausen Geo, A/P Langkilde Gunnar, Bolashikov Zhecho Dimitrov, Strøm-Tejsen Peter, Zukowska Daria, Schiavon Stefano, Haneda Masaoki and Simonsen Peter Slotved.

The financial supports from National University of Singapore, ASHRAE graduate Grant-in-aid (2007) and Chinese Government Award for Outstanding Self-financed students Abroad (2008) are gratefully acknowledged.

Yang Bin, in Singapore
Final submission in Dec. 2009

Table of Contents

Summary

As the contribution towards the goal of excellent and sustainable indoor environment, Ceiling mounted Personalized Ventilation (PV) has been developed based on conventional PV system. Personalized air, which is fresh, dry and cool, is supplied into breathing zone by ceiling mounted PV air terminal devices (ATD) without extending ducts into breathing zone. As a result, indoor aesthetics and flexibility of distributing indoor furniture are improved. However, the airflow characteristics and subjective assessments to this system have not been explored.

The first objective of this study is to evaluate the performance of prototype of ceiling mounted PV ATDs, with emphasis being placed on air movements characteristics around human body，cooling effect, draft rating, inhaled air temperature and inhaled air quality. This study is conducted at the Technical University of Denmark. The second objective of this study is to investigate the responses from tropically-acclimatized subjects to the local environment created with ceiling mounted PV system, with emphasis being placed on thermal sensation, air movement perception, acceptability and preference, perceived air temperature and perceived air quality. This study is conducted in Singapore, a place with hot and humid climate.

For the first purpose, thermal breathing manikin is utilized as main experimental facility, which can simulate breathing and heat generation of real person, give quantitatively evaluation of cooling effect for different body segments under this ceiling mounted PV system. The characteristics of flow field are measured by thermal anemometer.

For the second purpose, 32 tropically acclimatized subjects are chosen to give their assessment to ceiling mounted PV system with emphasis on thermal sensation, thermal comfort, air movement perception, acceptability and preference, perceived inhaled air quality and temperature, feeling of indoor environment.

This study reveals the feasibility of the newly developed ceiling mounted PV system for practical use in Tropic climate.

List of tables

List of Figures

List of Symbols

A	skin area (m^2)
a	coefficient (dimensionless)
C	constant dependent on clothing, body posture, chamber characteristics and thermal resistance offset of skin surface temperature control system ($K.m^2/W$)
$C_{R, SF6}$	SF_6 concentration in the climate chamber (ppm)
$C_{PV, SF6}$	SF_6 concentration in personalized air (ppm)
$C_{I, SF6}$	SF_6 concentration in the inhaled air (ppm)
D	diameter of nozzle outlet (m)
d_{outlet}	diameter of nozzle outlet (m)
H	human height (m)
Q	volumetric flow rate of personalized air (m^3/s)
Q_{outlet}	PV outlet flow rate (L/s)
Q_t	sensible heat loss (W/m^2)
Re	Reynolds number (dimensionless)
T_a	room temperature (°C)
t_{eq}	manikin-based equivalent temperature (°C)
T_{outlet}	PV outlet temperature (°C)
V_{outlet}	PV outlet velocity (m/s)
$v_{1.3}$	velocity at the 1.3 m vertical distance from nozzle outlet (m/s)
W	human weight (kg)
X	distance between nozzle outlet and human head level (m)

x_c length of core region (m)

X_{nl} neutral level (m)

Greek Symbols

υ kinetic viscosity (m^2/s)

δ_c radius at the end of core region (m)

$\delta_{1.3}$ radius at the 1.3 m vertical distance from jet outlet (m)

ΔT_{eq} manikin-based equivalent temperature difference (°C)

ε_p personal exposure effectiveness (dimensionless)

List of Appendices

Chapter 1: Introduction

1.1 Background and Motivation

The influence of indoor environment to human health, comfort and productivity is important (Wargocki et. al, 1999; Tham, 2004a) because people spend more than 90% of their time indoors (ASHRAE, 2003). In order to create comfortable and healthy indoor environment, mechanical ventilation and air-conditioning system (MVAC) is normally adopted. MVAC systems consume more than 55% of overall building related energy (Lee, 2004) and therefore their optimization is necessary for energy conservation purpose especially for tropical climate with hot and humid outdoor environment.

The most commonly used mechanical ventilation system is total volume ventilation. Two main air distribution principles are used: mixing and displacement. The strategy of the mixing ventilation is to control the temperature or volume of the air supplied through the ceiling-based diffusers to maintain a uniform indoor temperature distribution over space and relatively constant over time. The system is designed to promote complete mixing of supply air with room air through supply air jet momentum and buoyancy. The entire volume of air supplied to the space can be maintained at the desired room set point temperature and adequate quantity of conditioned outdoor air is delivered to the occupants as part of this total volume of supply air. The supply diffusers, usually mounted on the ceiling, are far away from the occupants and thus the supply air at a low contaminant concentration is mixed with the contaminated room air by the time it reaches the inhalation zone of the occupants. As a result, contaminant concentration is usually the same in the whole space and occupants breathe mediocre quality polluted instead of high quality outdoor air.

Another disadvantage of mixing air distribution is that overcooled conditions are usually created for the need of dehumidification which will cause energy waste (de Dear et. al, 1991). Occupants are found to wear jackets or sweaters since they do not have individual control of the system. In a displacement ventilation system, the cool supply air (3-5°C cooler than the room air) is delivered at a low velocity (e.g. 0.25-0.35m/s) through large-area supply devices close to the floor level, spreads over the floor area, and then rises through the room by a combination of lateral momentum and buoyancy forces. Unlike mixing ventilation where the driving force is mainly the momentum of supply air, here the momentum of the supplied air is small and the buoyancy is the dominant force for creating the room air movement. The buoyancy is caused by the presence of people or warm surfaces such as computers. Thus, air temperature and contaminant concentrations develop vertically, with cool and less contaminated air at low level and warm and more contaminated air at a higher level of the space. Therefore, this system has the potential to achieve considerably higher ventilation efficiency in the occupied zone at lower supply air volumes as compared to the mixing ventilation system. However, the supply diffusers, especially those sidewall-mounted, are also far away from the occupants and thus the supplied clean air is contaminated by materials and other emissions that are in contact with it. A field study in rooms with displacement ventilation has shown that almost 50% of occupants were dissatisfied with the air quality (Melikov et al. 2005). Furthermore, the draft at feet caused by the cool supply air and thermal asymmetry due to vertical temperature gradients are prone to incur local thermal discomfort. Such risk becomes higher for office configurations with higher heat load densities, which require larger amount of cool supply air.

Personalized ventilation (PV) system has recently been advocated for indoor environment to cater to the need of a paradigm shift from acceptable to excellent indoor environment (Fanger, 2001). Conditioned outdoor air is supplied to the breathing zone directly without mixing with re-circulated air. Individual control for PV airflow rate, direction and even temperature can be realized for changing from passive environmental adaptation to active environmental control. Occupant's satisfaction of inhaled air quality and thermal comfort could be improved significantly. For energy conservation purpose, PV system can efficiently utilize outdoor air by supplying it into the breathing zone directly without mixing with indoor contaminated air so as to reduce the absolute quantity of outdoor air. Meanwhile, indoor ambient temperature can be maintained higher with thermal comfort requirements achieved through local cooling of occupants' body. As a result, energy conservation can be achieved without affecting thermal comfort and inhaled air quality. The disadvantage is that fan energy for air transportation increases because of several extended PV air ducts.

A number of studies have been performed under laboratory conditions, with either a thermal manikin or human subjects, to evaluate the ability of a PV system to enhance inhaled air quality and/or thermal comfort. Most of them are conducted in temperate climatic zones (Bauman et. al, 1993; Tsuzuki et. al, 1999; Kaczmarczyk et. al, 2002a; Melikov et. al, 2002; Zeng et. al, 2002). These studies will be critically reviewed in Chapter 2.

It should be noted that the majority of PV-related studies, especially those with human subjects involved, were conducted in temperate climates. There have been very few

human subject studies in hot and humid climates (Sekhar et al., 2003a, 2003b, 2005; Tham et al., 2004b, 2004c; Gong et. al., 2006). Differences may be found in thermal sensation, perceived air quality, air movement perception, and draft sensation of tropically acclimatized subjects compared with subjects in temperate climates, due to differences in their physiological acclimatization, clothing, behavior, habituation, and expectation. Hence, the PV environmental parameters acceptable to tropically acclimatized occupants may be different from those identified in the temperate climates. For instance, the PV pilot study performed in the tropics (Sekhar et al., 2003a and 2003b) has observed that tropically acclimatized subjects prefer cooler local air movement with higher velocity than people in temperate climates. This suggests that, contrary to existing notions of air movement leading to draft as undesirable in temperate climates, air movement might be an important and positive factor in improving thermal comfort of occupants in the tropics; at least over a wider range than what is generally accepted in temperate climate. Furthermore, the enthalpy difference between outdoor and indoor air in the tropics consumes considerable energy to cool and dehumidify the outdoor air before it could be supplied. Thus, a PV system can be envisaged as a system with energy saving potential by virtue of the inherent possibility of supplying cool personalized air at a small quantity whilst maintaining the ambient space slightly warm through an ambient HVAC system.

Objective measurements of three prototypes of PV air terminal device (ATD) prototypes, which include high turbulence circular perforated panel (High-Tu CPP), low turbulence circular perforated panel (Low-Tu CPP) and desk mounted grill (DMG) have been conducted by using breathing thermal manikin in hot and humid climates (Zhou et al., 2005). Inhaled air temperature, inhaled air quality, cooling effect and

draft rating are used as index to compare different ATD prototypes. Corresponding subjective responses of two of these three PV ATD prototypes, High-Tu CPP and Low-Tu CPP, have been conducted by using tropically-acclimatized subjects. Inhaled air quality, inhaled air temperature, whole-body thermal sensation, facial thermal sensation, facial air movement perception and acceptability are used as indices to compare these two ATD prototypes (Gong et. al., 2006). The results reveal significant improvement of inhaled air quality, i.e. cleaner and cooler inhaled air, and increased satisfaction with the thermal environment.

Although the current PV ATD prototypes can both supply more outdoor air directly to the breathing zone and have potential to save energy (especially in hot and humid climate), room layouts and visual effects will be influenced negatively because of extended air ducts. A new approach, supplying outdoor air by utilizing high velocity circular outdoor air jet mounted on the ceiling without mixing with re-circulated air, is introduced. Because of the long distance from the ceiling mounted Air Terminal Device (ATD) to occupants' breathing zone, higher momentum of the supplied personalized flow and bigger outlet diameter than desk mounted PV ATD prototypes is necessary so as to keep the core region of personalized airflow as long as possible which will make it possible for supplying more fresh air into the breathing zone. The motivation of using high velocity personalized air in tropical climate is based on the previous results that air movement might be an important positive factor in improving thermal comfort for the tropics (Sekhar et al., 2003a and 2003b).

1.2 Research Objectives

The present study is aimed at exploring newly-developed ceiling mounted PV ATD

prototype not only to provide tropically acclimatized occupants with good local thermal environment and good inhaled air quality but also not to affect room layout and visual effects in an energy efficient way. The objectives of this thesis are as follows:

1. Evaluate the performance of ceiling mounted personalized ventilation system with regard to airflow interaction at the vicinity of human body, thermal comfort and inhaled air quality and temperature based on objective measurements

2. Study human response, including thermal sensation, air movement perception and preference, inhaled air quality, etc. created by individually controlled PV ATDs.

3. Evaluate the energy saving potential of the ceiling mounted PV system used in conjunction with background mixing ventilation system.

4. Evaluate the control strategy of ceiling mounted PV system.

1.3 Outline

The present chapter briefly discusses the characteristics of conventional total-volume ventilation and introduces the concept of the state-of-the-art personalized ventilation (PV). In tropical climate, the feasibility of ceiling mounted PV prototype without extended air duct is elaborated. The objectives of the study are stated.

Chapter 2, consisting of four parts, presents a holistic and critical review of PV. The first part describes the configurations of some commercially available PV systems as

well as those specifically developed for research purposes. The second and third parts review previous research work in terms of physical measurements of PV performance and human response to thermal environment and air quality generated by PV, respectively. The fourth part is devoted to research findings from limited PV-related studies in hot and humid climates. The research gaps are identified.

Chapter 3 presents the research methodology and results of pilot study based on CFD simulations. The feasibility of ceiling mounted PV is demonstrated.

Chapter 4 is dedicated to the research methodology for the objective measurements with a breathing thermal manikin and comprises experimental conditions, experimental protocol and evaluating index. Then, the results and discussion are presented from these objective measurements. The interaction of the personalized flow supplied from ceiling mounted nozzle with the thermal plume generated by a seated thermal manikin and its impact on the body cooling is studied. Relevant thermal and ventilation characteristics in the vicinity of thermal manikin are explored.

Chapter 5 is focused on the subjective response studies, covering the experimental conditions, basic information pertaining to subjects participating in the experiments, questionnaire, experimental procedure and methods used in data analysis. Possible parametric variation and combination for subjective response studies are also listed.
Then, the major findings are presented from subjective response studies. Human preference for local air movement and local thermal environment is the focus of data analysis.

Chapter 6 is focused on energy saving potential including the effect of control strategy. Energy consumption of ceiling mounted PV system is compared with mixing ventilation system and mixing ventilation system plus desk fans under different control strategies.

Chapter 7 reviews the objectives and presents a summary of significant findings. Finally, some suggestions and recommendations for further research and application of PV system in the tropics are pointed out.

Chapter 2: Literature Review

This chapter, consisting of four parts, presents tropical climate and conventional air-conditioning and mechanical ventilation (ACMV) system, a holistic and critical review of PV, human response study of thermal environment and air movement, research findings from limited PV-related studies in hot and humid climates. Knowledge gaps are then summarized and hypotheses are proposed.

2.1 Tropical Climate and Conventional ACMV system

Tropical zone is defined as the zone spanning the Tropic of Cancer (latitude 23.5°North) and the Tropic of Capricorn (latitude 23.5°South). Half of the world's population lives within this zone, which shares 40% land surface of the earth. The characteristics of tropical climate are abundant rainfall and high humidity associated with a low diurnal temperature range and relatively high air temperatures throughout the year.

Singapore's climate is characterized by uniform temperature and pressure, high humidity and abundant rainfall without distinct seasons because of geographic location and maritime exposure. Temperatures range fluctuate a minimum of 23-26°C and a maximum of 31-34°C. Relative humidity has a diurnal range in the high 90% in the early morning to around 60% in the mid-afternoon. During prolonged heavy rain, relative humidity often reaches 100%. Singapore is influenced by northeast monsoon (wetter season) which lasts from October to March and southwest monsoon (drier season) from May to September (Dutt and de Dear, 1991).

ACMV system plays an important role for improving indoor environment in the

Tropics given the feature of high temperature and humidity. Total-volume mechanical ventilation for air-conditioning is normally adopted by commercial office buildings. It includes two concepts, mixing and displacement. As already discussed in Chapter 1, mixing ventilation (MV) aims to maintain uniform and constant indoor environments while displacement ventilation (DV) aims to maintain a temperature and contaminant gradient with the most acceptable region occurring in occupant zones. However, such environments may not satisfy individual thermal requirement due to huge individual difference. As a result, ACMV systems with individual control become necessary.

Under both mixing and displacement ventilation systems, air inhaled by occupants is the mixing of outdoor air and ambient air (although outdoor air at different levels of the two types of ventilation), which can not satisfy air quality requirements. In the case of total volume air distribution typically 10 L/s· person outdoor air is supplied to spaces. The air inhaled by each occupant is in average only 0.1 L/s. the inhaled air (only 1% of the supplied air) is polluted by bioeffluents from occupants or emissions from building materials (Fanger, 2000). As a result, a small amount of high quality conditioned outdoor air should be supplied into breathing zones directly instead of supplying large amount of mediocre air in the whole room (Fanger, 2000).

Personalized ventilation, also known as Task/Ambient Conditioning (TAC), is such a ventilation system which provides personalized air. Under a PV system, conditioned outdoor air is supplied directly to the occupant's breathing zone without mixing with contaminated re-circulated air. The concept of PV has potential for both improving thermal environment around occupied zone by spot cooling and enhancing ventilation effectiveness (inhaled air quality) in breathing zone by supplying outdoor air directly

into the breathing zone. Individual control for PV air parameters such as airflow rate/velocity, temperature can compensate the large individual differences between people with regard to preferred environment.

2.2 Personalized Ventilation

2.2.1 Air Terminal Device and Air Flow

- **Air Terminal Device**

Unlike mixing ventilation which supply fully mixed air from ceiling mounted diffusers and displacement ventilation which supply air from sidewall mounted DV cylinders, the concept of PV aims to shorten the distance of ATDs and human occupants so as to improving both thermal environment and inhaled air quality in working areas. The present PV differentiates from other ventilation approaches by its air supply parameters (conditioned outdoor air) and supply position (close to breathing zones).

Before the consideration of PV for office applications, localized ventilation has been used in vehicle cabin (bus, car, and aircraft) and theater buildings for many years, with focus mainly on occupants' thermal comfort. Air quality is usually not a concerned issue and therefore re-circulated air was used in localized ventilation. Some of the commercially available localized systems as well as those specifically developed for research purposes with focus mainly on improving occupants' thermal comfort are shown in Figure 2.1.

a. Personal Environmental Module (PEM)

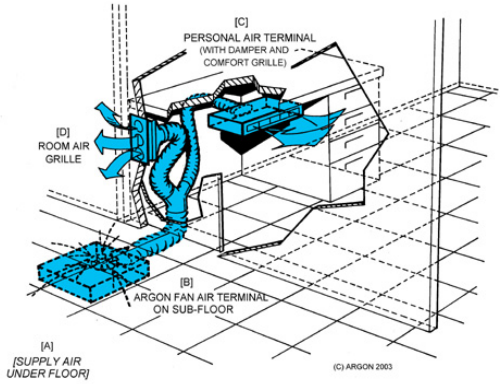

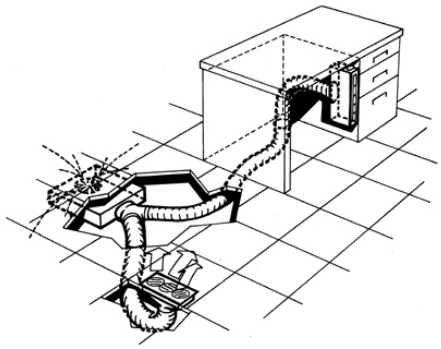

b. De ure:

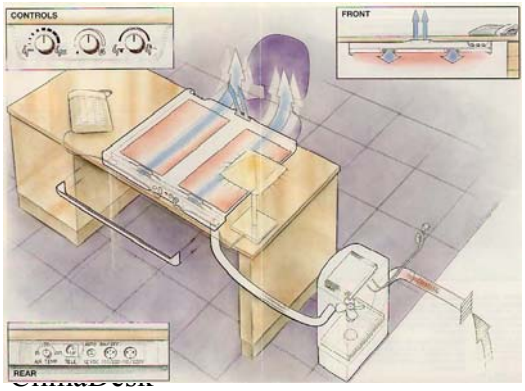

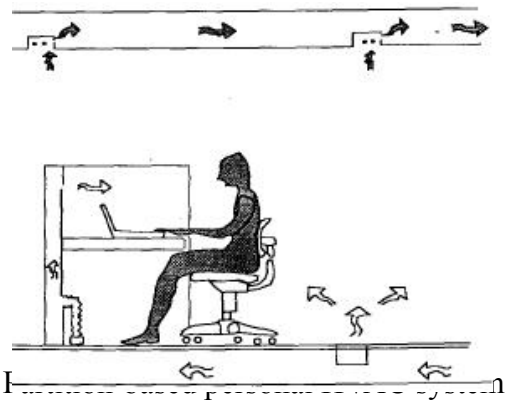

c. d. I n

Figure 2.1 Prototype of some localized ventilation air terminal devices (figure a from Johnson Controls (2005), figure b from Argon Corporation (2005), figure c from Bauman and Arens (1996), figure d from Matsunawa et al. (1995))

The potential of PV for improvement of occupants' inhaled air quality has been studied during the last decade. Different to previous ATDs used for localized cooling, only conditioned outdoor air is supplied by PV ATDs aiming for improvement of inhaled air quality. Figure 2.2 shows some of the studied PV ATD. The designs of

different PV ATDs have similar considerations for achieving both better thermal microenvironment by spot cooling of occupied zones and better inhaled air quality by minimizing mixing between personalized air and ambient air with individual control.

a. Round movable panel

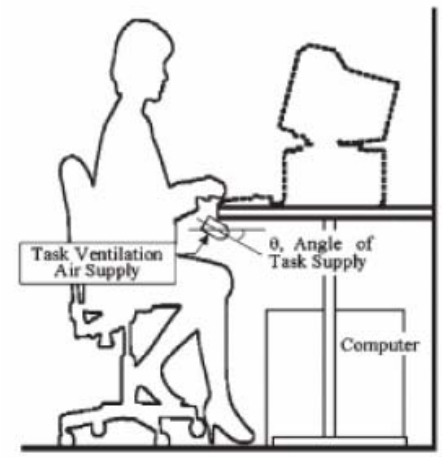

b. Desk-edge-mounted task ventilation system

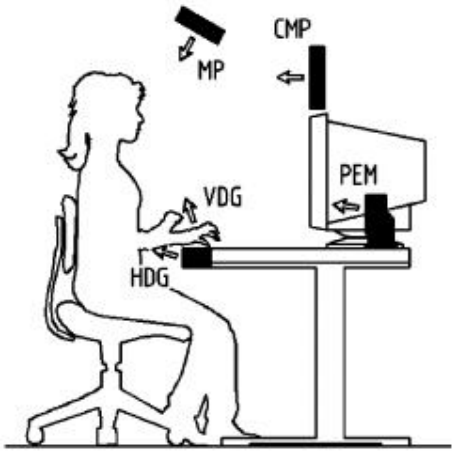

c. Five types of ATDs (MP-Movable Panel; CMP-Computer Monitor Panel; VDG-Vertical Desk Grill; HDG-Horizontal Desk Grill; PEM-Personal Environments Module)

d. Headset-Incorporated Supply

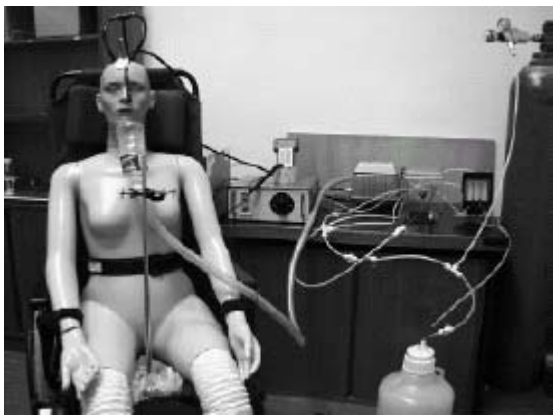

e. Microphone-like air supply nozzle

Figure 2.2 Prototype and some PV ATDs (figure a from Bolashikov et. al (2003), figure b from Faulkner et. al (2004), figure c from Melikov (2004), figure d from Bolashikov et. al (2003), figure e from Zuo et. al (2002))

- **Air Flow under PV**

Airflow under PV configuration is very complex. As shown in Figure 2.3 in an office with PV supply, there are at least five airflows interacting with each other around human body, i.e., free convection flow around human body, personalized airflow, respiration flow, ventilation flow and thermal flow (Melikov, 2004). Thermal microenvironment and inhaled air quality in breathing zone is influenced by combined effects of all these flows.

Figure 2.3 Airflow interaction around human body: (1)—free convection flow, (2)—personalized airflow, (3)—respiration flow, (4)—ventilation flow, (5)—thermal flow (Source: Melikov (2004))

Personalized airflow is typically a free jet, which includes core region, characteristic decay region, Axisymmetric decay region and terminal region. The length of core region is about 4 to 5 times of jet outlet. It is suggested by Melikov (2004) that core region should reach breathing zone when the location of ATD is considered. Reasonably increasing the diameter of jet outlet will increase the length of core region. Only when personalized airflow penetrates free convection flow it can be inhaled.

Upward free convection flow exists around human body because in comfortable environment its surface temperature is higher than the room air temperature. This flow is slow and laminar with thin boundary layer at the lower parts of the body and becomes faster and turbulent with thick boundary layer at the breathing level. A large portion of air that is inhaled by sedentary and standing persons is from this free

convection flow (Melikov, 2004).

Respiration creates alternating inhalation and exhalation flows. The exhalation generates jets with relatively high velocity, 1m/s and more, which can penetrate the free convection flow around human body, effectively rejecting exhaled air from the flow or air that may subsequently be inhaled (Melikov, 2004). The design of personalized air should avoid mixing with exhalation, and also avoid the exhalation which will be inhaled again.

The ambient ventilation flow normally has lower velocity when it is near to occupants. The detailed description of all airflows and their interaction is given in Melikov (2004).

2.2.2 PV Performance

This section reviews some previous studies reporting on PV system performance based on results from physical measurements. The studies provide evidence that occupant satisfaction is improved with the use of PV as compared to mixing ventilation. The majority of the studies are conducted in laboratory with major performance evaluation indices including manikin-based equivalent temperature, inhaled air temperature, ventilation effectiveness, personal exposure effectiveness, draft rating, etc. The definitions of these indices will be introduced where they first appear in the following review. Some of the indices used in the present study will also be described in detail in Chapter 3.

Previous studies demonstrate that PV system could accommodate different cooling

loads and subjects perceive a better thermal environment with local body cooling (Bauman et. al., 1993; Bauman et. al., 1998; Arens et. al., 1991; Tsuzuki et. al., 1999; Melikov et. al., 2002; Kaczmarczyk et. al., 2002a; Kaczmarczyk et. al., 2004). PV system could accommodate different heat loads up to 446 W in one workstation (Bauman et. al., 1993) and could improve the micro thermal satisfaction at the workstation to "near very satisfied" (Bauman et. al., 1998). Cooling effect on body by different types of PV ATDs has been explored (Tsuzuki et. al., 1999; Melikov et. al., 2002). Cooling effect is significant which can lead to whole-body heat loss (determined by thermal manikin) equivalent to room air temperature decrease of 9.0 °C (Tsuzuki et. al., 1999). The performance of five PV ATDs, i.e., Horizontal Desk Grill, Vertical Desk Grill, Personal Environmental Module, Computer Monitor Panel and Movable Panel, was investigated (Melikov et. al., 2002). It was found that Vertical Desk Grill provided greatest cooling of manikin's head (manikin based equivalent temperature decrease by -6 °C when PV airflow is 10 L/s). Corresponding subjective tests demonstrated that subjects could maintain their whole body thermal neutrality (Kaczmarczyk et. al., 2002a) and the operation of PV system did not cause any thermal discomfort (Faulkner et. al., 2004) although the subjects were exposed to thermally asymmetrical environment with air movement and radiation directed onto only some parts of the body.

Ventilation related indices, e.g., ventilation effectiveness and personal exposure effectiveness (see chapter 3), were also measured with PV system (Faulkner et. al., 1999; Melikov et. al., 2002; Kaczmarczyk et. al., 2004). Numerous laboratory and field studies were performed in the past decade. The performance of two desk mounted PV systems was compared in terms of air quality in breathing zone

(Faulkner et. al., 1999). Air Change Effectiveness (ACE) and Pollutant Removal Efficiency (PRE) are used as indices to access ventilation condition in breathing zone. Ventilation effectiveness of a desk-edge-mounted PV system was explored and about 1.5 could be achieved which means 50% increasing for ventilation effectiveness compared with mixing ventilation (Faulkner et. al., 2004). The impact of airflow interaction on inhaled air quality and transport of contaminants between occupants in rooms with personalized and total volume ventilation was explored (Melikov et. al., 2003). PV system supplying air against face improved ventilation efficiency in regard to the floor pollution up to 20 times and up to 13 times in regard to bioeffuents and exhaled air compared to mixing and displacement ventilation alone.

Subjective studies demonstrated that PV can effectively improve inhaled air quality in comparison with mixing ventilation (Kaczmarczyk et. al., 2002b; Zeng et. al., 2002; Kaczmarczyk et. al., 2004). PV system also decreased SBS symptoms (decrease complains of headache and improve thinking ability) and increased self-estimated performance compared to mixing system (Kaczmarczyk et. al., 2004). The best condition of perceived air quality, perception of freshness and intensity of Sick Building Syndrome (SBS) symptoms was when PV system supplied outdoor air at 20 °C (Kaczmarczyk et. al., 2002a). Elevated velocity for facial air movement significantly improved the acceptability of the air quality at 26 °C room air temperature and 70% relative humidity and compensated for the negative impact of relative humidity on perceived air quality at low velocity level. The impact of the elevated velocity on perceived air quality at low level of relative humidity (30%) diminished. This in some climatic conditions such as the tropics may eliminate the need for dehumidification of outdoor air and lead to energy savings (Melikov et. al.,

2008)

A field study on PV system in office buildings using pre-post intervention with control group methodology was reported (Bauman et. al., 1998). Three buildings with 42 desktops with Personal Environmental Module (PEM), one kind of PV systems, were tested. Occupants without PV systems on their workstations were also used as a control group. Intensive measurements and questionnaire surveys were performed in different periods within five months. Six building evaluating categories, i.e. thermal quality, air quality, lighting quality, acoustical quality, spatial layout and office furnishings were used. The results showed that PV system increased integrated occupant satisfaction.

It was reported that PV system could also realize energy conservation (Niu, 2003). Energy saving potential was attributed to high ventilation effectiveness (Faulkner et. al., 1999) and raising ambient temperature (Bauman et. al., 1993). Energy usage simulation for Personal Environment Control (PEC) was conducted. The results showed that PEC system lead to 7% saving and cause 15% penalty in lighting and electrical usage. However, the penalty could be offset by only about 0.08% annual increase in working productivity. In tropic climate, the use of a secondary PV system in conjunction with a primary air-conditioning system not only enhances thermal comfort and IAQ acceptability but can reduce energy consumption by 15-30% (Sekhar et. al., 2005). Some corresponding studies in the Tropics will be elaborated in section 2.4.

2.3 Human Response to Thermal Environment and Air Movement

Apart from improving air quality in occupied zones, another important function of PV system is to supply spot cooling for occupied zones so as to creating comfortable thermal environment. As a result, personalized air movement parameters and individual control become research focus. The question about nuisance of draft, defined as unwanted local cooling of the body caused by air movement (ASHRAE 2003), and the pleasure of fresh breeze has puzzled researchers for decades (e.g., from the study of Houghten et. al., 1938) and there is still no clear understanding how human perception develops from desirable cooling to uncomfortable draft among scientific community. The relation between human occupants and PV airflow still remains unknown especially human perception to non-isothermal PV/ambient system (Melikov et. al., 2004). The perception of air movement depends not only on air velocity and thermal environment parameters, but also on personal factors such as activity level, physiological acclimatization, clothing, habituation and expectation (Toftum, 2004). Huge individual differences do exist — some occupants perceive air movement as pleasant while others feel unpleasant draft at the same room air temperatures.

Numerous experiments of human perception on air movement were conducted under indoor temperature less than 26°C, which can be regarded as moderate and cool environments (Fanger and Peterson, 1977; Fanger and Christensen, 1986; Fanger et. al., 1988; Toftum, 1994; Toftum and Nielsen, 1996; Griefahn et. al., 2000; Griefahn et. al., 2001; Griefahn et. al., 2002). In addition to air velocity and temperature, the influence of turbulence intensity on draft discomfort was identified and incorporated into a model which predicts the percentage of dissatisfied due to draft (PD) (Fanger et. al., 1988). Corresponding extension for the model was developed by adding metabolic

rate (Toftum, 1994) and clothing (Griefahn, 2001). Elevated air velocity with individual control has been recommended to offset thermal discomfort at increased ambient temperature (ASHRAE Standard 2004). Even though it is possible to maintain thermal comfort and sensation by high air velocity at elevated temperature, subjects' dominant preference is for lower air velocity and a temperature in the comfort range (Toftum et. al., 2002; ASHRAE, 2003). Individual control helps to compensate huge individual differences between people with regard to preferred thermal environment and to minimize draft risk. In addition to draft discomfort due to cooling effect, air movement also causes annoying effect due to air pressure at high velocity (Xia et. al. 2000, Melikov, et. al. 1994a, 1994b).

2.4 PV Related Studies in Hot and Humid Climates

Relatively few studies on the performance of the PV concept at hot and humid climates/conditions have been reported (Fountain et al., 1994; Sekhar et al., 2003a, 2003b, 2005; Tham et al., 2004a, 2004b).

Fountain et al. (1994) studied the locally controlled air movement preferred by human subjects exposed to hot isothermal environments. The experiment was performed in a controlled environment chamber (Bauman et al., 1993) in which the nominal room air temperatures were set at 25°C to 28°C. Three different air terminal devices (ATD) for local supply were used: a desk fan, a Task Air Module (TAM), and a Personal Environmental Module (PEM). The experiment lasted approximately 3.5 hours and had 54 subjects involved. The first hour served as an acclimatization period during which the subjects adjusted the level of the local air movement (but not the direction or the position of the ATD) for thermal comfort. Every 15 minutes throughout the test,

the subjects were required to fill in a comfort survey questionnaire. Every 45 minutes they were asked to move away from the desk in order for detailed physical measurements of the local environments they produced to be taken for 5 minutes. When the measurements were completed, the subject returned to the desk and switched to a different ATD for next session. The order in which the ATDs were adjusted by the subjects was randomized. A wide range of preferred air velocities was observed. With the increase of air temperature, the range of preferred air velocities increased. The effect of air turbulence on preferred air velocities was not evident. A model that predicts the percentage of satisfied people as a function of air temperature and air movement in hot conditions was developed. The model recognizes that people actively participate in regulating their local environments.

A pilot study of PV application in typical tropical area as Singapore conducted by Sekhar et al. (2003a, 2003b, 2005) with the aims of investigating tropically acclimatized occupants' perception of thermal comfort and IAQ achieved with PV and exploring the energy saving potential of PV in the tropics. The experiments were performed in a controlled environmental chamber having 6 workstations provided with 6 independent PV ATDs. The ATD used was the movable panel (MP) fabricated according to the reported work by DTU. The experimental design consisted of 17 combinations of room ambient temperature (23°C and 26°C), personalized air temperature (20°C, 23°C, and 26°C), and the personalized air flow rate (7, 11, and 15L/s/person). Eleven tropically acclimatized human subjects participated in the experiment and filled in questionnaires. The results showed that PV in conjunction with conventional MV yielded high ventilation effectiveness in the inhalation zone ranging between 1.42 and 1.90 and lowered the average temperature of inhaled air in

the immediate inhalation zone by 2°C to 5°C compared to reference conditions without PV. The energy saving potential of the PV system supplying air at 7L/s/person and 23°C in conjunction with the MV system maintaining room temperature at 26°C was about 30% when compared with the MV system operating alone to maintain room temperature at 23°C and provide outdoor air of 15L/s/person. Analysis of subjective response revealed that PV improved the thermal comfort and IAQ acceptability by 58% and 64% respectively, in terms of mean values. Both thermal comfort and IAQ ratings generally increased as personalized air flow rate increased and decreased as personalized air temperature increased at ambient temperature of 26°C. It was observed that most subjects had placed the ATD close to their breathing zone or face under all experimental conditions. A preliminary finding that need further substantiation was that tropical subjects perceived an increased thermal comfort and air movement acceptability at higher draft rating values, which was an observation that differed significantly from what was seen in temperate climates.

The draft perception of tropically acclimatized subjects was further explored by Tham et al. (2004a, 2004b). The experimental facilities were identical to those employed by Sekhar et al. (2003a, 2003b, 2005). The ambient temperature was kept nominally at 23 or 26ºC, and personalized air temperatures were controlled at 20°C, 23°C, or 26ºC at the outlet surface of the PV ATD. Three levels of personalized air flow rate, 4.5, 7.3, 11.2 L/s/person, were presented to the subjects. Each experimental condition lasted 2.5 hours. 18 subjects participated in the experiments to respond to computer-administered questionnaires on their thermal and draft sensations using visual-analogue scales at the 1^{st}, 15^{th}, 30^{th}, 45^{th}, 60^{th}, 80^{th}, 100^{th}, 120^{th}, 135^{th} and 150^{th} minute. The study showed that, during long time exposure of 2.5 hours, thermal

sensation of facial parts and whole-body gradually decreased reaching steady state after one hour. The perception of air movement at higher flow rates (7.3 and 11.2L/s) was significantly better than that at lower flow rate (4.5L/s), suggesting that tropically acclimatized subjects preferred higher air flow or air movement up to a certain point. The change pattern of percentage of dissatisfied was observed decreasing when air velocity was below 0.3 to 0.4 m/s, and increasing when velocity above 0.4 m/s. Such a trend indicated that air movement may be considered subjectively to be too low or too high under PV conditions. Regression of optimal air velocity with time showed that optimal air velocities decreased fast before first 80 minutes and then became almost stable for the rest of the time of the exposure (R^2=0.9).

The above-mentioned studies conducted in tropical climates have to a certain extent underpinned the hypothesis that potential differences may exist in thermal sensation and air movement perception of tropically acclimatized occupants compared with those of people in temperate climates, due to differences in physiological acclimatization, clothing, behavior, habituation, and expectation. Therefore, PV environmental parameters that have been widely identified and accepted in the temperate climates might differ from tropically acclimatized people. Thus, it is of great importance to identify and establish comfort ranges of environmental parameters of PV with high degree of feasibility and viability in the tropical context.

Furthermore, in the hot and humid tropical climate like Singapore, the enthalpy difference between outdoor and indoor air requires considerable energy to cool and dehumidify the outdoor air before it could be supplied. Most of the HVAC systems are operated with high ratio (70%-90%, depending upon types of buildings) of

re-circulated air in order to save energy. Thus, the judicious use of PV whilst keeping the ambient temperature slightly warm such that their combination achieves good air quality and thermal comfort is clearly advantageous. The energy needed for ambient conditioning is optimized, while the individual is empowered to adjust his/her local environment to his/her preference. It is therefore envisaged that PV concept might be more applicable and certainly has the potential for the Tropics. One of the challenges is to develop suitable ATDs that optimize the inhaled air quality and thermal comfort of tropically acclimatized occupants in an energy efficient manner.

Motivated by the promising results of the PV pilot study by Sekhar et al. (2003a, 2003b, 2005) and Tham et al. (2004a, 2004b), follow-up studies are conducted by Gong and Zhou (2005) which are aimed at exploring PV designs capable of creating thermally comfortable local environment with good air quality for tropical applications through more rigorous experimental protocols involving both intensive physical measurements with thermal manikin and subjective measurements with tropically acclimatized subjects.

The performance of objective measurements for three prototypes of air terminal devices (ATD) for personalized ventilation (PV), circular perforated panel supplying personalized air at low initial turbulence intensity (abbreviated as Low-Tu CPP), circular perforated panel supplying personalized air at high initial turbulence intensity (abbreviated as High-Tu CPP), and desktop-mounted grille with adjustable horizontal vanes (abbreviated as DMG), is evaluated and compared under different experimental conditions by Zhou (2005). Major performance assessment indices included personal exposure effectiveness (ε_p, the percentage of personalized air in the inhaled air, an

index suggested by Melikov et al. 2002), inhaled air temperature, Δt_{eq} (change in manikin-based equivalent temperature, t_{eq}, (Nilsson et al. 1997) from the reference condition without PV), cooling effects and draft rating.

It was found that both CPPs were able to enhance the portion of fresh personalized air in the inhaled air, lower the inhaled air temperature, and provide more cooling effects as compared with reference conditions without PV. The impact of turbulence intensity was significant: under a certain temperature combination, Low-Tu CPP yielded significantly higher personal exposure effectiveness and lower inhaled air temperature than High-Tu CPP over the flow rate range studied. The maximum values of ε_p achieved with the Low-Tu CPP and High-Tu CPP at the highest flow rates were approximately 0.46 and 0.35, respectively. The maximum facial and whole-body cooling effects were -8.6°C and -1.3°C for Low-Tu CPP and -6.1°C and -1.2°C for High-Tu CPP. Under a given temperature combination, Low-Tu CPP yielded significantly greater facial cooling effect than High-Tu CPP over the flow rate range. However, whole-body cooling effect appeared to be much less affected by the turbulence intensity. Under an identical condition, the calculated draft rating of Low-Tu CPP was significantly higher than that of High-Tu CPP. The reason was that the effect of the low air temperature and high velocity achieved with the Low-Tu CPP at the measuring point far outweighed that of the high turbulence intensity caused by the High-Tu CPP.

It was also found that the ε_p, personal exposure effectiveness, increased with the increase of the personalized air flow rate up to approximately 7L/s, beyond which the effect of increasing flow rate on the increase of ε_p was marginal. At flow rates higher

than 7L/s, the dependence of ε_p on the relative difference between the personalized air and ambient air temperatures was little. The maximum ε_p of 0.7 was achieved at the highest flow rate of 12.2L/s. The inhaled air temperature decreased with the increase of the relative difference between the ambient and personalized air temperatures. The maximum decrease in inhaled air temperature from that measured under reference condition was approximately 5.1°C at flow rate of 12.2L/s under condition of 26/21°C. The dependence of inhaled air temperature on the flow rate above 7L/s was little. The manikin's facial parts were the most cooled body segments. The maximum cooling effect was -7.2°C for the facial parts and -0.9°C for the whole-body achieved at the highest flow rate of 12.2L/s under condition of 26/21°C. The calculated draft rating increased with the increase of flow rate and the decrease of the personalized air temperature. The impact of the variation of the absolute temperatures of the ambient and personalized air on the DMG's performance was identified by performing the testing under temperature combinations of 23.5/23.5°C and 23.5/21°C at the ten flow rate levels. Compared to conditions of 26/26°C and 26/23.5°C, the conditions of 23.5/23.5°C and 23.5/21°C resulted in lower ε_p and cooling effects for both facial parts and whole-body because of the increased strength of the free convection flow around the manikin. The cooler temperature combinations led to significantly lower temperatures of inhaled air and greater draft rating values. Supplementary measurements performed with the DMG's vanes set at 45° and 20° from the horizontal plane indicated that the 60° was the optimal angle to deliver inhaled air of best quality (highest ε_p and lowest inhaled air temperature) and strongest cooling effect at facial parts. The comparison between the DMG and the Low-Tu CPP revealed that the DMG yielded a significantly higher ε_p but slightly warmer inhaled air than the Low-Tu CPP over the flow rate range studied under a given temperature

combination. The relative difference in cooling effects on facial parts between the two ATDs was influenced by the flow rate. Below a certain threshold, the DMG yielded greater Δt_{eq}; above it, the CPP yielded greater Δt_{eq}. The threshold flow rate was determined by the specific temperature combination. The relative difference in draft rating between the two ATDs depended upon the flow rate: the two curves intersected at a certain point. On the two sides of the point, the relative position of the curves reversed. The flow rate corresponding to this point varied with different temperature combinations.

The subjective measurements by using two of the three PV ATD prototypes (Low-Tu CPP and High-Tu CPP) were conducted by Gong (2005). The combinations of ambient and personalized air temperatures adopted were identical to those in the objective measurements with the manikin. Less levels of personalized air flow rate were supplied. Twenty-four tropically acclimatized subjects participated in the experiments. Each subject underwent 48 conditions, i.e. 4 (temperature combinations) by 6 (personalized air flow rates) by 2 (ATD prototypes), in a reasonably randomized sequence.

Large individual variability in perception of the local environment created with the PV existed amongst the 24 subjects exposed to an identical condition. Subjective perceptions were strongly affected by the personalized air flow rate, temperature, turbulence intensity, and the ambient air temperature. Fairly strong correlations were found between the subjects' facial thermal sensation and whole-body thermal sensation (for High-Tu CPP, $R^2 \geq 0.83$ for each temperature combination; for Low-Tu CPP, $R^2 \geq 0.90$ for 26°C/26°C, 26°C/23.5°C, and 23.5°C/21°C, $R^2=0.67$ for

23.5°C/23.5°C) and between facial air movement perception and acceptability (for High-Tu CPP, $R^2 \geq 0.88$ for each temperature combination; for Low-Tu CPP, $R^2 \geq 0.89$ for 26°C/26°C, 23.5°C/23.5°C, and 23.5°C/21°C, $R^2 = 0.64$ for 26°C/23.5°C). However, the correlation between perceived inhaled air quality and temperature was rather weak ($R^2 < 0.43$). Multiple linear regression models were established for perceived inhaled air quality (PIAQ) and temperature (PIAT) as a function of other responses. For Low-Tu CPP, PIAT related to facial thermal sensation (FTS), facial air movement perception (FAMP), and facial air movement acceptability (FAMA); and PIAQ related to PIAT, FAMP, and FAMA. For High-Tu CPP, PIAT related to FTS and FAMP. Certain correlations between the mean subjective responses and the corresponding physical parameters measured with the manikin were observed. Linear regression of the perceived inhaled air temperature as a function of measured inhaled air temperature yielded a R^2 value of 0.81 for Low-Tu CPP and 0.74 for High-Tu CPP. R^2 values for the correlation between the facial thermal sensation and the corresponding Δt_{eq} at facial parts were 0.79 for Low-Tu CPP at ambient temperature of 23.5°C, 0.71 for Low-Tu CPP at ambient of 26°C, 0.65 for High-Tu CPP at ambient of 23.5°C, and 0.74 for High-Tu CPP at ambient of 26°C. As for the correlations between the whole-body thermal sensation and the whole-body Δt_{eq}, the obtained R^2 values were relatively lower: 0.66 for ambient of 23.5°C and 0.50 for ambient of 26°C when Low-Tu CPP was employed; 0.61 for ambient of 26°C and less than 0.1 for ambient of 23.5°C when the High-Tu CPP was operating. The exception was perceived inhaled air quality, which appeared to be independent of the personal exposure effectiveness (ε_p). The calculated draft rating below 60% was positively judged by the tropically acclimatized subjects: higher facial air movement acceptability was accompanied with higher draft rating. This substantiated the

previous finding of PV study in tropical climate (Sekhar et al., 2005) and identified a much broader acceptable range of draft rating (up to 60%) than the narrow range of 0 to 15% reported in the referred study.

2.5 Knowledge Gap

The review presented above demonstrates that supply of clean outdoor air to the breathing zone improves inhaled air quality. The clean and cool personalized air can penetrate the free convection flow around manikin/subjects so as to realizing spot cooling, decreasing inhaled air temperature, improving inhaled air quality. The cooling effect caused by the personalized flow, especially at the head, improves people's thermal comfort as well.

However, desk based and partition based PV ATDs decrease the flexibility of indoor furniture. Once the PV air duct has been mounted to the desk or partition, the distribution of indoor furniture cannot be changed easily. Room layouts and aesthetic effects will be influenced negatively because of the extended PV air duct to workstation. Floor based PV ATD, which is often used in under floor air supply system by using raised access floor, will essentially reduce floor height and affect visual effects. The combination of floor based and partition based PV ATDs is even worse for aesthetic effects and room layouts.

In order to realize the advantages of PV ATD without affecting room layouts and aesthetic effects, it would be desirable to void extended PV air duct. As a result, ceiling mounted PV ATD, which can be regarded as remote PV ATD, is worth exploring. In this case higher personalized airflow rates are necessary to offset the

free convection flow around manikin/subjects because of the reasonable long distance from PV ATD to the breathing zone of manikin/subjects. However it may increase the risk of draught when the personalized air flow rate is increased. This needs to be studied. The motivation for studying this kind of PV ATD in tropical climate stems from the research results that a much broader acceptable range of draft rating (up to 60%) for tropically acclimatized subjects (Sekhar et al., 2005).

As a newly developed PV system, the performance of ceiling mounted PV system has not been tested yet in the tropics. PV airflow is supplied in opposite direction of free convection flow, which will offset, not just penetrate, the free convection flow. The effects of personalized air movement direction on air movement perception are obviously different, which may make higher PV airflow rate possible for ceiling mounted PV than that of conventional PV.

The following hypotheses are therefore proposed:

PV system in conjunction with ceiling supply air distribution system improves occupants' thermal comfort and perceived air quality in tropical buildings;

PV system has a potential to save cooling energy consumption in tropical building designs.

people prefer different local air movement range for ceiling mounted PV compared with desk mounted PV ATD because of different supply direction;

people prefer different local air movement range for ceiling mounted PV at different PV/ambient temperature combination.

Chapter 3: Pilot Study

3.1 Introduction

The objective of the pilot study is:

To evaluate and verify the feasibility of newly developed ceiling mounted personalized ventilation air terminal device by using isothermal CFD simulation and objective measurements. The isothermal CFD model, validated by objective measurements, is used to conduct small number of parametric studies in order to find the means of making ceiling mounted personalized ventilation air terminal devices more flexible and optimal.

3.2 Research Methodology

3.2.1 Physical Measurements

The measurements were performed in the indoor environmental chamber in the Department of Building at National University Singapore (NUS). This $6.6\times3.7\times2.6m^3$ chamber was built to simulate a typical office environment with movable interior partitions dividing the whole chamber into six workstations. The chamber was enclosed by a $25m^2$ annular space called control room to minimize the external environmental interferences. The control room was used to accommodate equipment that condition the mixing and personalized ventilation air delivered to the chamber, e.g. the Honeywell building automation system (BAS), as well as part of ductwork for mixing ventilation and plenum box and major part of ductwork for personalized ventilation. Some equipment and instruments measuring physical parameters involved in the experiments were also placed in the control room, for instance, INNOVA multi-gas monitoring system and computer, thermocouple data-logger and computer,

etc. The layout plan of the indoor environmental chamber and the annular control room are schematically shown in Figure 3.1.

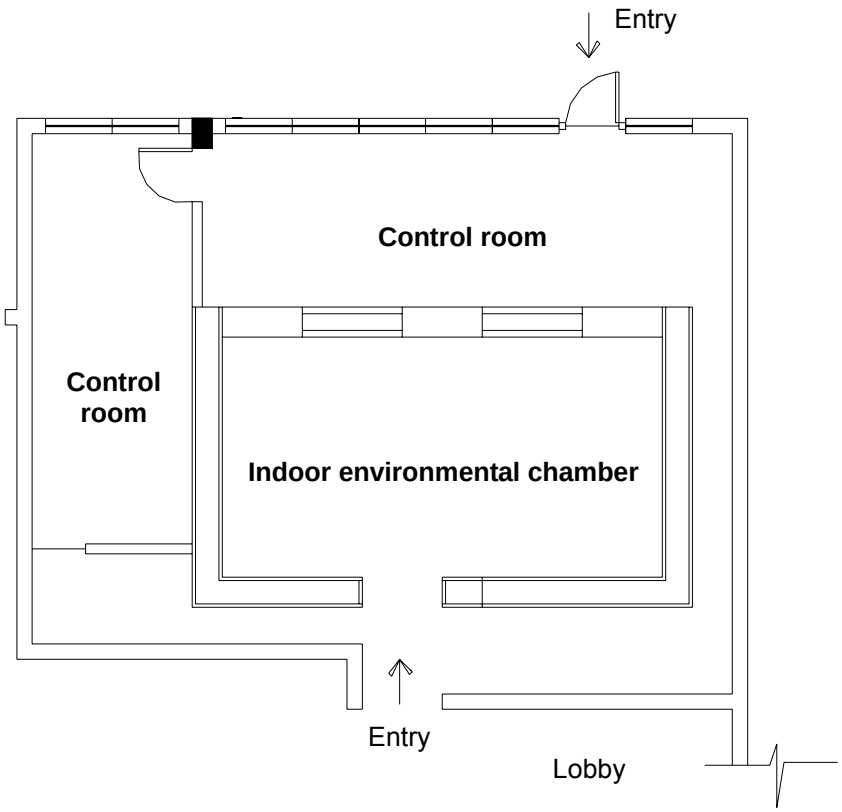

Figure 3.1 Schematic layout of the indoor environmental chamber

The ambient cooling to the chamber was served by re-circulated air stream, which was conditioned in re-circulated air compartment of single coil twin fan (SCTF) air handling unit (AHU) and distributed by ceiling-based re-circulated air duct. Two main supply diffusers controlled by a VAV box controller were centrally and symmetrically located at the suspended ceiling of the chamber. In the pilot study, only one which attaches with high velocity personalized air jet concentrically was used. Two return air grilles were diagonally located at the suspended ceiling and a completely ducted return route was used. Room air temperature was controlled at about 23°C. Figure 3.2 is a snapshot of part of the chamber's ceiling.

Figure 3.2 The ceiling supply diffuser and return grilles of mixing ventilation system

The personalized ventilation system was the primary system serving the chamber. It provides 100% outdoor air through an air jet nozzle locally mounted at the center of ambient air diffuser. Outdoor air was conditioned in the outdoor air compartment of SCTF AHU. The outdoor air in the plenum box was distributed to outdoor air nozzle through PVC pipe with 50mm diameter (Figure 3.3). Total air change rate was 7.4 air changes per hour (ACH) and 23.5 m^3/h per person outdoor air (2 persons) with 23°C supply temperature was supplied approximately when running outdoor air fan and re-circulated air fan at full load.

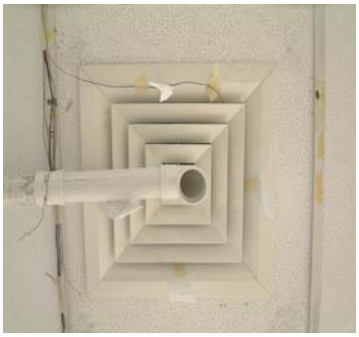

Figure 3.3 The PVC pipe for distributing personalized air

Measurement points were distributed at several locations especially at the breathing zone within the chamber as shown in Figure 3.4. Plane A stood for the plane with 1.2 meter height and plane B stood for the plane pass through the center line of ambient

air diffuser. Measurement of ventilation parameters included outlet velocity of personalized air, ambient air flow rate, air velocity in breathing zone and noise level.

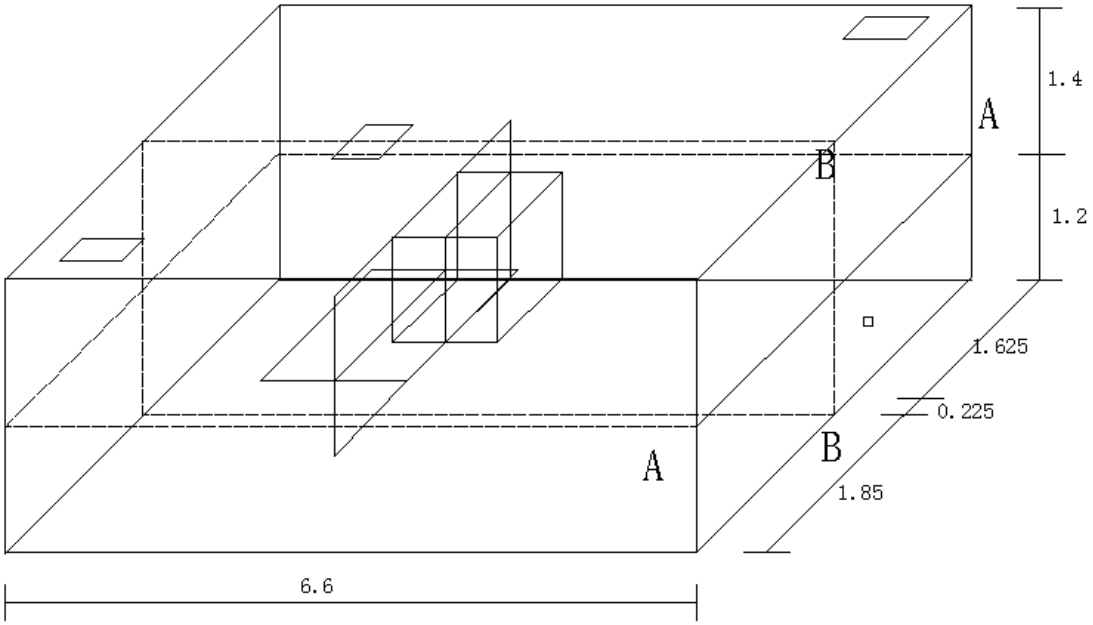

a.

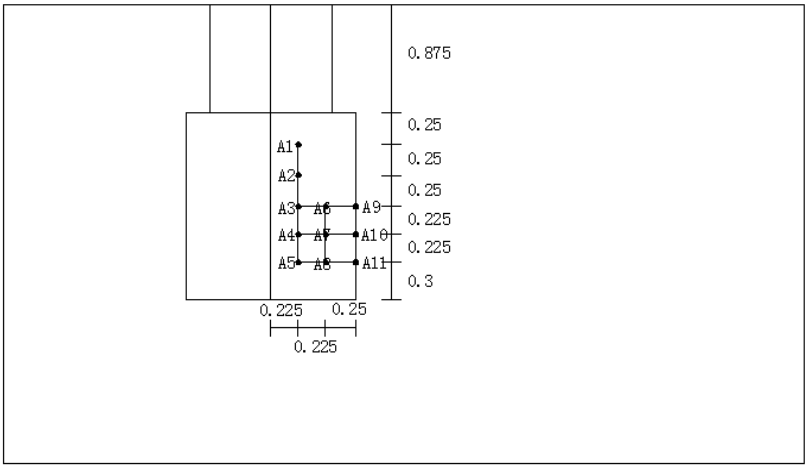

b.

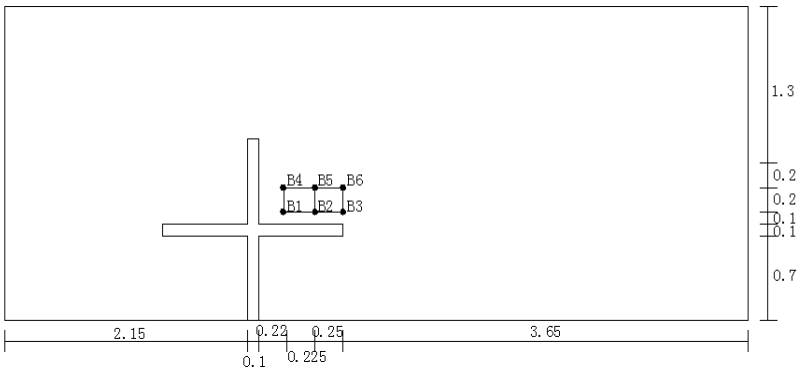

c.

Figure 3.4 Measuring points for velocity in breathing zone

Outlet velocity of personalized air from the circular nozzle was measured using airflow anemometer with 50 mm diameter. Ambient air flow rate was measured using airflow hood (Figure 3.5). Air velocity was measured over five-minute period for each measuring point in the breathing zone using a thermo-anemometer. Time-averaged values for the measuring points were used to validate the simulation results. Noise level was measured at several points inside the chamber using sound level meter and average values were used (Figure 3.6).

Figure 3.5 airflow anemometer and airflow hood

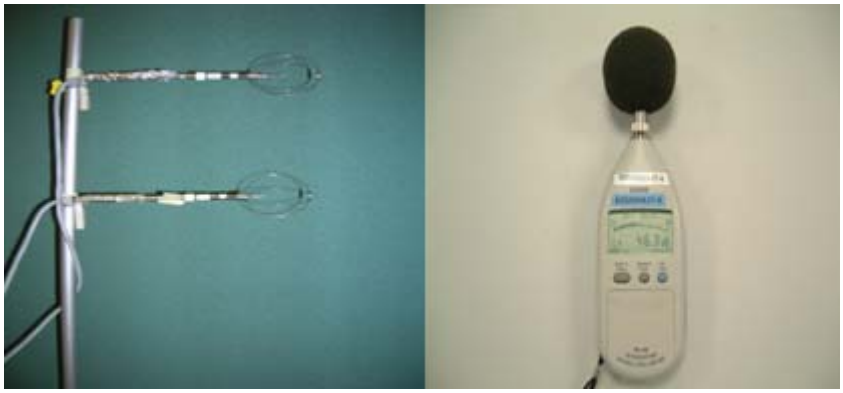

Figure 3.6 Thermo-anemometer and sound level meter

3.2.2 CFD Simulation

The simulated model which includes human body and furniture had geometrically approximate configuration compared with the real one in the chamber. Non-uniform grids were used to consider locations with large gradients of the solution variables (e.g., air velocity, outdoor air percentage) which might occur in regions near supply diffusers, occupants and furniture. Continuity equation and momentum equations were solved to obtain velocity distribution. Species transportation equation was activated and outdoor air was set as the minor species. As a result, distribution of outdoor air percentage (the ratio of outdoor air and total air) can be obtained. To account for turbulence flow, the standard k- ε model was applied in this study. Only isothermal cases were simulated and energy equation had not been activated. This implicate that upwards free convection flow around manikin/subject body caused by buoyant force had not been taken into consideration. Sensitivity analysis was conducted to obtain grid independent and accurate solutions.

Since boundary conditions had critical impact on the predicted airflow, a simplified model for air supply diffuser without compromising on the accuracy of predicted results was needed to be developed. Several methods had been developed such as conventional method (Huo et al, 2000), box method (Nielsen, 1992), momentum method (Chen et al, 1991), etc. A series of square 4-way ceiling diffuser models which include model A to E were developed and validated recently (Cheong et al, 2001). Model D which consider the nature of air jet around diffuser, had been validated to be the best one in simulating mixing ventilation system air diffuser was added with circular outdoor air jet and shown in Figure 3.7. The boundary conditions at re-circulated air diffuser, outdoor air jet and return air grills were shown in Table 3.1.

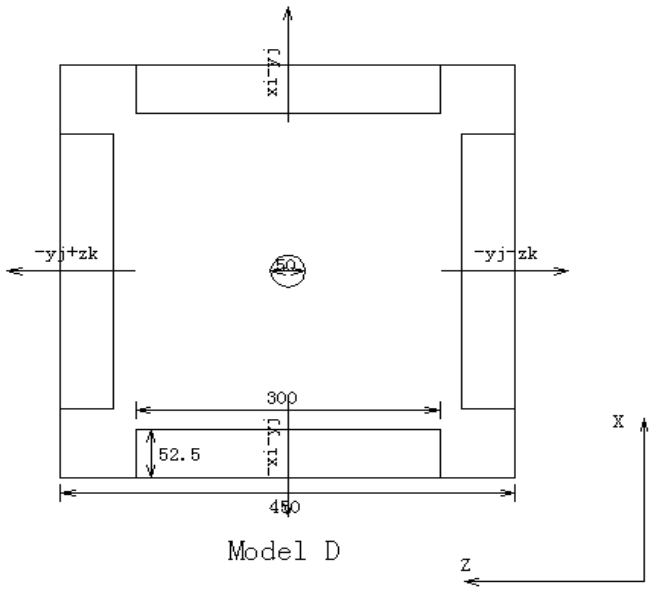

Figure 3.7 Models D for air diffuser

Table 3.1 Boundary conditions for supply diffusers and exhaust grills

Location	Velocity components(m/s)			Velocity(m/s)	Boundary type
	x	y	z	Normal	

Recirculated-air1	0	-1.855	3.213		Velocity inlet
Recirculated-air2	3.213	-1.855	0		Velocity inlet
Recirculated-air3	0	-1.855	-3.213		Velocity inlet
Recirculated-air4	-3.213	-1.855	0		Velocity inlet
Outdoor Air				6.65	Velocity inlet
Exhuast1					Pressure Outlet
Exhuast2					Pressure Outlet

3.2.3 Parametric Studies

In order to make the ceiling mounted jet more optimal and flexible, corresponding parametric studies were shown in Table 3.2. The study was focused on the interaction of the generated airflows from the re-circulated air diffuser and the personalized flow nozzle. The parameters changed were:

Table 3.2 Different simulation cases

	protrusive length(cm)	Blade angle	Outdoor air velocity(m/s)	Outdoor air jet angle
base case	10	30	6.65	90
case1	20	30	6.65	90
case2	10	20	6.65	90
case3	10	30	10.17	90
case4	10	30	6.65	45

In case 1, protruding outdoor air jet with length (20 cm) was compared with the base case (10cm). The possibility of enhancing full use of outdoor air was further predicted.

In case 2, different angle of re-circulated air diffuser blades (20 degrees) was compared with the base case (30 degrees), as shown in Figure 3.8.

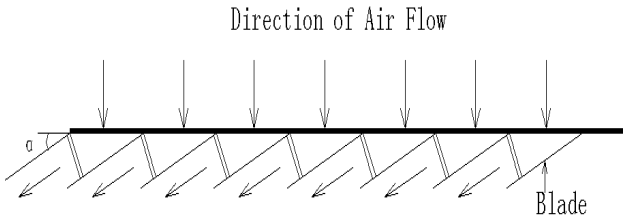

Figure 3.8 Angles of ambient air diffuser blade

In case 3, higher outdoor air flow rate (10L/sec. person, 72m^3/h) was compared with the base case (6.5L/sec. person, 47m^3/h). Correspondingly, outdoor air inlet velocity changed from 6.65 m/s to 10.17 m/s.

In case 4, protruding outdoor air jet with different angle (45 degree) was compared with the base case (90 degree). The possibility of enhancing flexibility of this newly developed ventilation strategy was further predicted.

3.3 Results and Discussion

The main objective of the pilot study was to predict the advantages and feasibilities of this newly developed ceiling mounted PV ATD, which are mainly focused on the improvement of local outdoor air percentage in the occupied zones without causing excessive draught rating. Hence, the typical parameters such as air velocity in the occupied zone were measured. The results of simulation airflow and local outdoor air percentage depict the spatial distribution of air velocity and its components. Small number of parametric studies, using simulation model validated by experiments, pave

the way for further objective measurements by using breathing thermal manikin (Yang and Sekhar, 2007).

3.3.1 Physical Measurements

Measured values of air velocity at different points in the occupied zone are below 0.25 m/s, which will not cause draft sensation. Detailed results will be compared with the simulation results for the base case later.

Whilst measured values of noise level at outdoor air inlet (60dB) and ambient (45dB) are high relative to conventional design, it is envisaged that the acoustic issues can be effectively addressed. Suitable nozzle with noise attenuation is recommended.

3.3.2 CFD Simulation

3.3.2.1 CFD Simulation for Base Case

The predicted outdoor air percentage and air velocity profiles for the base case are shown in Figure. 3.9 and Figure 3.10, respectively. Here, only plane B is presented, since this is the best representation of the condition in the chamber.

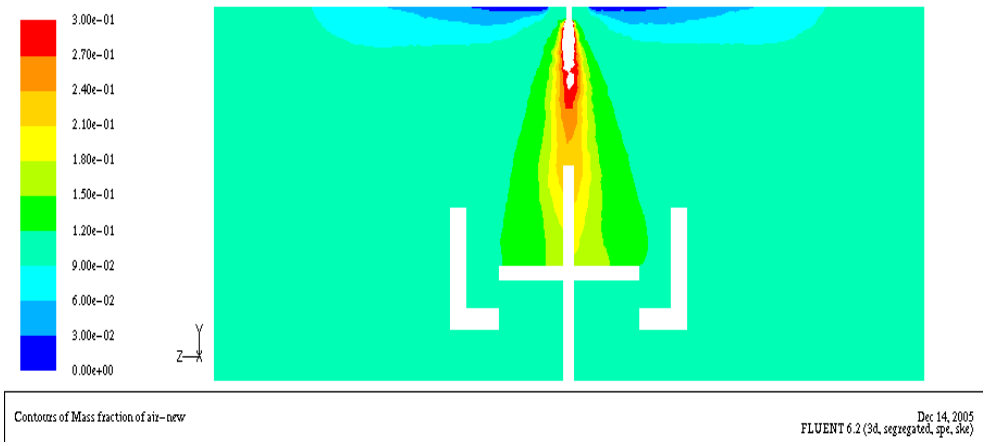

Figure 3.9 Local outdoor air percentage (base case, plane B)

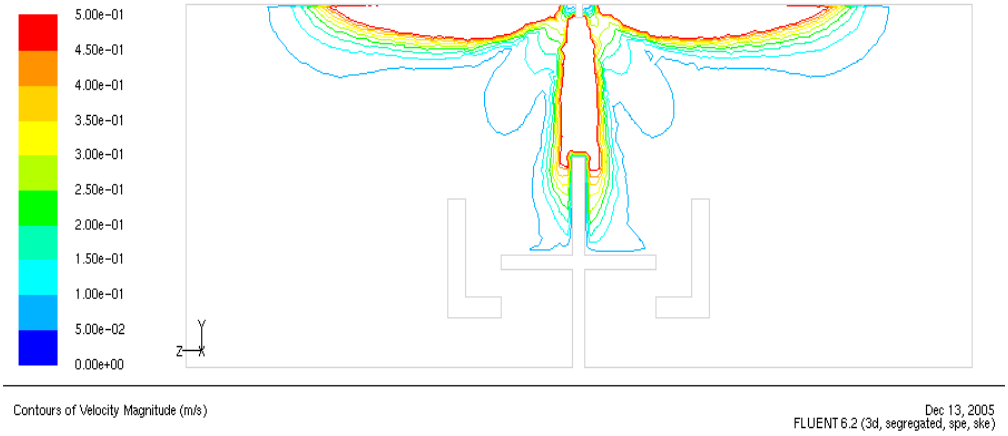

Figure 3.10 Air velocity (base case, plane B)

In this base case, 7.35 ACH of total air change rates (467m^3/h) and 23.5 m^3/h person outdoor air (totally 47m^3/h) were used. By using mixing ventilation strategy, outdoor air and re-circulated air are fully mixed before supply, which causes evenly distribution of local outdoor air percentage (10%). However, higher values of local outdoor percentage (15%-20%) in base case (Figure 3.9) are observed in the breathing zone from the simulation results. That means more outdoor air is supplied directly into the breathing zone without fully mixing with re-circulated air and better air quality in the breathing zone can be realized.

The air velocity of base case (Figure 3.10) will rise because of the long distance between the nozzle and occupied zone. Outdoor air from the circular nozzle comes down at high velocity through the partition and the tables and then reaches breathing zones. The predicted air velocity profile of occupied zone has reached the recommended threshold value (0.25m/s), above which may cause draft sensation.

3.3.2.2 CFD Simulation for Parametric Studies

Since the outdoor air nozzle has a protruded part from ceiling, the induction of re-circulated air can be avoided effectively the length increases. In case 1, local outdoor air percentage (Figure 3.11) can be improved further to 20%-25% compared with base case (Figure 3.9). However, air velocity in occupied zones (Figure 3.12) will increase and will exceed the threshold value (0.25m/s). The protruding part of outdoor air jet can not be too long from considerations of the visual effects and indoor layouts.

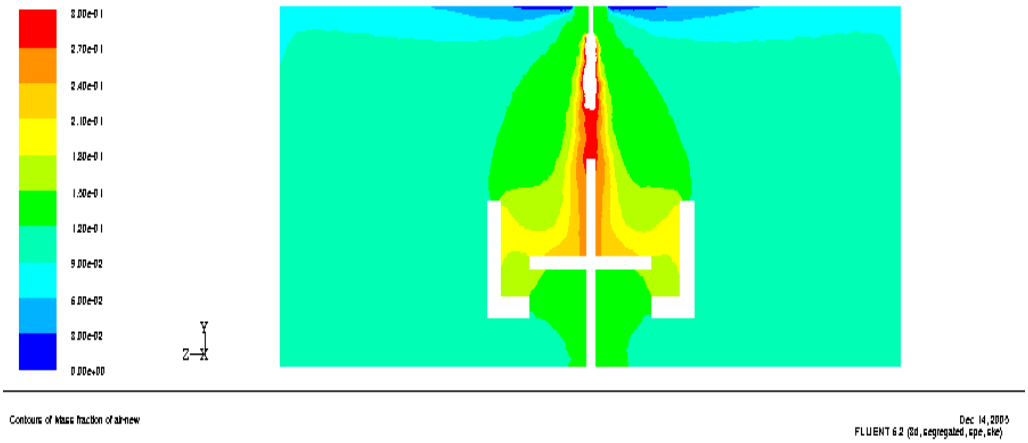

Figure 3.11 Local outdoor air percentage (case1, plane B)

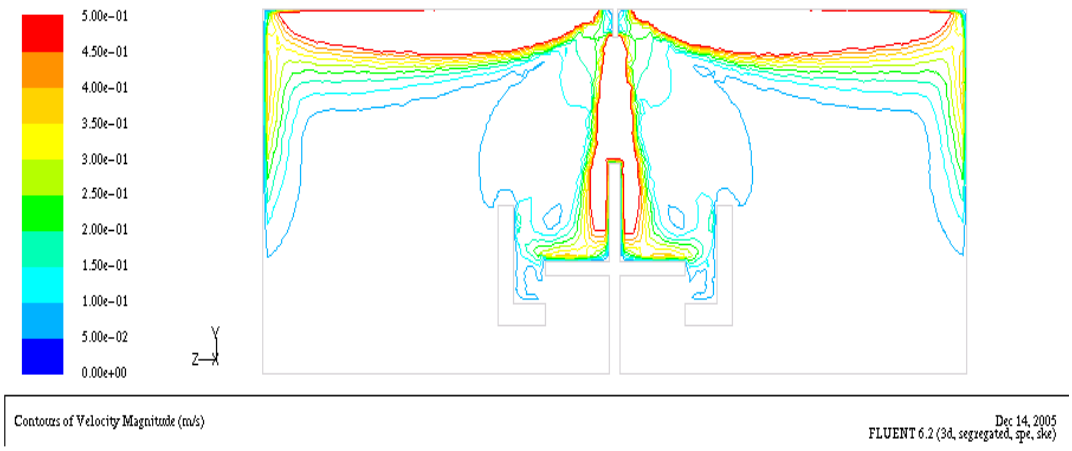

Figure 3.12 Air velocity (case1, plane B)

In case 2, less re-circulated air is induced into outdoor air and higher local outdoor air percentage (20%-25%) in occupied zones appears because the angle of re-circulated air diffuser blades varies from 30 degrees (Figure 3.9) to 20 degrees (Figure 3.13). However, the increasing of local air velocity in occupied zones (Figure 3.14) is not obvious compared with base case (Figure 3.10). This might be optimized in the future.

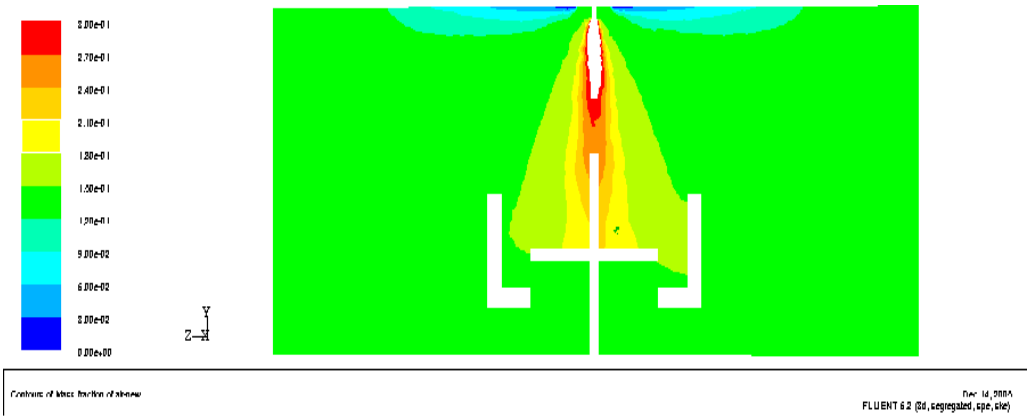

Figure 3.13 Local outdoor air percentage (case2, plane B)

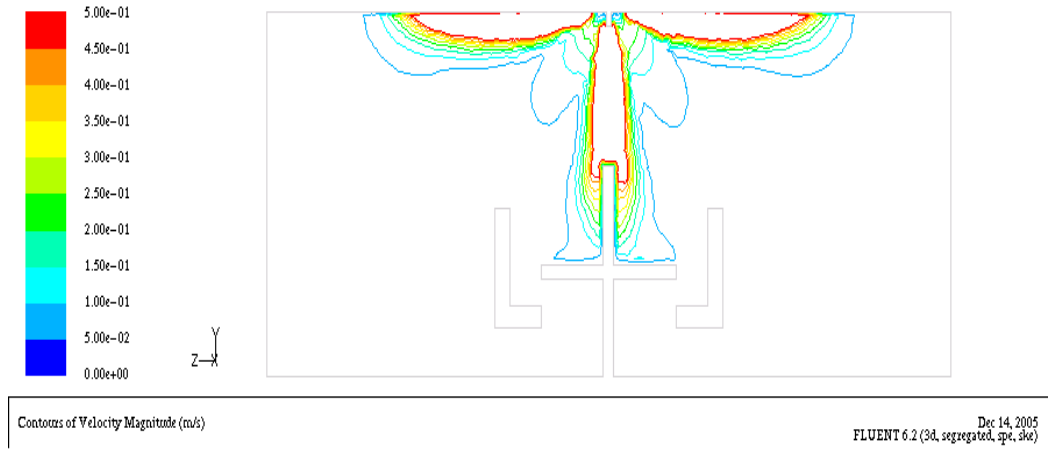

Figure 3.14 Air velocity (case2, plane B)

In case 3, higher local outdoor air percentage (25%-30%) in the occupied zone (Figure 3.15) can be obtained compared with base case (Figure 3.9) because outdoor air outlet velocity changes from 6.65 m/s to 10.17 m/s. As compensation, air velocity in the occupied zone (Figure 3.16) exceeds substantially the threshold value (0.25 m/s). Although people in tropical climate are not very sensitive for draught, the extent of air velocity that people can accept need to be verified through subjective response study.

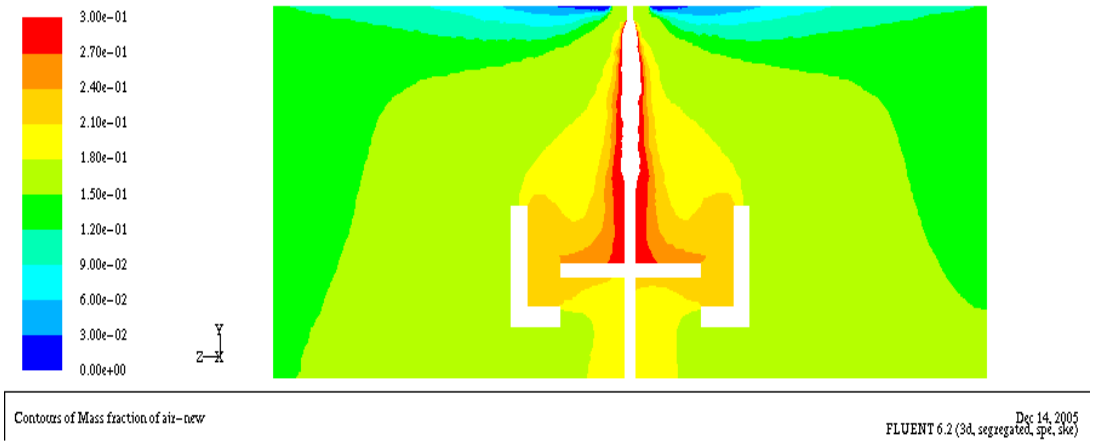

Figure 3.15 Local outdoor air percentage (case3, plane B)

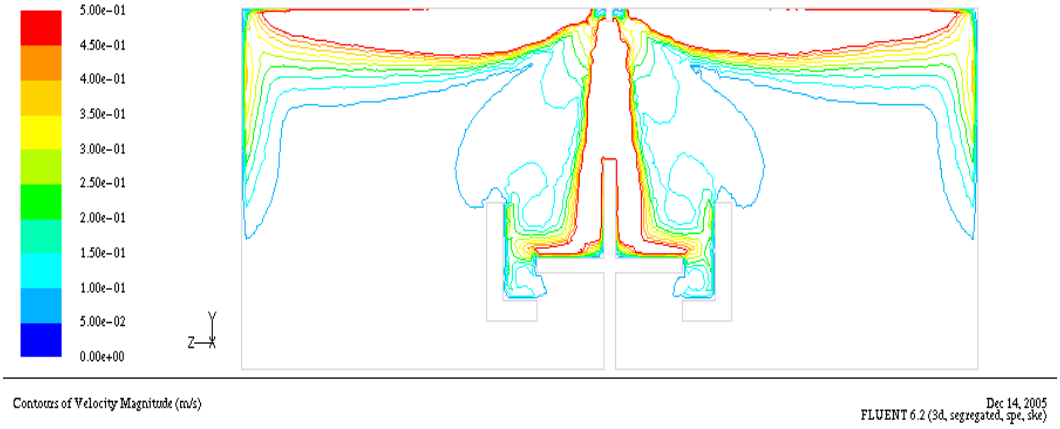

Figure 3.16 Air velocity (case3, plane B)

In case 4, protruding outdoor air jet with angle (45°) is compared with the base case (90°). Local outdoor air percentage (Figure 3.17) and air velocity (Figure 3.18) in the breathing zone which is faced with outdoor air jet is almost the same as base case. It can be used for breathing zones near sidewall.

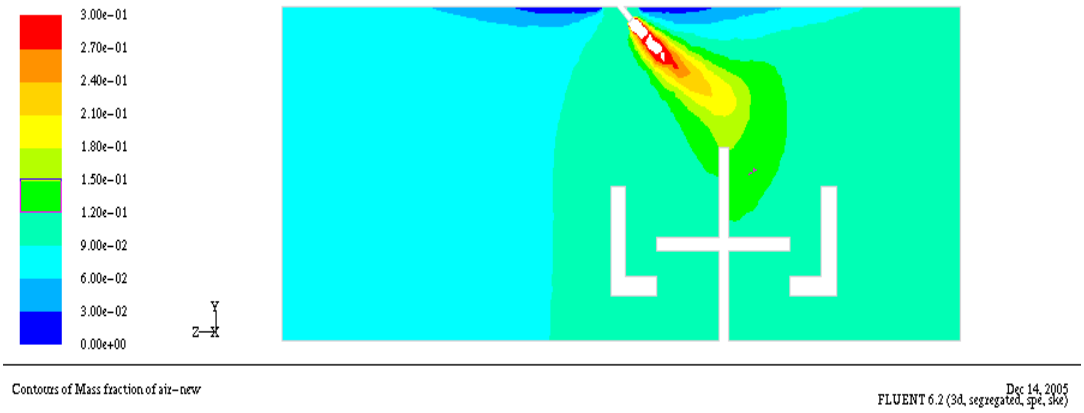

Figure 3.17 Local outdoor air percentage (case4, plane B)

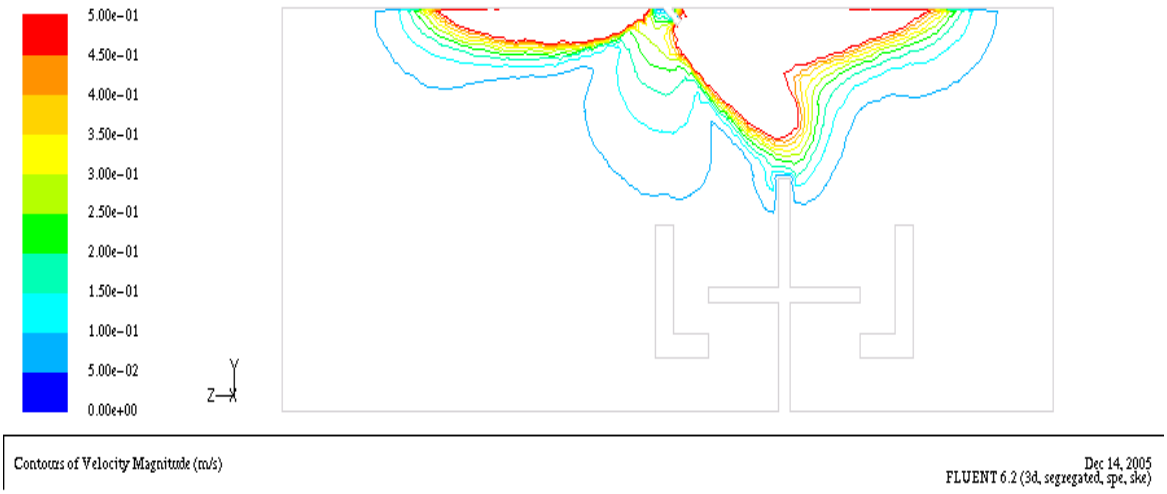

Figure 3.18 Air velocity (case4, plane B)

3.3.3 Comparison of the Results between Physical Measurements and CFD Simulations

Measured values of air velocity at different points in the occupied zone are compared with the simulation results in Table 3.3 for the base case. Good agreement validates the accuracy of the simulation model.

Table 3.3 Comparison between the measured and predicted results for air velocity at occupant level (Location of measuring points as shown in Figure 3.4)

				Air velocity(m/s)		
points	x(m)	y(m)	z(m)	Meas(vm)	Sim(vs)	% Diff (vm-vs)/vm
A1	-0.85	-0.1	-0.25	0.05184	0.0443	14.5
A2	-0.6	-0.1	-0.25	0.07887	0.0858	-8.8
A3	-0.35	-0.1	-0.25	0.15326	0.1493	2.6
A4	-0.125	-0.1	-0.25	0.07158	0.0757	-5.8
A5	0.1	-0.1	-0.25	0.02503	0.0277	-10.7
A6	-0.35	-0.1	-0.45	0.04665	0.0407	12.7
A7	-0.125	-0.1	-0.45	0.03177	0.0302	5
A8	0.1	-0.1	-0.45	0.02923	0.0256	12.4
A9	-0.35	-0.1	-0.65	0.03742	0.0314	16.1

A10	-0.125	-0.1	-0.65	0.03274	0.0272	16.9
A11	0.1	-0.1	-0.65	0.02613	0.0226	13.5
B1	-0.35	-0.45	-0.25	0.08813	0.0835	5.3
B2	-0.35	-0.45	-0.45	0.07394	0.068	8
B3	-0.35	-0.45	-0.65	0.04223	0.0356	15.7
B4	-0.35	-0.25	-0.25	0.11252	0.1104	1.9
B5	-0.35	-0.25	-0.45	0.04329	0.0444	-2.6
B6	-0.35	-0.25	-0.65	0.03136	0.0328	-4.6

3.4 Preliminary Conclusions

According to experimental and simulation results, the new ventilation strategy does have an ability to improve local outdoor air percentage in the occupied zones without causing excessive draught rating. Long protruding distance of outdoor air jet and small blade angle of re-circulated air are observed to make this new method more efficient. Different angles of the protruding outdoor air jet are observed to make this new method more flexible for different occupied zones.

3.5 Recommendations

Based on the findings from pilot study mainly focused on isothermal case, ceiling mounted PV system have the ability to improve outdoor air percentage in the occupied zones without causing excessive draught rating. Another possible advantage of ceiling mounted PV system is to create better local thermal environment by spot cooling, which will be explored in the main study. Based on the observation of CFD results, the control area by jet flow in occupied area is too small to cover human torso. Nozzles with bigger outlet diameter will be used for generating larger control area.

Chapter 4: Performance characteristics of ceiling mounted PV system -- objective measurements

4.1 Objectives

The aim of this part of the study was to evaluate the performance of a prototype of ceiling mounted PV ATDs, with emphasis being placed on air movement characteristics around human body， cooling effect, draft rating, inhaled air temperature and inhaled air quality.

The outline of research methodology for objective measurements is as follows.

- Experimental Design
- Experimental Conditions
- Experimental Protocol and Evaluation Index

4.2 Experimental Design

4.2.1 Facility

The objective measurements are performed in the personalized ventilation laboratory at The International Centre for Indoor Environment and Energy (ICIEE), Department of Civil Engineering, Technical University of Denmark. This 5.6×5.6×2.6m^3 chamber is built to simulate a typical office environment with six workstations. The chamber is adjacent to a control room. One of the walls with windows faces a garden, i.e. it is exposed to the outdoor environment. The control room is used to accommodate

equipment that condition the mixing and personalized ventilation air delivered to the chamber as well as part of ductwork for mixing ventilation and major part of ductwork for personalized ventilation.

The ambient cooling and ventilation of the chamber is served by an air handling unit (AHU) and ceiling-based mixing air distribution system. Four swirl supply diffusers are centrally and symmetrically located on the ceiling of the chamber. The diffusers are type Lindab RKG-200. One return air grille is located at the upper part of one side wall and a completely ducted return route is used. The airflow rate through the supply diffusers is balanced by four manual dampers installed on the branch of each diffuser. The supply air temperature is regulated by adjusting the off-coil temperature and flow rate is regulated by adjusting fan speed using control system to provide ambient cooling and to achieve desired indoor temperature. The mixing ventilation system is also called secondary system. Figure 4.1 is a scheme of mixing ventilation system for the PV laboratory.

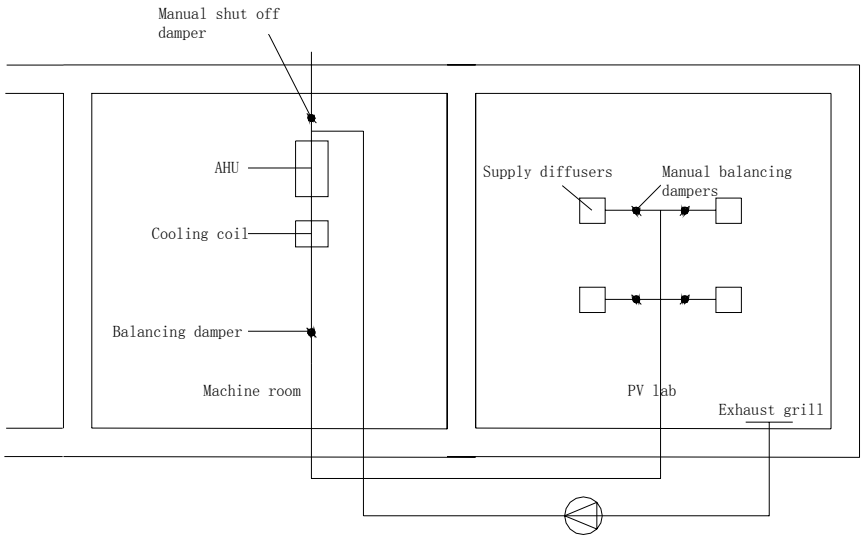

Figure 4.1 Schematic layout of mixing ventilation system for PV lab

The personalized ventilation system is the primary system serving the PV room. It

provides six workstations with personalized air which is 100% outdoor air. The supply air treated in the air handling unit (AHU) with an integrated electric heater, external cooling coil and external humidifier is brought to an air distribution box (ADB) which distribute personalized air to the workstations (Figure 4.2). Six small DC fans mounted at the ADB help to distribute personalized air via ducts to the workstations located in PV chamber (only one workstation located at the center of PV chamber was used for objective measurements). Additional local heater is used to control individually the personalized air supplied to each of the six workstations. In this case an electrically heated wire wrapped around part of the duct with length of approximately 1 meter is used to heat the duct wall and thus to transit the heat to the supplied personalized air for final tuning of its temperature. The six fans on the ADB can be regulated either by the occupants according to their preference for personalized airflow rate (velocity) or by operator located in the machine room. In this way the supply flow rate of personalized air can be regulated separately at each workstation. The airflow rate supplied to ADB is preset by the motorized balancing damper installed on the air supply duct after the components of the AHU. On the intake duct of the AHU, there is a manual shut-off damper installed to cut out the PV system from the outdoor air. Figure 4.2 is a scheme of personalized ventilation system for PV chamber. PV air terminal devices (ATD) of different design can be installed to each of the workstations.

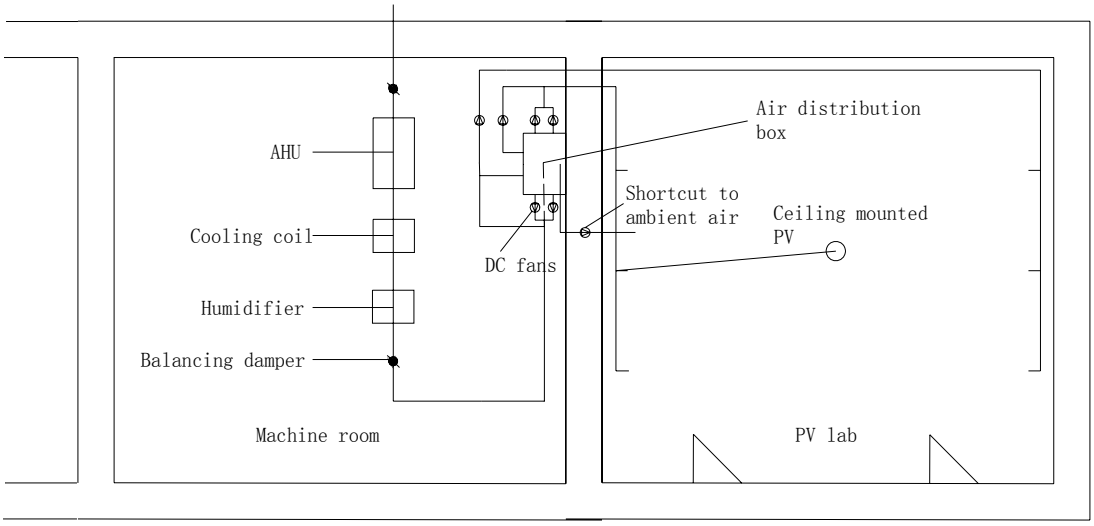

Figure 4.2 Schematic layout of personalized ventilation system for PV chamber

For the purpose of this study, one of the workstations was equipped with the ceiling ATD used later during the human subject study. The ATD was mounted on the ceiling above the workstation. The ATD was a nozzle made of aluminum, with a round outlet having a diameter of 95mm. The nozzle had a diameter of 160mm on the other side, which was connected to ductwork by suitable transition. The length of the nozzle was 140mm. The details of geometrical parameters of the nozzle are shown in Figure 4.3. The nozzle is suitable for ventilation of large areas where long jet throws were required. The nozzle delivered personalized air with low turbulence intensity (turbulence intensity lower than 20% as measured). The low turbulence intensity ATD was chosen in order to reduce heat transfer and mass mixing between PV air and ambient air so as to achieve maximum cooling effect and to provide as clean as possible air to the breathing zone. The distance between the nozzle and floor was 2.5 m. The distance between the nozzle and the head of the thermal manikin (described later in this chapter) was 1.3 m.

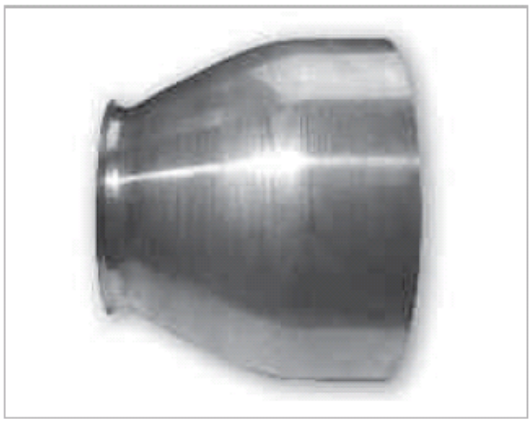

Description

LAD is an supply air nozzle suitable for ventilation of large areas where long throws are required. The nozzle can be used for both heated and cooled air. LAD has a standard MF measure and can be installed directly on a male spigot in the desired direction.

- Directional airflow
- Long throws
- Simple installation

Dimensions

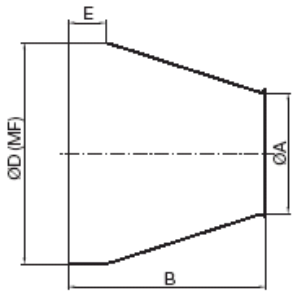

Size	ØA mm	B mm	ØD mm	E mm	Free area A[m²]	m kg
125	60	116	125	40	0.0029	0.10
160	95	140	160	40	0.0071	0.10
200	110	160	200	40	0.0095	0.20
250	145	205	250	60	0.0165	0.30
315	180	235	315	60	0.0254	0.50
400	225	270	400	80	0.0398	0.60

Lindab

Figure 4.3 Technical details of the jet diffuser for ceiling mounted PV ATD

Table 4.1 Jet parameters under different outlet flow rates with 95mm outlet diameter

Case No	Diameter(m)	Volumetric flow rate $Q_0(m^3/s)$	Outlet Velocity (m/s)	Re	a	X_c(m)	δ_c(m)	$V_{m1.3}$(m/s)	$\delta_{1.3}$(m)
1	0.095	0.002	0.282	1776	2.8	0.266	0.072	0.127	0.166
2	0.095	0.004	0.565	3552	3.3	0.314	0.085	0.253	0.201
3	0.095	0.006	0.847	5328	3.6	0.342	0.092	0.38	0.218
4	0.095	0.008	1.129	7104	3.9	0.371	0.1	0.506	0.232
5	0.095	0.01	1.412	8880	4.2	0.4	0.108	0.633	0.244
6	0.095	0.0135	1.906	11988	4.5	0.428	0.115	0.854	0.254
7	0.095	0.017	2.4	15097	4.7	0.447	0.121	1.076	0.260

Preliminary calculations based on the theory of free circular jet were performed to identify the length of the potential core of the flow, a, the coefficient, X_c, the length of core region of the personalized flow generated by the nozzle at different flow rate Qo, outlet velocity and Re number (Table 4.1). The calculations showed that the used nozzle with 95 mm outlet diameter would have long core region (0.25-0.45m),

suitable air velocity downwards at the breathing level (0.13-1 m/s) to offset free convection flow upwards around human body (0.2-0.25m/s) and suitable diameter at the breathing level to cover a person (0.35m-0.5m). Increasing the jet outlet diameter would reduce the air velocity downwards at the breathing level, which decreases cooling effect. Decreasing the jet outlet diameter would reduce the diameter at the breathing level so as not to cover a person. Isothermal case, which refers to the case with same temperature of both PV air from the jet and ambient air, was used to conduct the theoretical analysis (Appendix 2). Non-isothermal case, which refers to the case with different temperature between PV air from the jet and ambient air, had similar trend except the influence from buoyancy effect. In objective measurements, cooler PV air was supplied from the nozzle, which enforced throw length of the jet because the buoyancy force acted in the same direction as the inertia force. It was also called positive buoyancy.

The control system was designed in accordance with the system requirements and principles. It comprised control systems of personalized ventilation system and mixing ventilation system. The two systems were controlled by a computer. The software was installed on the computer. Complete program of the control system was made in Vee software. Agilent VEE was a graphical programming environment optimized for use with electronic instruments. The program's structure was made of blocks and data lines. The blocks interpreted different types of functions, formulas and connected instruments. The software was installed with support drivers of the used output and input devices. The software had two interfaces, user and programmer. The programmer interface displayed all the blocks and lines. The user interface

displayed only selected blocks from the programmer interface. Therefore the user interface was used only to run the completed program. On the user interface, there were usually displayed only the necessary measured and controlled data. The personalized ventilation system control consisted of airflow rates controls and supply temperature controls. As mentioned before, a computer was used as a general control component. As an input (measured) signal process unit, a data logger was used. The data logger was Agilent HP34970A. An output (control) signal was generated by two digital/analog output cards. The cards were Data Translation DT 332 and Data Acquisition PCI 6208V. The control software HP Vee6.0 was used and to execute the data. The mixing ventilation system control consisted of airflow rates and room temperature controls. The same computer as for the control of personalized ventilation system was used.

4.2.2 Instruments

4.2.2.1 Thermal Manikin

A thermal manikin with body shape and size of an average Scandinavian woman was used during the experiments to simulate a person exposed to the personalized flow from the ceiling mounted diffuser. The manikin was placed under ceiling mounted PV ATD in sedentary posture to simulate human-being with the generated thermal plume during the experiments. The manikin was shaped as a 1.68m high average-size female as shown in Figure 4.4. It was made of high quality glass fiber which gives a short time constant. The manikin had movable joints made of aluminum and plastic in neck, hands, shoulders, hip and knees, allowing its body to be adjusted to many postures

mimicking human-beings. The manikin's body was divided into 23 segments. The manikin was dressed with long sleeve shirt, trousers, underwear, socks and shoes at about 0.7 clo thermal insulation and was seated on an office chair with thermal insulation of approximately 0.15-0.2 clo.

Figure 4.4 Breathing thermal manikin

A comfort control mode was used, i.e. the surface temperature of the manikin was controlled to be the same as the skin temperature of an average person in state of thermal comfort under the exposed environmental conditions.

Skin temperatures and heat losses from all 23 body segments of the thermal manikin were measured and recorded. Detailed description was in Appendix 3. The manikin was calibrated before the measurements under well defined conditions. The calibration of the manikin is described in Appendix 1.

4.2.2.2 Temperature and Velocity Measurements

Temperature inside the chamber was controlled by BAS system and recorded by

HOBO meters. The relative humidity inside the chamber was not controlled but measured and recorded using an ONSET HOBO meter placed on every workstation. The relative humidity measurement range of the HOBO meter was 25%-95% with an accuracy of ±5%. Throughout all experimental conditions, the indoor relative humidity fluctuated within the range of 40%-55%.

The personalized air temperature as well as velocity, turbulence intensity, and draft rating were measured by Thermo-anemometer Measurements System HT400. Eight omnidirectional low velocity probes were used to perform simultaneous measurements. The characteristics of the anemometer comply with the requirements for such instruments in the standards (ASHRAE Standard 113, 2005, ISO Standard 7726, 2004). A detailed description is presented in Appendix 3.

Inhaled air temperature was measured at the lip of manikin's mouth by a small thermistor sensor (Crafttemp). It was recorded by a datalogger. The accuracy of the temperature measurement was ±0.2 °C. The temperature sensor and other measuring instruments are described in detail in Appendix 3.

Tracer gas (SF_6) measurements were performed to investigate the performance of the CMPV ATD in terms of ability to provide occupants with fresh outdoor air. Gas analyzer was used. A detailed description of the tracer gas measuring instruments is presented in Appendix 3.

Measure points for SF_6 concentration were shown in Figure 4.5. SF_6 concentration in

personalized air, inhaled air and climate chamber were measured at nozzle outlet, manikin's mouth and return air grill, respectively.

Figure 4.5 Measurement points of SF_6 concentration

Previous study by Melikov and Kaczmarczyk (2007) identified that trace gas concentration sampling at a point between the mouth and the nose of thermal manikin at distance less than 10 mm from the face represents accurately the trace gas concentration in the air inhaled by people. The placement of SF_6 sampling points and dosing point as well as connection of the sampling and dosing system are schematically shown in Figure 4.6.

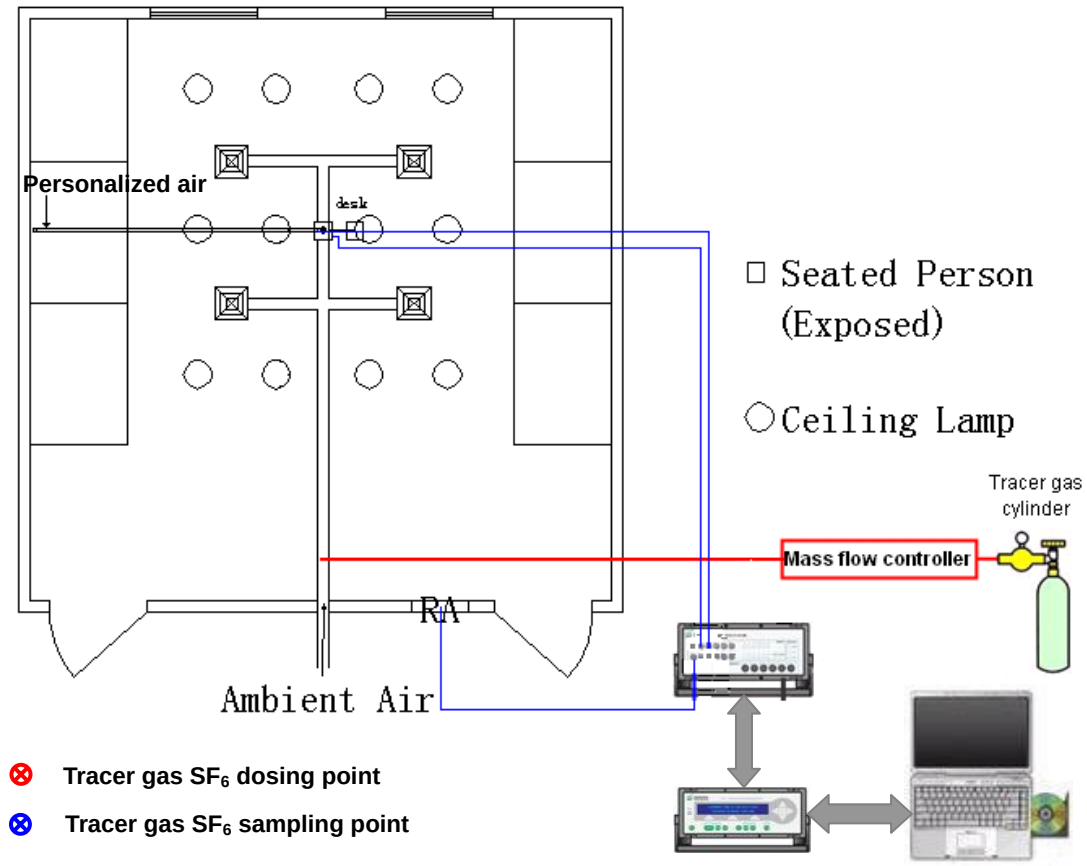

Figure 4.6 Schematic representation of distribution of SF_6 dosing and sampling points

4.3 Experimental Conditions

Experiments were designed to simulate typical office conditions and to utilize both isothermal and non-isothermal combinations of PV air temperature and ambient temperature so as to explore the acceptability of human subjects and the impact of personalized air on microenvironment of the respondents. Typically, the most common office temperature observed in Singapore is 23.5°C, which was used as one of the conditions. Another set of experiments were planned to have ambient temperature of 26°C to substantiate improvements of cooling effect and inhaled air quality as well as energy conservation in elevated ambient thermal environment. Three different PV air temperatures were studied, namely 21°C, 23.5°C and 26°C.

Four different PV flow rates (4, 8, 12, 16 L/s·person) were chosen. 4 L/s·person PV airflow rate was used to test the minimum threshold value for satisfying thermal comfort and air quality requirements especially under cases with low personalized air temperature. 8 L/s·person PV airflow rate was near outdoor air requirements of local standards (CP13, 1999). In many ventilated rooms, outdoor air supplied is of the order of magnitude of 10 L/s·person (Fanger, 2000). Therefore 12 L/s·person PV airflow rate was chosen as the third flow rate. 16 L/s·person PV airflow rate was used because of the relatively long distance between the ceiling mounted PV ATD and human breathing zone so as to improve both thermal quality and air quality in the breathing zone. Previous results with desk mounted PV ATD performed in the Tropics revealed that tropically acclimatized subjects preferred air movement with velocity as high as 1 m/s.

The thermal manikin was placed bellow the ceiling mounted PV ATD. It was adjusted so that the top of the head of the manikin to meet the centerline of the personalized flow. The distance between the outlet of the ceiling mounted PV ATD and the head of seated manikin was 1.3 m, i.e. the manikin was located in the axisymmetric decay region of the jet (x/D_= 13.7).

The matrix of the experiments is presented in Table 4.2. The experimental design also considered the option of running the same system under same conditions without

personalized air supply in order to demonstrate that PV concept does work. In the experiments with only mixing ventilation, i.e. PV flow rate was 0 L/s, the outdoor air was mixed with re-circulated air and supplied through ambient air diffusers. The experiments included 8 reference cases with primary system operating without PV air supply as listed in Table 4.2.

Table 4.2.Experimental conditions

Room temperature (°C)	26			23.5		
Use of PV	with PV		without PV	with PV		without PV
PV temperature (°C)	23.5	26	–	21	23.5	–
PV flow rate (L/s)	4,8,12,16	4,8,12,16		4,8,12,16	4,8,12,16	

Note: For experiments without PV, outdoor air is mixed with re-circulated air in AHU as part of total supply air.

Furthermore, experiments with manikin moved 0.2 m forward, backward and sideward were performed to simulate occupant's movement in reality at workplace and to study its impact on the airflow interaction and the local cooling of the body. During these experiments all temperature combinations under different personalized airflow rates (Table 4.2) were explored.

4.4 Experimental Protocol and Evaluation Index

The objective measurements included determination of velocity profile of the personalized flow, its cooling effect, inhaled air quality and inhaled air temperature. The procedures and indices for evaluation of the above parameters are introduced in the following sections.

4.4.1 Airflow Profile

It was already discussed that the airflow at the vicinity of human body with desk mounted PV is usually very complex. For a ceiling mounted PV, the personalized air is supplied from the ceiling towards the top of head of human occupants. The supply momentum is high so as to offset the upward free convection flow. Compared with the personalized airflow and the free convection flow, the influence of other airflows such as respiration flow, ventilation flow, etc. on the airflow interaction and body cooling is negligible. Therefore the interaction of these two flows was the focus of the present study.

The airflow from the ceiling mounted PV ATD was a typical circular free jet, which had potential core region, characteristic decay region, axisymmetric decay region and terminal region. The spread angle was between 20 to 30 degree for the convergent nozzle used (Awbi, 2003). Therefore, the omni-directional thermal anemometer probes for measurement of velocity magnitude were distributed in the jet as shown in Figure 4.7. The selected measuring points allowed for measurement of the centreline velocity and velocity distribution across the jet.

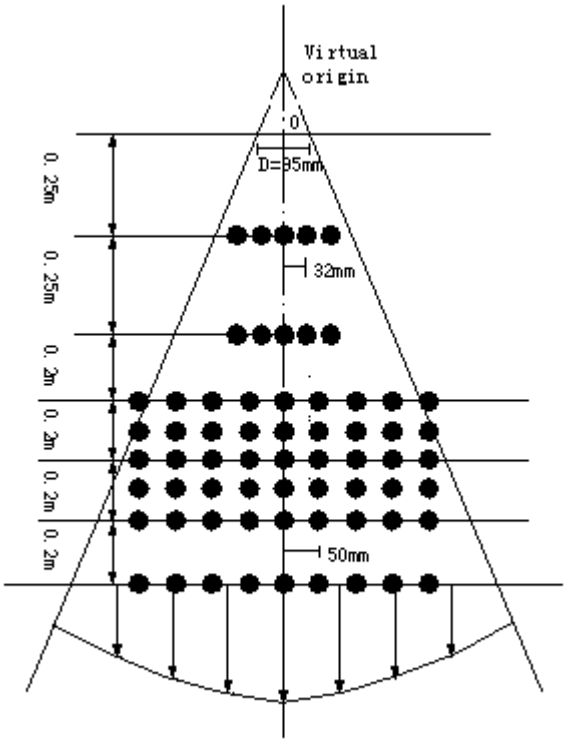

Figure 4.7 Distribution of Omni-directional thermal anemometer probes

When the thermal manikin (simulating an occupant) is present the development of the personalized flow, i.e. the circular jet, will be influenced by its body which will act as an obstacle and by the thermal plume generated. These two impacts of these effects on the airflow interaction were analyzed in the present study.

- **Blockage Effect of the Manikin**

The manikin located below the ceiling mounted PV ATD was an obstacle which disturbs the personalized airflow. A bypass flow was generated when the downward personalized airflow reaches the top of manikin's head, which is solid boundary (Figure 4.8). The centerline velocity was reduced in this area due to the blocking effect of the manikin. The blocking effect on the development of the centerline

velocity in the personalized flow and the velocity distribution across the flow was studied when the manikin was unheated. The measurements were performed at 8 cross sections. The measurements were performed at different personalized airflow rates under isothermal condition 23.5°C/23.5°C, i.e. room air temperature equal to the personalized air temperature.

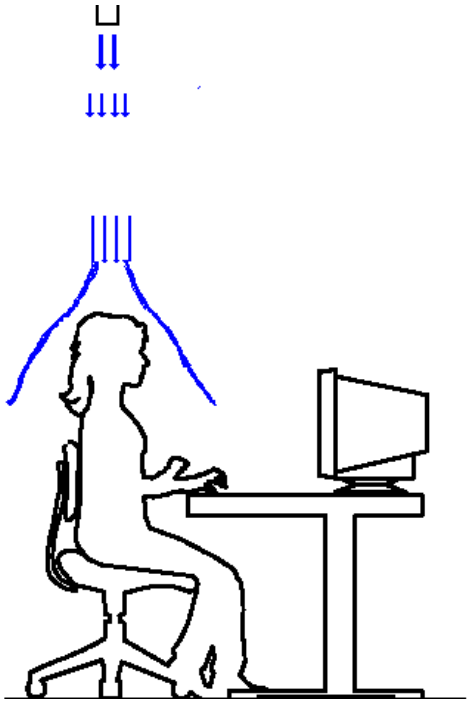

Figure 4.8 Blockage effect for ceiling mounted PV airflow from unheated manikin

- **Neutral Level**

The heated thermal manikin will generate a thermal plume with relatively high velocity 0.2 to 0.25 m/s (Melikov 2004). The generated thermal plum will inevitably influence the downward personalized airflow. In this study, this influence was evaluated by the neutral level (Figure 4.9). The neutral level, X_{nl}, was defined as the vertical distance from the nozzle to the point where the impact of the thermal plume on the velocity distribution in the personalized airflow begins to be observed, i.e. the

vertical distance from the nozzle to the point where the difference in velocity distribution across the airflow with and without the presence of manikin was observed. The neutral level was explored quantitatively based on different personalized airflow rates under 23.5°C/23.5°C isothermal case.

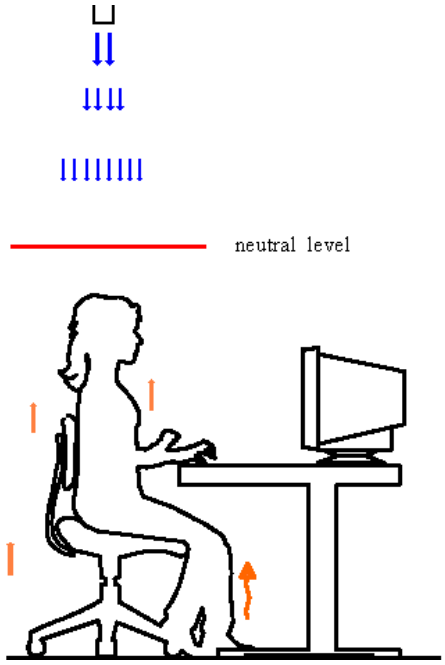

Figure 4.9 Neutral level for evaluating influence of free convection flow on PV airflow

4.4.2 Cooling Effect

In order to quantify the cooling effect of the thermal environment which the manikin was exposed to, sensible heat loss measured from each body segment as well as from the whole-body of the manikin was transformed into a parameter named manikin-based equivalent temperature. The manikin-based equivalent temperature was defined as the temperature of a uniform enclosure in which a thermal manikin with realistic skin surface temperature would lose heat at the same rate as it would in the actual environment (Nilsson et al. 1997). The manikin based equivalent temperature can be expressed as a function of the sensible heat loss from each body

segment:

$$T_{eq} = 36.4 - C(Q_t) \quad (4.1)$$

Where t_{eq} is manikin based equivalent temperature, °C,

Q_t is sensible heat loss, W/m^2,

36.4 is deep body temperature, °C,

C is constant dependent on clothing, body posture, chamber characteristics and thermal resistance offset of skin surface temperature control system, K.m^2/W. The difference of manikin based equivalent temperature with and without personalized air supply (ΔT_{eq}) calculated for each body segment and for the whole body was used as an evaluating index. The manikin was calibrated before the experiments.

4.4.3 Inhaled Air Quality and Temperature

The indices for evaluating the performance of the ceiling mounted PV ATD in terms of the air quality they deliver to occupants included Personal Exposure Effectiveness (ε_p), and inhaled air temperature. The definitions of these indices are presented in the following.

- **Personal Exposure Effectiveness**

The aim of PV was to provide occupants with 100% fresh and clean personalized air. An index expressing the percentage of personalized air in inhaled air, namely personal exposure effectiveness, ε_p, was derived from the following equation (Melikov et al., 2002):

$$\varepsilon_P = \frac{C_{R,SF6} - C_{I,SF6}}{C_{R,SF6} - C_{PV,SF6}} \quad (4.2)$$

Where $C_{R, SF6}$ is SF_6 concentration in the climate chamber (ppm),

$C_{PV, SF6}$ is SF_6 concentration in personalized air (ppm),

$C_{I, SF6}$ is SF_6 concentration in the inhaled air (ppm).

The concentrations were averaged values taken over concentration measurement curves when steady-state conditions were reached. This index is equal to one when 100% of personalized air was inhaled and it is equal to zero when no personalized air was inhaled.

- **Inhaled Air Temperature**

Data acquisition sensor was mounted in the mouth of manikin, through which air was inhaled. Average readings were taken and analyzed when steady-state conditions were reached.

4.5 Experimental Results

4.5.1 Flow Interaction

Comprehensive measurements of the velocity field across the personalized airflow at eight different cross sections were performed in the case of free vertical jet without manikin, with unheated manikin and with heated manikin. The mean velocity profiles measured at the 8 cross sections without manikin at 4 l/s are shown in Figure 4.10. Mean velocity profiles measured at selected cross sections without manikin, with

unheated manikin and with heated manikin are compared for exploring the blockage effect and the neutral level. These are shown in Figures 4.11 a, 4.10b and 4.11c in the case of 4 L/s. Velocity profiles similar to those shown in Figure 4.10 and 4.11 are obtained for the remaining flow rates of 8, 12 and 16 L/s. These are shown in Appendix 5. At the two cross sections close to nozzle outlet, centerline velocities are only slightly lower than the velocity at nozzle outlet because they were within the core region. The comparison of the results in Figures 4.11a and 4.11b show that at 4 L/s the blocking effect of the unheated manikin on velocity distribution in the personalized flow is observed after approximately 10.5 initial nozzle diameters, i.e. approximately at distance of 1.1 m from the exit of the nozzle and 0.2 m from manikin's head. The centerline velocity in the personalized flow at distance x/D=11.58 is substantially lower with manikin present than without manikin. The velocity measurements at 8, 12 and 16 L/s are analyzed in similar way. Figure 4.12 compares the dimensionless centerline velocity V/V_o without manikin and with unheated manikin at 4, 8, 12 and 16 L/s. The results identify that the blockage effect of the unheated manikin is observed almost at the same cross section, which was 0.2 m above manikin's head. Centerline velocity begins to reduce at that level under different personalized airflow rates. Although the absolute values of the reductions are different, the reduction ratios defined as the centerline velocity with unheated manikin divided by the centerline velocity without manikin are almost the same, 85% (Table 4.3). Air velocity along jet radius at this cross section increases slightly because of the bypass flow.

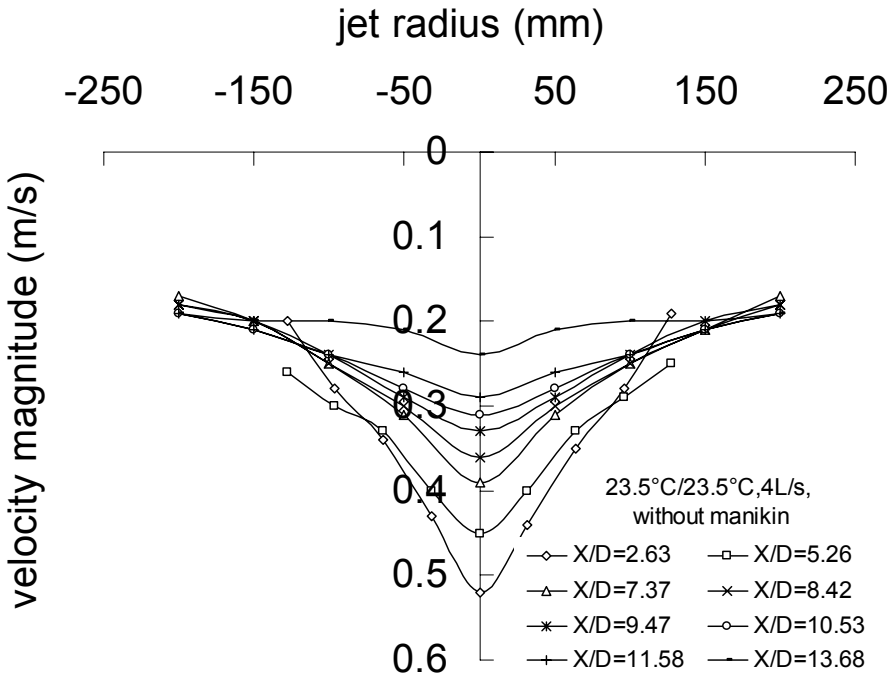

Figure 4.10 Air velocity profile with 4 L/s personalized airflow rate under 23.5°C/23.5°C isothermal case for all cross sections (X/D: dimensionless distance, X: absolute distance, D: nozzle diameter)

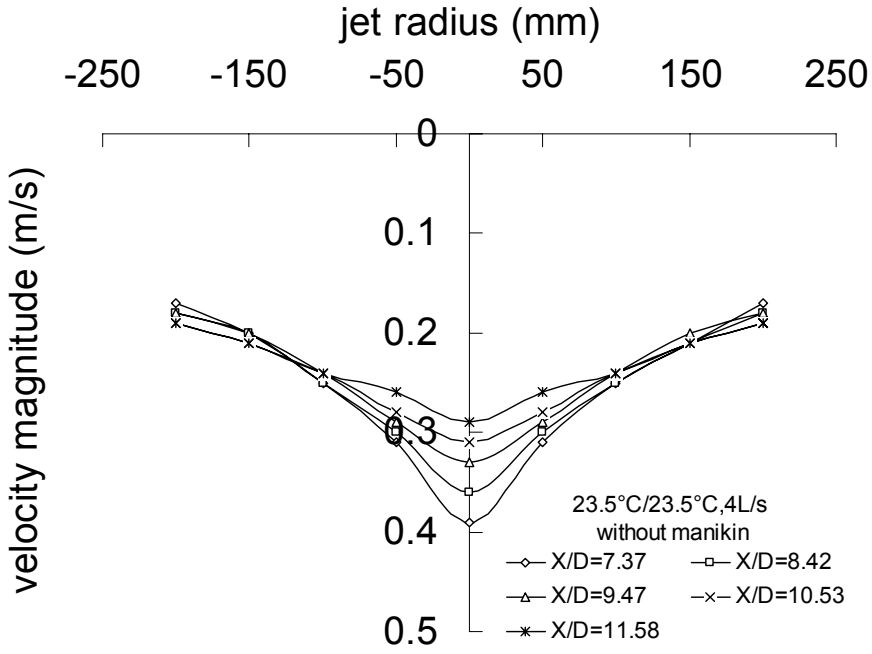

Figure 4.11a Air velocity profile with 4 L/s personalized airflow rate under

23.5°C/23.5°C isothermal case without manikin (X/D: dimensionless distance, X: absolute distance, D: nozzle diameter)

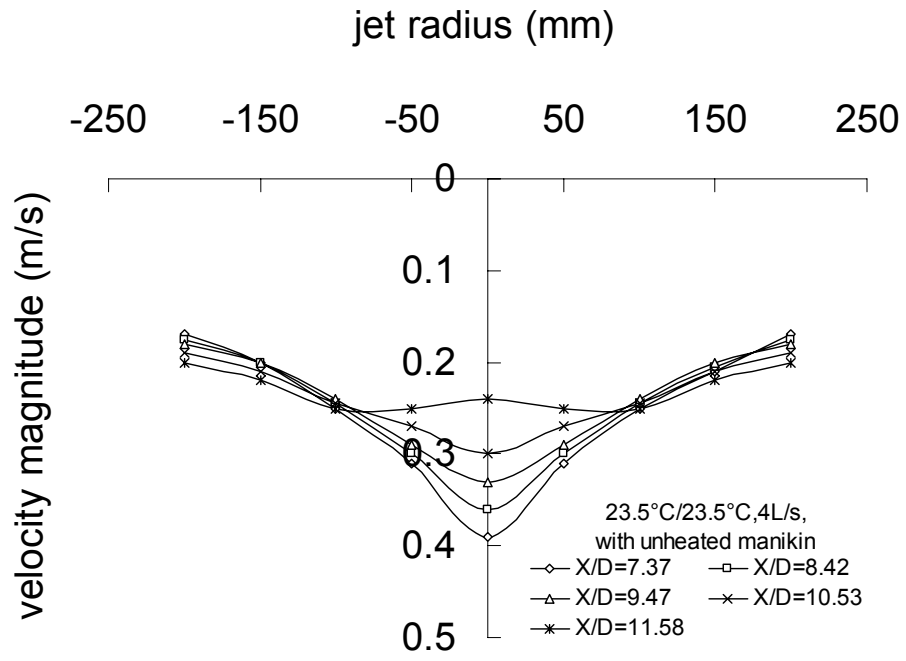

Figure 4.11b Air velocity profile with 4 L/s personalized airflow rate under 23.5°C/23.5°C isothermal case with unheated manikin (X/D: dimensionless distance, X: absolute distance, D: nozzle diameter)

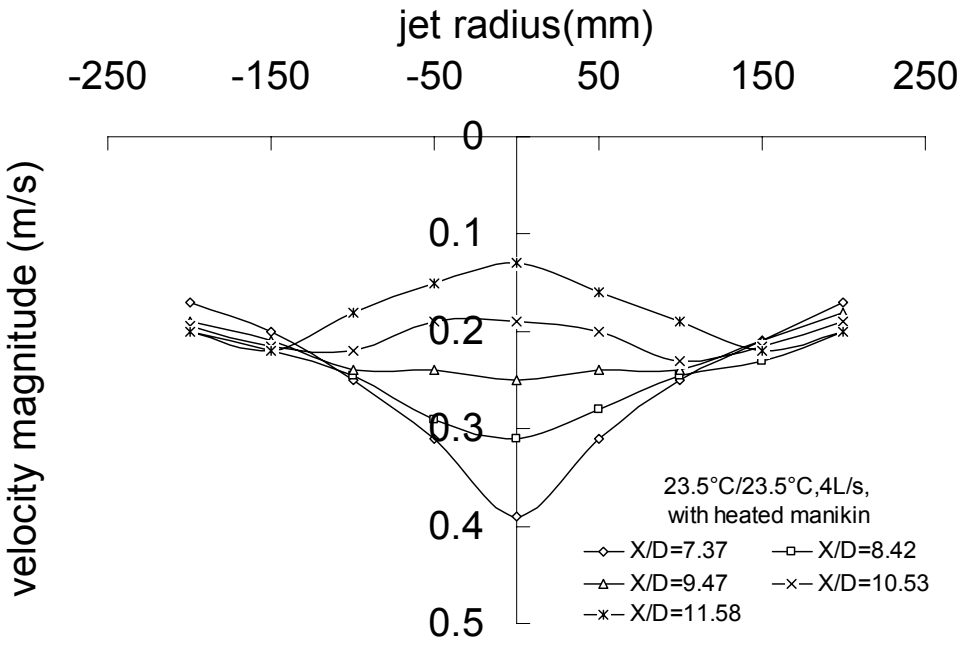

Figure 4.11c Air velocity profile with 4 L/s personalized airflow rate under 23.5°C/23.5°C isothermal case with heated manikin (X/D: dimensionless distance, X: absolute distance, D: nozzle diameter)

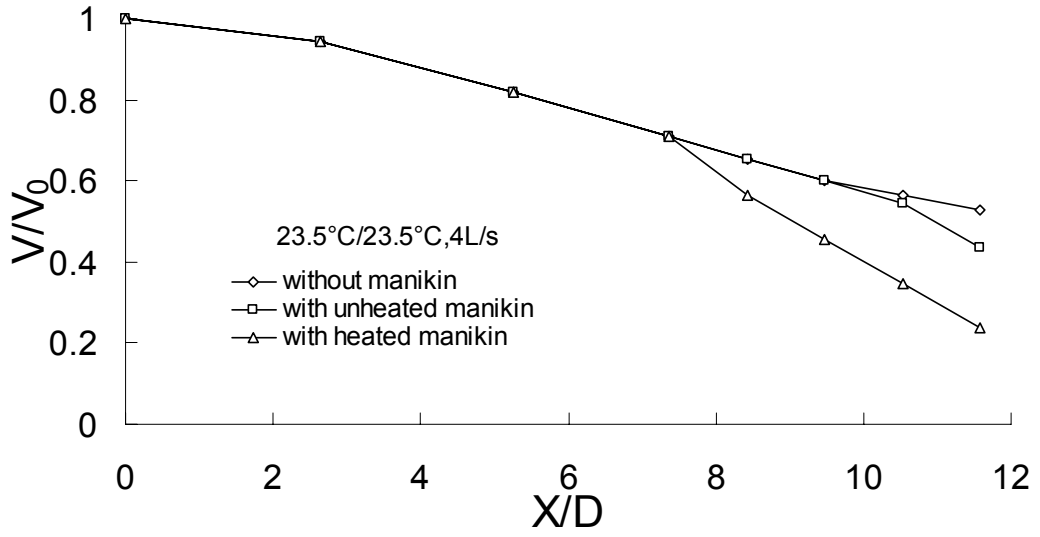

.

Figure 4.12a Comparison of centreline velocity distribution without, with unheated and with heated manikin at 4 L/s and 23.5°C/23.5°C isothermal case.
V (m/s) – centreline mean velocity; V_0 (m/s) – mean velocity at nozzle outlet
X (m) – distance between measuring point and nozzle outlet; D (m) – nozzle diameter

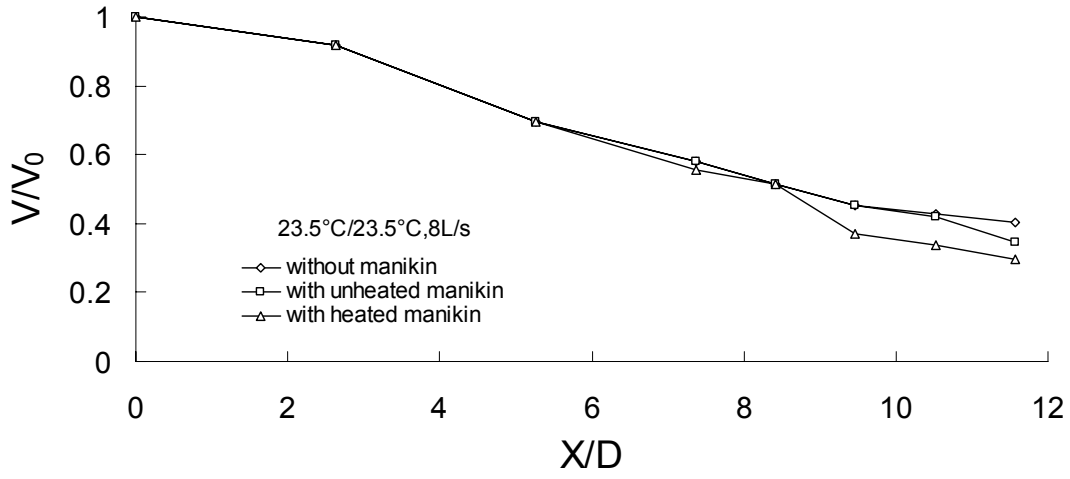

Figure 4.12b Comparison of centreline velocity distribution without, with unheated and with heated manikin at 8 L/s and 23.5°C/23.5°C isothermal case.
V (m/s) – centreline mean velocity; V_0 (m/s) – mean velocity at nozzle outlet
X (m) – distance between measuring point and nozzle outlet; D (m) – nozzle diameter

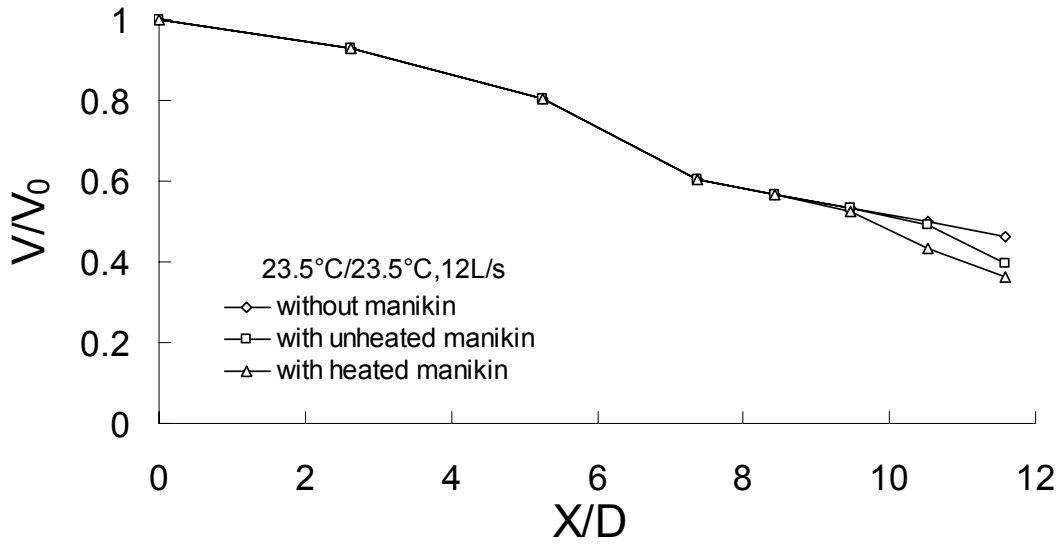

Figure 4.12c Comparison of centreline velocity distribution without, with unheated and with heated manikin at 12 L/s and 23.5°C/23.5°C isothermal case.
V (m/s) – centreline mean velocity; V_0 (m/s) – mean velocity at nozzle outlet
X (m) – distance between measuring point and nozzle outlet; D (m) – nozzle diameter

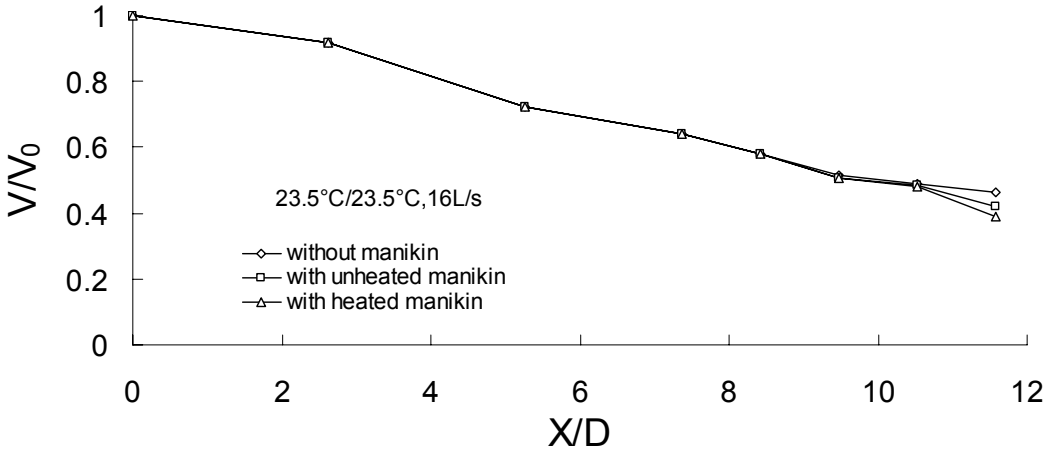

Figure 4.12d Comparison of centreline velocity distribution without, with unheated and with heated manikin at 16 L/s and 23.5°C/23.5°C isothermal case.
V (m/s) – centreline mean velocity; V_0 (m/s) – mean velocity at nozzle outlet
X (m) – distance between measuring point and nozzle outlet; D (m) – nozzle diameter

Table 4.3 Centreline velocity and Reduction ratio of centreline velocity at 0.2 m above manikin's head

	4L/s	8L/s	12L/s	16L/s
Centerline velocity without manikin (m/s)	0.29	0.49	0.7	0.92
Centerline velocity with unheated manikin (m/s)	0.24	0.42	0.6	0.81
Reduction ratio (%)	82.8	85.7	85.7	88.0

The thermal plume generated by the heated manikin creates further resistance for the personalized flow. For example, the comparison of the centerline velocity measured with heated manikin at x/D= 10.53 and 11.58 (Figure 4.11c) is lower than the centerline velocity measured with unheated manikin (Figure 4.11b) and without manikin (Figure 4.11a). Clear deformation of the velocity profiles and reduction of the centerline velocity due to the impact of the interaction of the personalized airflow and thermal plume from the manikin can be seen in Figure 4.11c already at distance of x/D= 7.37 (0.8 m) that is much closer to the nozzle exit, i.e. further from the manikin's head (0.5 m), than in the case of unheated manikin (Figure 4.11b). As expected, stronger deformation of the velocity field of the personalized flow is seen at low flow rates, because the personalized flow is not strong enough to offset the thermal plume close to the manikin, i.e. the strength of the thermal plume (centerline velocity of about 0.25 m/s) is comparable to the strength of the personalized flow (centerline velocity of 0.3 m/s). The neutral level at 4 L/s personalized airflow rate is 0.8 m. Similarly, the interaction of the two flows and the neutral levels are identified under all personalized airflow rates. At 16 L/s, the personalized airflow is strong enough to almost completely destroy the thermal plume. This can be seen from the

centerline dimensionless velocity shown in Figure 4.12. The neutral levels increase from 0.8m to 1.1 m when personalized airflow rates increase from 4 L/s to 16 L/s (Figure 4.13); the stronger the personalized airflow, the easier it could offset the opposing thermal plume generated by the heated manikin. The results in Figure 4.12d show that the blockage effect of the unheated manikin and neutral level appeared at the same cross section at 16 L/s personalized airflow rate, which confirms that the personalized airflow at 16 L/s is strong enough to destroy the thermal plume.

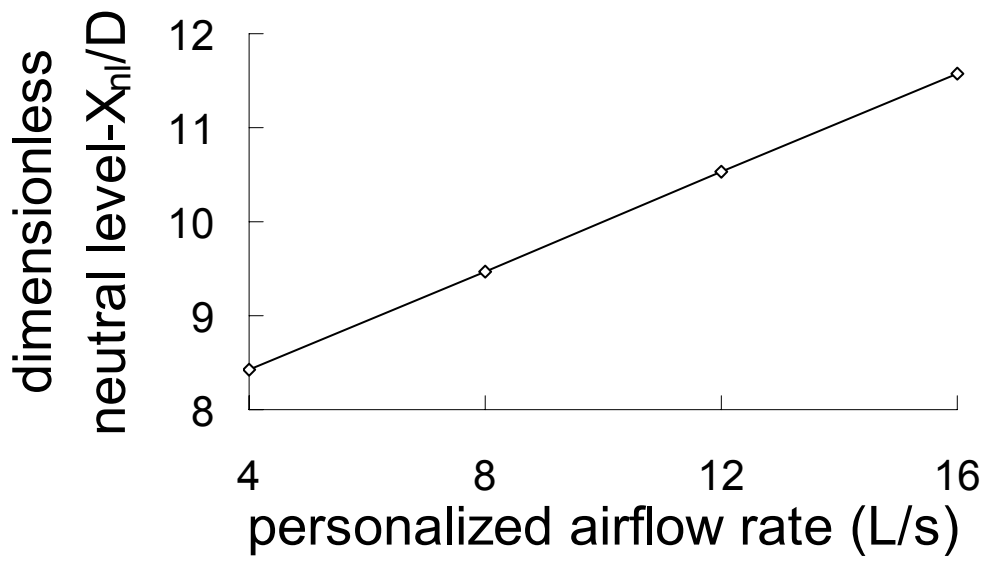

Figure 4.13 Dimensionless neutral level as a function of personalized airflow rates
X_{nl} (m) – neutral level; D (m) – nozzle diameter

4.5.2 Cooling Effect

The interaction of the personalized flow with the thermal plume generated by the manikin has direct effect on the equivalent temperature determined by the manikin. Figure 4.14 shows the difference in segmental equivalent temperature determined from the reference measurement, i.e. without personalized flow, and the

measurements with personalized jet at different airflow rates. As expected, the results identify that the head region of the manikin (scull, left/right face, back of the neck) are the body segments most cooled by the personalized flow. For left/right face, ΔT_{eq} changed from -1°C to -6°C under 23.5°C/21°C case and from -0.5°C to -4°C under 26°C/26°C case, which are the two extreme cases among the four cases, when the flow rate increased. For scull, ΔT_{eq} changed from -0.5°C to -4°C under 23.5°C/21°C case and from -0.25°C to -2°C under 26°C/26°C case. For back of the neck, ΔT_{eq} changed from -0.7°C to -4.5°C under 23.5°C/21°C case and from -0.5°C to -2.5°C under 26°C/26°C case. This means that the cooling due to the personalized flow is as much as the cooling which would be obtained when corresponding room air temperature drop is achieved. For left and right chest, ΔT_{eq} changed from -0.5°C to -3.5°C under 23.5°C/21°C case and from -0.25°C to -2°C under 26°C/26°C case, when the flow rate increased. The cooling effect of whole body was smaller, from -0.25°C to -2°C under 23.5°C/21°C case and from -0.1°C to -1.5°C under 26°C/26°C case, when the flow rate increased. Figure 4.15 shows the difference in segmented equivalent temperature determined from the reference measurement, i.e. without personalized flow, and the measurements with personalized jet at different PV/ambient temperature combinations. Under the lowest personalized airflow rates (4 L/s), ΔT_{eq} changed from -0.6°C to -1.1°C, from -0.2°C to -0.6°C, from -0.3°C to -0.7°C and from -0.3°C to -0.7°C for left/right face, for scull, for back of the neck, for left and right chest, respectively. Under the highest personalized airflow rates (16 L/s), ΔT_{eq} changed from -4°C to -6.2°C, from -2°C to -4.5°C, from -2.5°C to -4.7°C and

from -2.5°C to -4°C for left/right face, for scull, for back of the neck, for left and right chest, respectively.

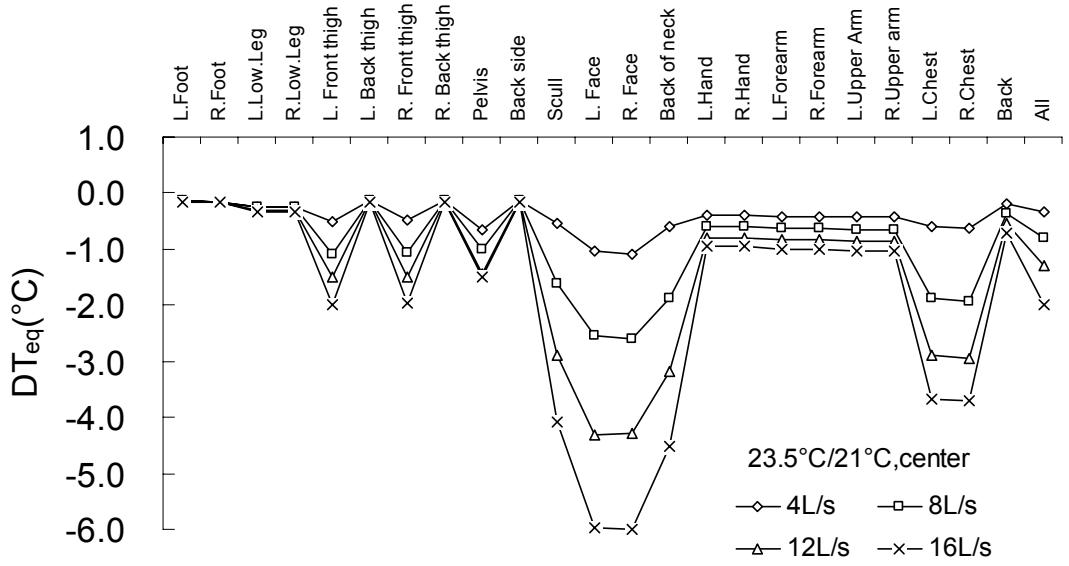

Figure 4.14a Cooling effect analysis under different personalized airflow rates.at 23.5°C/21°C

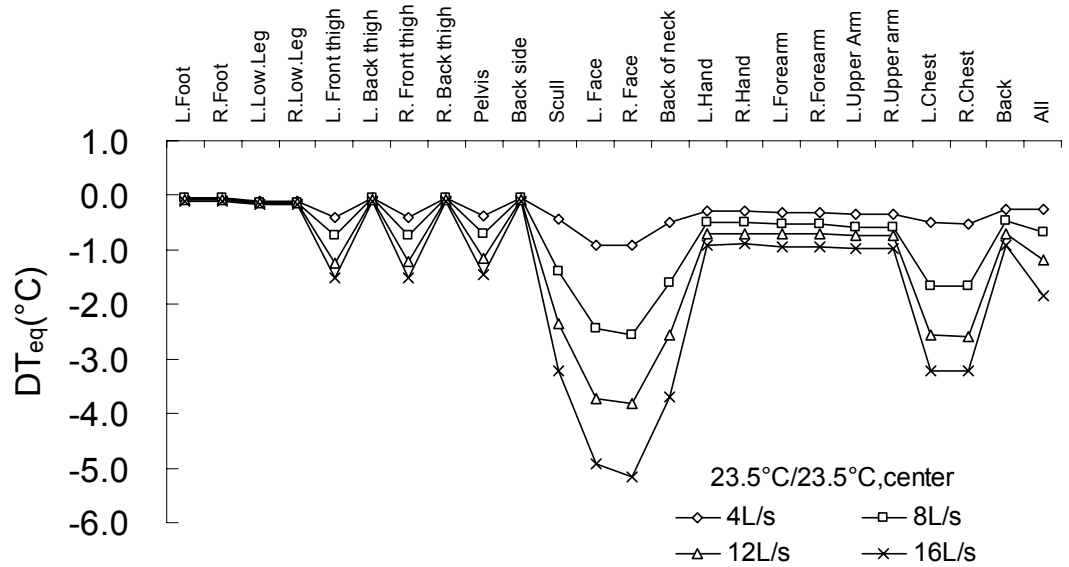

Figure 4.14b Cooling effect analysis under different personalized airflow rates.at

23.5°C/23.5°C

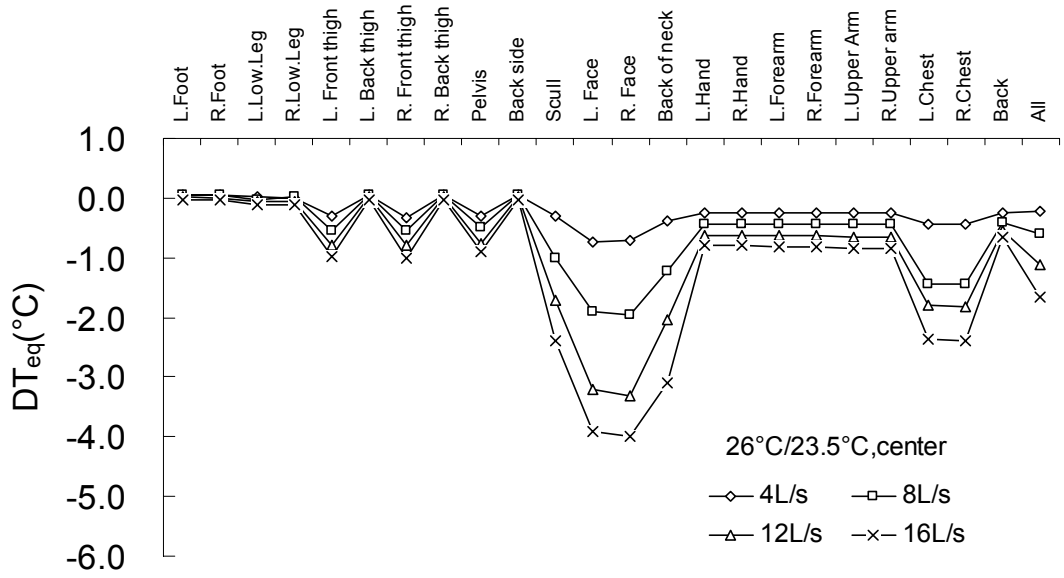

Figure 4.14c Cooling effect analysis under different personalized airflow rates.at 26°C/23.5°C

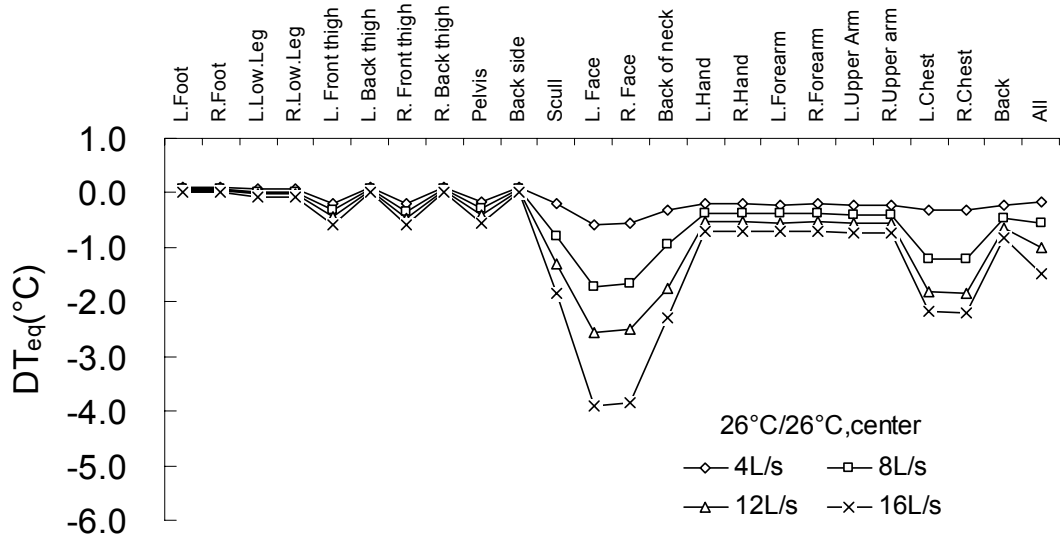

Figure 4.14d Cooling effect analysis under different personalized airflow rates.at 26°C/26°C

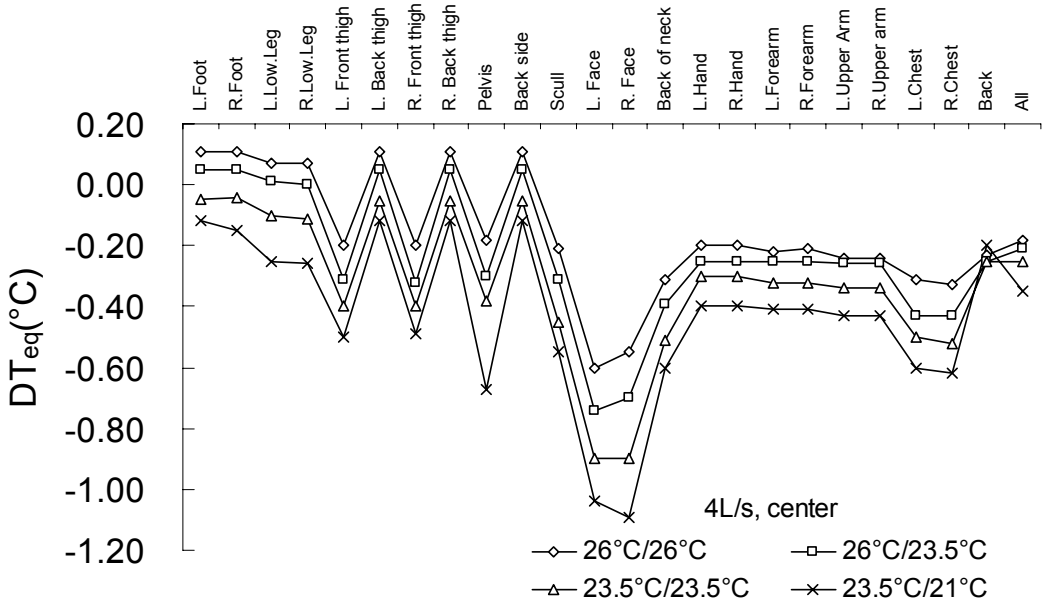

Figure 4.15a Cooling effect analysis under different temperature combinations.at 4 L/s personalized airflow rate

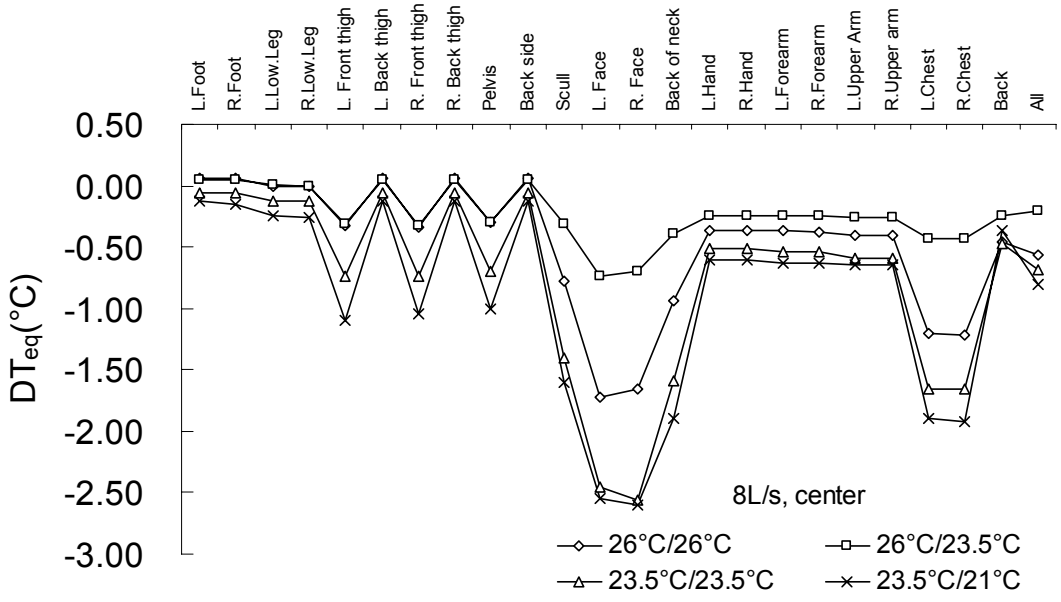

Figure 4.15b Cooling effect analysis under different temperature combinations.at 8 L/s personalized airflow rate

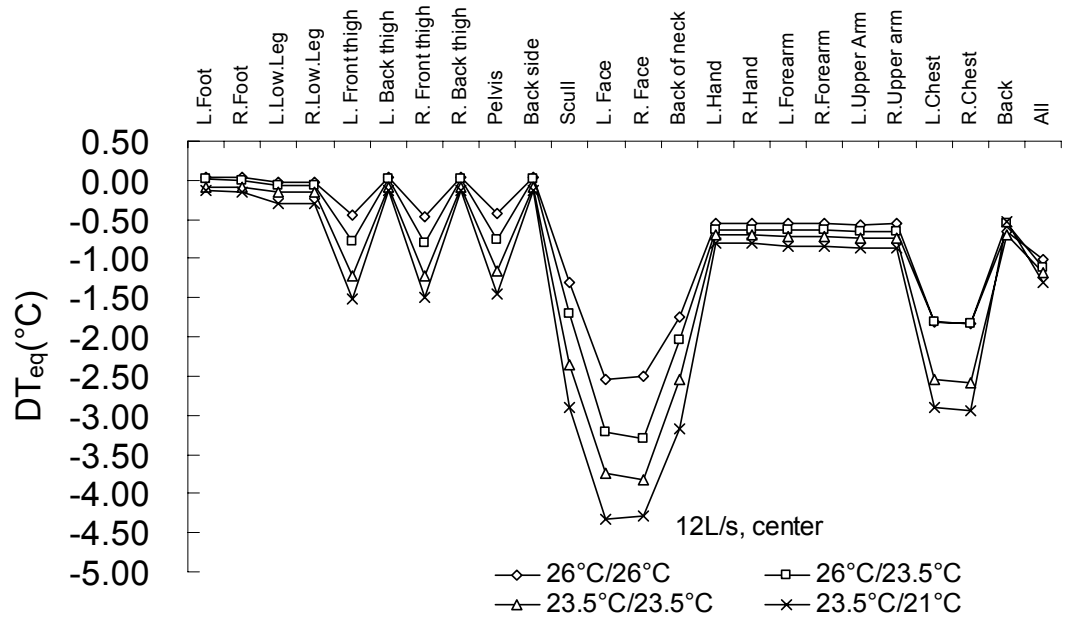

Figure 4.15c Cooling effect analysis under different temperature combinations.at 12 L/s personalized airflow rate

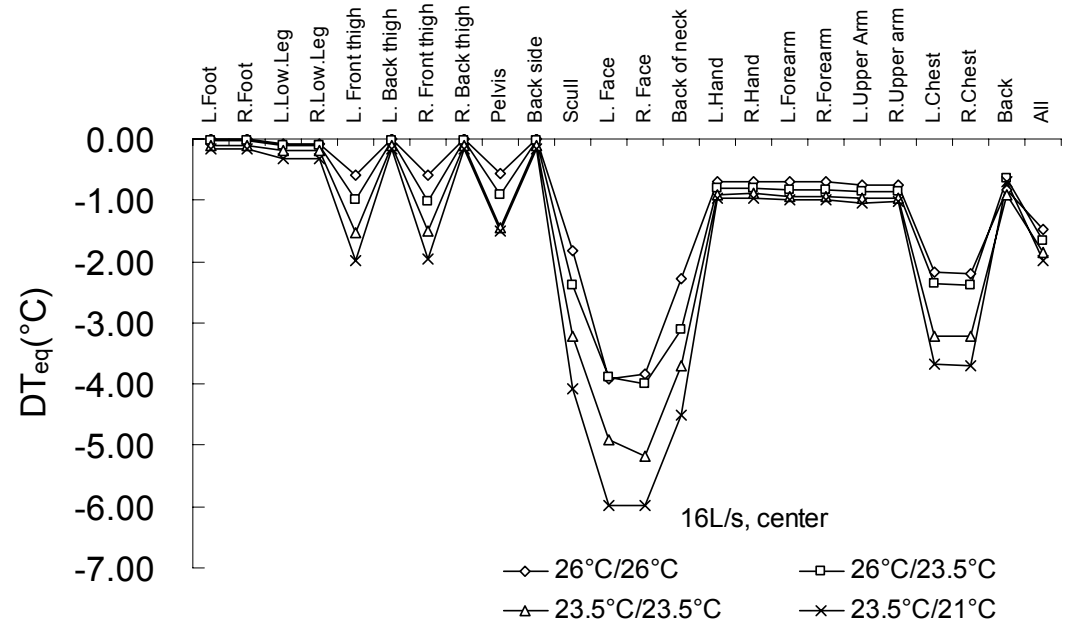

Figure 4.15d Cooling effect analysis under different temperature combinations.at 16 L/s personalized airflow rate

The impact of room air temperature and personalized air temperature on the equivalent temperature are demonstrated from Figure 4.16a to Figure 4.16d. Due to an increase in the airflow rate, the segmented equivalent temperature at the face decreased by 5°C at 21°C personalized air and by 4°C at 23.5°C personalized air when room air temperature is 23.5°C (Figure 4.16a and Figure 4.16b). The segmented equivalent temperature at the face decreased by 3.4°C at 23.5°C personalized air and by 3.3°C at 26°C personalized air when room air temperature is 26°C (Figure 4.16c and Figure 4.16d). This indicates that the influence of personalized air temperature on equivalent temperature at the face becomes striking when room air temperature becomes low. Due to an increase in the airflow rate, the segmented equivalent temperature at the face decreased by 4°C at 23.5°C room air temperature and by 3.4°C at 26°C room air temperature when personalized air temperature is 23.5°C (Figure 4.16b and Figure 4.16c). This indicates that the equivalent temperature at the face is also affected by room air temperature. The lowest whole-body equivalent temperature is 21.5°C at 23.5°C/21 °C temperature combination and 24.3°C at 26°C /23.5°C temperature combination.

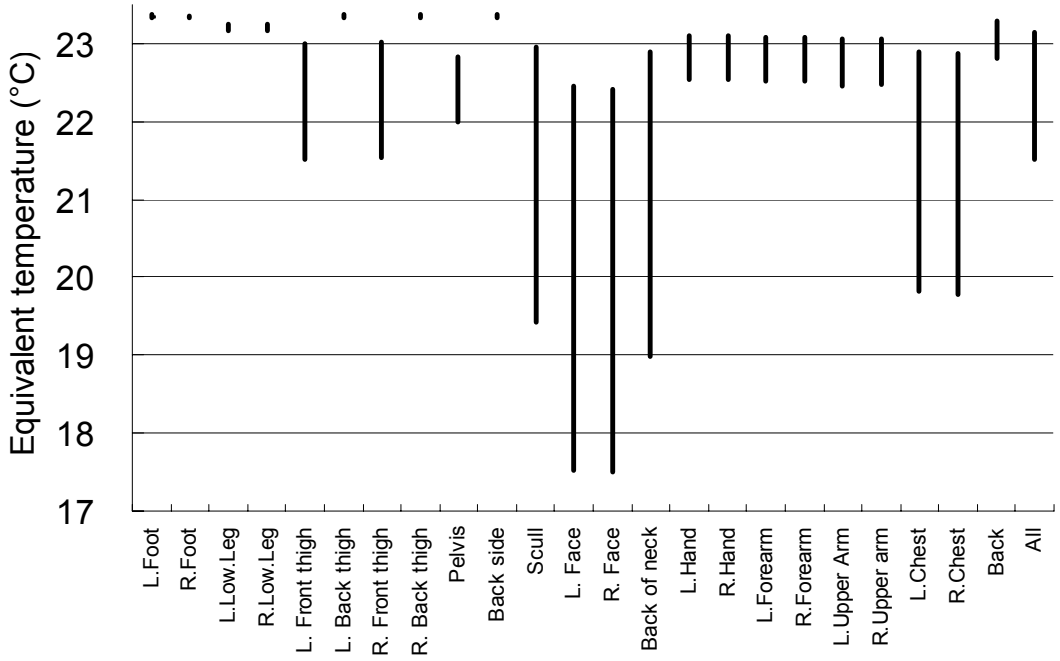

Figure 4.16a Ranges of the segmented and whole-body equivalent temperature tested at room air temperature of 23.5°C and personalised air temperature 21°C. Each line end indicates the highest and lowest of equivalent temperature

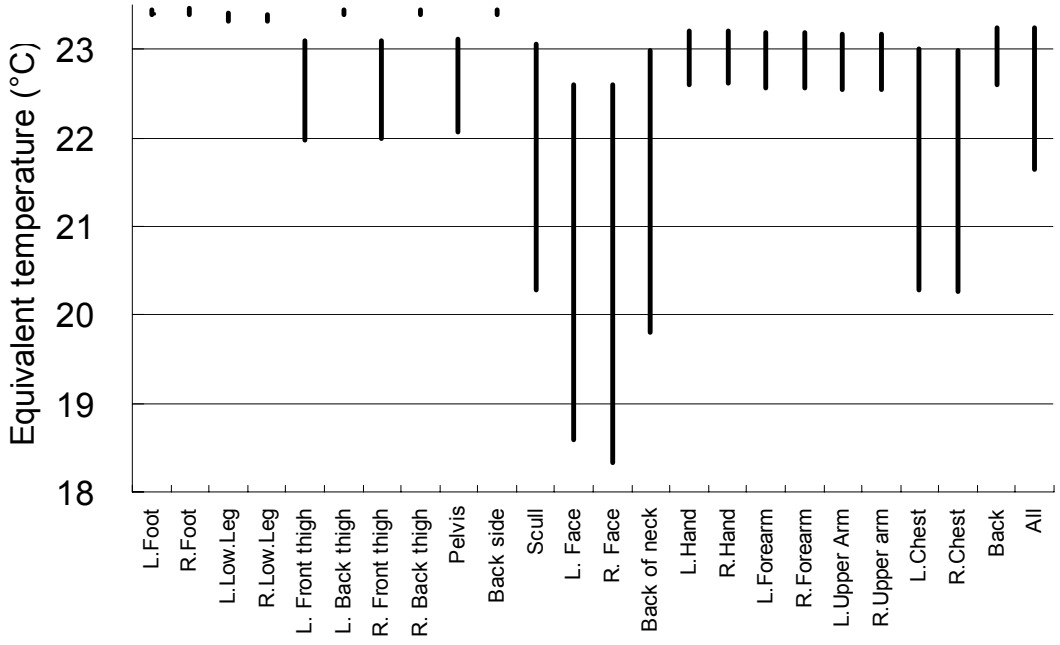

Figure 4.16b Ranges of the segmented and whole-body equivalent temperature tested at room air temperature of 23.5°C and personalized air temperature 23.5°C. Each line end indicates the highest and lowest of equivalent temperature

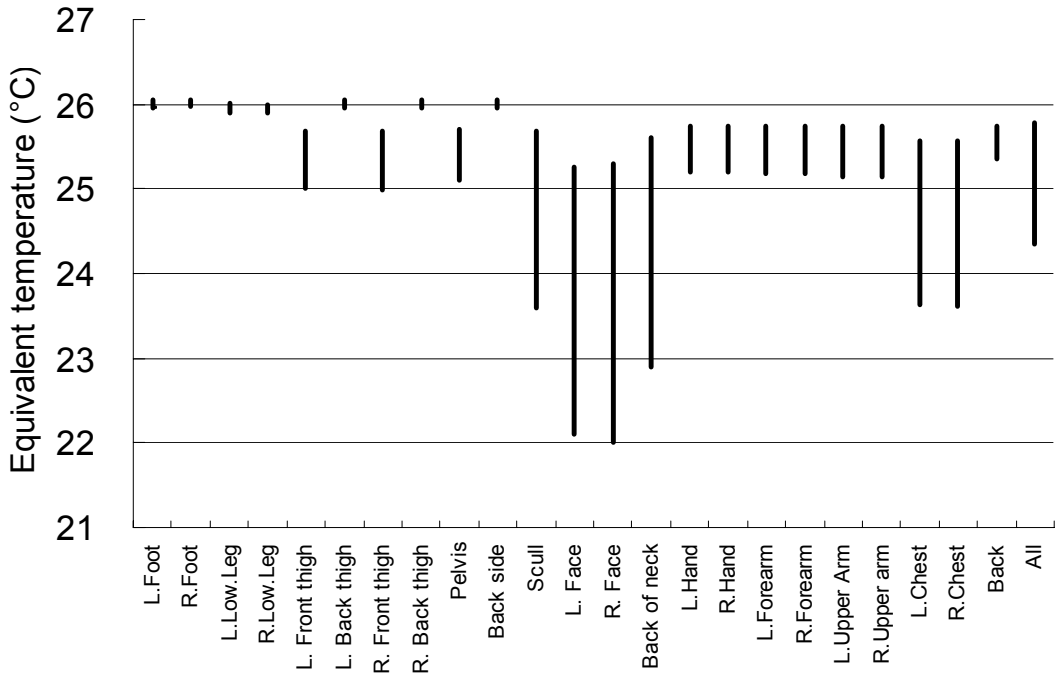

Figure 4.16c Ranges of the segmented and whole-body equivalent temperature tested at room air temperature of 26°C and personalized air temperature 23.5°C. Each line end indicates the highest and lowest of equivalent temperature

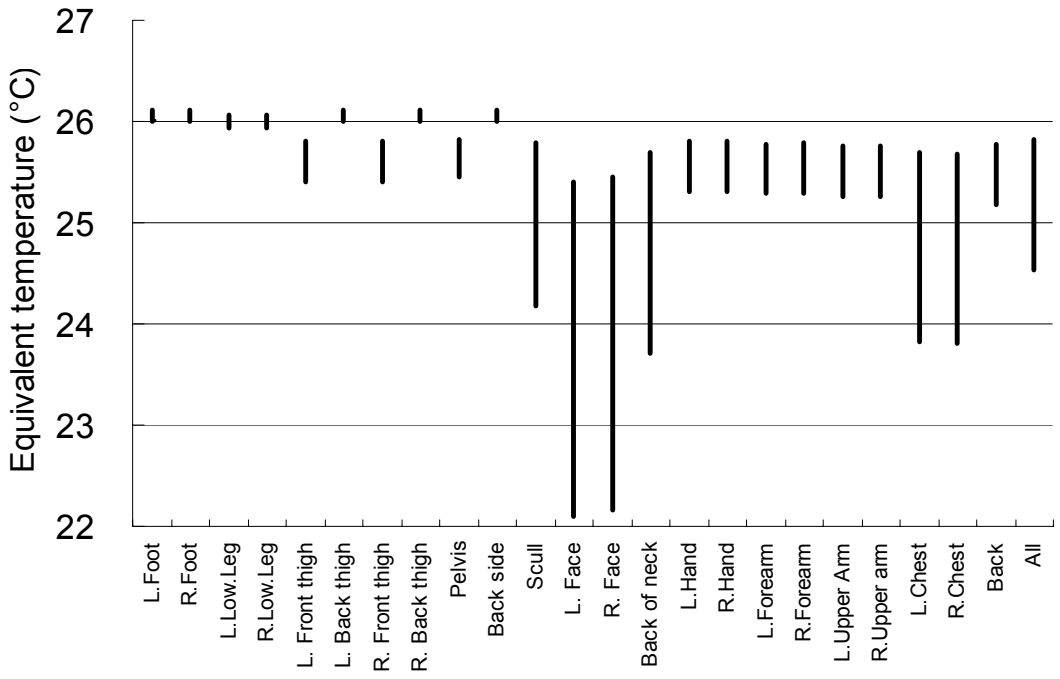

Figure 4.16d Ranges of the segmented and whole-body equivalent temperature tested at room air temperature of 26°C and personalized air temperature 26°C. Each line end indicates the highest and lowest of equivalent temperature

Because of obvious cooling effects of the face and the chest, six body segments are selected for further analysis, including the scull, the left face, the right face, the back of neck, the left chest and the right chest. The results from the analyses of the results for these body segments are shown in Figures 4.17 and 4.18. The decrease of the equivalent temperature in comparison with the reference case without personalized airflow is shown in the figures. The results in the figures reveal that the influence of the PV airflow rate is not striking when it is lower than 8 L/s. This influence becomes obvious when PV airflow rate is greater than 12 L/s especially at personalized air temperature of 21°C. The ranges of the equivalent temperature determined for the selected six body segments at the four temperature combinations studied when the personalized airflow changed from 4 l/s to 16 l/s are shown in Figure 4.19. Figure 4.20 shows the ranges of equivalent temperature obtained for the 4, 8, 12 and 16 l/s at the studied temperature combinations. The left face and the right face are the two body segments cooled mostly when the airflow increased from 4 l/s to 16 l/s. At 26°C, the equivalent temperature for the left and right face decreased by 4°C when the airflow rate increased and by 5°C to 6°C at 23.5°C room air temperature (Figure 4.19). The cooling effect of the increased airflow rate on the remaining four body segments is about 2°C at 26°C room air temperature and 3°C to 4°C at 23.5°C room air temperature. The influence of the PV airflow rate on the equivalent temperature becomes obvious when PV airflow rate is greater than 12 L/s (Figure 4.20). The decrease in the equivalent temperature is largest when the PV airflow rate changes from 12 L/s to 16 L/s, i.e. the penetration effect of the personalized air over thermal

plume felt at 8 L/s increases with the increase of the airflow rate and causes more cooling of the body.

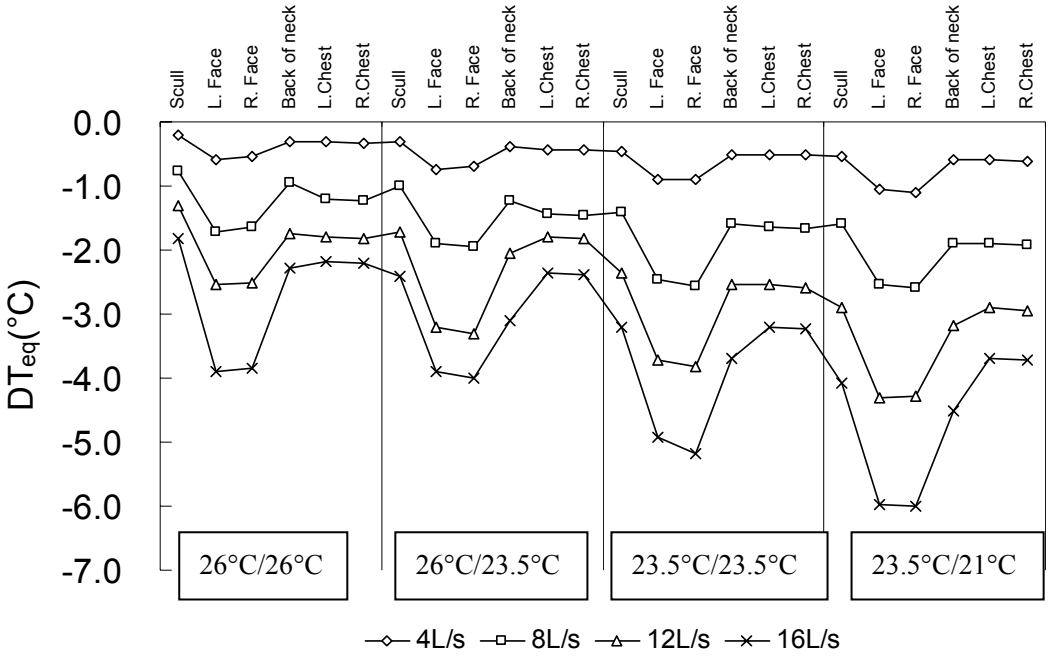

Figure 4.17 Cooling effect analysis under different personalized airflow rates for six body segments.

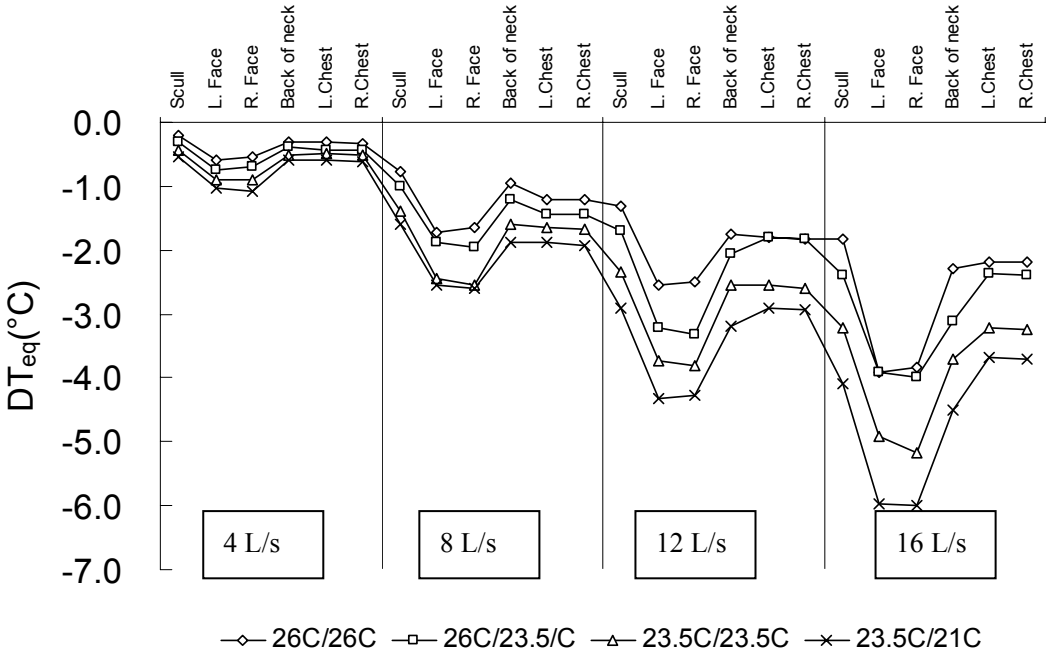

Figure 4.18 Cooling effect analysis under different ambient/PV temperature combinations for six body segments.

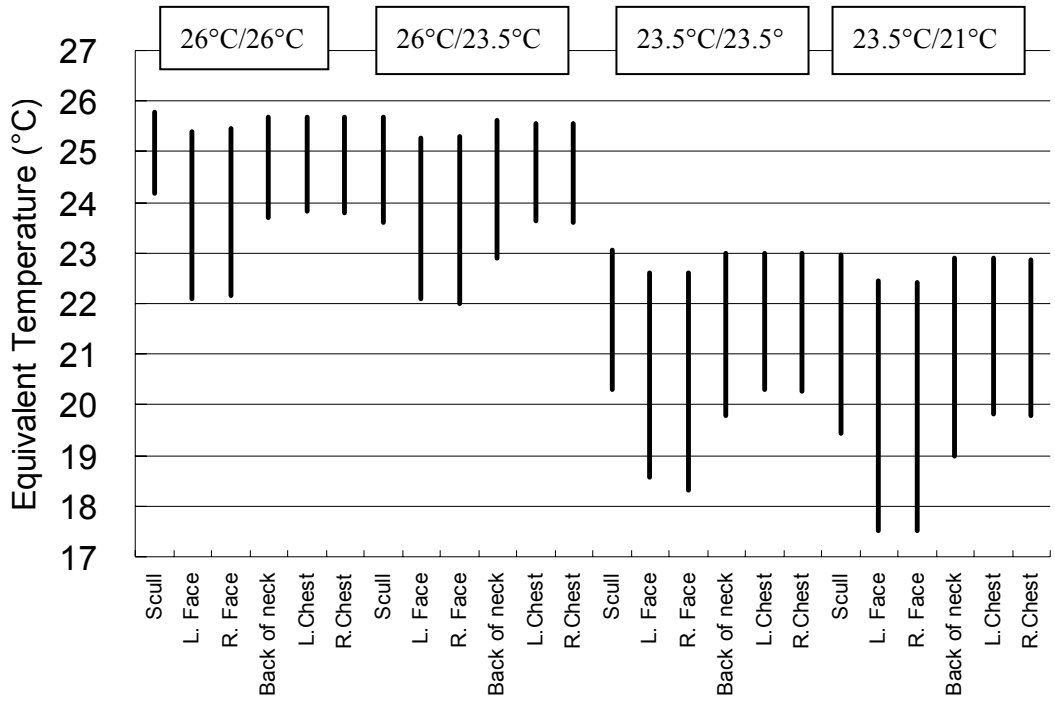

Figure 4.19 Ranges of segmented equivalent temperature determined at four PV/Ambient temperature combinations when PV airflow rate was changed from 4 l/s to 16 l/s for six body segments. Each line end indicates the highest and lowest of equivalent temperature

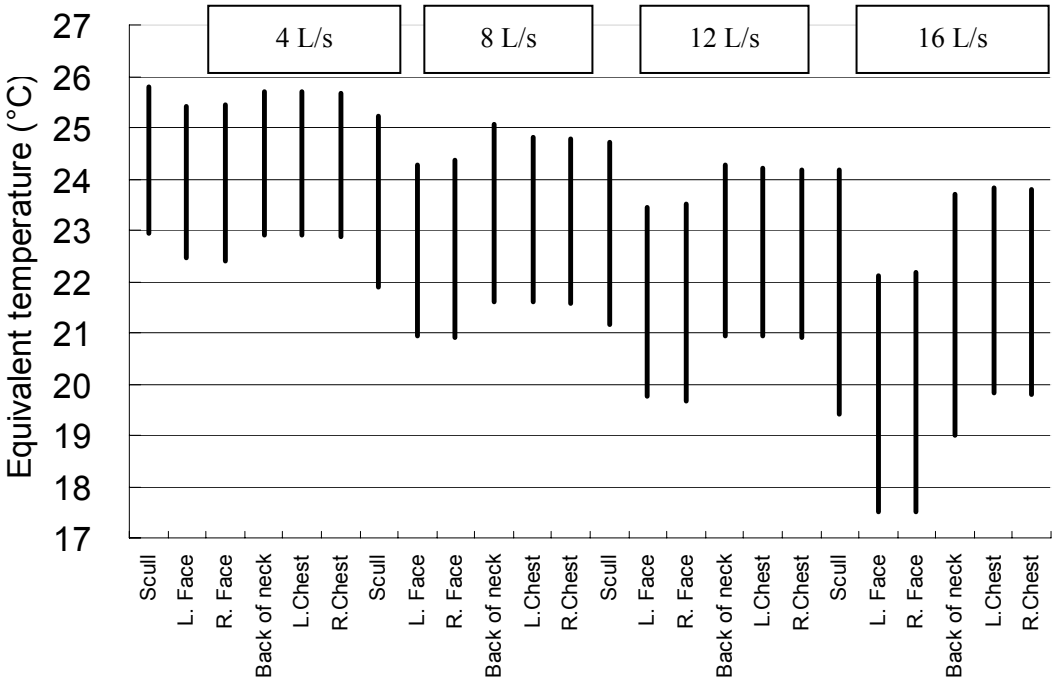

Figure 4.20 Ranges of segmented equivalent temperature determined at four PV airflow rates under four different PV/Ambient temperature combinations for six body segments. Each line end indicates the highest and lowest of equivalent temperature

The impact of the body position with regard to the personalized flow on its cooling effect was studied under all experimental conditions. The cooling effect, i.e. ΔT_{eq}, at personalized flow rate of 16 L/s and different temperature combinations is shown in Figure 4.21. At this highest flow rate, the asymmetrical cooling effect of the body is strongest. The trends of other personalized airflow rates are same as that under 16 L/s personalized airflow rate. For the cases introducing the movement of manikin forward or backward, cooling effect of corresponding body segments moving outside the personalized flow is reduced. As expected for the cases of moving the manikin sideward, obvious asymmetry for cooling effect is observed in the following body segments: face, hand, forearm, upper arm and chest. For whole-body cooling effect, the case of moving the manikin forward is the worst case because lower body part is moved far away from the jet target area. Cooling effect under 23.5°C/23.5°C temperature combination and different personalized airflow rates is shown in Figure 4.22. The asymmetry in the local cooling of the body is enforced when personalized airflow rates changed from 4L/s to 16 L/s.

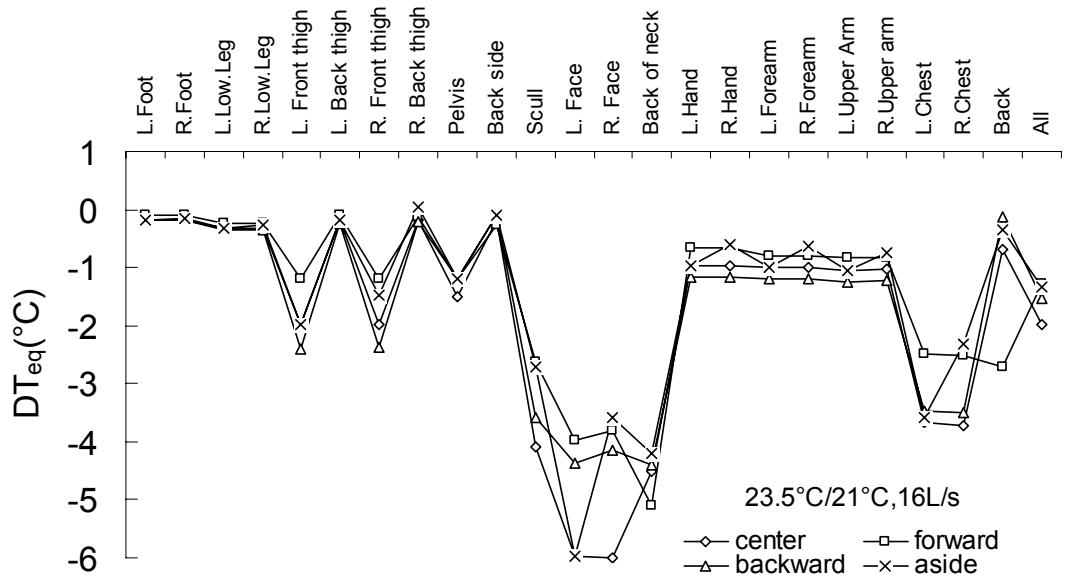

Figure 4.21a Occupant movement analysis under different moving directions. at 16 L/s personalized airflow rate and 23.5°C/21°C temperature combinations

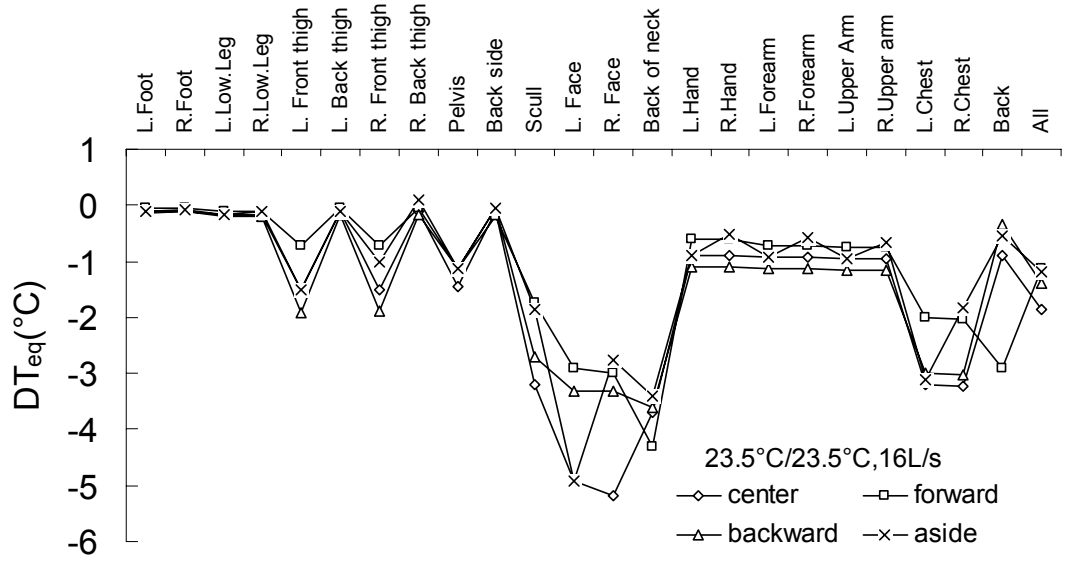

Figure 4.21b Occupant movement analysis under different moving directions. at 16 L/s personalized airflow rate and 23.5°C/23.5°C temperature combinations

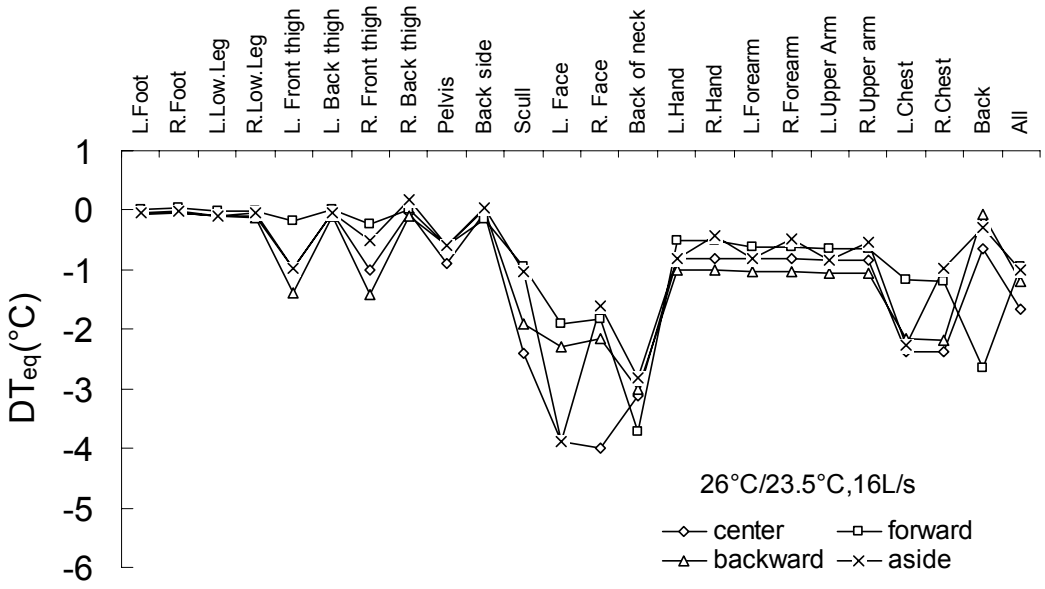

Figure 4.21c Occupant movement analysis under different moving directions. at 16 L/s personalized airflow rate and 26°C/23.5°C temperature combinations

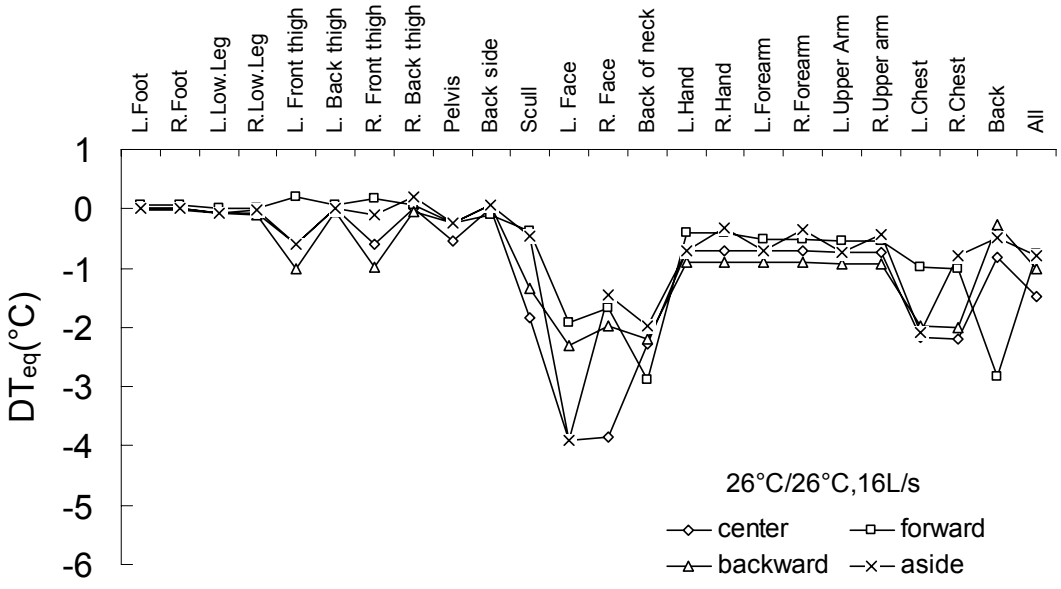

Figure 4.21d Occupant movement analysis under different moving directions. at 16 L/s personalized airflow rate and 26°C/26°C temperature combinations

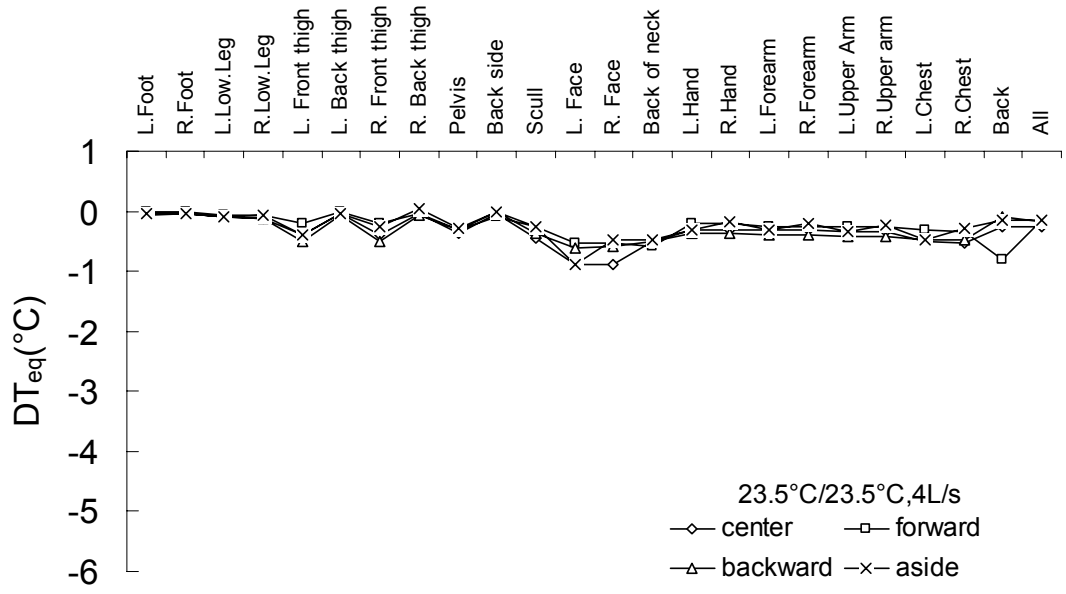

Figure 4.22a Occupant movement analysis under different moving directions. at 4 L/s personalized airflow rate and 23.5°C/23.5°C temperature combinations

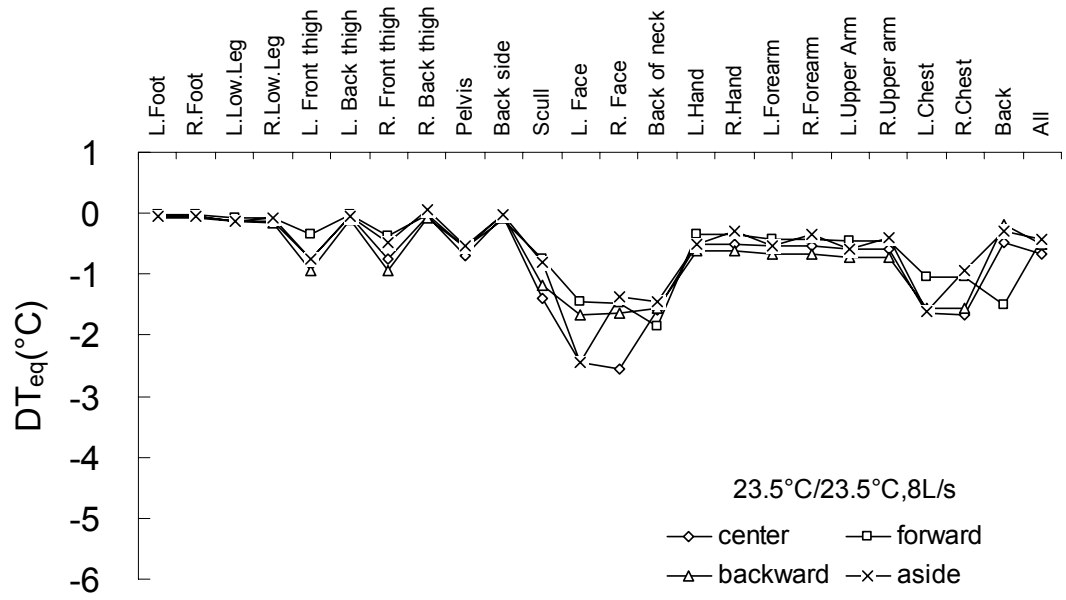

Figure 4.22b Occupant movement analysis under different moving directions. at 8 L/s personalized airflow rate and 23.5°C/23.5°C temperature combinations

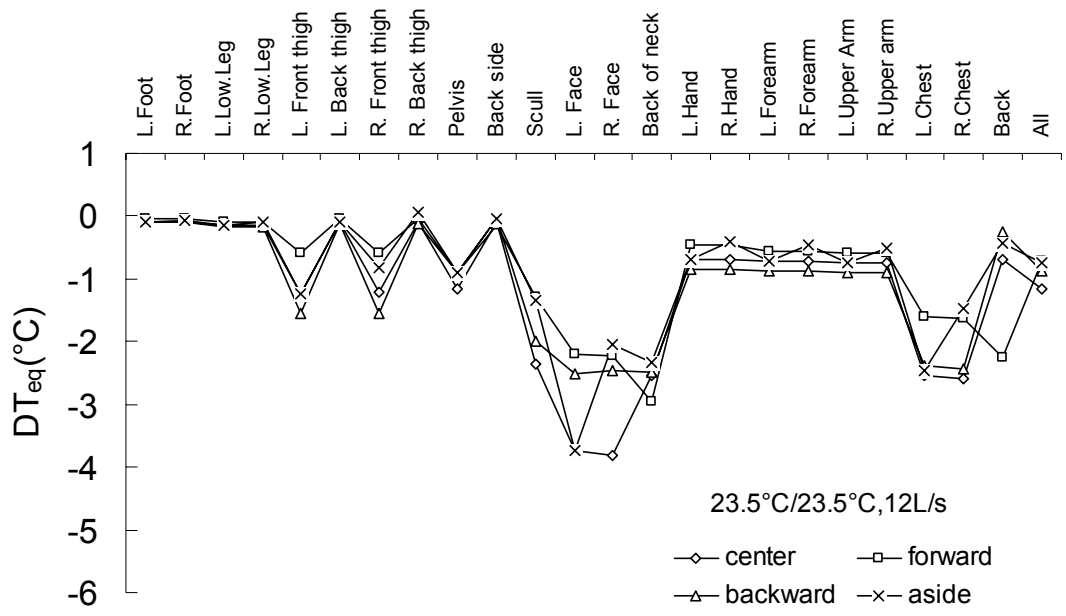

Figure 4.22c Occupant movement analysis under different moving directions. at 12 L/s personalized airflow rate and 23.5°C/23.5°C temperature combinations

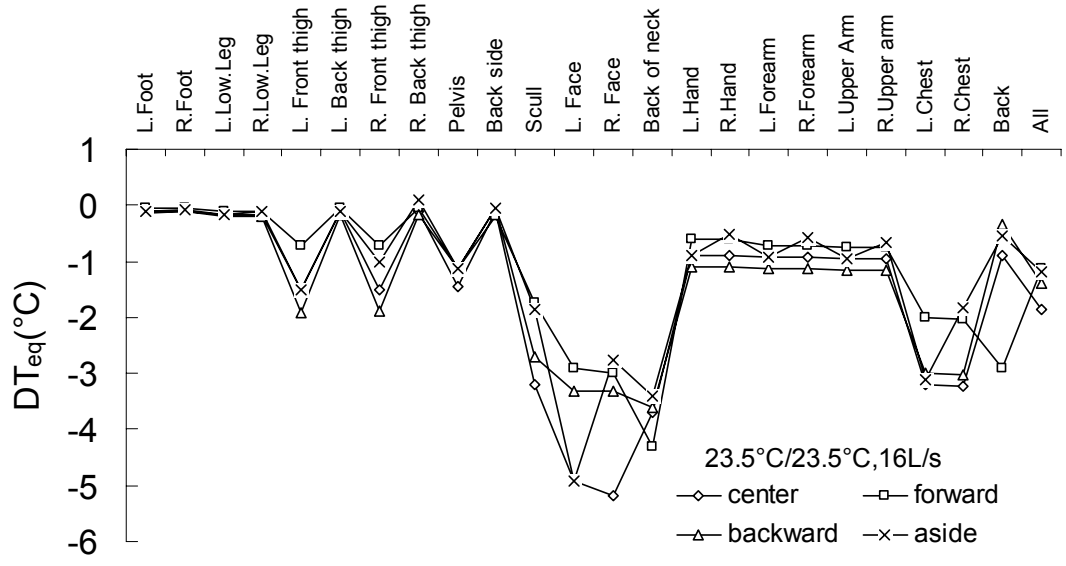

Figure 4.22d Occupant movement analysis under different moving directions. at 16 L/s personalized airflow rate and 23.5°C/23.5°C temperature combinations

4.5.3 Inhaled Air Quality

The personal exposure effectives, used to assess the percentage of personalized air in the inhaled air, is plotted against personalized air flow rate under experimental conditions of 23.5°C/21°C and 23.5°C/23.5°C in Figure 4.23. Under both isothermal and non-isothermal conditions, the personal exposure effectiveness increases with the increase of air flow rate. The curves keep increasing with the increase of the flow rate, indicating that the impact of increasing PV flow rate on elevating the percentage of personalized air in the inhaled air is important.

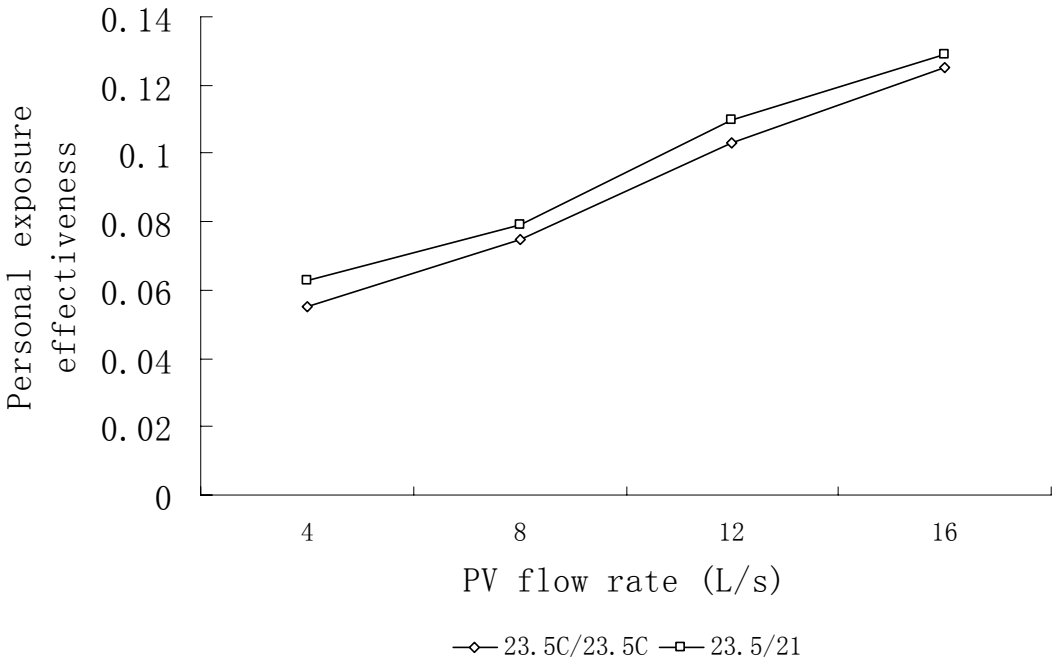

Figure 4.23 Personal exposure effectiveness as a function of personalized air flow rate (23.5°C/23.5°C and 23.5°C/21°C)

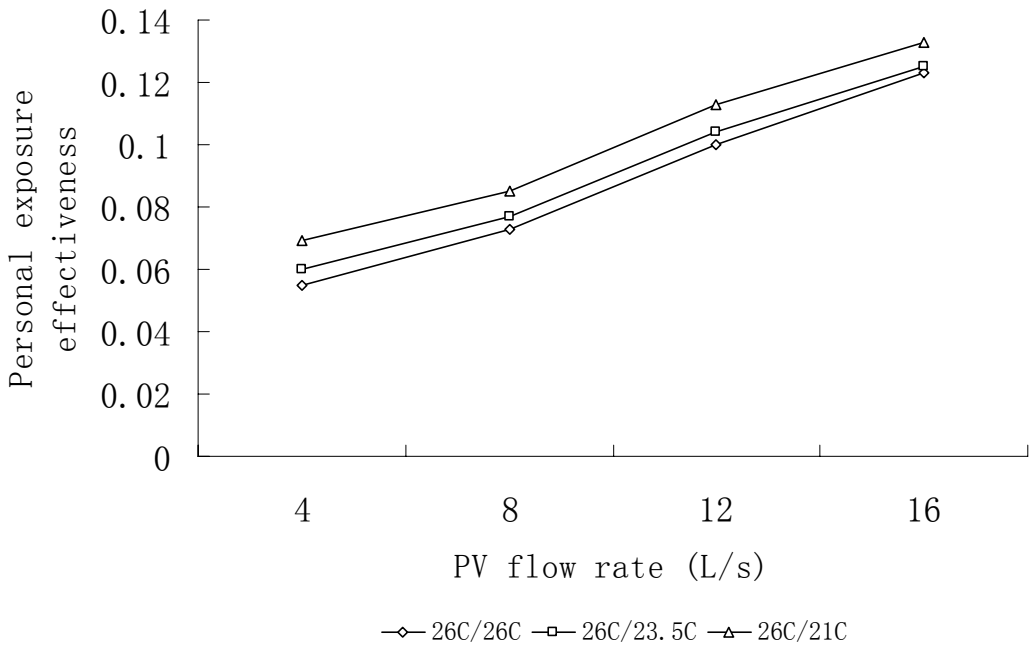

Figure 4.24 Personal exposure effectiveness as a function of personalized air flow rate (26°C/26°C, 26°C/23.5°C and 26°C/21°C)

The personal exposure effectiveness curves under conditions of 26°C/26°C, 26°C/23.5°C and 26°C/21°C (Figure 4.24) followed the same trends as their counterparts under 23.5°C/23.5°C and 23.5°C/21°C.

The results in Figures 4.23 and 4.24 indicate that the personal exposure index increases when the difference between the room temperature and personalized air temperature increases, i.e. as cooler the personalized air than the room air is as higher the portion of the clean air in inhalation is. However the differences are not large for the studied temperature combinations.

Compared with totally mixing ventilation which has 0 value for PEE, ceiling mounted PV system can increase the amount of the clean personalized air from 6% to 12% when PV flow rate increases.

4.5.4 Inhaled Air Temperature

The inhaled air temperature is measured simultaneously with the tracer gas measurements. Inhaled air temperature under both isothermal and non-isothermal conditions when ambient air temperature is 23.5°C is plotted against personalized air flow rate, as shown in Figure 4.25. The inhaled air temperature when the manikin is exposed to the reference condition (without PV) at ambient air temperature of 23.5°C is approximately 26.6°C, i.e. much higher than the ambient temperature. This is because an upward free convection flow of warm air exists around the human body (Homma and Yakiyama, 1988; Melikov and Zhou, 1996). A large portion of the manikin's inhaled air is from the free convection flow, which has a higher temperature than the ambient air.

It is to be noted that, compared to the free convection flow, the exhalation of manikin, had very little influence on the inhaled air temperature. The reason is because the two independent air jets emerging from the nostrils have sufficiently high velocities so that they could penetrate the free convection flow boundary around the human body and spread away from the face. Consequently, very little exhaled air would be re-inhaled by the manikin in next breathing cycle. According to study by Cermak and Majer (2000), exhalation through nostrils and inhalation through mouth, the maximum amount of re-inhaled air in inhaled air is found to be lower than 1%. It is also found by Hyldgard (1994) that the exhalation formed one (from mouth) or two

(from nostrils) jets penetrating the boundary layer locally and no short circuiting took place between the exhalation and inhalation at usual conditions. That is the reason why breathing mode is not used.

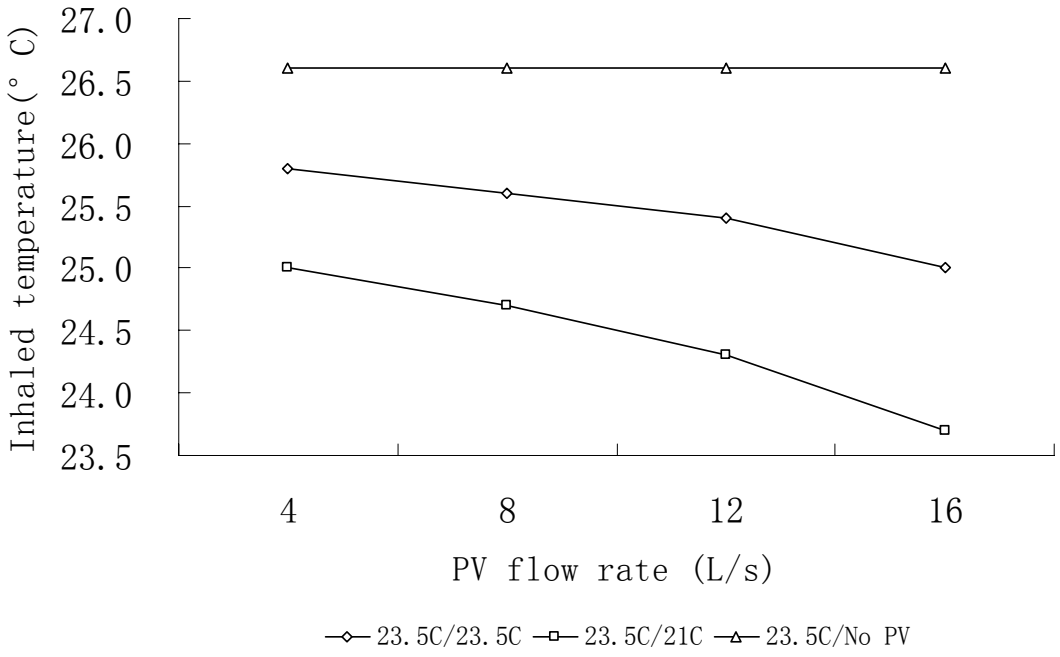

Figure 4.25 Inhaled air temperature as a function of personalized air flow rate (23.5°C /23.5°C, 23.5°C /21°C and 23.5°C /No PV)

In the present experiments the airflow pattern in the inhalation zone became more complicated because of downward personalized air supplied from ceiling mounted PV ATD directed towards manikin's head. Thus, the inhaled air temperature is affected by the interaction of the downward personalized air flow with the upward free convection flow. Under both non-isothermal and isothermal conditions, the decrease of inhaled air temperature becomes quick with the increase of the personalized air flow rate. At flow rate level of 16L/s, the inhaled temperature is 23.7°C for non-isothermal case (23.5°C/21°C), approximately 2.9°C lower than that under

reference condition, and 25°C for isothermal case (23.5°C/23.5°C), approximately 1.6°C lower than that under reference condition. This is because the downward cool personalized air at higher flow rates is strong enough to offset the warmer free convection flow layer and reached the manikin's inhalation zone.

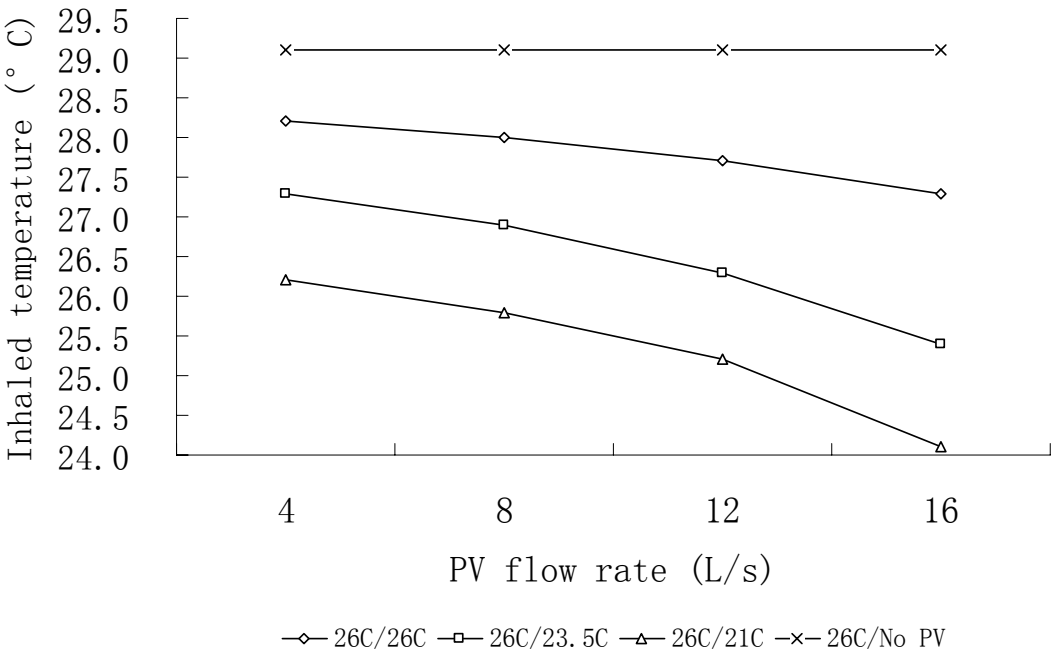

Figure 4.26 Inhaled air temperature as a function of personalized air flow rate (26°C /26°C, 26°C /23.5°C, 26°C /21°C and 26°C /No PV)

Inhaled air temperature under both isothermal and non-isothermal conditions when ambient air temperature is 26°C is plotted against personalized air flow rate, as shown in Figure 4.26. Under both non-isothermal and isothermal conditions, the decrease of inhaled air temperature becomes quick with the increase of the personalized air flow rate. At flow rate level of 16L/s, the inhaled temperature is 24.1°C for non-isothermal case (26°C/21°C), approximately 5°C lower than that under reference condition, and

27.3°C for isothermal case (26°C/26°C), approximately 1.8°C lower than that under reference condition. It should be noted that during the reference measurements the PV was not used but the clean and cool personalized air was mixed with the background air supplied to the room.

4.6 Discussion

The airflow rate and the temperature of the personalized air and the ambient air temperature influence the cooling effect of the jet from the ceiling mounted nozzle. For the ranges of these three parameters studied, the personalized airflow rate is the most important factor which influences the equivalent temperature, i.e. the heat loss from the manikins' body. The cooling of the body segments is strongly asymmetrical, i.e. the head (scull, left/right face, back of neck) and left/right chest are the most cooled body segments. For example, the equivalent temperature at the face decreases from 3°C to 5°C in comparison with the reference condition without personalized airflow when personalized airflow rate changes from 4L/s to 16 L/s. For the face segment, the equivalent temperature decreases by 0.5°C when the personalized airflow increases by 1 L/s under the temperature conditions 23.5°C/21°C (ambient temperature/PV temperature). The equivalent temperature decreases by 0.3°C when PV temperature decreases by 1°C at 16 L/s personalized airflow rates and 23.5°C room air temperature. Similarly, decrease in the equivalent temperature is obtained when at 16 L/s and 23.5°C PV temperature the room temperature decreases by 1°C. The whole body cooling is much less affected by the change of the airflow rate than

the cooling of the segments directly exposed to the personalized flow. The feet, lower legs, back thighs and the back side of the manikin's body are almost not cooled (ΔT_{eq} < 0.2°C) and the hands, forearms, upper arms and back are cooled only slightly (ΔT_{eq} <0.5°C) by the personalized airflow. The large asymmetry identified in the body cooling suggests that in practice the maximum cooling of individually controlled personalized air flow from ceiling mounted nozzles will be limited due to the risk of local thermal discomfort for the occupants.

Due to the positioning of the air supply nozzles far from the occupant, the cooling effect of ceiling mounted personalized ventilation system is lower than the cooling effect of desk mounted PV system. For example, the manikin based equivalent temperature obtained for the face with desk mounted PV at 23.5°C/21°C with personalized flow rate of 16 L/s as reported by Gong et al. (2006) is 4°C lower than the equivalent temperature obtained in this study with ceiling mounted nozzle.

The pressure exercised by the personalized airflow locally on the body (mainly the top of the head), will be another factor which will influence the human response to the vertically applied personalized airflow and thus the performance of personalized ventilation with ceiling mounted nozzles in practice. The results suggest that individual control of the personalized airflow rate is essential in practice for compensating the large differences which exist between people with regard to preferred thermal sensation and air movement. Individual control of personalized

airflow rate should also be considered as an important factor in the design of ceiling mounted personalized ventilation nozzles.

People, while performing work at their desks, will typically move their body and this will affect the interaction of the thermal plume above the body with the personalized airflow from the ceiling. The asymmetrical cooling effect of the body increased when personalized airflow rate increased. For the cases introducing the movement of manikin forward or backward, cooling effect of corresponding body segments moving outside the personalized airflow is reduced. As expected, for the cases of moving the manikin sideward, obvious asymmetry for cooling effect is observed in the following body segments: face, hand, forearm, upper arm and chest.

For energy conservation purpose, supplying warmer personalized air is better than supplying cooler personalized air so as to obtain the same cooling effect. The largest equivalent temperature differences obtained for different body segments change from -1°C to -6°C under 23.5°C/21°C temperature combination when personalized airflow rates increase from 4 L/s to 16 L/s. 23.5°C/21°C temperature combination is the case which can achieve highest cooling asymmetry among the 4 temperature combinations. 16 L/s personalized airflow rate, which can destroy thermal plume completely, is suggested as maximum airflow rate acceptable to people.

Compared with totally mixing ventilation which has 0 value for PEE, ceiling mounted

PV system can increase the mount of the clean personalized air from 6% to 12% when PV flow rate increases. By decreasing inhaled air temperature, perceived air quality will become much better with ceiling mounted PV than without it. This phenomenon has been demonstrated in previous study (Fang et. al., 1998). Furthermore, elevated personalized air movement velocity will offset the negative effect of air temperature and humidity on perceived air quality, which will save energy for dehumidification especially for the tropics with high humidity (Melikov et. al., 2008).

4.7 Conclusions of Objective Measurements

The most important conclusions of the objective measurements are:

a. The blocking effect of unheated manikin on the personalized airflow supplied from above is observed up to 0.2 m above manikin's head and is not affected by the personalized airflow rate. The centerline velocity is reduced by 85%.

b. The neutral level obtained with heated manikin increases from 0.8 m to 1.1 m with the increase of the airflow rate.

c. Under the set-up used in the present study (nozzle diameter 0.095m and distance between the nozzle and the manikin's head of 1.3 m) the personalized airflow at 16 l/s is strong enough to destroy the thermal plume from the manikin and to efficiently provide cooling to manikin's body.

d. The scull, the left/right face and the back of neck are the body segments most cooled by the personalized airflow. The cooling effect increased with the increase of the personalized airflow rate and the decrease of the room and personalized air temperature. The maximum cooling of the left/right face is comparable with the cooling effect caused by 6°C decrease of the room air temperature without personalized airflow. The cooling effect of the personalized airflow on the whole body is smaller.

e. The influence of personalized air temperature on equivalent temperature at the face becomes striking when room air temperature becomes low. The equivalent temperature at the face is also affected by room air temperature. Personalized airflow rate is the most important factor which influences the equivalent temperature most.

f. For the ranges of change of these three parameters studied, the personalized airflow rate is the most important factor which influences the equivalent temperature, i.e. the heat loss from manikins' body.

g. Obvious asymmetry for cooling effect is observed when manikin is moved forward, backward and sideward. The whole-body cooling effect of the personalized airflow is minimal when the manikin is moved forward and its lower body part remain out of the jet.

h. Under both isothermal and non-isothermal conditions, personal exposure effectiveness increases with the increase of air flow rate. Personal exposure effectiveness under non-isothermal condition is slightly higher than that in isothermal condition.

i. Inhaled air temperature is affected by the interaction of the downward personalized air flow with the upward free convection flow. Under both non-isothermal and isothermal conditions, the decrease of inhaled air temperature becomes quick with the increase of the personalized air flow rate. Compared with totally mixing ventilation which has 0 value for PEE, ceiling mounted PV system can increase the amount of the clean personalized air from 6% to 12% when PV flow rate increases. Lower inhaled air temperature will also improve the perceived air quality.

Chapter 5: Human response studies of ceiling mounted PV system -- subjective assessments

5.1 Objectives

The objectives of this part of the study was to evaluate human response to the ceiling mounted PV ATD with regard to local and whole body thermal sensation and its acceptability, thermal comfort, air movement perception, acceptability and preference. An important aim of the study was to identify relationship within and between these responses.

The outline of research methodology for subjective assessments is as follows.

- Experimental Facilities
- Experimental Conditions
- Subject Selection
- Questionnaire Design
- Experimental Procedure

5.2 Experimental Design

In order to examine human perception in an unbiased manner, experimental design was considered carefully. The consideration included selection of experimental conditions, subject selection, questionnaire design and design of experimental procedure.

5.2.1 Experimental Facilities

The experiments were conducted in the Field Environmental Chamber (FEC) already described in detail in Chapter 3 of this report.

5.2.2 Experimental Conditions

The personalized air parameters were controlled at the ATD outlet. The experimental conditions were identical with the experimental conditions of the objective study (Chapter 4). Based on the results of the objective measurements, elevated air velocities by higher airflow rates were selected so as to achieving velocity in breathing zone up to 1 m/s. Personalized air temperature of 21°C, 23.5°C and 26 °C at ATD outlet were adopted with ambient temperature of 23.5°C and 26 °C (Table 5.1). In the chamber, 16 workstations were divided into 4 groups, with 4 workstations in each group. The ceiling mounted ATD at each of the 4 workstations was different, respectively 4, 8, 12, 16 L/s respectively. Thus 4 subjects who participated in the same time in the experiments could choose a workstation with any of the flow rates.

Table 5.1 Experimental conditions for subjective assessments

Room Temperature T_a(°C)	26			23.5	
PV Outlet Temperature T_{outlet}(°C)	21	23.5	26	21	23.5
PV Outlet Flow rate Q_{outlet}(L/s)	4,8,12,16				
PV Outlet Velocity V_{outlet}(m/s)	0.565,1.13,1.695,2.26				

5.2.3 Subject Selection

Thirty-two subjects, 16 males and 16 females, participated in the experiments in 8 separate groups of four. The reason for this arrangement was that each group member

could choose to be exposed to four different PV airflow rates from low to high so as to simulate individual control of the personalized flow (5.2.4). All the subjects were healthy, without chronic disease or allergy and were non-smokers. The subjects were instructed to eat normally before attending the experiments and not to drink alcohol and take drugs 24 hours before the experiment. They were also asked to wear normal attire for office working. The anthropometric data of the 32 subjects is shown in Table 5.2.

Table 5.2 Anthropometric data for the subjects

Sex	No. of subjects	Age(years)	Height (m)	Weight (kg)	Skin Area* (m^2)
Females	16	20.6±1.0	1.74±0.06	63.8±8.0	1.77±0.12
Males	16	22.6±1.5	1.60±0.05	48.4±5.8	1.48±0.09
Females and Males	32	21.6±1.6	1.67±0.09	56.1±10.4	1.63±0.18

* In the thesis, skin area is calculated from Dubois-area $A_{Du}=0.203W^{0.425}H^{0.725}$

5.2.4 Questionnaire Design

Three computer-administered questionnaires were used in the experiments of subjective assessment. Questionnaire 1 included questions regarding thermal sensation, air movement perception, air movement acceptability and preference. Questionnaire 2 included questions regarding thermal comfort, perceived air quality and the feeling of environment. Questionnaire 3 included questions about subjects' attire. All these questions can be referred in Appendix 4.

a. Questionnaire 1

ASHRAE 7-point scale (ASHRAE, 2004) was used to evaluate thermal sensation for

the whole body and for the various body parts: +3 Hot; +2 Warm; +1 Slightly warm; 0 Neutral; -1 Slightly cool; -2 Cool; -3 Cold. In the questionnaire, a diagram of a human body with each body segments clearly demarcated was used to indicate the thermal sensation of each body segments. Thermal sensation of the whole-body was also solicited.

Subjects were also asked whether they felt any air movement at any body segment. If they felt, they were required to assess the air movement. The perception of air movement at each body segment was evaluated on the same diagram of human body: +3 Much too air movement; +2 Too breezy; +1 Slightly breezy; 0 Just right; -1 Slightly still; -2 Too still; -3 Much too still.

Subjects were asked to assess their acceptability for air movement at top of the head, face, neck, chest, shoulder, upper arm, lower arm, hands; back, and lower body. The end-points of the linear visual scales were coded as -1 (very unacceptable) and 1 (very acceptable), with an interval in between at -0 (just unacceptable) and +0 (just acceptable) for assessment of air movement acceptability (Figure 5.1).

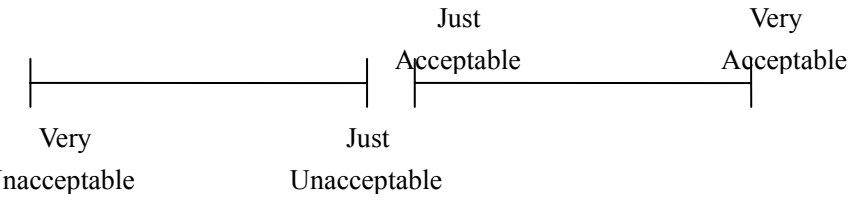

Figure 5.1 Linear visual analogue scales with intervals for assessment of air movement acceptability

Subjects were also asked to indicate their preferred change for air movement at different body parts. They were provided with three options: less air movement, no change, more air movement (Figure 5.2).

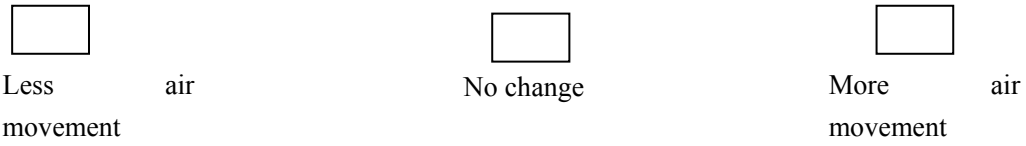

Figure 5.2 three options for assessment of air movement preference

b. Questionnaire 2

In questionnaire 2, the questions were about thermal comfort, inhaled air quality, inhaled air temperature, inhaled air humidity, odor of inhaled air, freshness of inhaled air and feeling of indoor environment. For the questions about thermal comfort and perceived air quality, the same linear visual analogue scales with intervals were used. The linear visual analogue scales without intervals in between were used for other questions including perceived inhaled air temperature (cold -3 to hot +3), humidity (humid 0 to dry 100), odor of inhaled air (no odor 0 to overwhelming odor 100), and freshness of inhaled air (air stuffy 0 to air fresh 100). The questions of feeling of the environment were all coded from 0 to 100.

c. Questionnaire 3

In questionnaire 3, the types of attire were listed for subjects to select. During the experiments, all attire were illustrated by pictures in aiding subjects to choose. In the data analysis, the clothing information was then converted into clothing thermal

insulation (in Clo).

5.2.5 Experimental Procedure

One week before the formal experiments, all subjects visited the FEC and attended a briefing session so they could become familiar with the operation of computer-administered questionnaire system and the experimental procedures.

Both 16 male and 16 female subjects were divided into eight groups randomly with 4 members in each group, 2 male and 2 female subjects. The subjects reported 15 minutes before the start of the experiment in an air-conditioned corridor where temperature differed only slightly from the temperature in the control room and the experimental chamber. Thereafter, subjects were required to acclimatize for 30 minutes in the control room, which was maintained at the same ambient temperature as the experimental chamber (Figure 5.3). During their stay in the control room, the subjects were allowed to change their attires in order to achieve thermally neutral status. After that, subjects entered the experimental chamber and were not allowed to change their attire during the following two-hour-exposure. At the beginning of the exposure in the experimental chamber, the subjects were asked to fill in questionnaire regarding their attire and anthropometric information (Table 5.2). The clothing insulation was around 0.7 clo and was almost the same for males and females with small individual differences during the exposures. Each group member could choose one of 4 workstations with different PV airflow rates (4, 8, 12, and 16 L /s) based on

their preference. This provided the subjects with some degree of "individual control" of PV airflow rates. They were exposed to the PV flow for 15 minutes. The subjects could then either move to adjacent workstation or keep staying in the same workstation, which was based on their air movement preference. The subjects had the possibility of changing workstation four times during the first hour (after each 15 minutes' exposures). The subjects were encouraged to use the workstations with different PV airflow rates in order to be able to move at the end of the 1 hour exposure to the workstation with most preferred air movement. The subjects, depending on their preference were or were not exposed to all four PV airflow rates. The actual PV airflow rates were blind to the subjects. They were only told about the varying trend (increasing PV air flow in a particular direction) which would aid them to move in the correct direction based on their air movement preference. At the end of the first hour, the subjects were asked to move to a workstation which they had not visited and to stay there for 30 minutes. This session, called make-up session, aimed to verify that the subjects really did not prefer the conditions at the workstation. For the subjects who had visited 3 workstations during the first hour, they were asked to choose the one they had not visited during the first hour. For the subjects who had visited only 1 or 2 workstations during the first hour, they could choose any other workstations they had not visited during first hour. After that, the subjects could make their final choice of the workstation with the most preferred PV airflow rate. The subjects who had visited all 4 workstations during the first hour were allowed to stay in their preferred workstation. During the last 30 min of the experiment the subjects

stayed 30 min at the workstation with the most preferred environment. This concluded the experiment for the particular subject. Subjects were asked to complete questionnaires regarding their thermal sensation, thermal comfort, air movement sensation and preference, inhaled air quality, inhaled air temperature and feeling of indoor environment six times, i.e. after each of the first 15 min exposures and after the following two exposures of 30 min (Table 5.4). The subjects in the eight groups followed exactly the same experimental procedure (Table 5.3). Every subject participated in five experiments. Thus he/she was exposed to five different ambient/PV temperature combinations. The exposure of the subjects to the different temperature combinations was randomized and completely blind.

Before the formal experiments, the PV air parameters of air velocity, temperature and room parameter of room temperature were set and they were controlled during the experiment by Building Automation System (BAS). Room air relative humidity was not controlled but recorded by HOBO meters.

Figure 5.3 Subjects in the control room (left) and in the FEC.

Table 5.3 Sequence of experiment and respective timings that each group attended

		Air-conditioned area	Control room	Chamber room					
				stochastic choice	second choice	third choice	fourth choice	make-up choice	final choice
Group A	Day 1	07:15-07:30	07:30-08:00	08:00-08:15	08:15-08:30	08:30-08:45	08:45-09:00	09:00-09:30	09:30-10:00
Group B	Day 1	09:15-09:30	09:30-10:00	10:00-10:15	10:15-10:30	10:30-10:45	10:45-11:00	11:00-11:30	11:30-12:00
Group C	Day 1	12:15-12:30	12:30-13:00	13:00-13:15	13:15-13:30	13:30-13:45	13:45-14:00	14:00-14:30	14:30-15:00
Group D	Day 1	14:15-14:30	14:30-15:00	15:00-15:15	15:15-15:30	15:30-15:45	15:45-16:00	16:00-16:30	16:30-17:00
Group E	Day 2	07:15-07:30	07:30-08:00	08:00-08:15	08:15-08:30	08:30-08:45	08:45-09:00	09:00-09:30	09:30-10:00
Group F	Day 2	09:15-09:30	09:30-10:00	10:00-10:15	10:15-10:30	10:30-10:45	10:45-11:00	11:00-11:30	11:30-12:00
Group G	Day 2	12:15-12:30	12:30-13:00	13:00-13:15	13:15-13:30	13:30-13:45	13:45-14:00	14:00-14:30	14:30-15:00
Group H	Day 2	14:15-14:30	14:30-15:00	15:00-15:15	15:15-15:30	15:30-15:45	15:45-16:00	16:00-16:30	16:30-17:00

Table 5.4 Questionnaires to be answered during the course of experiments corresponding to the time scale in Table 5.3 (Questionnaires can be referred in Appendix 2, human subjects keep staying in control room without filling in the questionnaires before 30 minutes)

Time (mins)	30	45	60	75	90	120	150
Questionnaire 1		√	√	√	√	√	√
Questionnaire 2		√	√	√	√	√	√
Questionnaire 3	√						

5.3 Human Perception Analysis

The impact of the airflow rate and the studied temperature combinations on subjects' thermal sensation, air movement perception acceptability and preference, thermal comfort, etc. was analyzed and is discussed in the following sections.

5.3.1 Thermal Sensation

- **Thermal Sensation and PV Airflow Rate**

PV airflow rates are 4, 8, 12, 16 L/s at the outlet of ceiling mounted PV ATDs. Corresponding air velocities are about 0.13, 0.35, 0.55, 0.77 m/s with 20 cm distance on top of head based on objective measurements (Chapter 4).

The local thermal sensation for head, face, neck, chest, shoulder, upper arm, lower arm, hands, back, lower body and the whole body thermal sensation based on average value of 32 subjects are plotted against PV airflow rates respectively in Figures 5.4 through 5.11. Logarithmic regression is used to describe the correlation between the thermal sensation and the flow rate. The R^2 of logarithmic regression curves in Figure 5.4 to Figure 5.11 is listed in Table 5.5.

As expected, the thermal sensation decreases with the increase of the flow rate, i.e. subjects feel cooler with the increase of the flow rate. Under the same PV airflow rate and temperature combination, the lower body segments (Figure 5.10) feel warmer

than the upper body segments and the neck (Figure 5.6) feel cooler (thermal sensation reported is 0.2-0.3 units low) than the face (Figure 5.5). Objective measurements performed with thermal manikin show that the neck and the face are symmetrically exposed to the flow field generated by the ceiling mounted PV ATD. Airflow and thermal characteristics are almost the same for these two body parts. Therefore, the differences obtained in the response of the subjects can be attributed to the neck being much more sensitive than face when exposed to the ceiling PV flow. Similarly, the back (Figure 5.7) is found to be more sensitive to the personalized flow than the chest, shoulder and upper arms (Figure 5.8). However, in this case the difference is not so striking because of the longer distance to ceiling mounted PV ATD. The protection of attire also reduces the difference in sensitivity of the back and the chest/shoulders/upper arms. At the same temperature combination and flow rate the head (Figure 5.4) felt warmer (thermal sensation with 0.2 units higher) than the face (Figures 5.5). This is attributed to the protection and thermal resistance from hair. The results in Figure 5.9 reveal that the difference in the thermal sensation of the lower arms and hands reported at the temperature combinations 26°C/21°C and 23.5°C/23.5°C becomes small especially at low PV airflow rate. The reason is that these body parts may be occasionally placed under the table and thus be protected from the flow. Similar are the results for the lower body (Figure 5.10). One intersection appears on the thermal sensation curves of these two cases (26°C/21°C and 23.5°C/23.5°C). When PV airflow rate is lower than this intersection (about 6 L/s), room air temperature has more influence on lower body thermal sensation than the influence of PV air temperature. The influence of both PV air temperature and room air temperature will be elaborated in the following part.

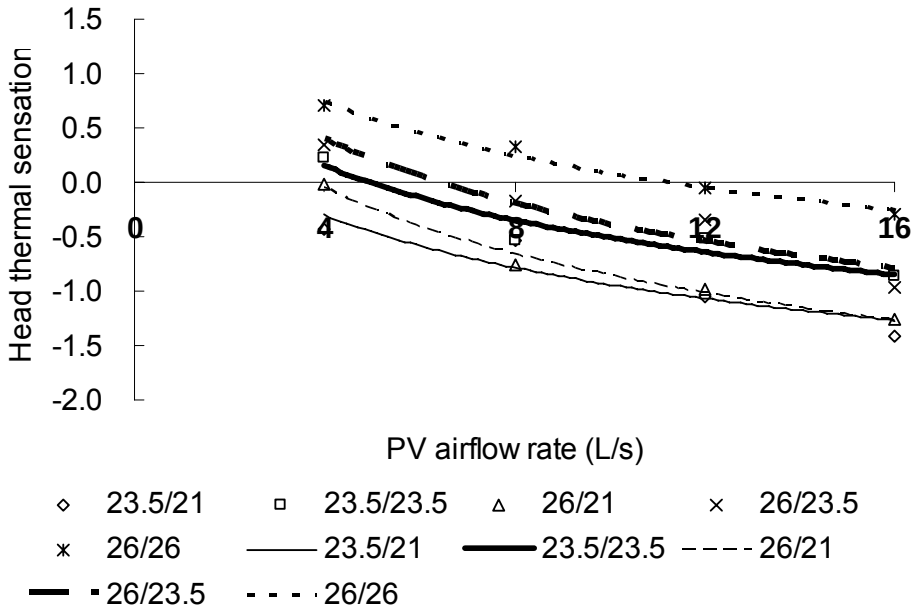

Figure 5.4 Logarithmic regression of head thermal sensation as a function of the personalized flow rate. Y-axis: -3=Cold; -2=Cool; -1=Slightly cool; 0=Neutral; 1=Slightly warm; 2=Warm; 3=Hot.

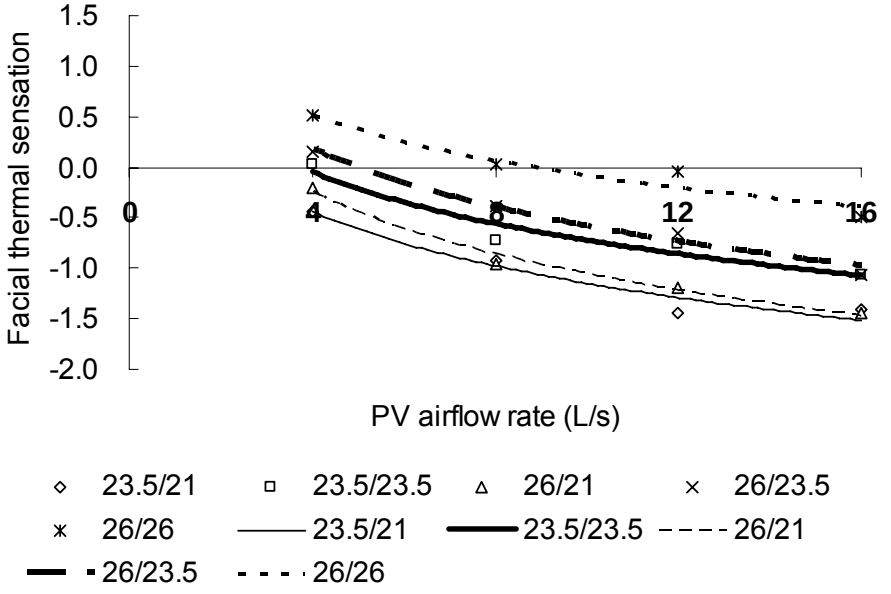

Figure 5.5 Logarithmic regression of facial thermal sensation as a function of the personalized flow rate. Y-axis: -3=Cold; -2=Cool; -1=Slightly cool; 0=Neutral; 1=Slightly warm; 2=Warm; 3=Hot.

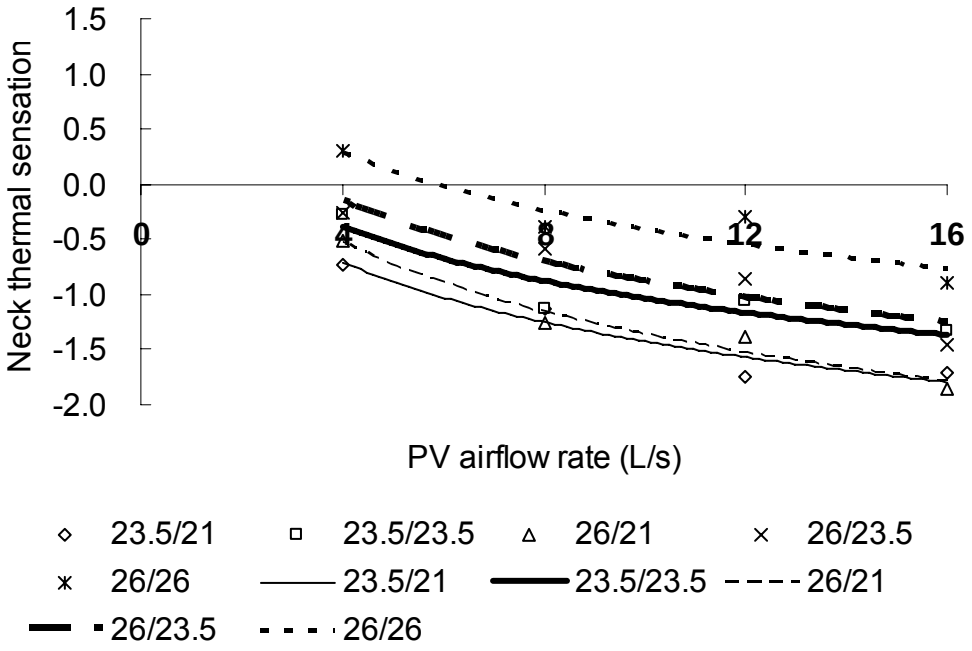

Figure 5.6 Logarithmic regression of neck thermal sensation as a function of the personalized flow rate. Y-axis: -3=Cold; -2=Cool; -1=Slightly cool; 0=Neutral; 1=Slightly warm; 2=Warm; 3=Hot.

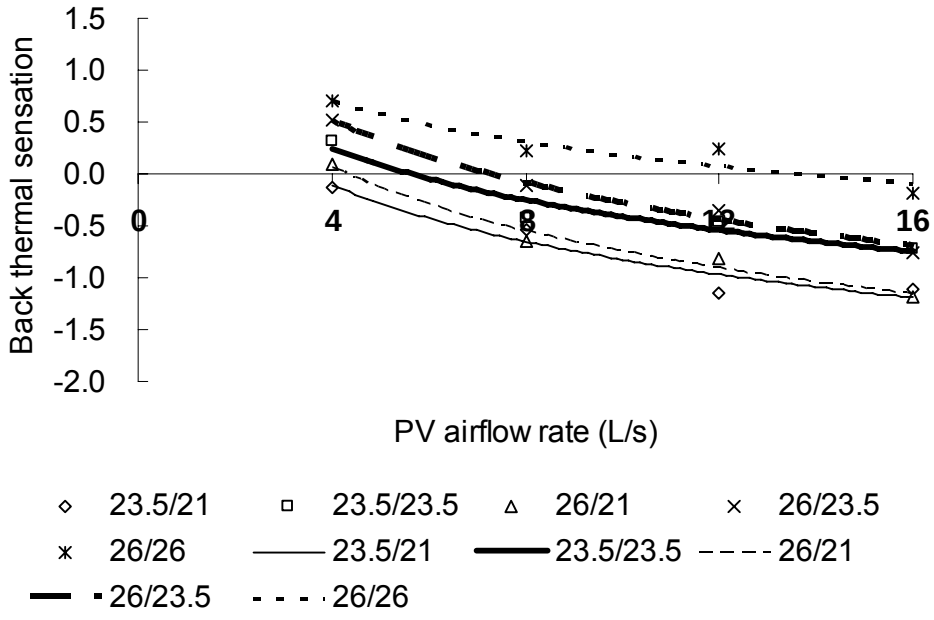

Figure 5.7 Logarithmic regression of back thermal sensation as a function of the personalized flow rate. Y-axis: -3=Cold; -2=Cool; -1=Slightly cool; 0=Neutral; 1=Slightly warm; 2=Warm; 3=Hot.

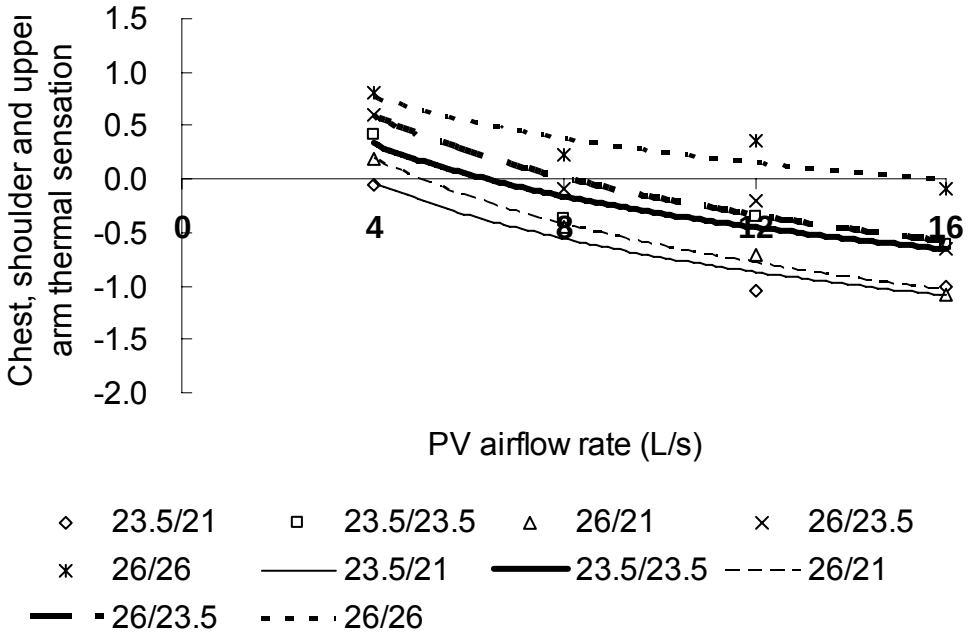

Figure 5.8 Logarithmic regression of chest, shoulder and upper arm thermal sensation as a function of the personalized flow rate. Y-axis: -3=Cold; -2=Cool; -1=Slightly cool; 0=Neutral; 1=Slightly warm; 2=Warm; 3=Hot.

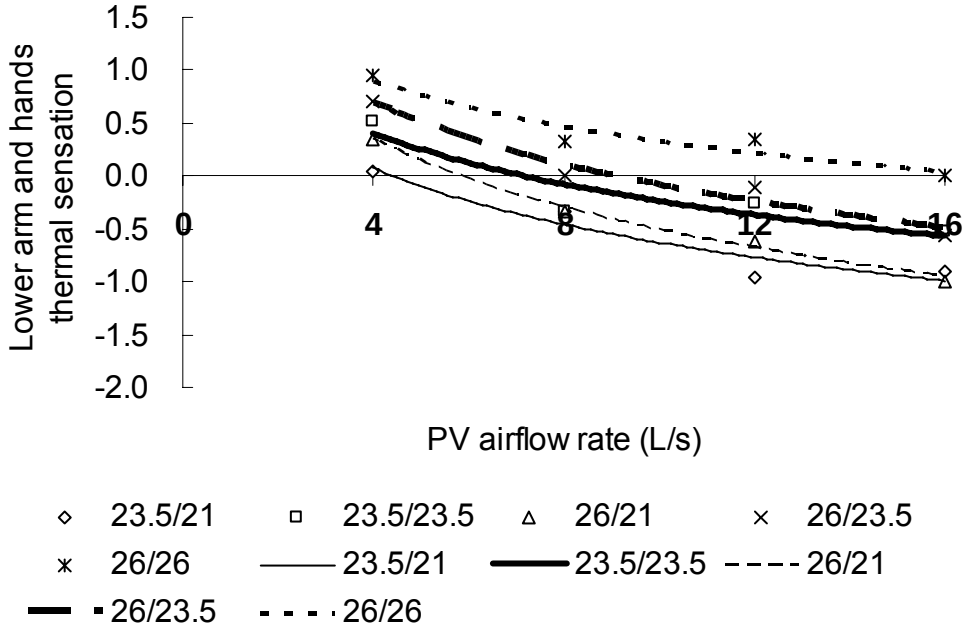

Figure 5.9 Logarithmic regression of lower arm and hands thermal sensation as a function of the personalized flow rate. Y-axis: -3=Cold; -2=Cool; -1=Slightly cool; 0=Neutral; 1=Slightly warm; 2=Warm; 3=Hot.

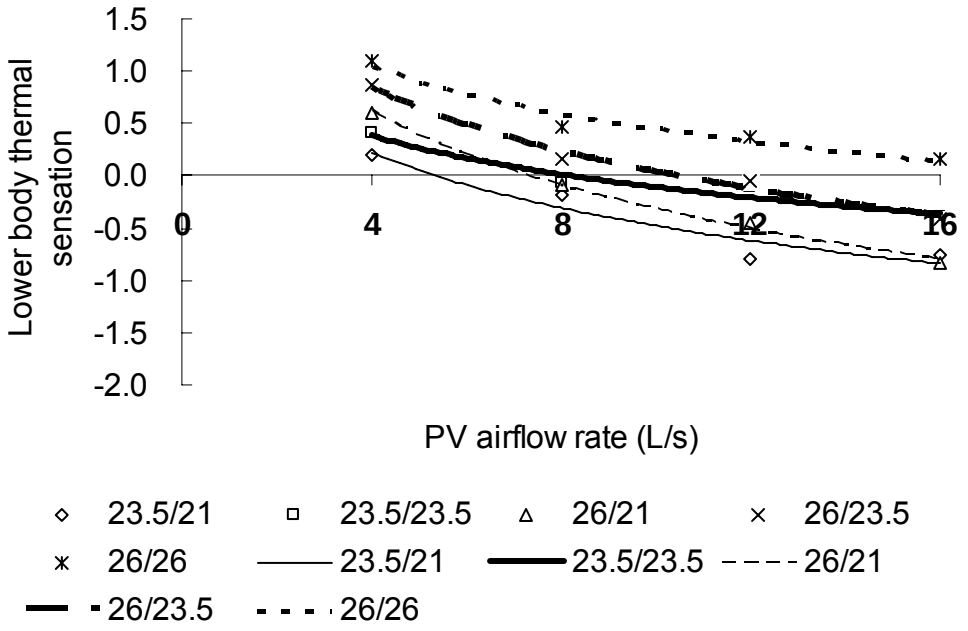

Figure 5.10 Logarithmic regression of lower body thermal sensation as a function of the personalized flow rate. Y-axis: -3=Cold; -2=Cool; -1=Slightly cool; 0=Neutral; 1=Slightly warm; 2=Warm; 3=Hot.

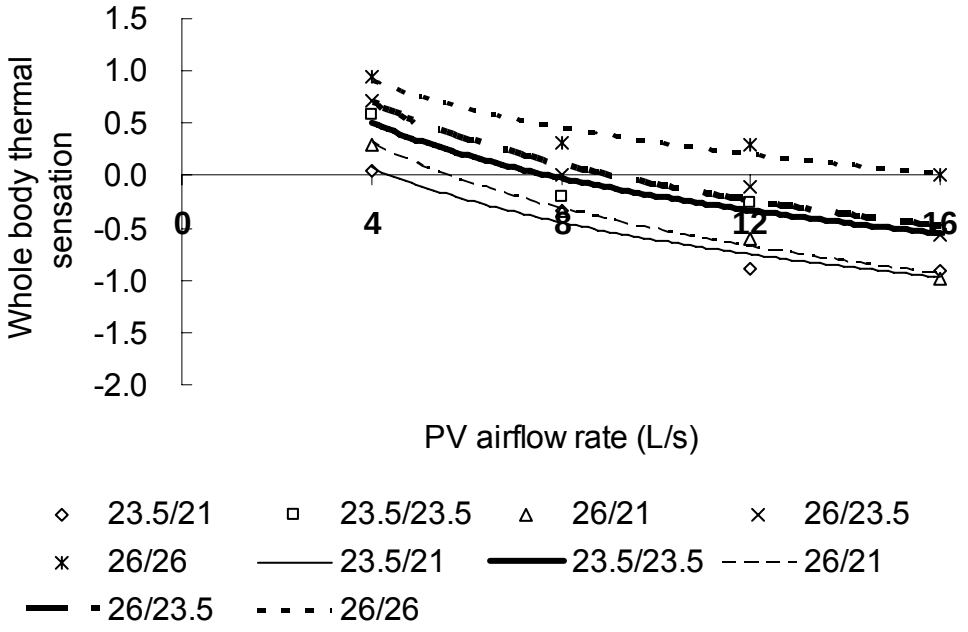

Figure 5.11 Logarithmic regression of whole body thermal sensation as a function of the personalized flow rate. Y-axis: -3=Cold; -2=Cool; -1=Slightly cool; 0=Neutral; 1=Slightly warm; 2=Warm; 3=Hot.

Table 5.5 R^2 of logarithmic regression in Figure 5.4 to Figure 5.11

Temperature (ºC)	Thermal sensation							
	head	face	neck	chest, shoulder and upper arm	lower arm and hands	back	lower body	whole body
23.5/21	0.80	0.94	0.92	0.92	0.92	0.92	0.92	0.94
23.5/23.5	0.91	0.98	0.86	0.90	0.85	0.93	0.78	0.94
26/21	0.84	0.93	0.96	0.99	0.99	0.98	0.97	0.98
26/23.5	0.92	0.98	0.88	0.96	0.96	0.98	0.99	0.96
26/26	0.98	0.93	0.87	0.83	0.91	0.88	0.96	0.93

- **Thermal Sensation and Temperature**

Figures 5.12 to 5.14 compare the average thermal sensation reported at the four airflow rates for each of the five temperature combinations. The results in Figure 5.12 show that the facial thermal sensation decreases when PV air temperature decreases under the same ambient temperature. The results in the figure also show that the facial thermal sensation under the same PV air temperature but different ambient temperatures are usually comparable to each other, i.e. the thermal sensation for the pair of 23.5°C /21°C and 26°C /21°C or pair 23.5°C /23.5°C and 26°C /23.5°C. It can be seen from Figure 5.14 that the whole body thermal sensation increases following the temperature combination sequence of 23.5°C/21°C, 26°C/21°C, 23.5°C/23.5°C, 26°C/23.5°C, 26°C/26°C. This indicates that both PV air temperature and room air temperature affect whole body thermal sensation and PV air temperature has more pronounced effect. All other body segments except the lower body (Figure 5.13) follow this sequence. For the lower body part, the room air temperature has more influence on the local thermal sensation than the PV air temperature when PV airflow rate is lower than 8 L/s. This is demonstrated by comparing cases 23.5°C/23.5°C and 26°C/21°C. The reason is that the influence from PV air temperature is reduced by decreasing PV airflow rate coupled with blockage effect by the table for lower body

part.

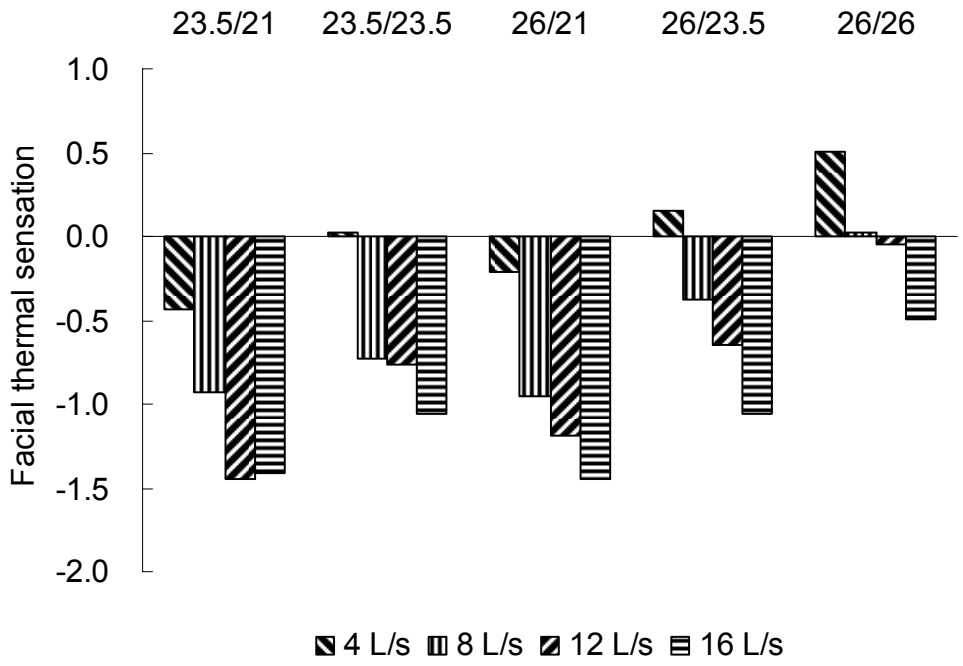

Figure 5.12 Facial thermal sensation at different temperature combinations and flow rate of 4, 8, 12 and 16 L/s. Y-axis: -3=Cold; -2=Cool; -1=Slightly cool; 0=Neutral; 1=Slightly warm; 2=Warm; 3=Hot.

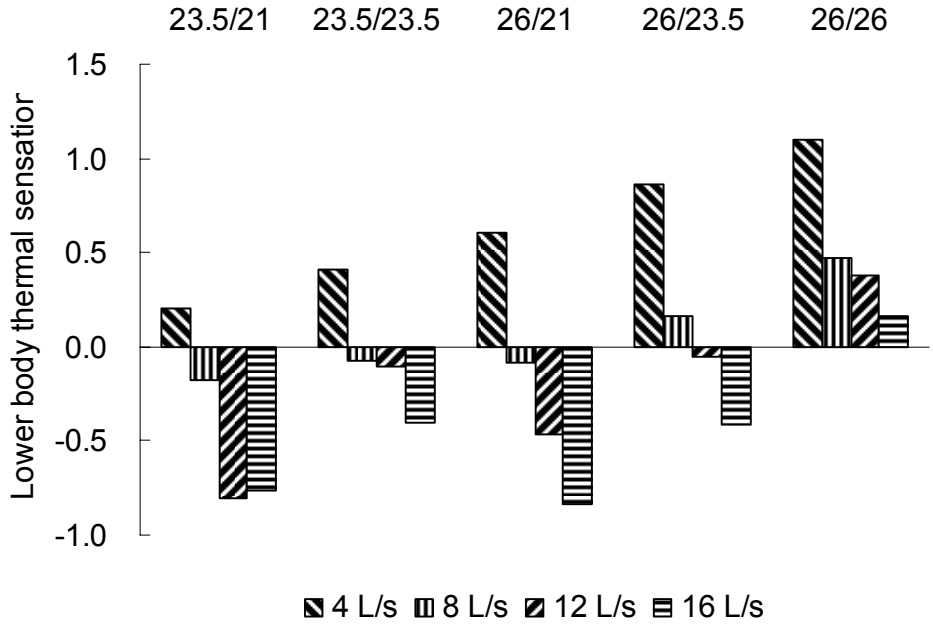

Figure 5.13 Lower body thermal sensation at different temperature combinations and flow rate of 4, 8, 12 and 16 L/s. Y-axis: -3=Cold; -2=Cool; -1=Slightly cool; 0=Neutral; 1=Slightly warm; 2=Warm; 3=Hot.

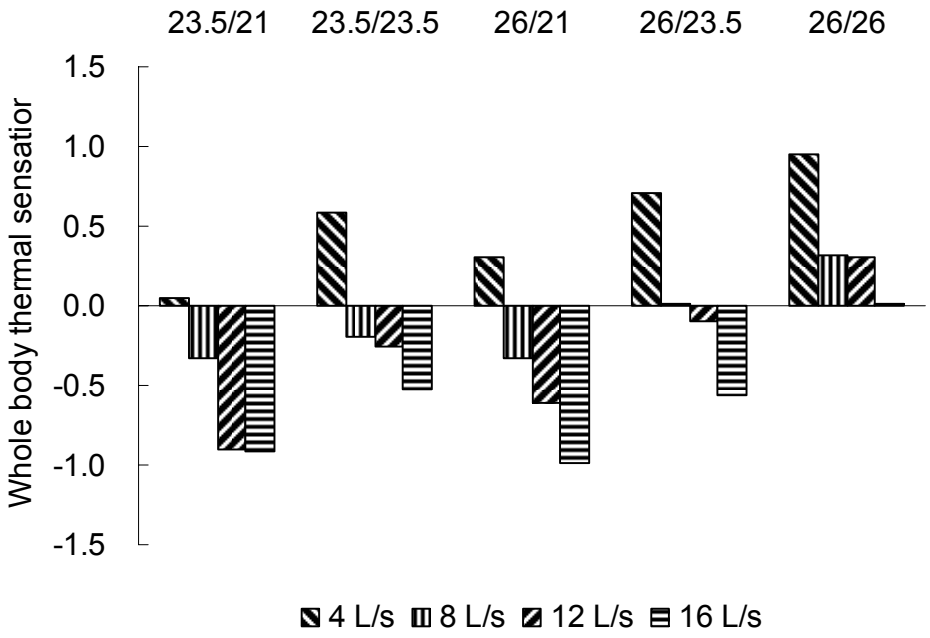

Figure 5.14 Whole body thermal sensation at different temperature combinations and flow rate of 4, 8, 12 and 16 L/s. Y-axis: -3=Cold; -2=Cool; -1=Slightly cool; 0=Neutral; 1=Slightly warm; 2=Warm; 3=Hot.

5.3.2 Air Movement Perception, Acceptability, Preference

Subjective assessment of local air movement includes air movement perception, acceptability and preference for different body segments and whole body. Logarithmic regression is applied to describe the relationship between the air movement perception (Figure 5.15 and Figure 5.16) and air movement preference (Figure 5.19 and Figure 5.20) and the flow rate and quadratic regression is applied to describe the relationship between the air movement acceptability (Figure 5.17 and Figure 5.18) and the flow rate. The correlation coefficients obtained are listed in Table 6.6.

- **Air Movement Perception**

Air movement perception for the body parts and the whole body increases when PV

airflow rate increases. This is demonstrated by the results for the face and the whole body shown in Figure 5.15 and Figure 5.16. The increase of the air movement perception is slightly faster at PV airflow rate from 4 L/s to 8 L/s and slows down when the flow rate increases from 8 to 12 L/s, i.e. the variation of subjects' air movement perception decreases with the increase of the velocity. One possible explanation is that relative value of PV airflow rate increasing reduces within the range of high PV airflow rate.

The comparison of the results in Figure 5.15 and Figure 5.16 reveal that the whole body air movement perception is lower than that of the facial air movement perception. The reason is that upper body part especially the head, the face and the neck are closer to the ceiling mounted PV ATD and are exposed to higher air velocity, while the whole body air movement perception also includes the perception at the lower body parts exposed to low velocity.

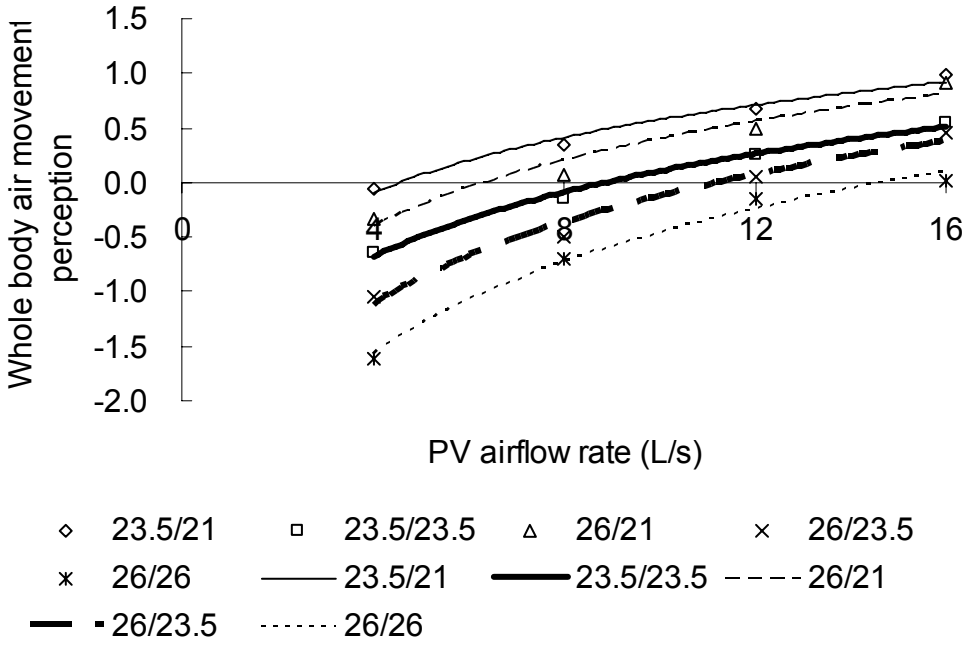

Figure 5.15 Logarithmic regression of whole body air movement perception as a function of the flow rate. Y-axis: -3=much too still; -2=too still; -1=slightly still; 0=just right; 1=slightly breezy; 2=too breezy; 3=much too breezy.

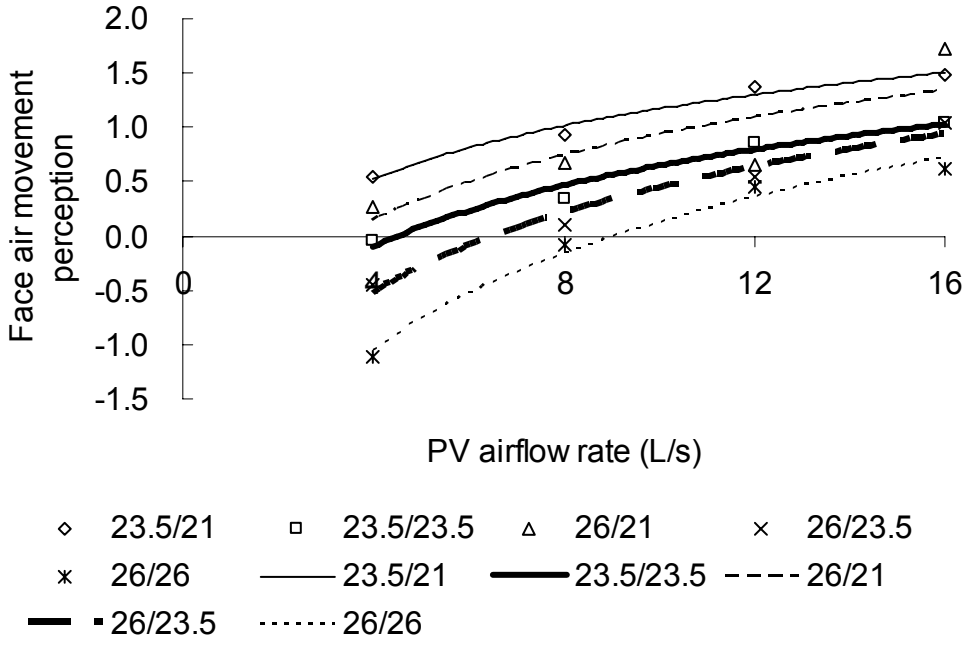

Figure 5.16 Logarithmic regression of face air movement perception as a function of the flow rate. Y-axis: -3=much too still; -2=too still; -1=slightly still; 0=just right; 1=slightly breezy; 2=too breezy; 3=much too breezy.

- **Air Movement Acceptability**

Figure 5.17 and 5.18 show air movement acceptability as a function of the flow rate. For the face and the whole body, the air movement acceptability increases initially and then decreases after a peak value is reached for the temperature combinations 26°C/21°C, 23.5°C /23.5°C and 26°C /23.5°C cases when PV airflow rate increases. It is only at the two extreme temperature combinations, i.e. the lowest and the highest temperatures, 23.5°C/21°C and 26°C/26°C, that the air movement acceptability respectively decreases and increases with the increase of the flow rate. The maximum values appear at 4 L/s for 23.5°C/21°C and at 16 L/s for 26°C/26°C.

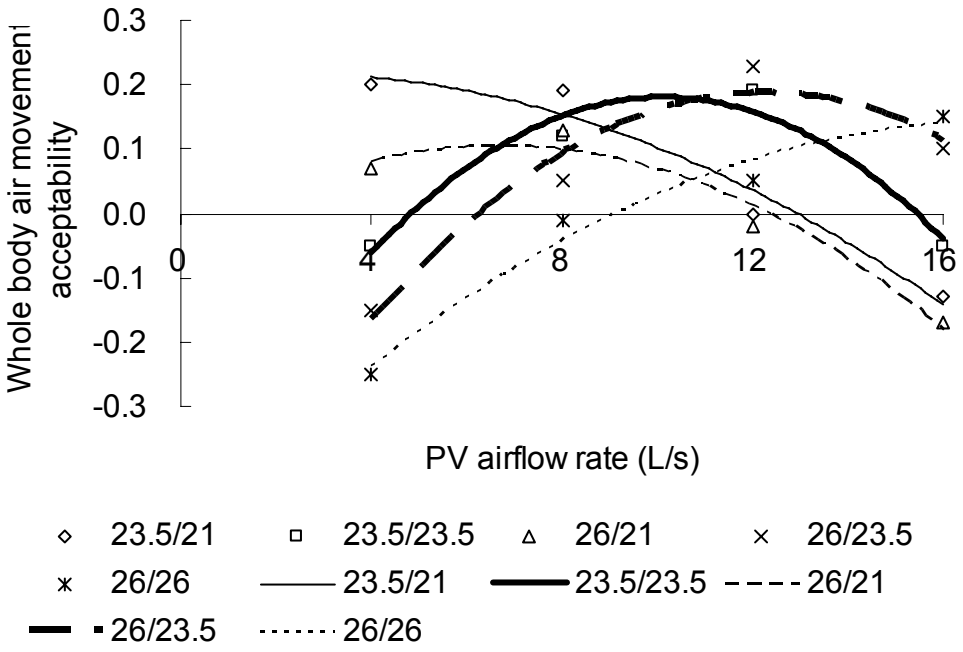

Figure 5.17 Quadratic regression of whole body air movement acceptability as a function of the flow rate. Y-axis: -1=very unacceptable; 0=just unacceptable/acceptable; +1=very acceptable.

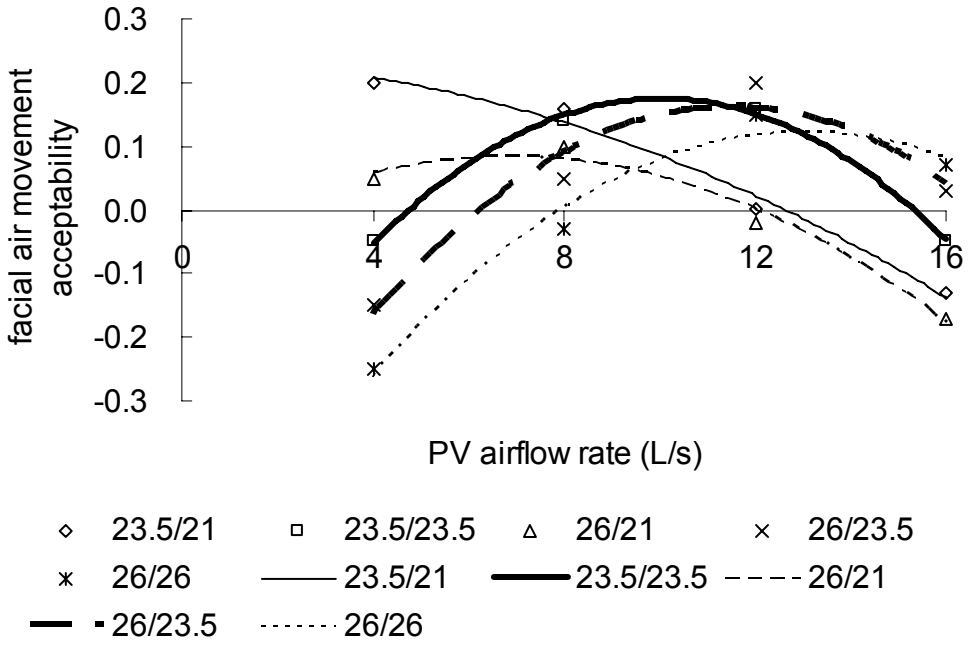

Figure 5.18 Quadratic regression of face air movement acceptability as a function of the flow rate. Y-axis: -1=very unacceptable; 0=just unacceptable/acceptable; +1=very acceptable.

- **Air Movement Preference**

Figures 5.19 and 5.20 show the air movement preference for the face and the whole body. The air movement preference decreases with the increase of the flow rate, i.e. with the increase of the air velocity. The decrease in the air movement preference is slightly faster at PV airflow rate from 4 L/s to 8 L/s than at flow rate from 8 to 12 L/s. This observation is consistent with the change of the air movement perception with the increase of the flow rate.

The comparison of the results in Figure 5.19 and Figure 5.20 show that the whole body air movement preference is higher than the facial air movement preference. This observation is consistent with the results obtained for the air movement perception

(Figures 5.15 and 5.16).

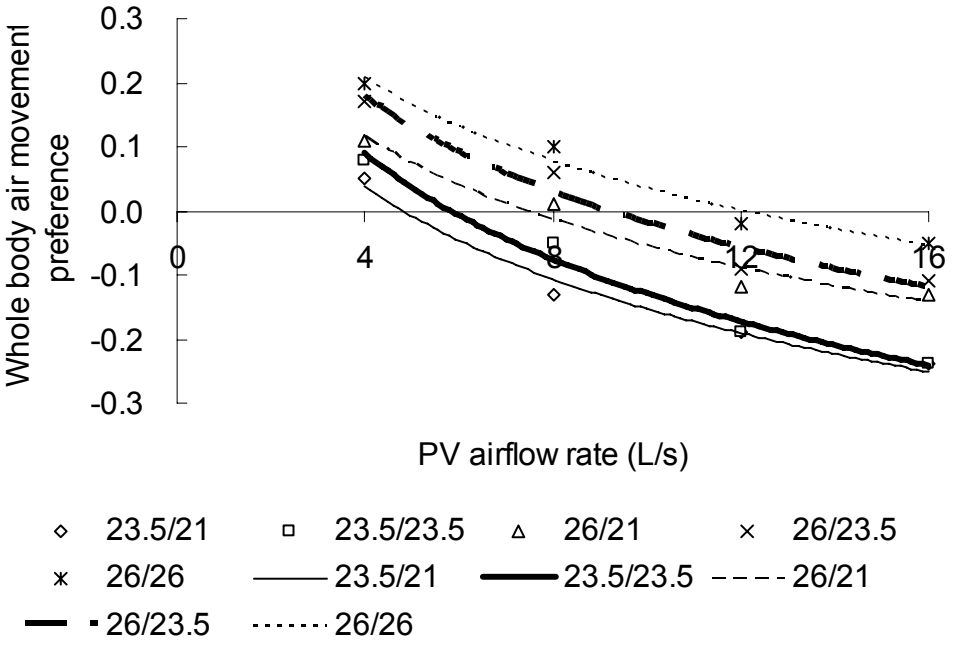

Figure 5.19 Logarithmic regression of whole body air movement preference as a function of the flow rate. Y-axis: -1=less air movement; 0=no change; +1=more air movement.

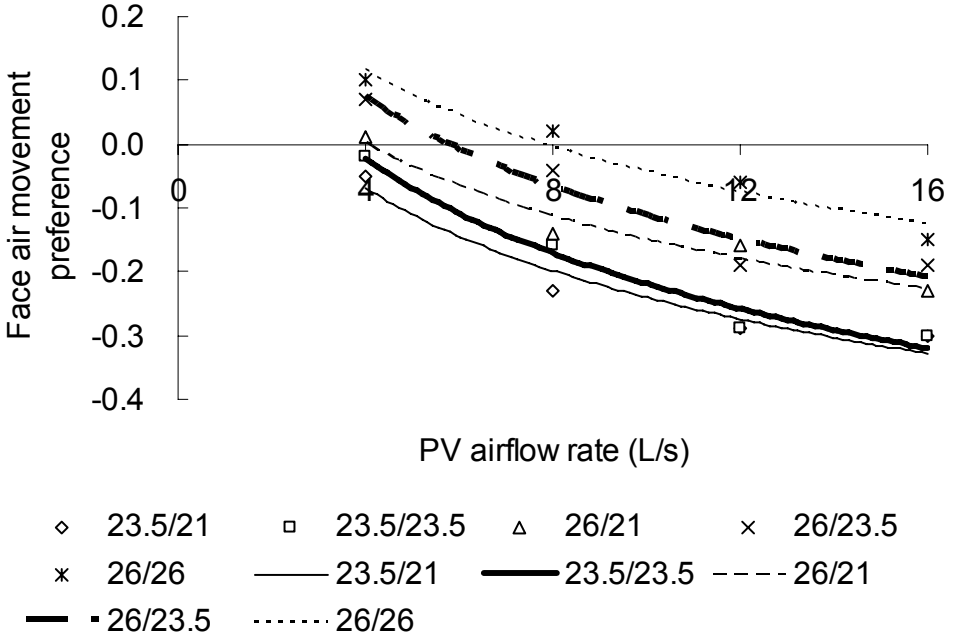

Figure 5.20 Logarithmic regression of face air movement preference as a function of the flow rate. Y-axis: -1=less air movement; 0=no change; +1=more air movement.

Table 5.6 R^2 of regression in Figure 5.15 to Figure 5.20 (prec, acc and pref respectively stand for air movement perception, acceptability and preference)

face	perc	acc	pref	whole body	perc	acc	pref
23.5/21	0.98	0.98	0.94	23.5/21	0.98	0.96	0.98
23.5/23.5	0.97	0.99	0.97	23.5/23.5	0.99	0.95	0.98
26/21	0.69	0.98	0.96	26/21	0.96	0.96	0.96
26/23.5	0.97	0.94	0.94	26/23.5	0.98	0.94	0.96
26/26	0.98	0.97	0.95	26/26	0.99	0.97	0.97

5.3.3 Thermal Comfort Acceptability

Subjects' thermal comfort acceptability as a function of the flow rate in shown in Figure 5.21. Quadratic regression is applied to describe the correlation between these parameters and the correlation coefficients are shown in Table 5.7. The convex shape of regression curves shows that thermal comfort is perceived better at certain PV airflow rate, which is in the middle of listed PV airflow rate range. The summit of convex shape shifts left or right when temperature reduces or increases respectively.

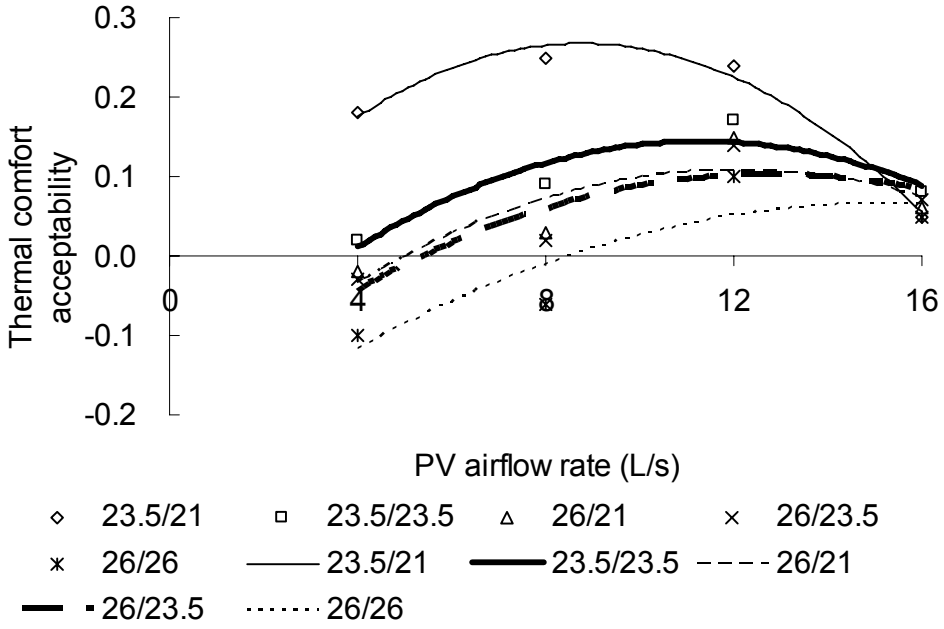

Figure 5.21 Quadratic regression of thermal comfort acceptability as a function of the flow rate. Y-axis: -1=very unacceptable; 0=just unacceptable/acceptable; +1=very acceptable.

Table 5.7 R^2 of regression in Figure 5.21 (TC-thermal comfort)

	23.5/21	23.5/23.5	26/21	26/23.5	26/26
TC	0.98	0.86	0.74	0.79	0.79

5.3.4 Indoor Air Quality

Subjective responses of indoor air quality including perceived inhaled air temperature, perceived air quality and freshness of inhaled air were analyzed. Relationships between these sensations and the flow rate are established. The correlation coefficients of the relationships are listed in Table 5.8. The results are discussed in this section.

- **Perceived Air Quality**

Under all experimental conditions, mean values of the PAQ are within the acceptable range. The PAQ as a function of the flow rate is shown in Figure 5.22. PAQ improves when PV airflow rate increases or temperature decreases.

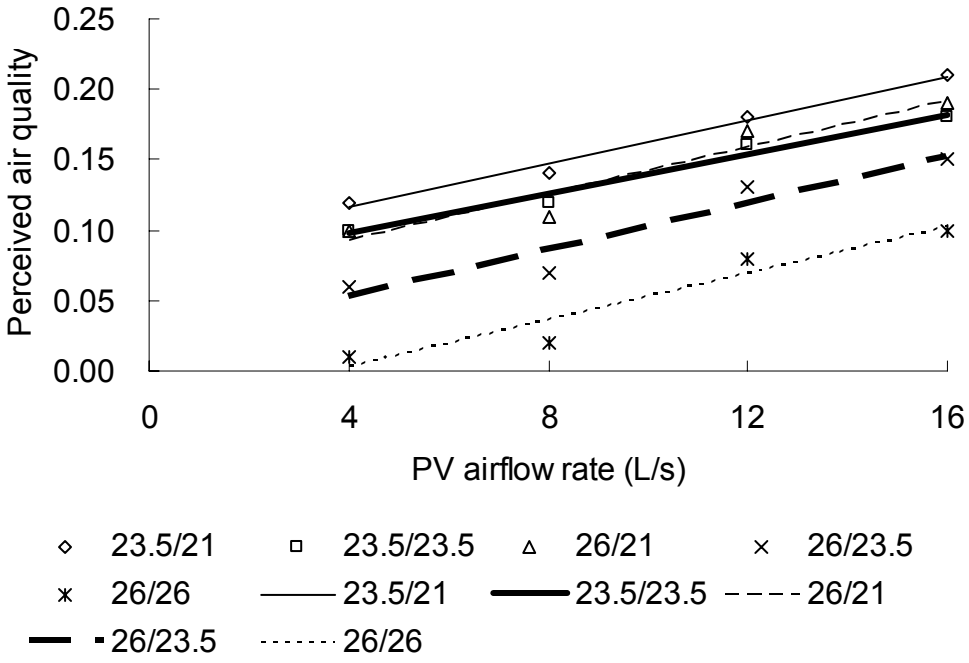

Figure 5.22 Linear regression of perceived air quality as a function of the flow rate. Y-axis: -1=very unacceptable; 0=just unacceptable/acceptable; +1=very acceptable.

- **Perceived Inhaled Air Temperature**

Logarithmic regression was used to describe the relationship between the perceived inhaled air temperature and the flow rate (Figure 5.23). Perceived inhaled air temperature becomes cooler when PV airflow rate increases. At the low flow rate, the importance of the ambient temperature for the perceived air temperature increases. This can be seen from the results reported by the subjects at the temperature combinations 26°C/21°C and 23.5°C/23.5°C and at flow rate of 4 l/s, i.e. at the low flow rate only small part of the personalized flow reaches the breathing zone of the subject.

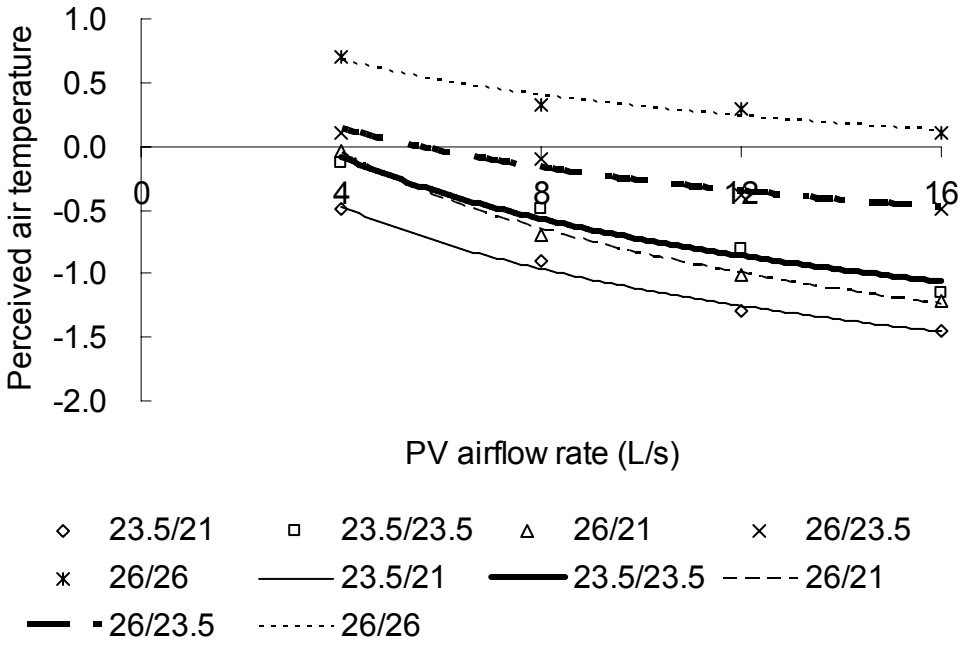

Figure 5.23 Logarithmic regression of perceived inhaled air temperature as a function of the flow rate. Y-axis: -3=Cold; +3=Hot.

- **Freshness of Inhaled Air**

The air freshness as a function of the flow rate as obtained at the temperature combinations studied is shown in Figure 5.24. The air freshness increases with the increase of the flow rate, i.e. with the increase of the velocity at the breathing zone. The air is perceived fresher at low temperatures than at high temperatures.

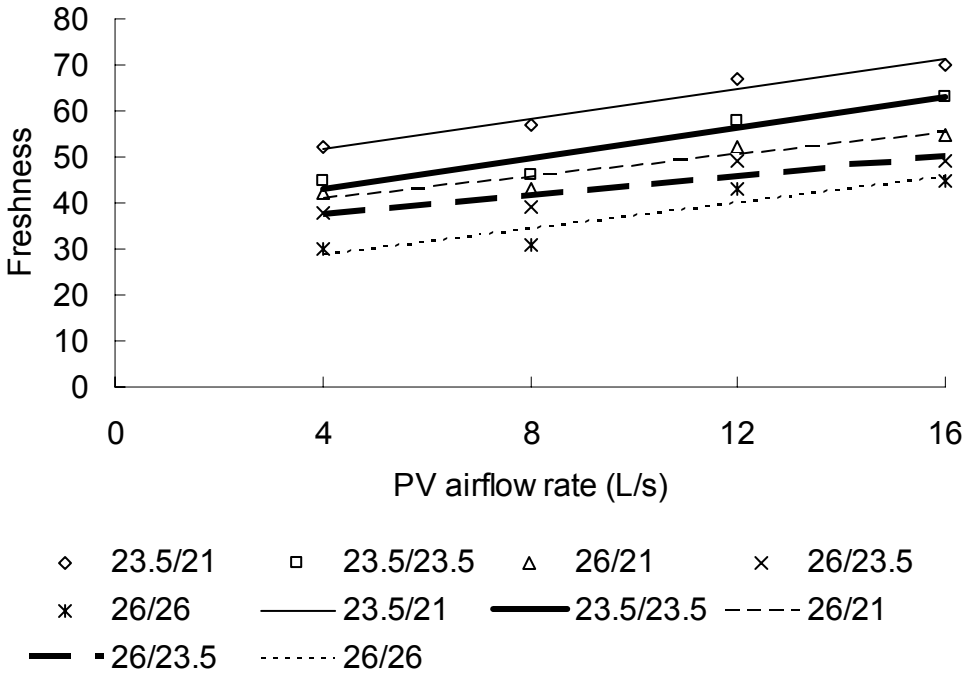

Figure 5.24 Linear regression of inhaled air freshness as a function of the flow rate. Y-axis: 0= Air stuffy; 100=Air fresh.

Table 5.8 R^2 of regression in Figure 5.22, Figure 5.23 and Figure 5.24 (PAT-perceived inhaled air temperature; PAQ-perceived air quality; Freshness-Freshness of inhaled air)

	23.5/21	23.5/23.5	26/21	26/23.5	26/26
PAT	0.99	0.96	0.99	0.96	0.96
PAQ	0.99	0.98	0.93	0.93	0.92
Freshness	0.96	0.91	0.91	0.83	0.87

5.3.5 Evaluation of Noise Level

The evaluation of noise level for ceiling mounted PV system is important because of high supply air momentum. Under all experimental conditions, the satisfaction with the noise level was in the acceptable range (Figure 5.25). The satisfaction with the noise level decreases when the PV airflow rate increases. Temperature does not have statistically significant impact on the satisfaction with the noise level. The satisfaction

with the noise level as a function of the flow rate could be described with a linear function. The correlation coefficients of the relationships are listed in Table 5.9.

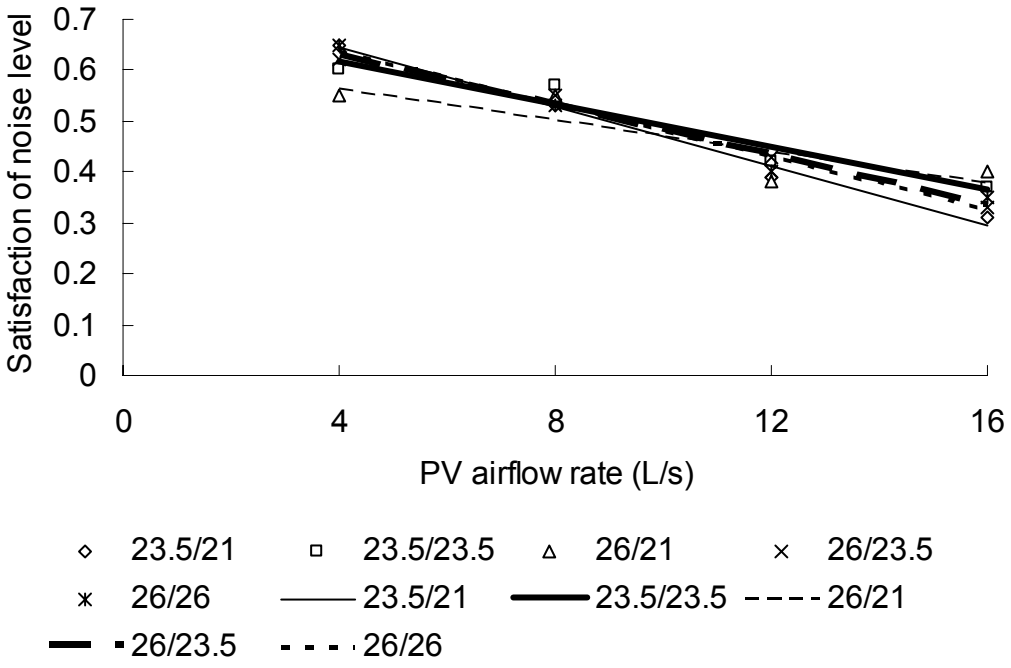

Figure 5.25 Linear regression of satisfaction of noise level as a function of the flow rate. Y-axis: -1= Dissatisfied; +1=Satisfied.

Table 5.9 R^2 of linear regression in Figure 5.25

	23.5/21	23.5/23.5	26/21	26/23.5	26/26
Noise level	0.99	0.93	0.75	0.99	0.97

5.3.6 Discussion

The explored relationship between subjects' thermal sensation and air movement perception and PV airflow rate at the studied temperature combination revealed expected relationships, i.e. the condition with higher PV airflow rate is perceived cooler and breezier, and the condition with lower air temperature is perceived as

cooler. Under the same PV airflow rate and temperature upper body parts especially neck, face and head are perceived cooler and breezier than the lower body parts and the whole body.

PV airflow rate has important effect on the body thermal sensation and the air movement perception, acceptability and preference. The correlations obtained between air movement acceptability/thermal comfort and PV airflow rate reveal that subjects prefer certain air velocity. The most acceptable PV airflow rate increases with the increasing of the temperature combinations. The preference of air movement is consistent with the results of de Dear and Fountain (1994), Tanabe and Kimura (1994) and Gong (2006).

Both the PV air temperature and the ambient air temperature influence subjects' local thermal sensation and the whole body thermal sensation. PV air temperature has stronger influence on thermal sensation than ambient temperature especially for upper body segments. It is only under low PV airflow rate (about 4 L/s) that the influence of the ambient temperature on the thermal sensation is comparable to that of the PV air temperature. It is only for lower body parts at low PV airflow rate (about 4 L/s) that the influence on thermal sensation from ambient temperature is more pronounced than the influence of the PV air temperature.

Perceived inhaled air temperature becomes cooler when PV airflow rate increases. Perceived air quality and inhaled air freshness improves when PV airflow rate increases or temperature reduces. Satisfaction of noise level decreases when PV

airflow rate increases.

5.4 Human Perception Relation

The human perception relations within and between the three categories, i.e., thermal sensation (face, neck, head and whole body), thermal comfort (whole body), feeling of air movement (facial region) are explored in this section of the thesis.

5.4.1 Correlation Analysis within Human Perceptions

- **Thermal Sensation**

The correlation between the local thermal sensations for the face, the neck and the head and the whole body thermal sensation are analyzed (Figure 5.26, Figure 5.27 and Figure 5.28). The statistical analyses performed identify that the correlations are strong with correlation coefficient above 0.97 for most of the temperature combinations studied (Table 5.10).

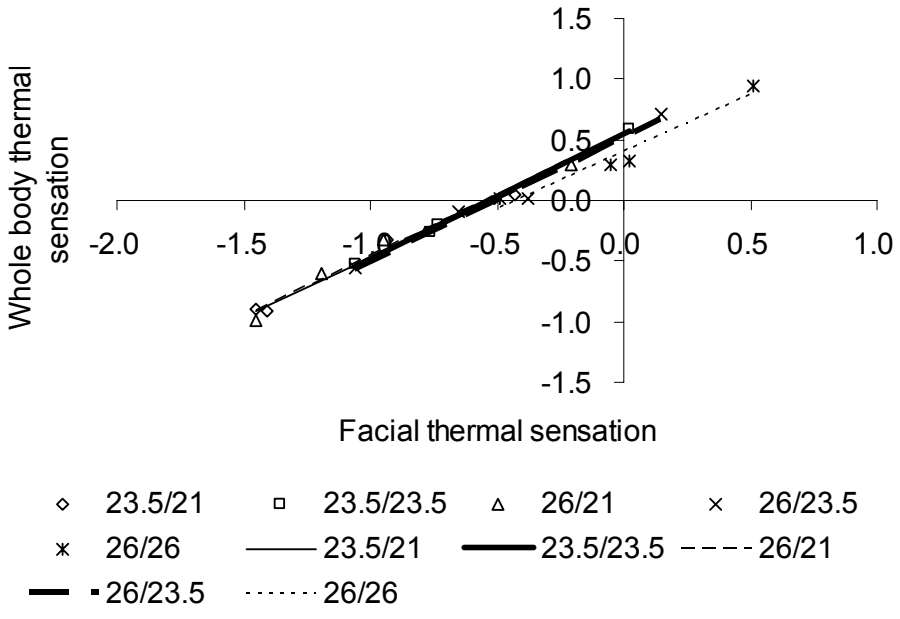

Figure 5.26 Linear regression of whole body thermal sensation and facial thermal sensation. Y-axis and X axis: -3=Cold; -2=Cool; -1=Slightly cool; 0=Neutral; 1=Slightly warm; 2=Warm; 3=Hot.

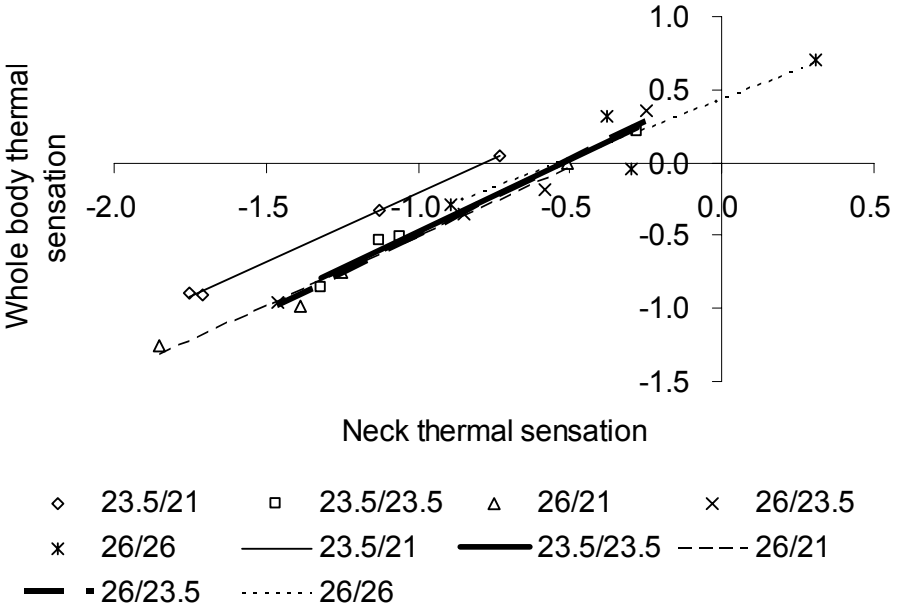

Figure 5.27 Linear regression of whole body thermal sensation and neck thermal sensation. Y-axis and X axis: -3=Cold; -2=Cool; -1=Slightly cool; 0=Neutral; 1=Slightly warm; 2=Warm; 3=Hot.

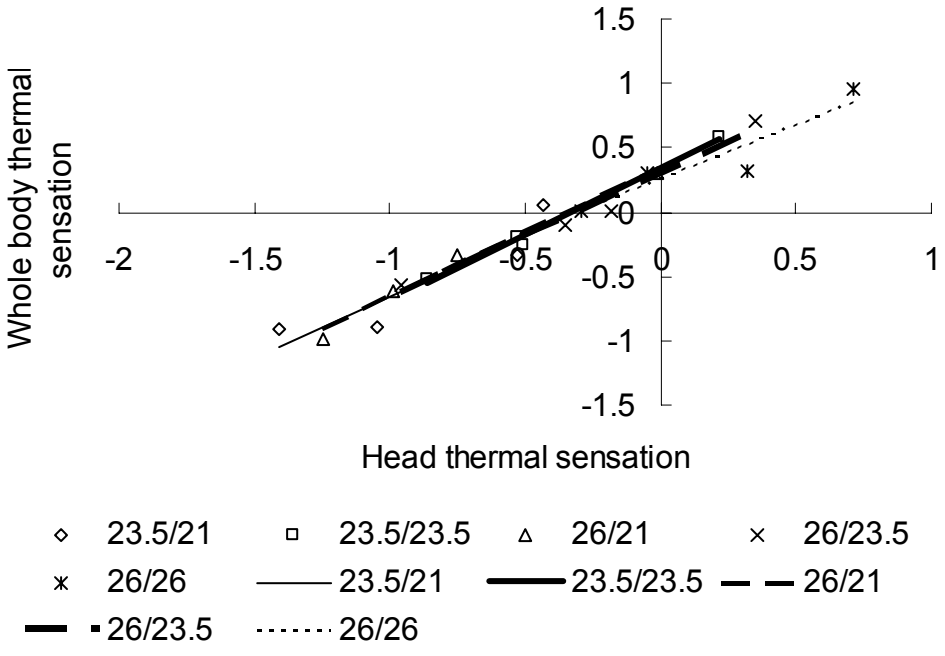

Figure 5.28 Linear regression of whole body thermal sensation and head thermal sensation. Y-axis and X axis: -3=Cold; -2=Cool; -1=Slightly cool; 0=Neutral; 1=Slightly warm; 2=Warm; 3=Hot.

Table 5.10 R^2 of regression in Figure 5.26, Figure 5.27 and Figure 5.28

	23.5/21	23.5/23.5	26/21	26/23.5	26/26
face	0.99	0.99	0.98	0.98	0.95
neck	0.99	0.98	0.98	0.98	0.83
head	0.85	0.99	0.98	0.97	0.88

The results of the analyses reveal that the local thermal sensation at the face and the neck is slightly cooler (0.5 units) than the whole body thermal sensation. The difference between the local thermal sensation for the head and the whole body thermal sensation is smaller, about 0.3 units, which can be explained by the protection of the hair. At the temperature combination 23.5°C /21°C, i.e. the coolest temperature combination the relationship for the local thermal sensation at the neck and the whole body thermal sensation is shifted toward the cooler side of the scale. Under these conditions, the neck is felt much cooler (0.75 units cooler) than the whole body thermal sensation. The possible reason is that neck becomes much more sensitive to air movement at lower temperatures.

The regression lines obtained at ambient temperatures of 26°C and 23°C almost overlap. This demonstrates that the influence of the ambient temperature on the whole body thermal sensation is not dominant compared with the influence of the PV air temperature. This is because most of the body parts, especially the upper body parts, are exposed to the PV airflow. The PV airflow has clear influences on the facial thermal sensation. The lower the temperature of the PV airflow, the lower is the

thermal sensation reported by the subjects.

- **Air Movement Perception, Acceptability, Preference**

Face and whole body are chosen for further investigation to explore the relationship between air movement acceptability and air movement perception, air movement acceptability and air movement preference, and air movement preference and air movement perception. The results of the analysis are shown in Figure 5.29 (correlation coefficient 0.68), Figure 5.30 (correlation coefficient 0.72), Figure 5.31 (correlation coefficient 0.24), Figure 5.32 (correlation coefficient 0.50), Figure 5.33 (correlation coefficient 0.59) and Figure 5.34 (correlation coefficient 0.84), respectively. Each point in the figures stands for the mean subjective response obtained for the combinations of personalized airflow rate, personalized temperature and ambient air temperature.

The relation of air movement acceptability and air movement perception for face (Figure 5.29) suggests that the subjects felt the air movement most acceptable when they felt it between just right and slightly breezy. The acceptability of the air movement decreased when the air movement perception moved toward either much too still or much too breezy. The relation of air movement acceptability and air movement perception for whole body (Figure 5.30) suggests that the subjects felt the air movement most acceptable when they felt it just right.

By utilizing first derivative of air movement acceptability and air movement

perception (dAcc/dPerc), the maximum value of air movement acceptability (0.093) is derived at air movement perception level of 0.502, i.e. the air movement acceptability was higher when the air movement was perceived stronger than "just right". The finding is in agreement with previously reported results obtained with tropically acclimatized subjects (de Dear and Fountain, 1994; Gong et. al., 2006).

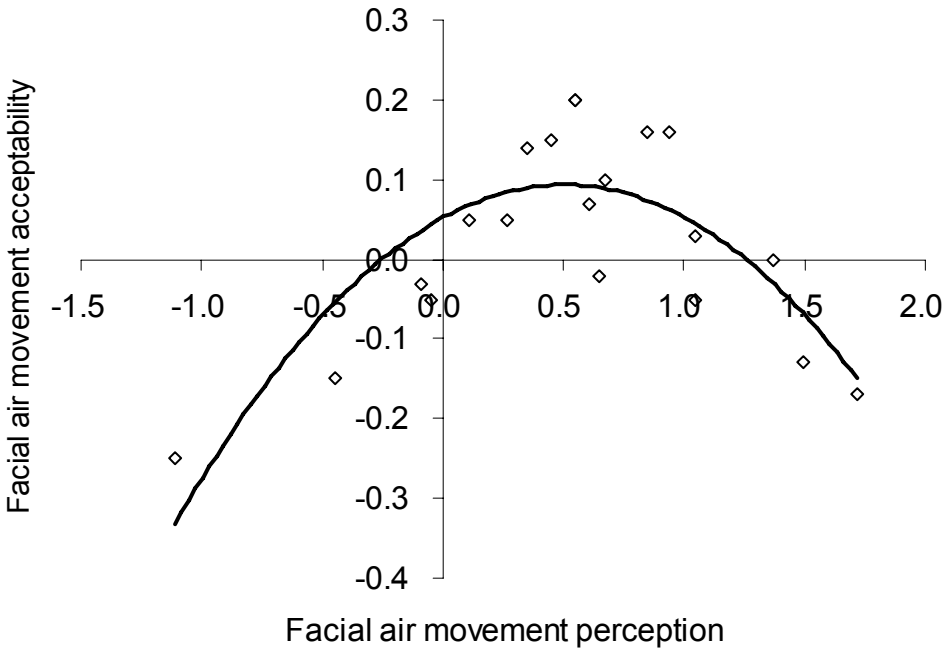

Figure 5.29 Quadratic regression of facial air movement acceptability and facial air movement perception. Y-axis: -1=very unacceptable; 0=just unacceptable/acceptable; +1=very acceptable. X-axis: -3=much too still; -2=too still; -1=slightly still; 0=just right; 1=slightly breezy; 2=too breezy; 3=much too breezy.

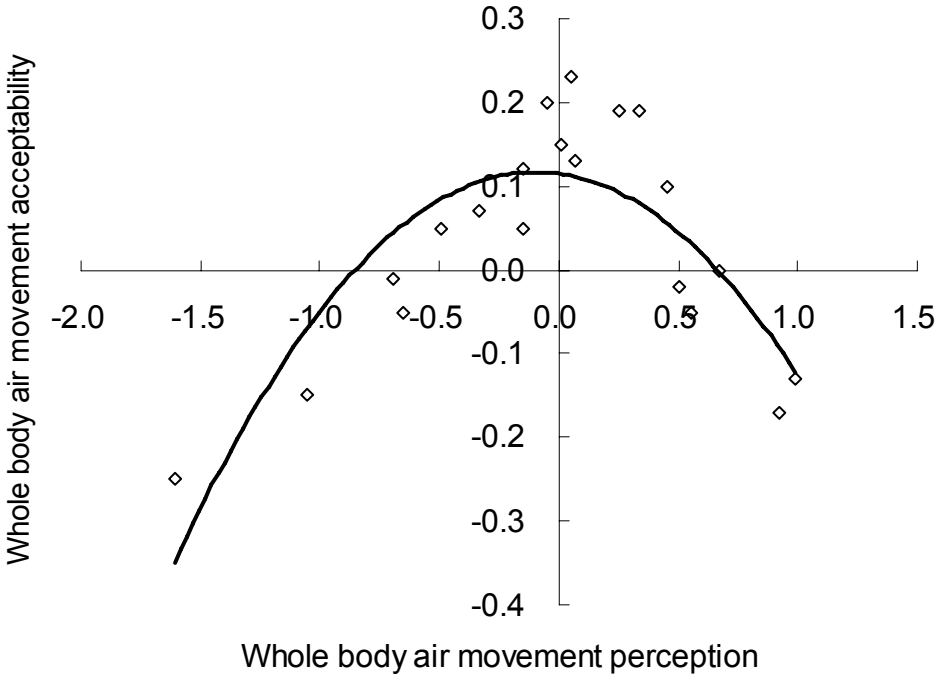

Figure 5.30 Quadratic regression of whole body air movement acceptability and whole body air movement perception. Y-axis: -1=very unacceptable; 0=just unacceptable/acceptable; +1=very acceptable. X-axis: -3=much too still; -2=too still; -1=slightly still; 0=just right; 1=slightly breezy; 2=too breezy; 3=much too breezy.

In the same manner by utilizing first derivative of air movement acceptability and air movement preference (dAcc/dPref) for face (Figure 5.31), the maximum value of air movement acceptability (0.068) is derived at air movement preference level of -0.062, i.e. the air movement acceptability was higher when subjects prefer slightly less air movement. The whole body analysis follows the similar trend (Figure 5.32).

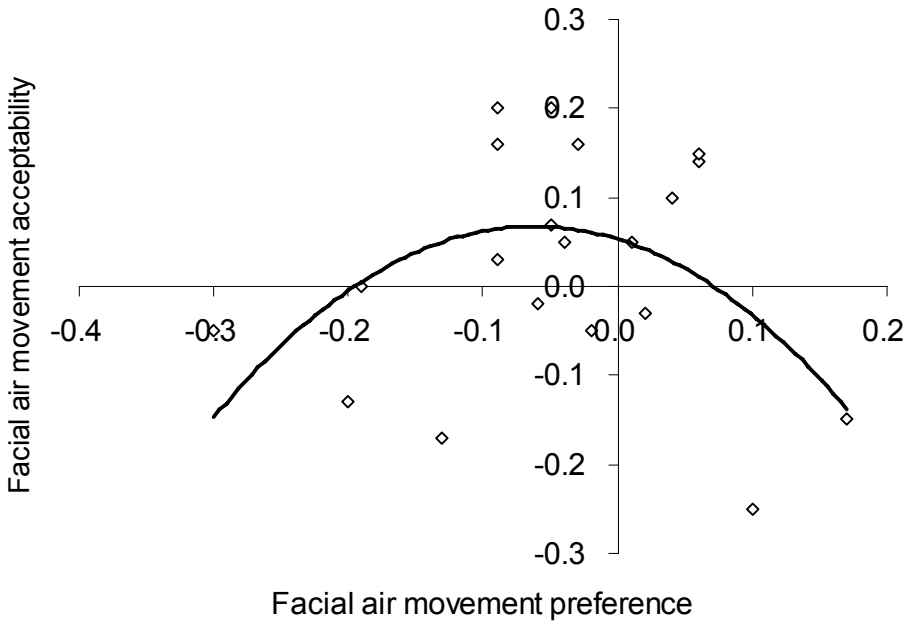

Figure 5.31 Quadratic regression of facial air movement acceptability and facial air movement preference. Y-axis: -1=very unacceptable; 0=just unacceptable/acceptable; +1=very acceptable. X-axis: -1=less air movement; 0=no change; +1=more air movement.

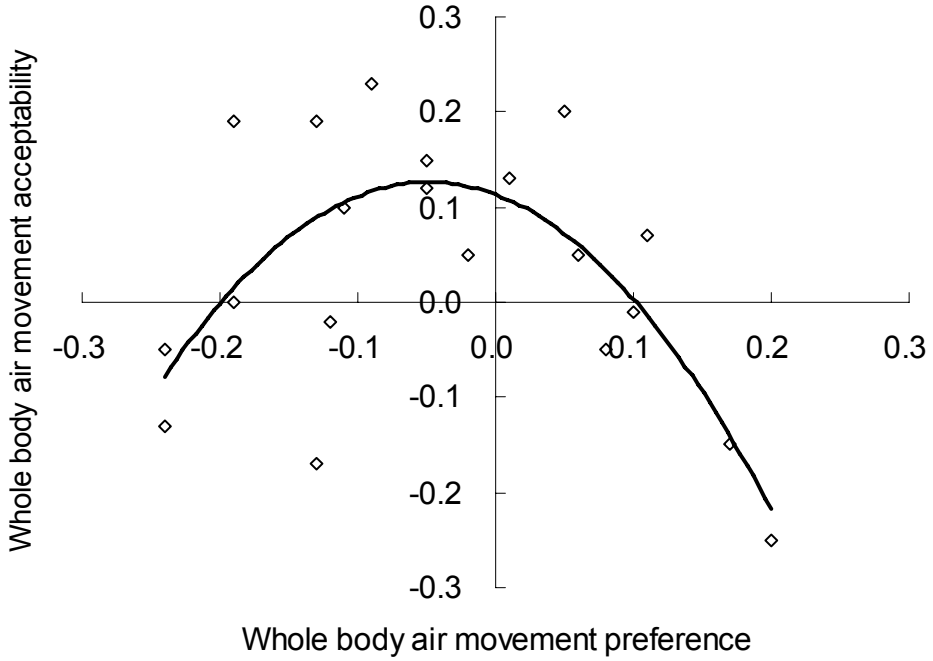

Figure 5.32 Quadratic regression of whole body air movement acceptability and whole body air movement preference. Y-axis: -1=very unacceptable; 0=just unacceptable/acceptable; +1=very acceptable. X-axis: -1=less air movement; 0=no change; +1=more air movement.

The correlation between air movement preference and air movement perception for face (Figure 5.33) revealed as expected that subjects preferred more air movement when their air movement perception decreased. The whole body analysis follows the similar trend (Figure 5.34). For face, the interception of the linear correlation between the responses of the subjects to these two parameters on the Y-axis is between "just right" and "slightly breezy", i.e. the subjects preferred slightly more air movement than "just right". For whole body, the interception of the linear correlation between the responses of the subjects to these two parameters on the Y-axis is between "just right" and "slightly still", i.e. the subjects preferred slightly less air movement than "just right". The observation is made without any apparent reason.

An empirical model of air movement preference and air movement perception for the face is derived from the correlation shown in Figure 5.33 by linear regression:

$$Pref=-0.1258Perc+0.0251 \ (R^2=0.6) \qquad (6.1)$$

Where, Pref is air movement preference (-1=less air movement, 0=no change, +1=more air movement), Perc is air movement perception (-3=much too still, -2=too still, -1=slightly still, 0=just right, 1=slightly breezy, 2=too breezy, 3=much too breezy).

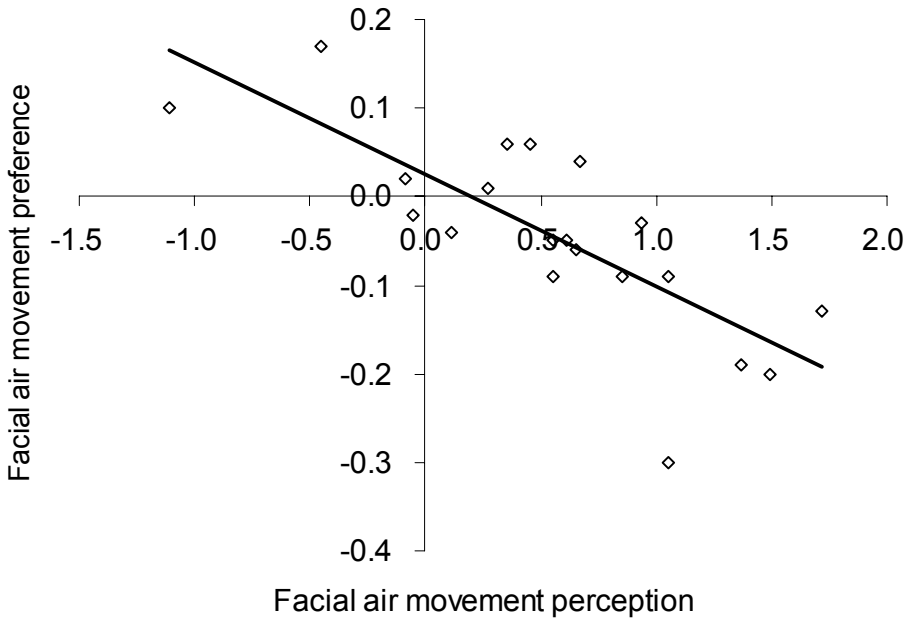

Figure 5.33 Linear regression of facial air movement preference and facial air movement perception. Y-axis: -1=less air movement; 0=no change; +1=more air movement. X-axis: -3=much too still; -2=too still; -1=slightly still; 0=just right; 1=slightly breezy; 2=too breezy; 3=much too breezy.

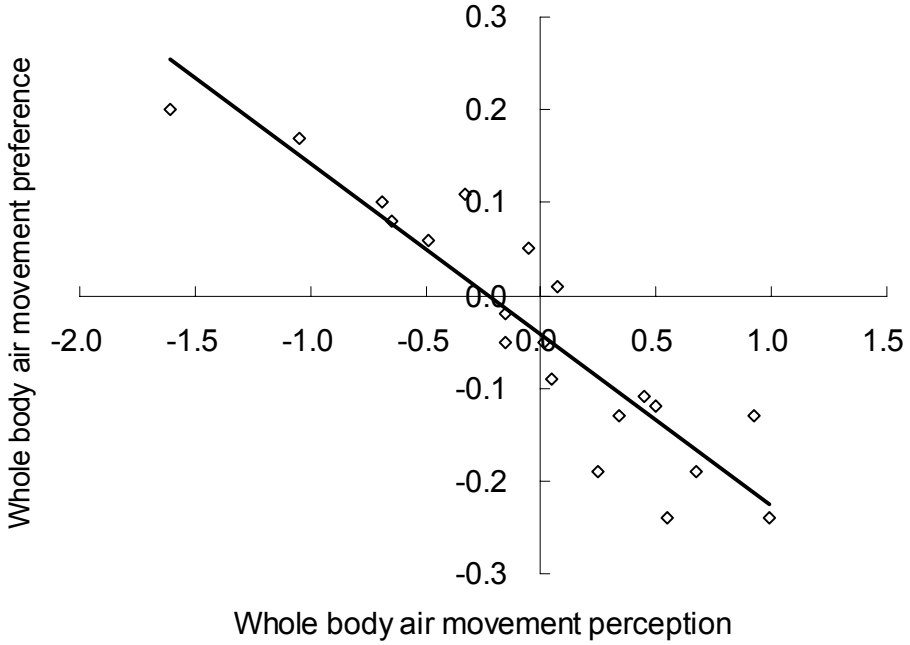

Figure 5.34 Linear regression of whole body air movement preference and whole body air movement perception. Y-axis: -1=less air movement; 0=no change; +1=more air movement. X-axis: -3=much too still; -2=too still; -1=slightly still; 0=just right; 1=slightly breezy; 2=too breezy; 3=much too breezy.

5.4.2 Correlation Analysis between Human Perceptions

The relationship between thermal comfort, thermal sensation and air movement perception, acceptability and preference was studied and the results of the analyses were presented. Each point in the figures represents the mean subjective response obtained for the combinations of personalized airflow rate, personalized temperature and ambient air temperature.

- **Thermal Sensation and Thermal Comfort**

The relationship between the thermal comfort and the local thermal sensation at the face and the thermal comfort vote and the whole body thermal sensation are shown respectively in Figure 5.35 (correlation coefficient 0.53) and Figure 5.36 (correlation coefficient 0.51). Quadratic regression is used to describe the relationships. The analyses reveal that the correlations are not statistically strong. The correlation coefficients are 0.53 and 0.51 respectively. Nevertheless the results in the figures indicate that subjects felt most comfortable when thermal sensation was between 'neutral' and 'slightly cool'. The optimum thermal comfort is examined by utilizing the first derivative of the relationships between whole body thermal sensation and thermal comfort, i.e. d thermal comfort/d thermal sensation. The optimal thermal comfort (0.1) is achieved at whole body thermal sensation of -0.36, i.e. slightly cooler than thermal neutrality.

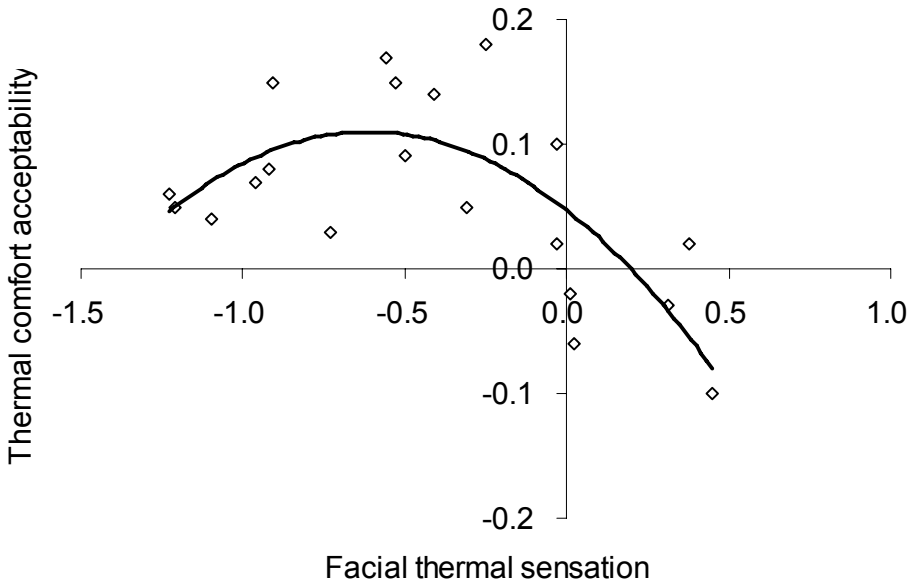

Figure 5.35 Quadratic regression of thermal comfort acceptability and facial thermal sensation. Y-axis: -1=very unacceptable; 0=just unacceptable/acceptable; +1=very acceptable. X-axis: -3=Cold; -2=Cool; -1=Slightly cool; 0=Neutral; 1=Slightly warm; 2=Warm; 3=Hot.

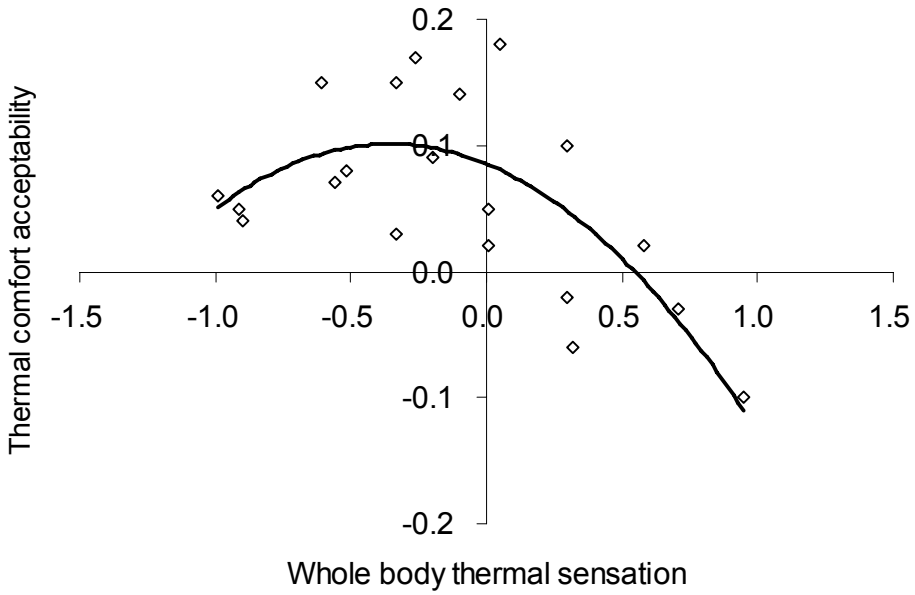

Figure 5.36 Quadratic regression of thermal comfort acceptability and whole body thermal sensation. Y-axis: -1=very unacceptable; 0=just unacceptable/acceptable; +1=very acceptable. X-axis: -3=Cold; -2=Cool; -1=Slightly cool; 0=Neutral; 1=Slightly warm; 2=Warm; 3=Hot.

- **Thermal Sensation and Feeling of Air Movement**

The relationship between air movement perception and thermal sensation, air movement acceptability and thermal sensation and air movement preference and thermal sensation was explored. The analyses were performed for the face and for the whole body. The results presented in Figures 5.37 to 5.42 are discussed below.

Strong correlation (0.86) between facial air movement perception and the facial thermal sensation was identified. The results are shown in Figure 5.37. Each point in the figures stands for the mean subjective response obtained for the combinations of personalized airflow rate, personalized temperature and ambient air temperature. As expected, the subjects felt cooler when they perceived the air movement stronger, i.e. when the convective cooling increased.

The relationship between the air movement perception and the whole body thermal sensation, presented in Figure 5.38 (correlation coefficient 0.92), reveal the same tendency, i.e. the subjects felt cooler when they perceived the air movement stronger.

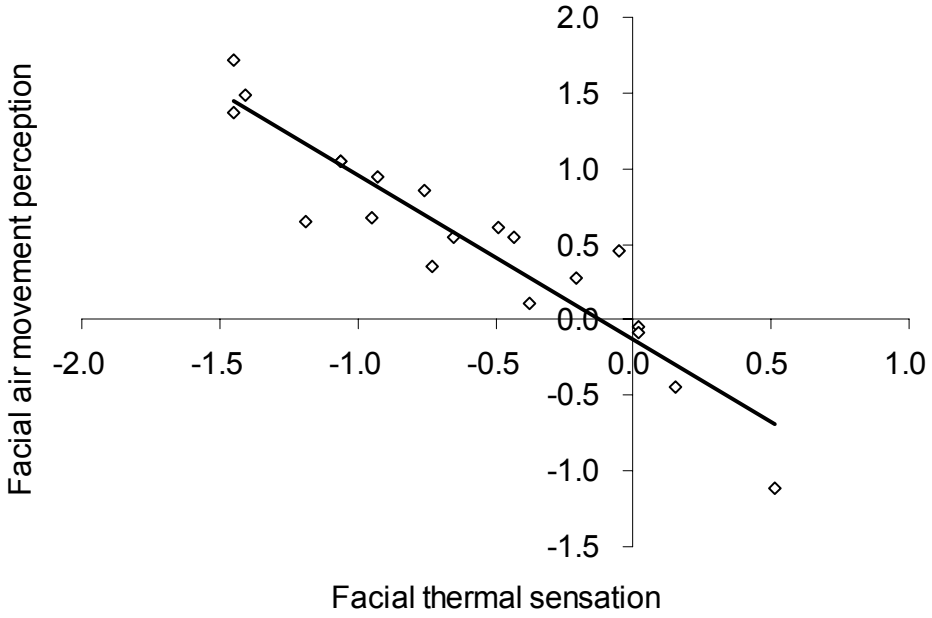

Figure 5.37 Linear regression of facial air movement perception and facial thermal sensation. Y-axis: -3=much too still; -2=too still; -1=slightly still; 0=just right; 1=slightly breezy; 2=too breezy; 3=much too breezy. X-axis: -3=Cold, -2=Cool, -1=Slightly cool, 0=Neutral, 1=Slightly warm, 2=Warm, 3=Hot.

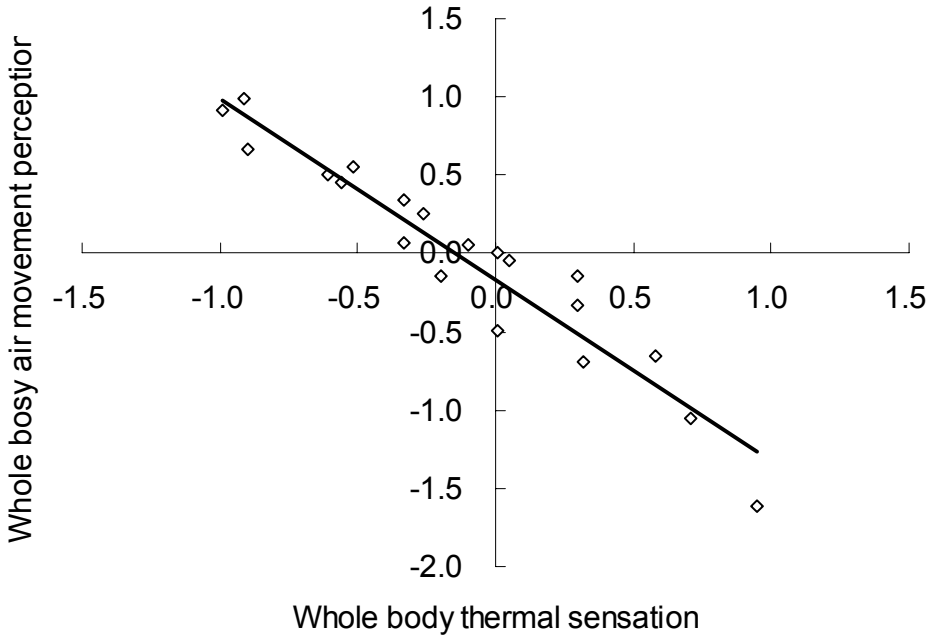

Figure 5.38 Linear regression of whole body air movement perception and whole body thermal sensation. Y-axis: -3=much too still; -2=too still; -1=slightly still; 0=just right; 1=slightly breezy; 2=too breezy; 3=much too breezy. X-axis: -3=Cold; -2=Cool; -1=Slightly cool; 0=Neutral; 1=Slightly warm; 2=Warm; 3=Hot.

The relationship between the facial air movement acceptability and facial thermal sensation was approximated with quadratic regression as shown in Figure 5.39 (correlation coefficient 0.74). Each point in the figures stands for the mean subjective response obtained for the studied combinations of personalized airflow rate, personalized temperature and ambient air temperature. The highest acceptability of the air movement was obtained at the cooler side of the thermal sensation scale, i.e. when subjects felt slightly cool. The first derivative of the relationship shown in the figure defines the maximum air movement acceptability (0.13) when the facial thermal sensation is -0.6 (close to 'slightly cool').

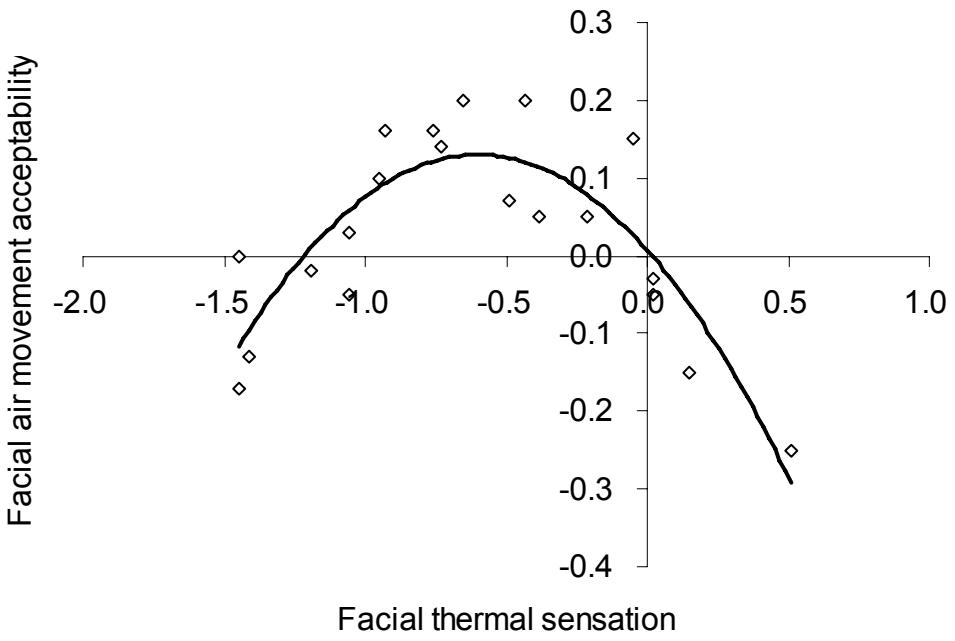

Figure 5.39 Quadratic regression of facial air movement acceptability and facial thermal sensation. Y-axis: -1=very unacceptable; 0=just unacceptable/acceptable; +1=very acceptable. X-axis: -3=Cold; -2=Cool; -1=Slightly cool; 0=Neutral; 1=Slightly warm; 2=Warm; 3=Hot.

The relationship between the whole body air movement acceptability and the whole

body thermal sensation shown in Figure 5.40 (correlation coefficient 0.80) was rather similar to the relationship for face. The highest acceptability of the air movement was also obtained at the cooler side but move towards neutral side slightly on the thermal sensation scale.

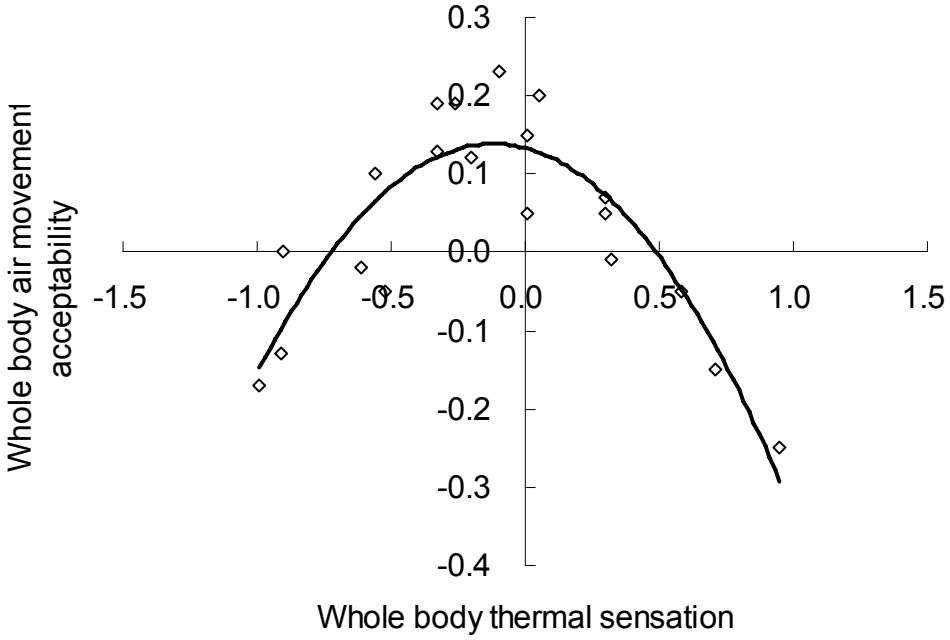

Figure 5.40 Quadratic regression of whole body air movement acceptability and whole body thermal sensation. Y-axis: -1=very unacceptable; 0=just unacceptable/acceptable; +1=very acceptable. X-axis: -3=Cold; -2=Cool; -1=Slightly cool; 0=Neutral; 1=Slightly warm; 2=Warm; 3=Hot.

Correlation between facial/whole body thermal sensation and air movement preference are shown in Figure 5.41 (correlation coefficient 0.81) and Figure 5.42 (correlation coefficient 0.52). The positive correlations show that when subjects feel warm they prefer more air movement. This is consistent with the observation in Figure 5.37 that subjects feel warm and they perceive air movement being still because air movement perception and air movement preference is negatively

correlated (Figure 5.33). Subjects prefer more air movement even when thermal sensation is in cool side (Figure 5.33). Facial thermal sensation is about -0.5 when air movement preference equals to 0 (prefer no change of air movement), and subjects prefer some air movement when facial thermal sensation is 0 (neutral status).

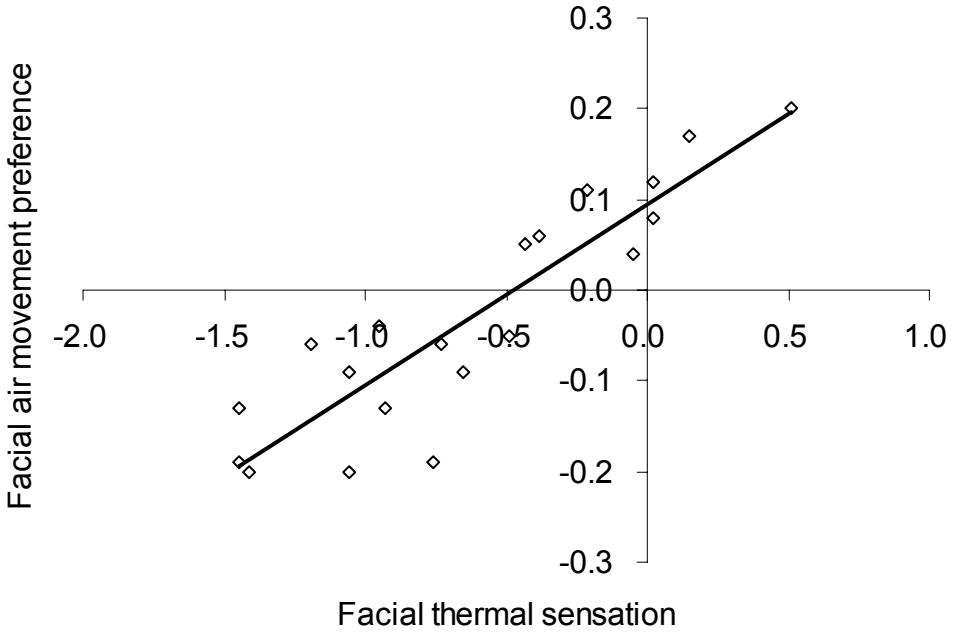

Figure 5.41 Linear regression of facial air movement preference and facial thermal sensation**.** Y-axis: -1=less air movement; 0=no change; +1=more air movement. X-axis: -3=Cold; -2=Cool; -1=Slightly cool; 0=Neutral; 1=Slightly warm; 2=Warm; 3=Hot.

The relationship between the whole body air movement preference and the whole body thermal sensation was explored and is presented in Figure 5.42 (correlation coefficient 0.77). It is observed that subjects prefer less air movement when whole body thermal sensation is in cool side and prefer more air movement when whole body thermal sensation is in warm side.

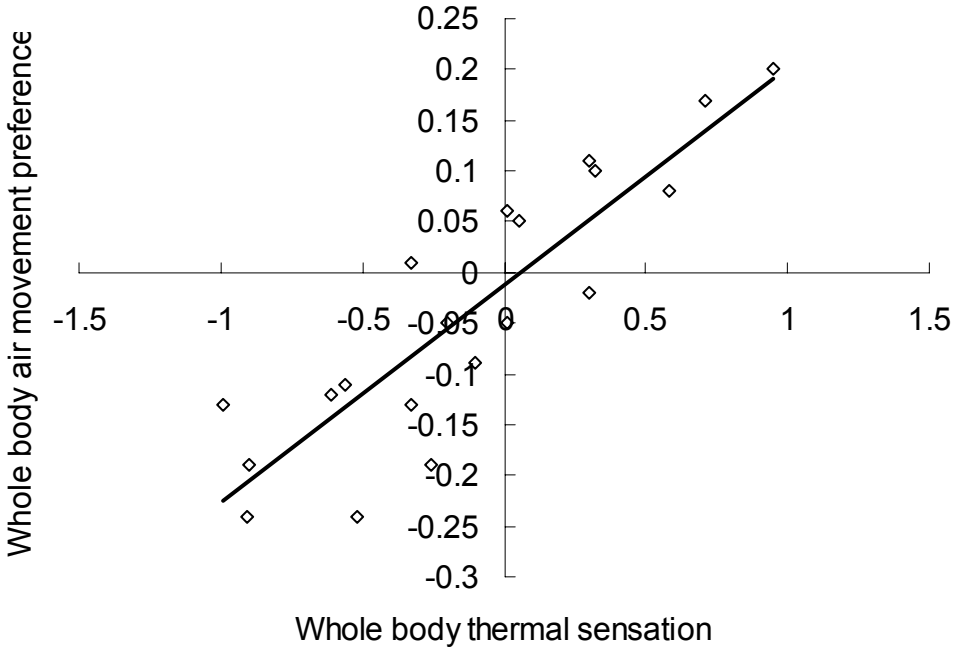

Figure 5.42 Linear regression of whole body air movement preference and whole body thermal sensation. Y-axis: -1=less air movement; 0=no change; +1=more air movement. X-axis: -3=Cold; -2=Cool; -1=Slightly cool; 0=Neutral; 1=Slightly warm; 2=Warm; 3=Hot.)

- **Thermal Comfort Acceptability and Feeling of Air Movement**

The relationship between subjects thermal comfort acceptability and the air movement perception, acceptability and preference was explored. The results are presented in Figures 5.43 (correlation coefficient 0.52), 5.44 (correlation coefficient 0.40) and 5.45 (correlation coefficient 0.58), respectively. Each point in the figures is based on the mean subjective response obtained for the combinations of personalized airflow rate, personalized temperature and ambient air temperature. From Figure 5.43, the optimum value of thermal comfort acceptability appears when air movement perception is between 'just right' and 'slightly breezy'. Positive linear correlation is observed between air movement acceptability and thermal comfort acceptability because both of them are influenced by local air movement as shown in Figure 5.44.

Figure 5.45 demonstrates that the optimum value of thermal comfort acceptability appears when air movement preference is between 'less air movement' and 'no change', which verifies the results from Figure 5.43.

The results of the analyses reveal that the subjects felt thermally most comfortable when they perceived the air movement between "just right" and "slightly breezy". Still or too breezy air movement perception decreased subjects thermal comfort (or acceptability of the thermal environment). Subjects' thermal comfort (acceptability of the thermal environment) increased with the increase of air movement acceptability (Figure 5.44) and was maximum when they reported no change in air movement or slightly less air movement.

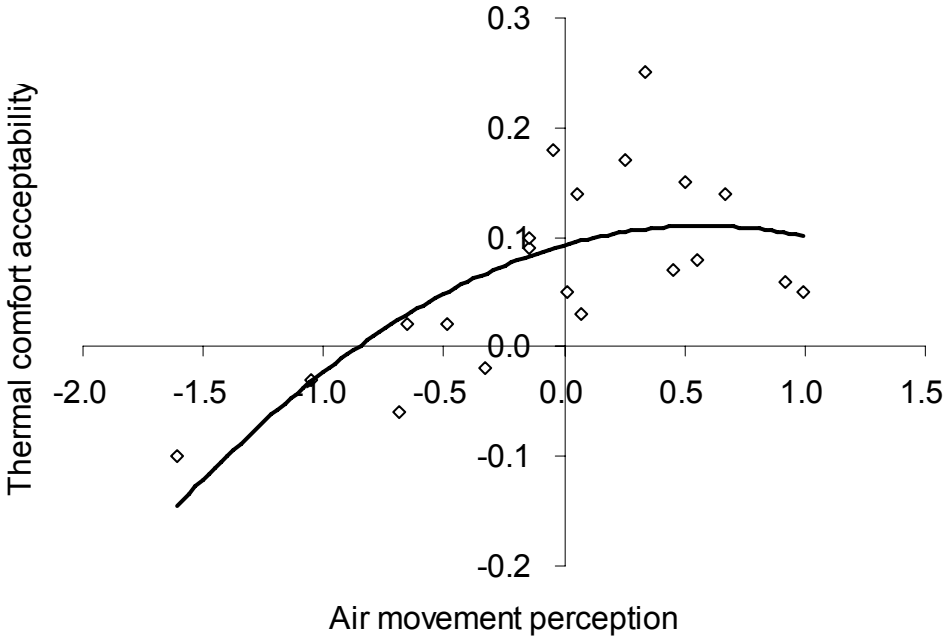

Figure 5.43 Quadratic regression of thermal comfort acceptability and whole body air movement perception. Y-axis: -1=very unacceptable; 0=just unacceptable/acceptable; +1=very acceptable. X-axis: -3=much too still; -2=too still; -1=slightly still; 0=just right; 1=slightly breezy; 2=too breezy; 3=much too breezy.

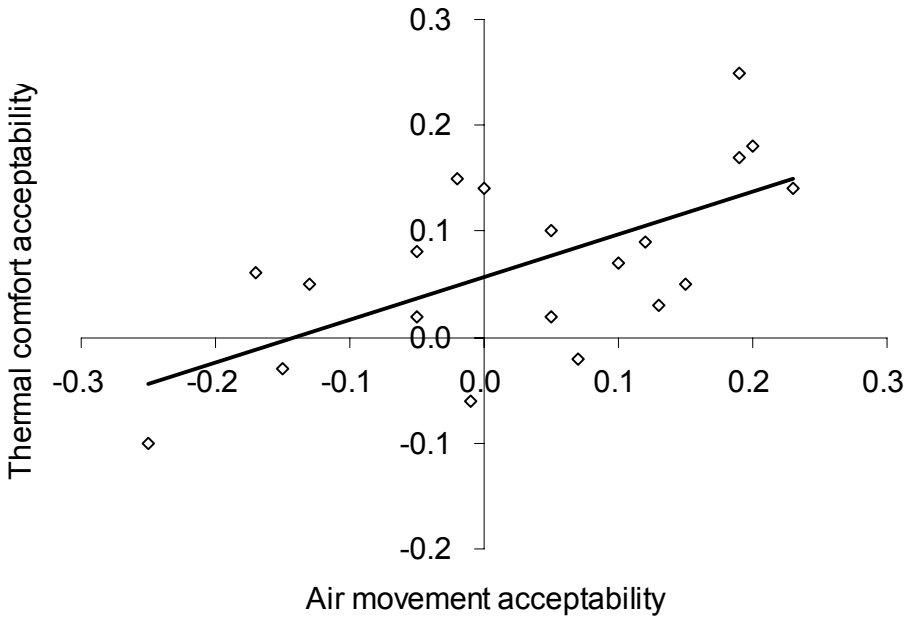

Figure 5.44 Linear regression of thermal comfort acceptability and whole body air movement acceptability. Y-axis and X-axis: -1=very unacceptable; 0=just unacceptable/acceptable; +1=very acceptable.

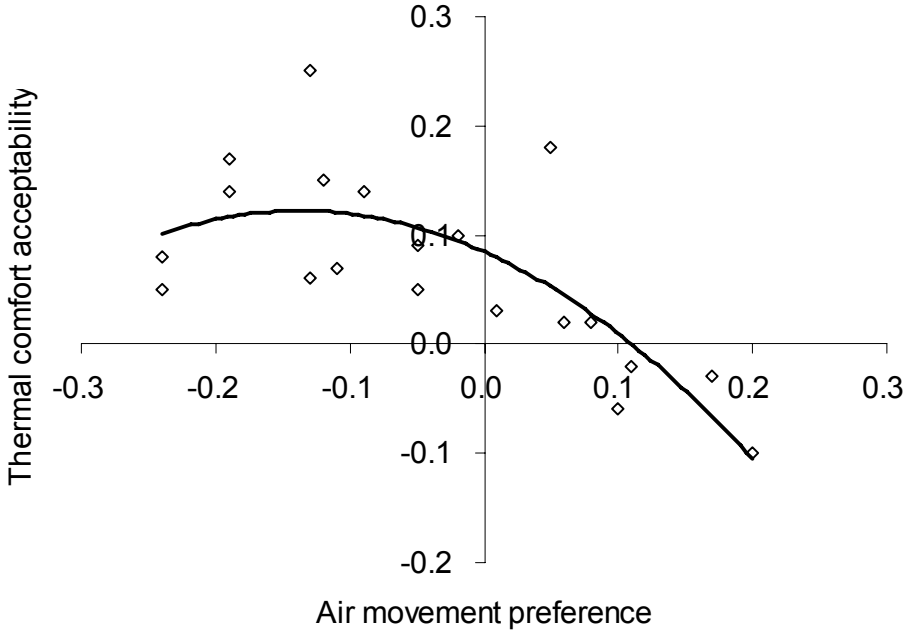

Figure 5.45 Quadratic regression of thermal comfort acceptability and whole body air movement preference. Y-axis: -1=very unacceptable; 0=just unacceptable/acceptable; +1=very acceptable. X-axis: -1=less air movement; 0=no change; +1=more air movement.

5.4.3 Concluding Remarks

The relationships explored between subjects' perception of the thermal environment and air movement reveal that the air movement was optimal when it was perceived between 'just right' and 'slightly breezy'. At this condition, the optimal thermal sensation between 'neutral' and 'slightly cool' was achieved. Stronger air movement caused more cooling while weaker air movement increased the warmth discomfort and thus decreased the acceptability of the thermal environment. However it should be noted that subjects preferred higher air velocity at ambient temperature 26°C and lower air velocity at ambient temperature 23.5°C.

The preference towards 'slightly cool' thermal sensation was identified in this study. This is in consistence with the findings that people in average prefer slightly cooler than neutral temperature (Schiller et. al., 1988). This implies that thermal comfort is not usually at 'neutral' thermal sensation.

5.5 Dissatisfaction due to Air Movement

In previous sections of this report, subjects' perception analyses were based on the mean vote of all subjects. The mean vote is an arithmetric average, which only expresses the general sensation for all subjects as a whole, but it doesn't reveal the percentage of subjects satisfied or dissatisfied with the thermal environment. The percentage of subjects dissatisfied with the thermal environment generated by the ceiling mounted PV ATD at the varied conditions studied is explored in this section. The reasons for dissatisfaction are analyzed. Furthermore the individual preferences for personalized flow rate and the ranges of acceptable and optimal local velocity are

identified.

5.5.1 Percentage Dissatisfied

Before exploring subjects' dissatisfaction with the thermal environment generated by the ceiling PV ATD, the individual preferences for air movement are analyzed. These analyzes are performed for each of the temperature combinations studied and each of the personalized flow rates. The results of these analyses are shown in Figures 5.46-5.50. The distribution of the percentage of subjects with preference for more/no change/less air movement is shown for different PV airflow rates under different temperature combination.

The results in the figures reveal large individual differences among the subjects and justify the need for individual control of at least the personalized flow rate. Nevertheless, general tendency for larger percentage of subjects with preference for less air movement and lower percentage of subjects with preference for more air movement is clear when PV airflow rate increases. At the same PV airflow rate, larger percentage of subjects prefers more air movement when the air temperature increases. Thus the need for individual control for the ceiling mounted PV system especially becomes essential when variations in room air temperature are present.

In all temperature combinations studied, subjects prefer to have the personalized flow provided by the ceiling mounted PV ATD. Only one subject exposed to personalized flow at 4 L/s requested less air movement at the lowest temperature combination of

23.5°C/21°C. This demonstrates the advantage of PV system compared with only mixing ventilation system.

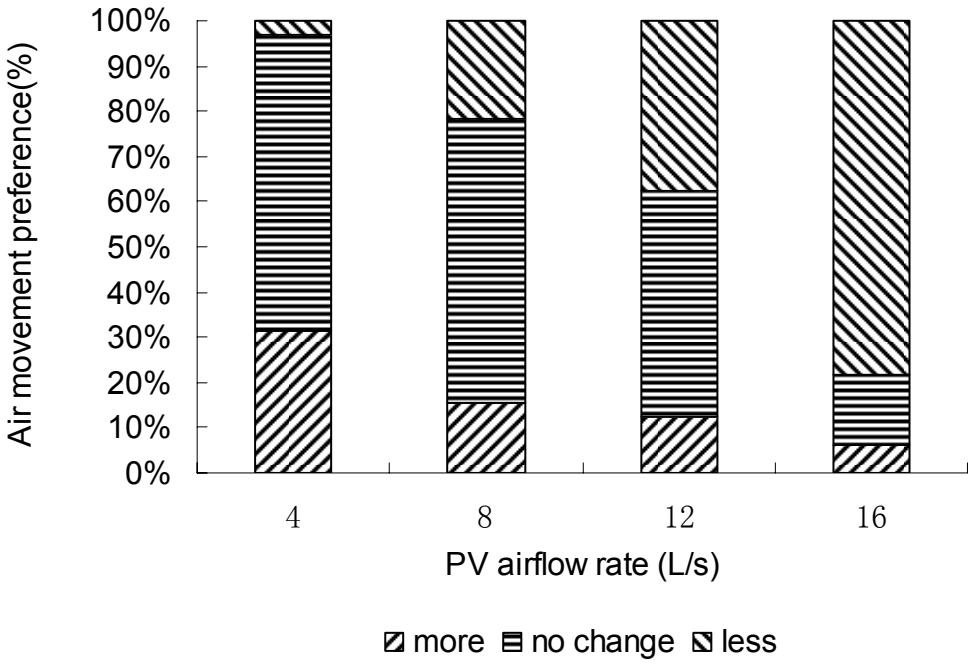

Figure 5.46 Percentage of subjects' air movement preference at 23.5°C/21°C

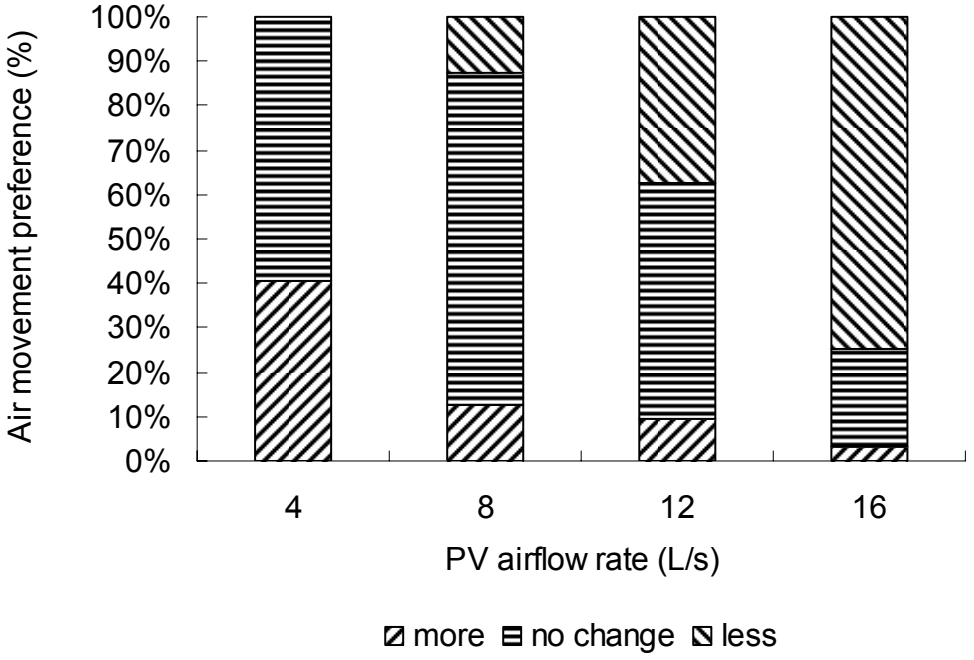

Figure 5.47 Percentage of subjects' air movement preference at 23.5°C/23.5°C

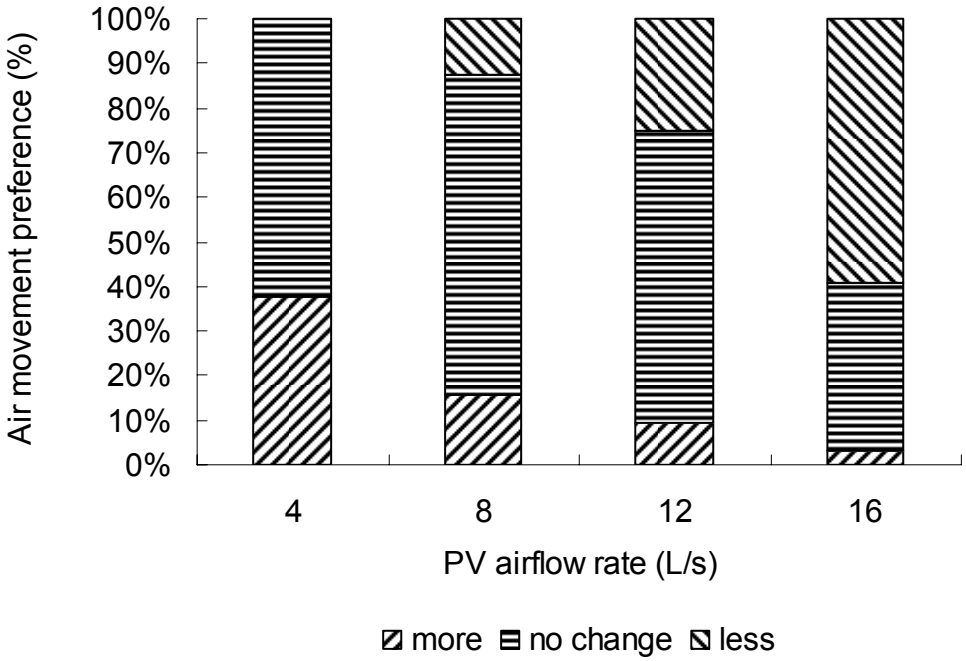

Figure 5.48 Percentage of subjects' air movement preference at 26°C/21°C

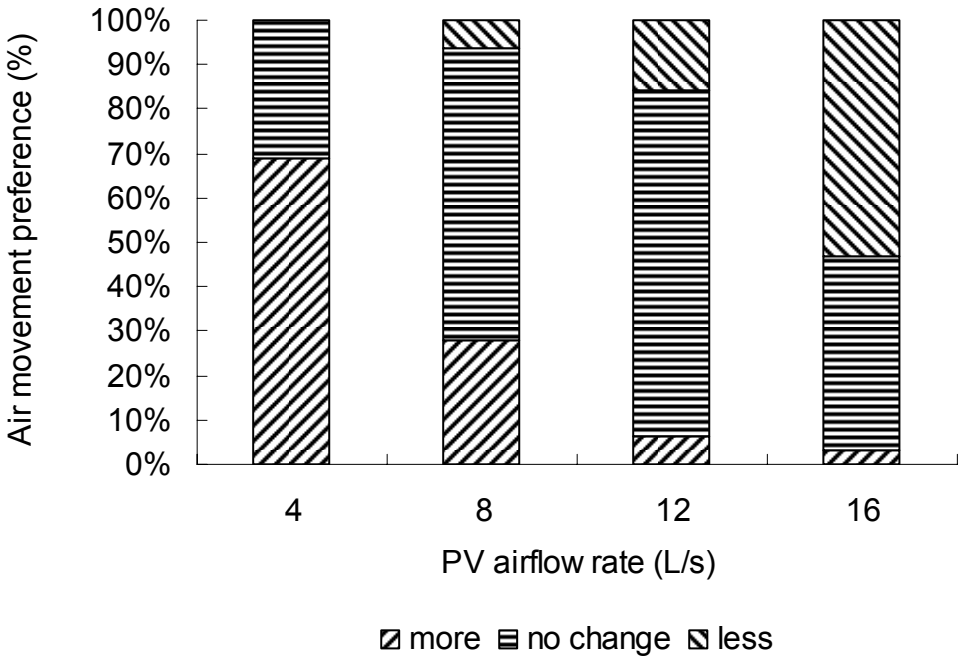

Figure 5.49 Percentage of subjects' air movement preference at 26°C/23.5°C

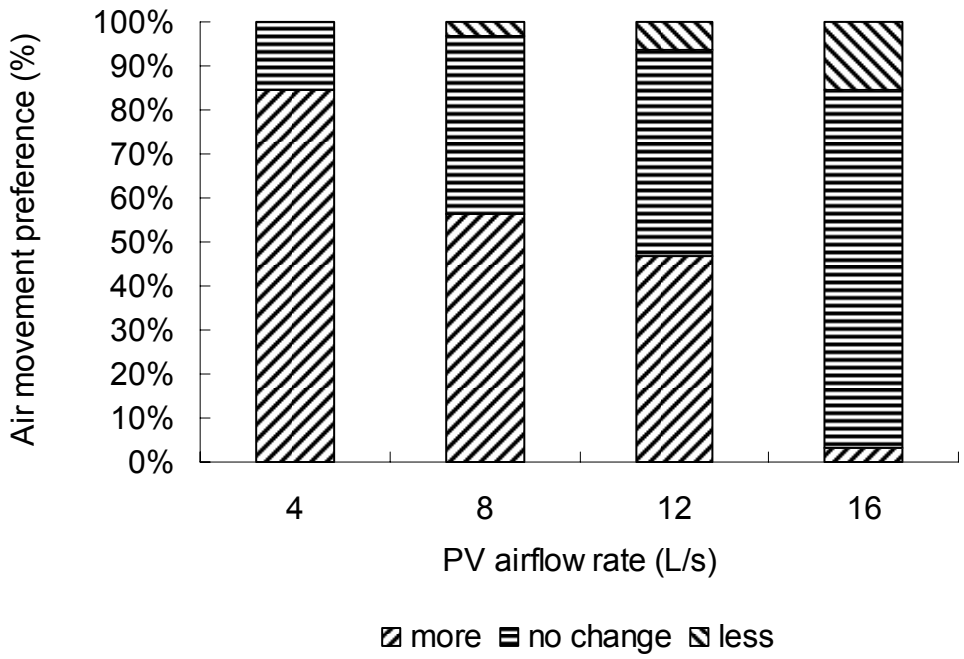

Figure 5.50 Percentage of subjects' air movement preference at 26°C/26°C

Figures 5.51 and 5.52 show the percent dissatisfied, i.e. those who prefer less air movement and those who prefer more air movement, as a function of the PV flow rate. Logarithmic regression is used to illustrate correlation between these quantities.

The percent dissatisfied due to strong air movement (those who prefer less air movement) increases with the increase of the flow rate, i.e. with the increase of the target velocity of the personalized flow (Figure 5.51). The results in the figure show the same trend obtained at different temperature combinations. The percentage of subjects dissatisfied increases with the decrease of the air temperature in the following order of PV and ambient air temperature combination: 23.5°C/21°C, 23.5°C/23.5°C, 26°C/21°C, 26°C/23.5°C, 26°C/26°C.

The percentage of subjects dissatisfied due to too weak air movement (those who

prefer more air movement) decreases with the increase of the flow rate, i.e. with the increase of the target velocity of the personalized flow (Figure 5.52). The results in the figure show the same trend obtained at different temperature combinations. The percentage of subjects dissatisfied increases with the decrease of the air temperature in the following order of PV and ambient air temperature combination: 26°C/26°C, 26°C/23.5°C, 26°C/21°C, 23.5°C/23.5°C, 23.5°C/21°C. The percent dissatisfied is rather similar at the temperature combinations 26°C/21°C, 23.5°C/23.5°C and 23.5°C/21 °C.

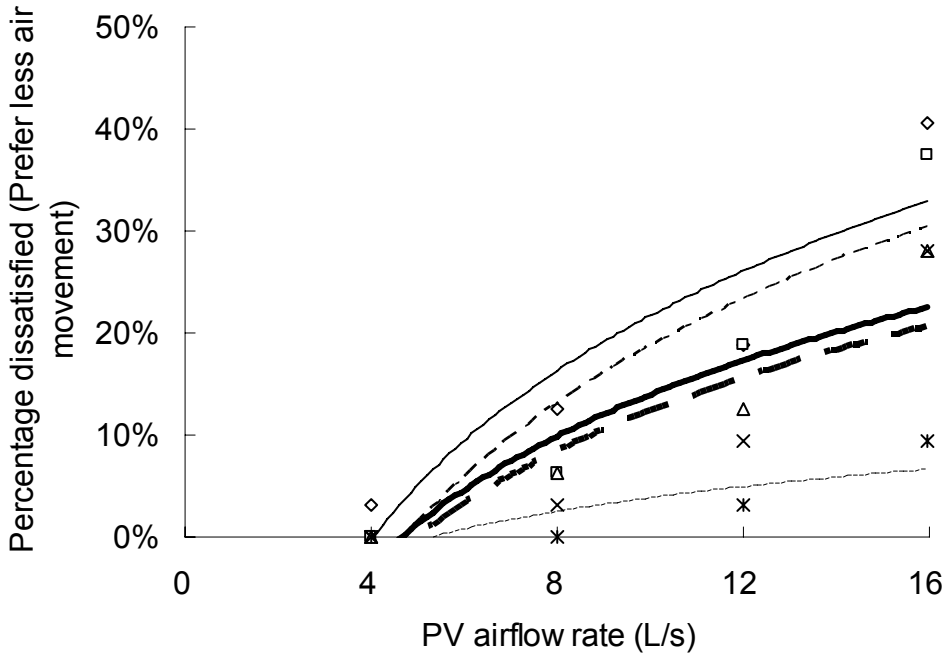

Figure 5.51 Percentage dissatisfied—prefer less air movement

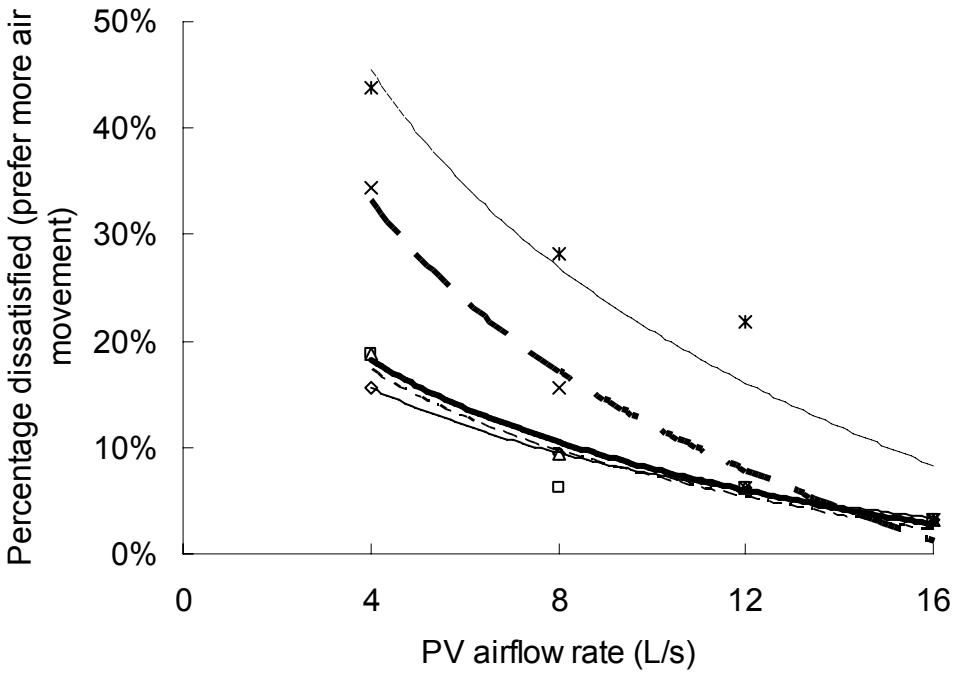

Figure 5.52 Percentage dissatisfied—prefer more air movement

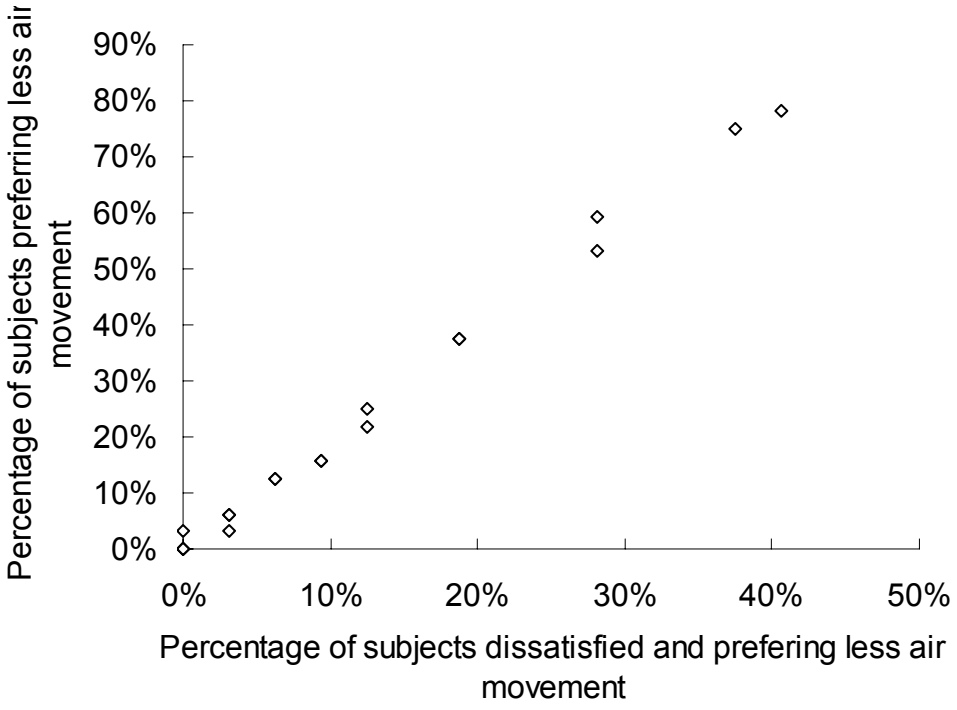

Figure 5.53 Comparison of the percentage of subjects preferring less air movement and the percentage of subjects dissatisfied and preferring less air movement

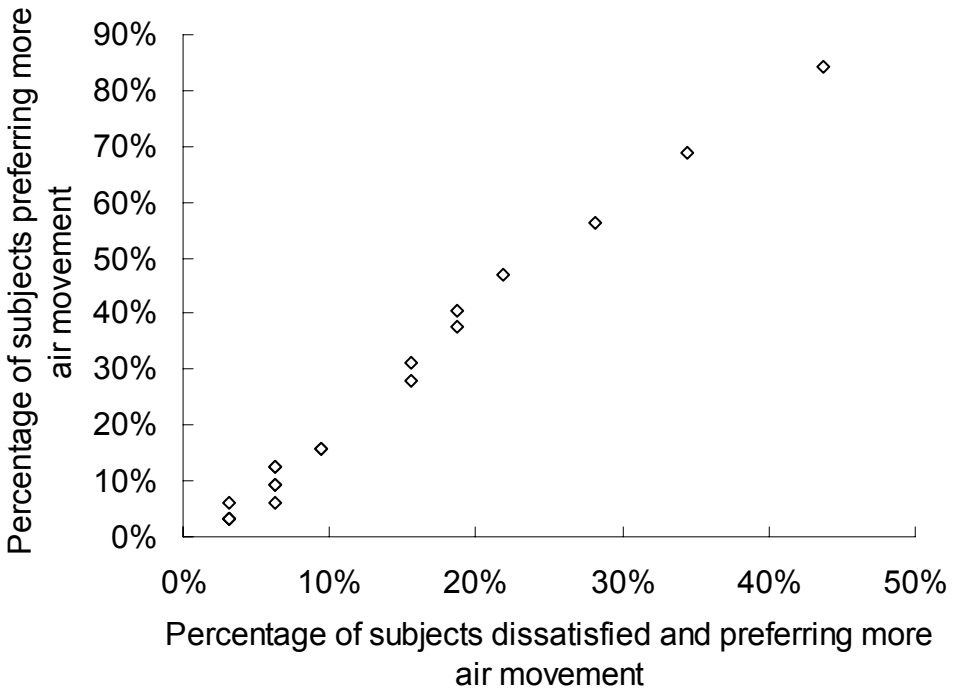

Figure 5.54 Comparison of the percentage of subjects preferring more air movement and the percentage of subjects dissatisfied and preferring more air movement

The relationship between percentage of subjects preferring less/more air movement and percentage of subjects dissatisfied preferring less/more air movement is explored in Figure 5.53 and Figure 5.54, respectively. About 50% of those subjects preferring less/more air movement is dissatisfied and preferred less/more air movement, which is similar as the results from Toftum et. al. (2002) and Gong et. al. (2006).

5.5.2 Final Choice of PV Airflow Rates under Individually Controlled System

The subjects were encouraged to change the workstation and select the one with most preferred personalized flow every 15 minutes. The analyses of the results from the final 15 min (after 1.5 hours) are shown in Figure 5.55. For the lowest temperature combination (23.5°C/21°C), 53% subjects chose 4 L/s PV airflow rate and nobody

chose 16 L/s PV airflow rate. At the temperature combination (26°C/21°C), 34% of the subjects preferred 4 L/s and only 12.5% preferred 4 L/s at 23.5°C/23.5°C. This result shows that the PV air temperature had stronger impact on the final choice of the PV airflow rates compared with room air temperature. The strong impact of the PV air temperature on the preferred flow rate can be seen from the results for 16 L/s: at ambient temperature of 26°C the percentage of subjects who preferred 16 L/s increased from 6% at PV temperature of 21°C to 31% and 56% when the PV air temperature increased to 23.5°C and 26°C respectively. At the same PV air temperature of 21°C, the percentage of subjects choosing 16 L/s PV airflow rate increased from 0 to 6% when room air temperature increased from 23.5°C to 26°C and at PV air temperature of 23.5°C, the percentage of subjects choosing 16 L/s PV airflow rate increased from 19% to 31% when room air temperature increased from 23.5°C to 26°C. These results confirm that the PV air temperature had more influence on the final choice of the PV airflow rates compared with room air temperature.

As the subjects made their final choice of PV airflow rates by experiencing the conditions at each of the workstations with different personalized airflow rates almost all of them found the local air movement acceptable. Only one subject preferred air movement more than generated at the workstation with 16 L/s PV airflow rate at all temperature combinations. One subject preferred air movement less than 4 L/s at the lowest temperature combination (23.5°C/21°C).

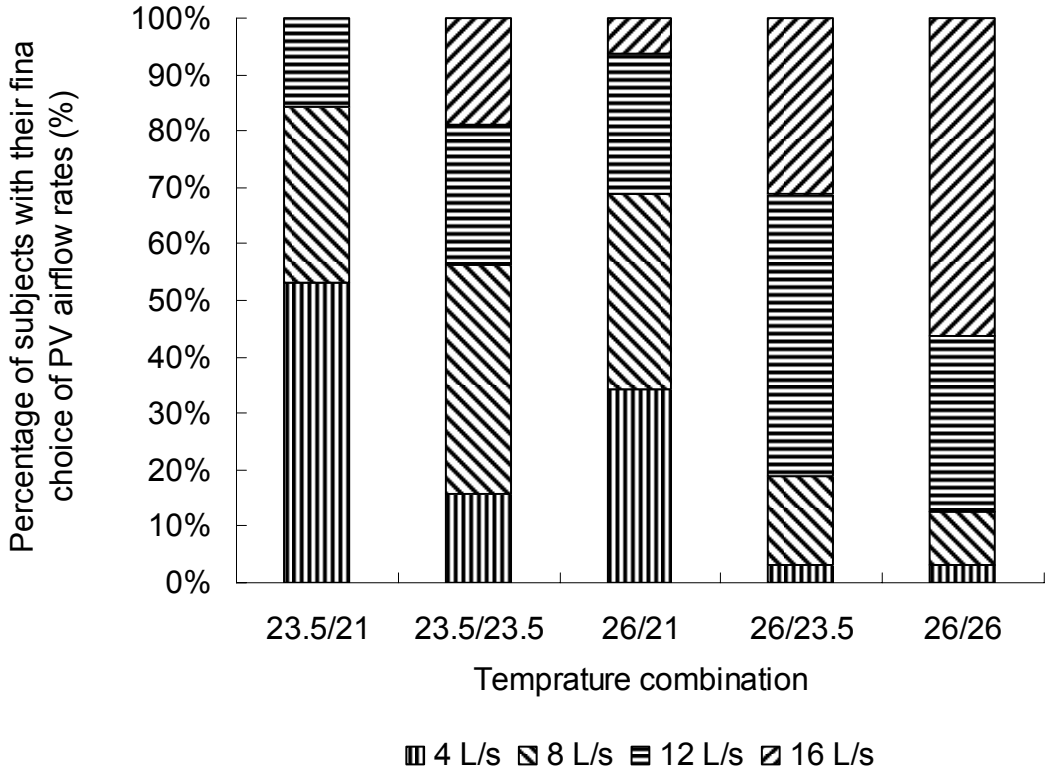

Figure 5.55 Percentage of subjects with their final choice of PV airflow rates

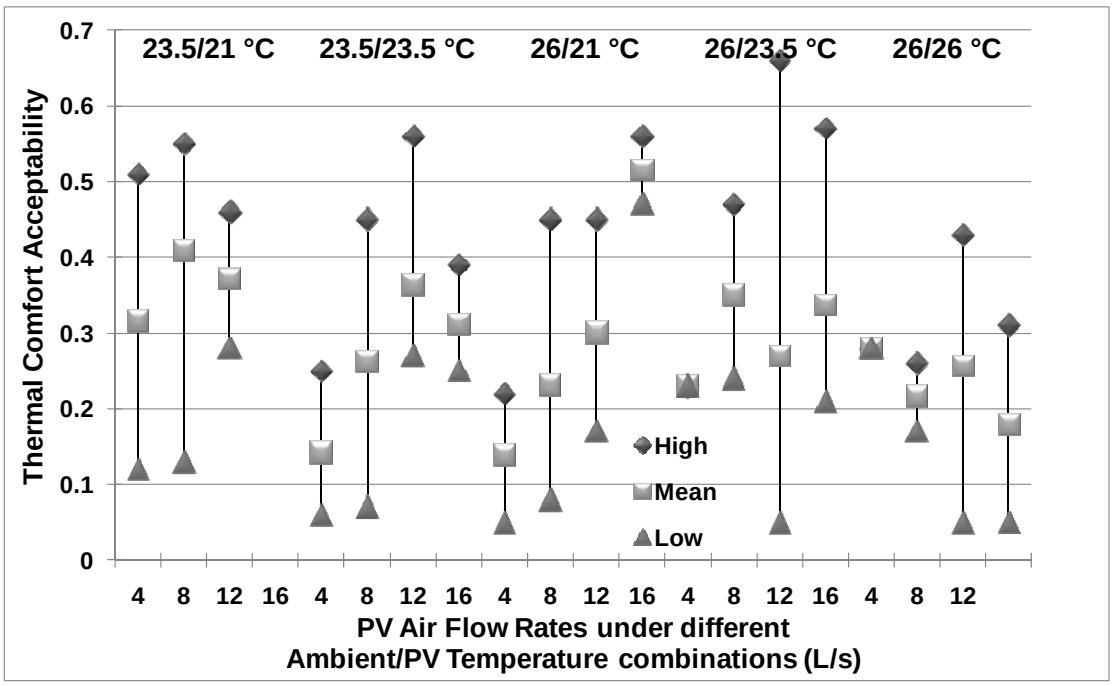

Figure 5.56 Maximum, minimum and mean values of thermal comfort acceptability based on subjects' final choice. Y-axis: -1=very unacceptable; 0=just unacceptable/acceptable; +1=very acceptable.

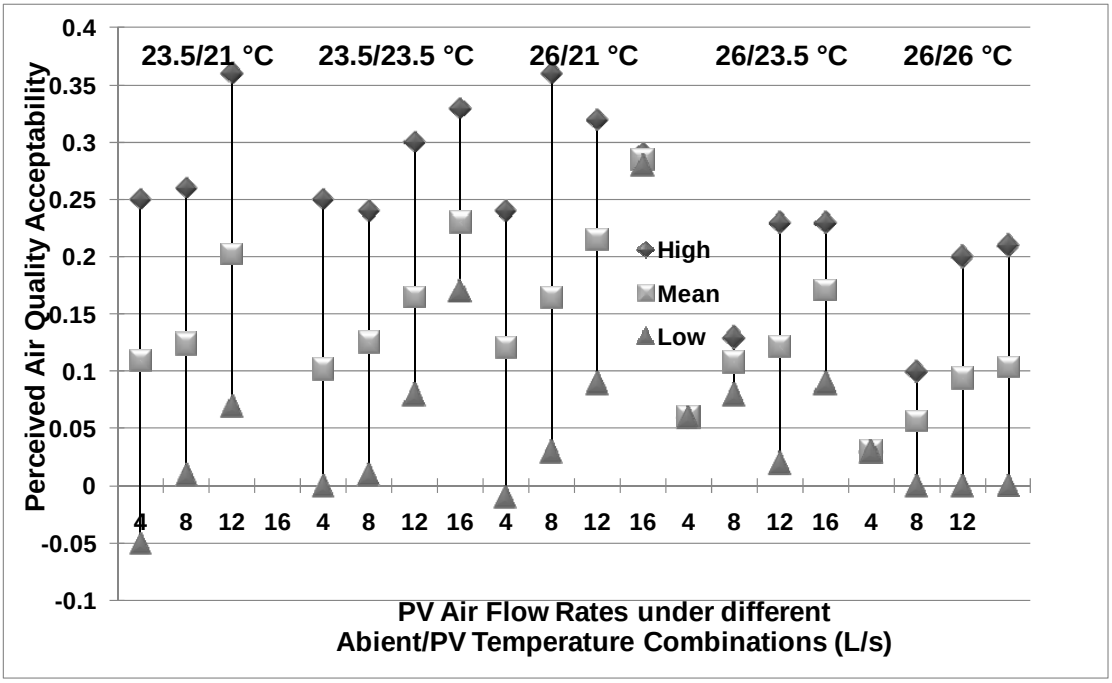

Figure 5.57 Maximum, minimum and mean values of perceived air quality acceptability based on subjects' final choice. Y-axis: -1=very unacceptable; 0=just unacceptable/acceptable; +1=very acceptable.

Based on the subjects' final choice of PV airflow rates under the different temperature combinations, the acceptability of the thermal environment and perceived air quality were analyzed. The maximum, minimum and mean values of these two quantities based on subjects' final choice at the different temperature combinations are presented in Figures 5.56 and 5.57 respectively. The acceptability scales for the thermal environment and for the perceived air quality is: "VERY UNACCEPTABLE" (-1) at the worst end of the scale and "VERY ACCEPTABLE" (+1) at the best end of the scale. 0 can be seen as neutral or "JUST RIGHT". The thermal comfort acceptability was found to be good and the average value varied from 0.14 to 0.52 under different final choice of PV airflow rates and temperature combinations. Inhaled air quality was also acceptable and the average values varied from 0.03 to 0.29 under different final choice of PV airflow rates and temperature combinations. At 16 L/s PV airflow rate

and 26°C room air temperature, average values of thermal comfort acceptability decreases from 0.52 through 0.34 to 0.18 when PV air temperature increases from 21°C through 23.5°C to 26°C. At 26°C (cases 26°C/23.5°C and 26°C/26°C) and 4 L/s the average value of inhaled air quality acceptability decreased strikingly to about 0.1. Possible reason can be the relatively high temperature of the inhaled air because the personalized flow was not strong enough to penetrate the thermal plume.

In order to understand individual preferences for facial air movement and PV airflow rates, the results of the subjects' thermal comfort and inhaled quality acceptability based on their final choice of PV airflow rates are analyzed as presented in Tables 5.11 and 5.12 respectively. Each row in the tables indicates a particular subject assessment and preference across different ambient and PV air temperature combinations. It is clearly observed that occupants with higher acceptability for thermal comfort and inhaled air quality under low PV airflow rates with low temperature combination are inclined to prefer either the same or slightly higher PV airflow rates under the next higher temperature combination, although the acceptability may reduce. The results from Tables 5.11 and 5.12 also indicate that the responses of subjects for thermal comfort and inhaled air quality follow similar trends.

Table 5.11 Thermal comfort acceptability based on final choice of PV airflow rates under different temperature combinations (based on subject number)

	23.5°C/21°C				23.5°C/23.5°C				26°C/21°C				26°C/23.5°C				26°C/26°C			
Subject No.	**4**	**8**	**12**	**16**	**4**	**8**	**12**	**16**	**4**	**8**	**12**	**16**	**4**	**8**	**12**	**16**	**4**	**8**	**12**	**16**
11	0.51				0.25				0.22				0.23				0.28			
22	0.51				0.19				0.21					0.47				0.26		
14	0.46				0.14				0.18					0.43				0.22		
29	0.46				0.07				0.17					0.28					0.43	
23	0.43				0.06				0.15					0.33				0.17		
1	0.39					0.38			0.12						0.38				0.32	
6	0.36					0.45			0.13					0.24					0.34	
8	0.35					0.34			0.09						0.36				0.27	
26	0.33					0.32			0.13						0.66				0.29	
18	0.28					0.31			0.08						0.36				0.26	
30	0.26					0.3			0.05						0.29				0.25	
4	0.25					0.29				0.45					0.28				0.22	
25	0.23					0.27				0.37					0.27				0.13	
21	0.17					0.25				0.26					0.26				0.05	
32	0.15					0.23				0.24					0.25					0.31
7	0.12					0.11				0.23					0.24					0.31
20	0.12					0.09				0.22					0.22					0.27
17		0.55				0.07				0.2					0.21					0.24
2		0.52					0.35			0.13					0.13					0.23
5		0.5					0.38			0.19					0.17					0.21

10	0.48			0.43		0.18			0.18	0.29
13	0.47			0.56		0.08			0.05	0.18
24	0.4			0.33			0.45		0.57	0.17
28	0.39			0.29			0.34		0.41	0.16
19	0.37			0.27			0.31		0.39	0.16
3	0.28			0.3			0.33		0.37	0.14
15	0.13				0.39		0.29		0.36	0.15
31		0.46			0.36		0.28		0.31	0.12
12		0.4			0.31		0.23		0.25	0.07
16		0.37			0.29		0.17		0.28	0.09
27		0.35			0.27			0.56	0.22	0.07
9		0.28			0.25			0.47	0.21	0.05

Note: -1=very unacceptable, 0=just unacceptable/acceptable, +1=very acceptable

Table 5.12 Inhaled air quality acceptability based on final choice of PV airflow rates under different temperature combinations (based on subject number)

	23.5°C/21°C				23.5°C/23.5°C				26°C/21°C				26°C/23.5°C				26°C/26°C			
Subject No.	**4**	**8**	**12**	**16**	**4**	**8**	**12**	**16**	**4**	**8**	**12**	**16**	**4**	**8**	**12**	**16**	**4**	**8**	**12**	**16**
22	0.25				0.25				0.24					0.13				0.1		
11	0.24				0.13				0.22				0.06				0.03			
14	0.21				0.07				0.16					0.12				0.07		
23	0.2				0.06				0.14					0.12				0		
29	0.18				0				0.13					0.08					0.13	
6	0.17					0.24			0.12					0.09					0.2	
8	0.13					0.22			0.11						0.23				0.13	
1	0.12					0.21			0.09						0.19				0.12	
18	0.11					0.14			0.08						0.15				0.11	
26	0.09					0.13			0.05						0.19				0.11	
30	0.06					0.13			-0.01						0.14				0.05	
4	0.05					0.12				0.36					0.13				0.05	
25	0.04					0.11				0.24					0.13				0.04	
21	0.03					0.11				0.22					0.12				0	
7	0.02					0.09				0.21					0.12					0.21
32	-0.05					0.05				0.15					0.11					0.19
17		0.26				0.01				0.14					0.1					0.16
10		0.22					0.3			0.14					0.08					0.14
13		0.18					0.24			0.09					0.1					0.15
5		0.17					0.23			0.07					0.04					0.13

2	0.14			0.15		0.03			0.02			0.11
3	0.09			0.12			0.32			0.23		0.11
19	0.06			0.09			0.23			0.2		0.08
28	0.06			0.11			0.27			0.21		0.08
24	0.05			0.08			0.22			0.19		0.08
16	0.01				0.33		0.22			0.18		0.08
12		0.36			0.26		0.19			0.19		0.08
15		0.28			0.22		0.18			0.17		0.06
31		0.16			0.21		0.09			0.14		0.02
9		0.14			0.19			0.29		0.11		0.01
27		0.07			0.17			0.28		0.09		0

Note: -1=very unacceptable, 0=just unacceptable/acceptable, +1=very acceptable

5.5.3 Individual analysis under different exposed conditions

In order to evaluate the process for each subject to make his/her final choice of PV flow rates, subjects' options for PV airflow rates and corresponding preferences at different time points are analyzed (Appendix 8). During the process of subjects changing their options, it is quite common that subjects preferring more air movement at previous time point will change to the workstation with higher PV airflow rate at the next time point, and vice versa. In the make-up session, subjects will choose more/less air movement if the PV airflow rate in this session is lower/higher than their final choice. For the final choice of their PV airflow rate, they prefer no change for air movement. The acceptability of both thermal comfort and air quality are also analyzed during this process (Appendix 6 and 7). Obvious trends are demonstrated for the acceptability of both thermal comfort and air quality that acceptability increases when subjects move towards their final choice of PV airflow rate.

5.5.4 Optimum Velocity and Acceptable Velocity Range

The results obtained on the percentage of subjects dissatisfied with the air movement as presented in Figures 5.51 and 5.52 were analyzed and quadratic regression was used to obtain the optimum PV airflow rate and optimal flow rate range. The results shown in Figure 5.58 for the temperature combinations studied reveal that the percentage dissatisfied first decreases, reaches a minimum and starts to increase when the PV airflow rate increases. There is an optimum PV airflow rate corresponding to a minimum percent dissatisfied for each of the temperature combinations. The optimum PV airflow rates are derived from first derivative of the regression equation and are listed in Table 5.13. If the optimum airflow rate is out of the range of 0-16 L/s, the

value will be set as this limit value. The optimum PV airflow rates increase when air temperature increases.

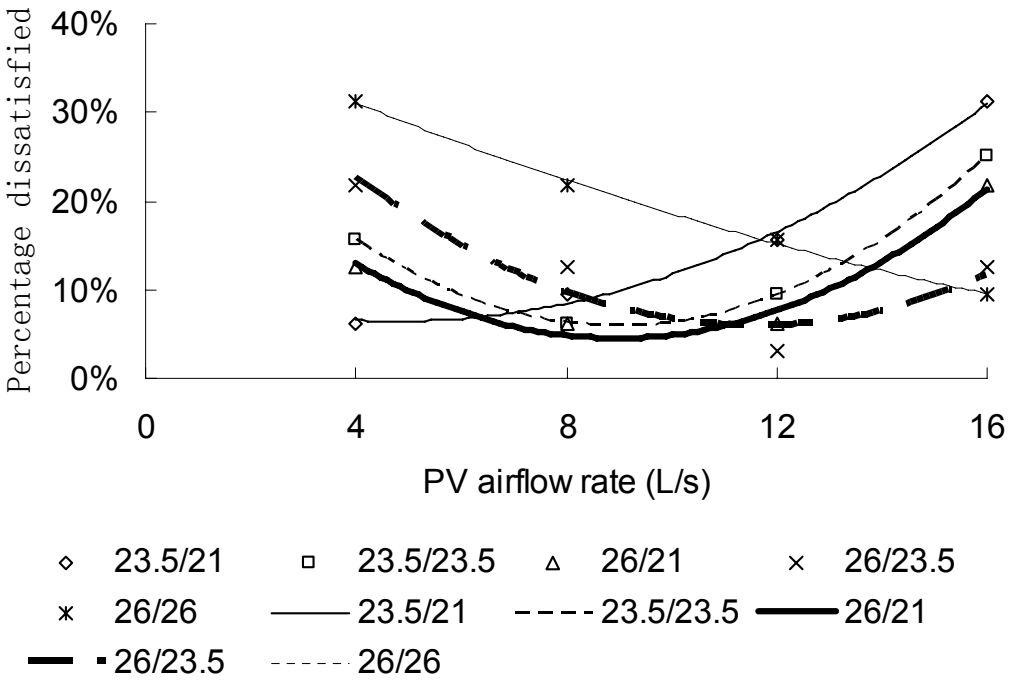

Figure 5.58 Quadratic regression of Percentage dissatisfied and PV airflow rate

Table 5.13 Optimum PV airflow rate and range

Experimental condition (°C)	23.5/21	23.5/23.5	26/21	26/23.5	26/26
Optimum PV airflow rate (L/s)	4.7	9	9	11.7	16
Most acceptable range of PV airflow rate (L/s)	0-11.2	4.2-13.9	3.4-9.6	6.0-16.0	12.3-16.0

The most acceptable range of the PV airflow rate for the temperature combinations studied was explored. The range was determined by applying the criteria that at least 85% of the subjects (in accordance with the limit of 15% dissatisfied occupants recommended in ASHRAE standard 55 2004) should be satisfied with the air movement. The range is derived by starting from an airflow that has the most satisfied votes. If the flow rate with its adjacent velocity can satisfy at least 85% of all subjects,

the range is extended to include the two velocities. If not, responses at other adjacent velocities are examined again. If the flow is out of the range of 0-16 L/s, the value will be set as limit value. The results are shown in Table 5.13, which demonstrates that the range moves to higher velocities when temperature increases. Compared with the study of conventional PV system in the Tropics (Gong et. al., 2006), the range span has become large. The optimum PV airflow rates under different temperature combinations vary from 4.7 L/s to 16L/s. At this range of personalized flow rate the velocity at the target area (the head of the manikin) ranged from 0.3 m/s to 1m/s. This result is important for design and implementation in practice of PV with ceiling mounted ATD.

Chapter 6: Energy Saving Potential and Effect of Control Strategy of Ceiling Mounted PV System

The results presented in the earlier chapters show that ceiling mounted PV system can improve thermal sensation and perceived air quality, which pave the way for saving air conditioning energy. A warmer space temperature, such as 26 °C, accompanied by a PV supply air temperature of 23.5 °C, implies that space cooling load is reduced by spot cooling in comparison when a space temperature is maintained at 23.5 °C by total volume mixing ventilation only. As a result of improving perceived air quality, less outdoor air is utilized to maintain a certain degree of air quality. This implies potential for saving cooling and dehumidifying energy of outdoor air especially for hot and humid climate.

In practice, individual control for PV airflow rate will be provided to each human occupant. Occupants can change PV airflow rate based on their preference. Some workstations are sometimes not occupied and these workstations will be switched off. These scenarios will cause different consumption of energy for air cooling and air transportation.

6.1 Definition of Control Strategies

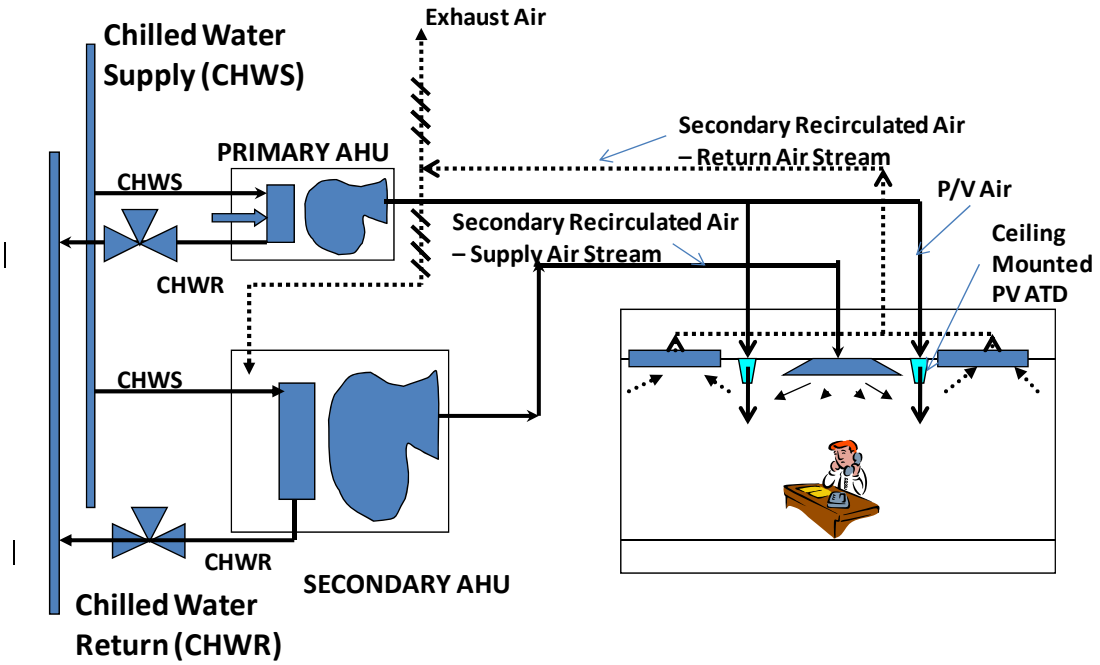

Figure 6.1 Air conditioning and air distribution system in field environmental chamber

The aim of this study is to evaluate energy saving potential of ceiling mounted PV system in conjunction with mixing ventilation compared with mixing ventilation system alone as well as compared with mixing ventilation system combined with desk fans for generating more air movement at each desk individually (if required). The energy calculations are performed through a simulated study based on the specifications of the field environmental chamber (FEC) at the National University of Singapore. The design conditions in Singapore are used during the analyses. The FEC is employed with 16 ceiling mounted PV ATDs that are aimed to provide personal control to 16 occupants in 16 work stations. PV Air is conditioned by using Primary AHU (Figure 6.1). There are 6 supply air diffusers for supplying ambient air. Air is conditioned by using Secondary AHU. The basis for the energy analysis is a simulation of different configurations of PV ATDs and occupant density and the

following three different control strategies are employed:

- Control Strategy 1: 10 effective PV ATDs, with 9L/s PV airflow rate for each one. This represents the presence of 10 occupants and each using a moderate PV airflow rate which, in this case, is also representative of typically recommended ventilation rate of 9 L/s.
- Control Strategy 2: 10 effective PV ATDs, with 4.5L/s PV airflow rate for each one. This represents a practical situation where some occupants prefer higher PV airflow rates and others prefer lower PV airflow rates.
- Control Strategy 3: All 16 PV ATDs, with 9L/s PV airflow rate for each one. This represents a situation when the PV system designed for the FEC is operating at a peak condition where all 16 PV ATDs are effective and each supplying 9 L/s PV airflow rate.

The various cases under different control strategies are shown in Table 6.1.

6.2 Energy Saving Potential

The three different control strategies are analyzed to simulate individual control and the variation in the effective number of PV ATDs in operation. Under each strategy, the case of PV in conjunction with MV at elevated ambient room temperature 26 °C is compared with cases of MV used alone to keep the room temperature at 26 °C or MV alone to keep the room temperature either at 26 °C or at 28 °C but with additional individually controlled desk fan at each desk to generate elevated air movement for occupants' thermal comfort. The supply temperature of the personalized air is 23.5°C.

6.2.1 Description of Cooling Loads in the Field Environmental Chamber

The field environmental chamber has a floor area of 84 m^2 (11.7 m by 7.2 m) and a height of 2.7 m. The external wall is constructed with plaster and brick and the external window is covered with dark black coating. Assuming no temperature difference between different internal zones, there is no heat transfer through internal walls, ceiling and floor. Thermal load from building envelope is listed in Table 6.2. For control strategy 1 and 2, there are 10 persons with 125 W total heat generated by each person. For control strategy 3, there are 16 persons with 125 W total heat generated by each person. There are 63 ceiling lamps with 18 W heat generated by each lamp. The intensity of equipment load is 15 W/m^2.

6.2.2 Design Parameters

Outdoor design condition is 32°C and 80% relative humidity. Room temperatures are kept at 28°C, 26°C and 23.5°C respectively. Room relative humidity is kept constant at 50%. For PV case in Control strategy 1, 10 PV ATDs are in operation with 9 L/s flow rate for each one. Ambient airflow rate is kept constant at 810 L/s. Ambient room temperature is kept at 26 °C and PV air is supplied at 23.5°C. For MV cases alone or with additional fans in Control strategy 1, the total supply airflow rate is kept constant at 900 L/s with 90 L/s outdoor air supply. For PV case in Control strategy 2, 10 PV ATDs are in operation with 4.5 L/s flow rate for each one. Ambient airflow rate is kept constant at 855 L/s. Ambient room temperature is kept at 26 °C and PV air is supplied at 23.5°C. For MV cases alone or with additional fans in Control strategy 2, the total supply airflow rate is kept constant at 900 L/s with 45 L/s outdoor air supply.

For PV case in Control strategy 3, 16 PV ATDs are in operation with 9 L/s flow rate for each one. Ambient airflow rate is kept constant at 756 L/s. Ambient room temperature is kept at 26 °C and PV air is supplied at 23.5°C. For MV cases alone or with additional fans in Control strategy 3, the total supply airflow rate is kept constant at 900 L/s with 144 L/s outdoor air supply. Each desk fan with 30 W power will be supplied for each occupant.

6.2.3 Energy Consumption

6.2.3.1 Cooling Energy Consumption for Air Conditioning

Cooling energy consumption for air conditioning is calculated for each case of control strategy 1 as shown in Table 6.3 as an example. Comparing case 1 and 3 under control strategy 1, cooling energy consumptions are the same when same room conditions are kept (temperature and relative humidity). When room air temperature is increased to 28°C or decreased to 23.5°C, cooling energy consumption will increase or decrease correspondingly. Cooling energy consumption will not be affected by PV air supply temperature.

Table 6.1 Various cases studied

Case	Control Strategy 1	No. of operating PV ATDs	PV airflow rate in each ATD(L/s)	Total PV airflow rate(L/s)	MV airflow rate(L/s)
1	26°C/23.5°C (PV)	10	9	90	810
2	23.5°C (MV)				900
3	26 (MV)+desk fans				900
4	28°C (MV)+desk fans				900
Case	Control Strategy 2	No. of operating PV ATDs	PV airflow rate in each ATD(L/s)	Total PV airflow rate(L/s)	MV airflow rate(L/s)
1	26°C/23.5°C (PV)	10	4.5	45	855
2	23.5°C (MV)				900
3	26 (MV)+desk fans				900
4	28°C (MV)+desk fans				900
Case	Control Strategy 3	No. of operating PV ATDs	PV airflow rate in each ATD(L/s)	Total PV airflow rate(L/s)	MV airflow rate(L/s)
1	26°C/23.5°C (PV)	16	9	144	756
2	23.5°C (MV)				900
3	26 (MV)+desk fans				900
4	28°C (MV)+desk fans				900

Table 6.2 Thermal load

	T_{room}=28°C	T_{room}=26°C	T_{room}=23.5°C
Building envelope (W)	235	353	500
Occupants (W)	1250/2000	1250/2000	1250/2000
Lighting (W)	1134	1134	1134
Equipment (W)	1264	1264	1264
Total (W)	3883/4633	4001/4751	4148/4898
Total intensity (W/m^2)	46.2/55.2	47.6/56.6	49.4/58.3

Table 6.3 Cooling energy consumption for air conditioning under control strategy 1

No.	Cases	$T_{outdoor}$ (°C)	$RH_{outdoor}$	T_{indoor} (°C)	RH_{indoor}	Q_{pv} (L/s)	$Q_{ambient}$ (L/s)	Q_{mv} (L/s)	E_{pv} (W)	$E_{ambient}$ (W)	E_{total} (W)
1	26°C/23.5°C (PV)	32	80%	26	50%	90	810		2700	5836	8536
2	23.5°C (MV)	32	80%	23.5	50%			900			9331
3	26 (MV)+desk fans	32	80%	26	50%			900			8536
4	28°C (MV)+desk fans	32	80%	28	50%			900			7879

Table 6.4 Transport energy consumption under control strategy 1

	PV flowrate (m^3/s)	ATD	Flowrate for each ATD (m^3/s)	Duct D (m)	v(m/s)	Fan power (W)	MV Flowrate (m^3/s)	ATD	Flowrate for each ATD (m^3/s)	Duct D (m)	v(m/s)	Fan power (W)	Desk fan (W)	Total (W)
1	0.09	10	0.009	0.1	1.15	100	0.81	6	0.135	0.3	1.91	45	0	145
2	0	0	0			0	0.9	6	0.15	0.3	2.12	50	0	50
3	0	0	0			0	0.9	6	0.15	0.3	2.12	50	300	350
4	0	0	0			0	0.9	6	0.15	0.3	2.12	50	300	350

6.2.3.2 Transport Energy Consumption

For MV cases, a total of 900L/s mixed air is supplied. Air is conditioned by using Secondary AHU (Figure 6.1). There are 6 supply air diffusers, each supplying 150 L/s mixed air.

For PV cases, the total airflow rate is also 900L/s but it consists of two parts, PV air and ambient air. By taking control strategy 1 as an example, each ATD supplies 9 L/s airflow for PV air. 10 PV ATDs are activated. PV Air is conditioned by using Primary AHU. Corresponding ambient airflow rate is 810L/s so as to maintain the same total airflow rate. Corresponding transport energy consumptions are listed in Table 6.4.

Transport energy consumption for PV air is much higher than that of ambient air. The reason is because airflow velocity in PV air duct is much higher, which causes high flow resistance.

6.2.3.3 Total Energy Consumption

The total energy consumption for the cases that are compared includes electrical energy consumption for air conditioning, energy consumption for transport of air and desk fan energy consumption. Based on a conventional COP of a chiller, its performance is estimated to be 0.6 kW/Ton. The power consumption by desk fan is 30W. By taking control strategy 1 as an example, corresponding total energy consumptions for different cases are listed in Table 6.5.

Table 6.5 Total energy consumption under control strategy 1

	$E_{cooling}$ (W)	$E_{electricity}$ (W)	$E_{transport}$ (W)	$E_{desk\ fan}$ (W)	E_{total} (W)
26°C/23.5°C (PV)	8536	1463	145	0	1608
23.5°C (MV)	9331	1600	50	0	1650
26°C (MV)+desk fans	8536	1463	50	300	1813
28°C (MV)+desk fans	7879	1351	50	300	1701

6.2.4 Energy Saving Potential Analysis

Figure 6.2 compares energy consumption for the cases studied under control strategy 1. By comparing 23.5°C MV and 26°C/23.5°C PV it can be seen that increasing room temperature can save cooling energy. Cooling effect will almost remain the same by local cooling from ceiling mounted PV. Although transport energy increases, total energy can still be saved. Comparing case 26°C /23.5°C PV with case 26°C MV+desk fans, ceiling mounted PV can not only realize better cooling effect but also save total energy consumption. Total energy consumption for MV+ desk fans case is still higher than that of 26°C /23.5°C PV case even though the room temperature is increased to 28°C. Compared with MV or MV+desk fans, total energy savings can be realized by using ceiling mounted PV system.

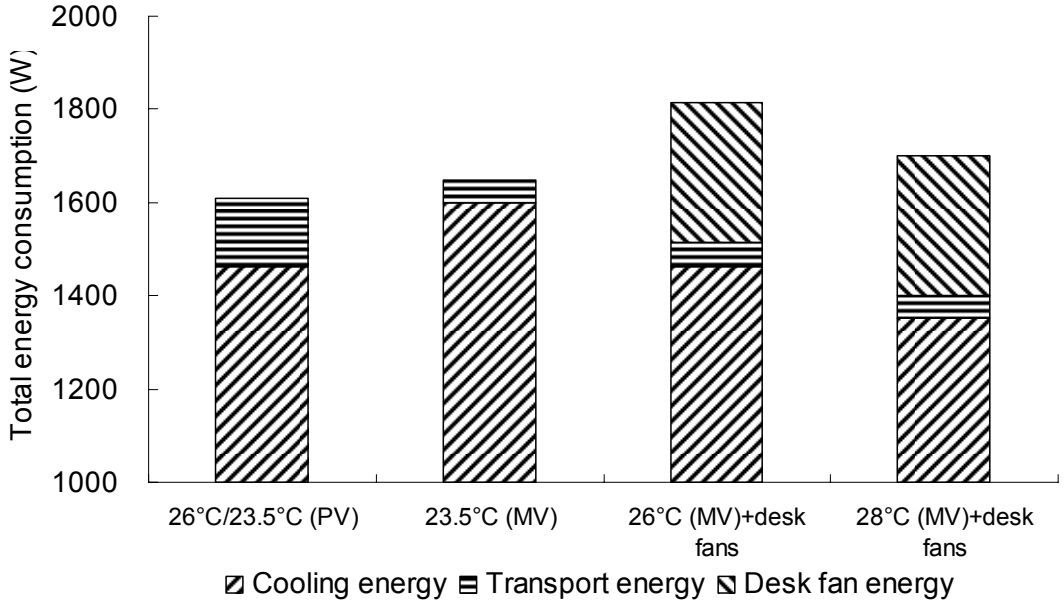

Figure 6.2 Total energy consumption for different cases under control strategy 1 (9L/s PV airflow rate, 10 ATDs)

The analyses of the other two control strategies are carried out in the same manner as that of the control strategy 1. Control strategy 2 supplies 4.5 L/s PV airflow rate through each of the 10 PV ATDs to simulate individual control from human occupants. Control strategy 3 supplies 9 L/s PV airflow rate through each of the 16 PV ATDs to simulate the case with more PV ATDs in operation.

As a result, control strategy 2 with 4.5 L/s PV air supply in each ATD is calculated. 10 PV ATDs are used. Total airflow rate is kept constant at 900L/s. This will provide a basis for evaluating the performance when the PV flow rate is controlled manually or automatically. Corresponding total energy consumptions are shown in Figure 6.3.

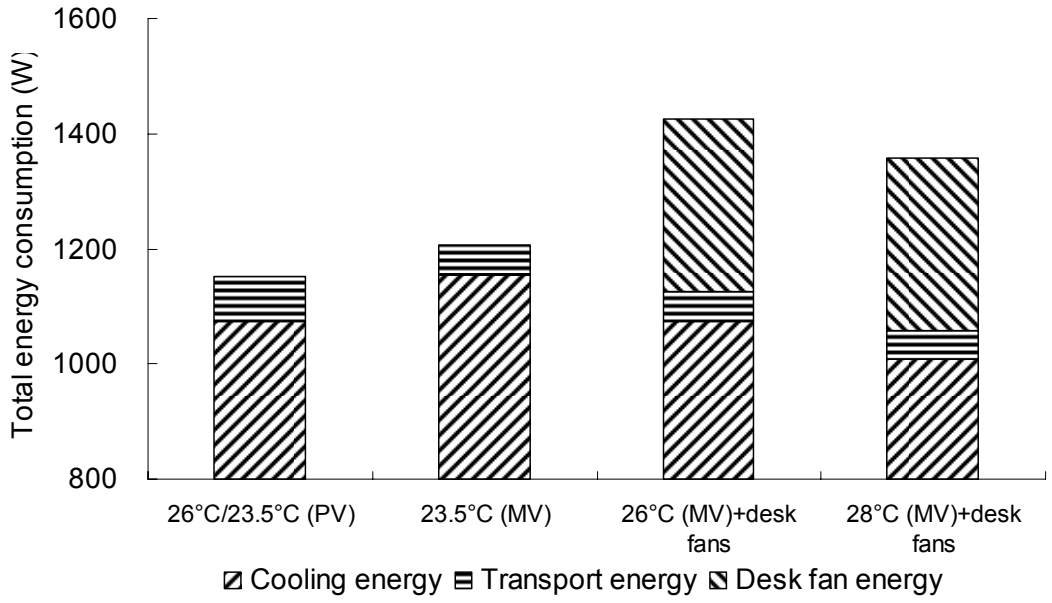

Figure 6.3 Total energy consumption for different cases under control strategy 2 (4.5L/s PV airflow rate, 10 ATDs)

Control strategy using 16 PV ATDs is also analyzed for comparison. Each ATD supplies 9 L/s personalized air. Total airflow rate is also kept constant at 900L/s. Corresponding total energy consumptions are shown in Figure 6.4.

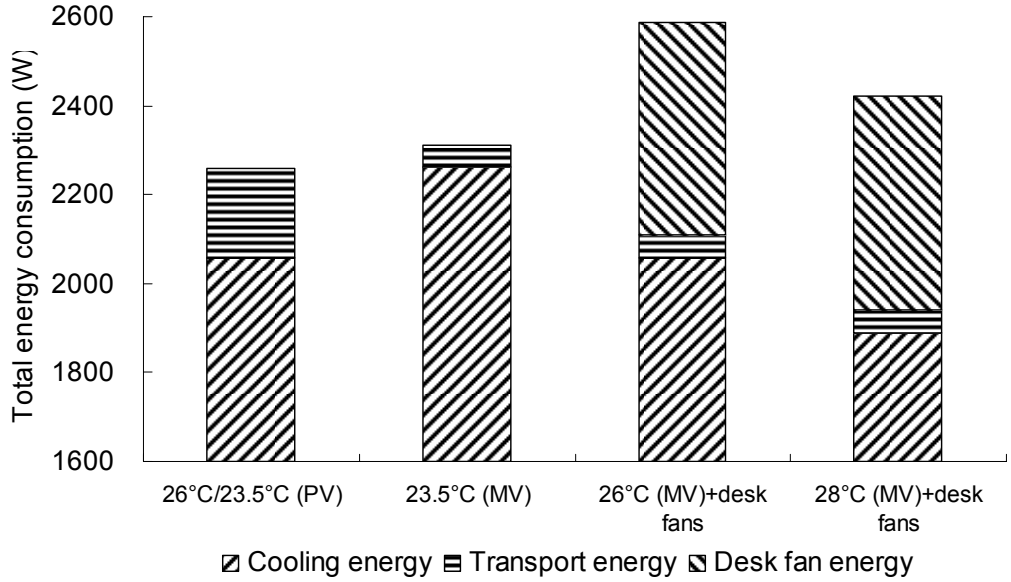

Figure 6.4 Total energy consumption for different cases under control strategy 3 (9L/s PV airflow rate, 16 ATDs)

For both control strategy 2 and 3, it is observed by comparing 23.5°C MV and 26°C/23.5°C PV (Figure 6.3, Figure 6.4) that increasing room temperature can save cooling energy. Cooling effect will almost remain the same by local cooling from ceiling mounted PV. Although transport energy increases, total energy can still be saved. Comparing case 26°C /23.5°C PV with case 26°C MV+desk fans, ceiling mounted PV can not only realize better cooling effect but also save total energy consumption. Total energy consumption for MV+ desk fans case is still higher than that of 26°C /23.5°C PV case even though the room temperature is increased to 28°C.

Comparing different cases under control strategy 2 with corresponding cases under control strategy 1, both cooling energy and transport energy are reduced because of reduced outdoor airflow rate. Comparing different cases under control strategy 3 with corresponding cases under base case, energy consumption increases for all components of total energy consumption.

Chapter 7: Conclusion and Recommendation

7.1 Review and Achievement of Research Objectives

The performance of newly developed ceiling mounted personalized ventilation system was studied in complementing objective and subjective experiments under well defined laboratory conditions. The objectives of the research and the results obtained are summarized as follows.

- **First Objective**

The first objective was to evaluate the performance of a prototype of PV with ceiling mounted ATD, with emphasis being placed on the characteristics of the generated personalized flow and its interaction with the human body as an obstacle and the thermal plume generated when it was heated, on its local and whole body cooling effect, inhaled air temperature and inhaled air quality.

During this study, the human body was simulated with a full scale breathing thermal manikin. The experiments were performed at personalized flow rate of 4, 8, 12 and 16 L/s and five combinations of ambient air temperature and personalized air temperature, respectively 23.5°C/21°C, 23.5°C/23.5°C, 26°C/21°C, 26°C/23.5°C, 26°C/26°C.

The most important conclusions of this part of the study are summarized as follows:

- The blocking effect of the unheated manikin's body was identified to be up to 0.2 m above manikin's head for the studied flow rates. The corresponding reduction

ratio of centerline velocity was 85%;

- The neutral level, X_{nl}, defined as the vertical distance from the nozzle to the point where the impact of the thermal plume on the velocity distribution in the personalized airflow begins to be observed increased from 0.8 m to 1.1 m with the increase of personalized airflow rate. Under the set-up used in the present study (nozzle diameter 0.095m and distance between the nozzle and the manikin's head of 1.3 m), the personalized airflow at 16 l/s was strong enough to destroy completely the thermal plume generated by the heated manikin and to efficiently provide cooling to manikin's body;
- Head region of the manikin (left/right sculls and face, and back of neck) is the body segment most cooled by the personalized flow. The local cooling increased with the increase of the personalized flow rate and with the decrease of the air temperature. For the flow rate (4, 8, 12 and 16 L/s) and combinations of personalized air temperature/ambient air temperature studied the local cooling was equivalent to decrease of air temperature in uniform environment (with low velocity) from -1°C to -6°C at 23.5°C/21°C and from -0.5°C to -4°C at 26°C/26°C case. The temperature of the personalized air had stronger impact of the local cooling of the head than the ambient air temperature. The lower part of the body was less cooled by the personalized airflow;
- The cooling effect of the personalized airflow for the whole body was smaller and equivalent to decrease of air temperature in uniform environment from -0.25°C to -2°C at 23.5°C/21°C and from -0.1°C to -1.5°C at 26°C/26°C. The influence of personalized air temperature was stronger than the influence of the ambient temperature.
- Personalized airflow rate was the most important factor which influences the body

cooling;

- Typical body movement at workplace with ceiling mounted PV ATD will cause asymmetry in the body cooling by the personalized airflow and may in practice cause local draught discomfort. The whole body cooling effect of the personalized airflow is minimal when the body is moved forward;
- The ceiling mounted PV ATD improved the inhaled air quality in comparison with the total volume mixing ventilation. The portion of clean personalized air in inhaled air increased from 6% to almost 14% when the flow rate increased from 4 L/s to 16 L/s. The inhaled air temperature decreased with the increase of the PV airflow rate and with the decrease of its temperature. Therefore it may be expected that the ceiling mounted PV ATD will improve occupants' perceived air quality.

- **Second Objective**

The second objective was to investigate the responses from tropically-acclimatized subjects to the local environment created with ceiling mounted PV system, with emphasis being placed on thermal sensation, air movement perception, acceptability and preference, perceived air temperature and perceived air quality.

The temperature combinations were the same as during the thermal manikin experiments. The subject were encouraged to choose the preferred workplace among 4 workplaces which differed only by the supplied personalized flow rate being respectively 4, 8, 12 and 16 L/s.

The most important conclusions of this part of the study are summarized as follows:

- The maximum acceptability of the thermal environment (average for the 32 subjects participating in the experiments) was obtained when the average thermal sensation was between 'neutral' and 'slightly cool'. This thermal sensation was achieved when the flow was perceived as "just right" or "slightly breezy". Stronger air movement caused more cooling while weaker air movement increased the warmth discomfort decreased the acceptability of the thermal environment.
- The optimal flow rate at which the lowest percentage of dissatisfied subjects was obtained increased from 4.7 L/s at 23.5°C/21°C to 16 L/s at 26°C/26°C, providing target velocity at the head of 0.32 m/s and 1 m/s respectively;
- The local and whole body thermal sensation, air movement perception, preference and acceptability were correlated with the PV airflow rate and the air temperature. The thermal sensation and the air movement preference decreased and the air movement perception increased when the PV flow rate increased and the air temperature decreased. The PV flow rate at which the maximum acceptability was obtained increased with the increase of the air temperature.
- The perceived air quality and the freshness of the inhaled air increased and the perceived inhaled air temperature decreased with an increasing of the flow rate and a reduction of the air temperature.
- The whole body thermal sensation and the local thermal sensation were significantly correlated. The air movement perception and preference were correlated with the thermal sensation;
- Large differences between the subjects were identified with regard to the preferred air movement at the same air temperature. The preferences for no change in air movement were reported at each of the four PV flow rates (4, 8, 12,16 L/s) for the

whole range of air temperature studied;

- The range of most acceptable PV airflow rate (85% satisfied subjects) increased with the increase of the air temperature and was more influenced by the PV air temperature and less by the room air temperature.
- The PV with ceiling mounted ATD has potential to improve perceived I inhaled air quality of the occupants by providing cleaner and cooler air to inhalation.
- In all temperature combinations studied, subjects preferred to have the personalized flow provided by the ceiling mounted PV ATD. Only one subject exposed to personalized flow at 4 L/s requested less air movement at the lowest temperature combination of 23.5°C/21°C. This demonstrates the advantage of PV system compared with only mixing ventilation system.

- **Third Objective**

The third objective was to evaluate energy saving potential of ceiling mounted PV system in conjunction with background mixing ventilation compared with mixing ventilation system alone and with mixing ventilation system when occupants are provided with individually controlled desk fans for generating additional air movement at each desk. Energy calculation is based on design conditions in Singapore.

The most important conclusions of this part of the study are summarized as follows:

- Increasing room temperature can save cooling energy. Cooling effect will keep almost the same by local cooling from ceiling mounted PV comparing ceiling

mounted PV with MV. Although transport energy increases, total energy still can be saved by elevating room temperature and use of ceiling mounted PV nozzles.

- Comparing ceiling mounted PV with MV plus desk fans, ceiling mounted PV can not only realize better cooling effect but also save total energy consumption.

- **Fourth Objective**

The fourth objective is to evaluate control strategy of ceiling mounted PV system. Control strategy is discussed when different number of PV ATD is used or different PV airflow rate is supplied from PV ATDs.

The most important conclusions of this part of the study are summarized as follows:

- When outdoor airflow rate is reduced, both cooling energy and transport energy are reduced. When more PV ATDs are used, energy consumption increases for all components of total energy consumption.

7.2 Recommendations

Based on the findings from this study, the following recommendations are drawn for practical applications.

- Design range of target velocity for this system is from 0.3 m/s to 1 m/s;
- Individual control of airflow rate is essential for providing occupants with preferred conditions when PV with ceiling mounted ATD is used in practice.
- Under non-isothermal case, subjects prefer less cool air which reduces the energy

consumption of PV supply fan.

Based on the findings from this study, the following recommendations are drawn for further research.

- The choice of nozzle diameter, which will influence the size of target area, is based on theoretical calculation without considering the influence from human occupants. The variation study of nozzle diameter is recommended.
- Changing installation height of the nozzle will influence this PV system performance, which need to be explored.
- Ambient temperature can be elevated to 28 °C or more for further study.
- Some other ceiling mounted PV ATDs, which are not directly above workstations, can be installed. They are useful for occupants when they move from their own workstation to public area.
- Continuous individual control for PV airflow rates instead of only four options (4, 8, 12, 16 L/s) should be studied.

Bibliography

www.absoluteastronomy.com/encyclopedia/S/Si/Singapore.htm, Absolute astronomy (2005), Singapore.

Arens, E., Bauman, F., Johnston L. and Zhang, H. (1991) Testing of localized ventilation systems in a new controlled environment chamber. Indoor Air, 3, 263-281.

ASHRAE (2003). ASHRAE handbook, fundamentals, SI Edition, American Society of Heating, Refrigeration and Air Conditioning Engineers, Inc.

ASHRAE Standard 55-2004 (2004) Thermal environmental conditions for human occupancy, Atlanta, GA, American Society of Heating, Refrigerating and Air-Conditioning Engineers, Inc.

Awbi, H. B. (2003) Ventilation of buildings, Spon Press, London, 2003.

Bauman, F. S. and Arens, E. A. (1996) Task/ambient conditioning systems: engineering and application guidelines, Berkeley, CA, Center for Environmental Design Research, University of California, Berkeley (Publication number CEDR-13–96).

Bauman, F. S., Carter, T. G., Baughman, A. V. and Arens, E. A. (1998) Filed study of the impact of a desktop task/ambient conditioning system in office buildings. ASHRAE Transactions, 104 (1), 1153-1171.

Bauman, F. S., Zhang, H., Arens, E. A. and Benton, C. C. (1993) Localized comfort control with a desktop task conditioning system: laboratory and field measurements. ASHRAE Transactions, 99 (2), 733-749.

Bolashikov, Z., Nikolaev, L., Melikov, A. K., Kaczmarczyk, J. and Fanger, P. O. (2003) New air terminal devices with high efficiency for personalized ventilation application. Proceedings of Healthy Buildings 2003, Singapore, 2, 850–855.

Brohus, H. and Nielsen, P. V. (1994) Personal exposure in a ventilated room with concentration gradients. Proceedings of Healthy Buildings '94, Budapest, 2, 559–564.

Cermak, R. and Majer, M. (2000) Development and evaluation of air terminal devices for personalized ventilation. ET-EP, 2000-09, Technical University of Denmark, Lyngby, Denmark.

Chen, Q. and Moser, A. (1991) Simulation of a multiple-nozzle diffuser. IEA Annex 20 Subtask 1 Research Item 1.20, 12th AIVC Conference.

Cheong, K. W. D., Tham, K. W., Ullah, M. B., Sekhar, S. C., Wong, N. H. and Djunaedy, E. (2001) Modeling of the air quality and ventilation in indoor environment. R-292-000-011-112: final report.

CP13, Singapore Standard, CP13: 1999, Code of practice for mechanical ventilation

in buildings, Singapore, 1999.

de Dear, R.J., Leow, K.G. and Foo, S.C. (1991) Thermal comfort in the humid tropics: Field experiments in an air conditioned and naturally ventilated buildings in Singapore. International Journal of Biometeorology, 34, 259-265.

Dutt, A.J., and de Dear, R.J. (1991) Study of wind patterns for Singapore. Unpublished NUS-HDB Research Report 7. NUS.

Fanger, P. O. (2000) Indoor air quality in the 21st century: search for excellence. Indoor Air, 10, 68-73.

Fanger, P.O. and Christensen, N.K. (1986) Perception of draught in ventilated spaces. Ergonomics, Vol. 29 (2), 215-235.

Fanger, P. O., Melikov, A. K., Hanzawa, H. and Ring, J. (1988) Air turbulence and sensation of draught. Energy and Buildings, 12, 1, 21-39.

Fanger, P.O. and Peterson, C.J.K. (1977) Discomfort due to air velocities in spaces, Proceedings of Meeting of Commission B1, B2, E1 of Int. Instit. Refig 4, 289-296.

Faulkner, D., Fisk, W. J., Sullivan, D. P. and Wyon, D. P. (1999) Ventilation efficiencies of desk-mounted task/ambient conditioning systems. Indoor Air, 9, 273–281.

Faulkner, D., Fisk, W. J., Sullivan, D. P. and Lee, S. M. (2004) Ventilation efficiencies and thermal comfort results of a desk-edge-mounted task ventilation system. Indoor Air, 14 (Suppl. 8), 92-97.

Fountain, M., Arens, E., De Dear, R., Bauman, F. and Miura, K. (1994) Locally controlled air movement preferred in warm isothermal environments. ASHRAE Transactions, 100(2), 937-952.

Gong, N., Tham, K.W., Melikov, A.K., Wyon, D.P., Sekhar, S.C., and Cheong, K.W. (2006) Local air movement in the tropics. HVAC&R Research, 12, 1065-1076.

Griefahn, B., Kunemund, C. and Gehring, U. (2000) The significance of air velocity and turbulence intensity for responses to horizontal drafts in a constant air temperature of 23 °C. International Journal of Industrial Ergonomics, 26, 639-649.

Griefahn, B. and Kunemund, C. (2001) The effects of gender, age and fatigue on susceptibility to draft discomfort. Journal of Thermal Biology, 26, 395-400.

Griefahn, B., Kunemund, C. and Gehring, U. (2001) The impact of draft related to air velocity, air temperature and workload. Applied Ergonomics, 32, 407-417.

Griefahn, B., Kunemund, C. and Gehring, U. (2002) Evaluation of draft in the workplace. Ergonomics, 45(2), 124-135.

Homma, H. and Yakiyama, M. (1988) Examination of free convection around occupant's body caused by its metabolic heat. ASHRAE Transactions, 93, 104-124.

Houghten, F.C., Gutberlet, C. and Witkowski, E. (1938) Draft temperatures and velocities in relation to skin temperature and feeling of warmth, ASH and VE Transactions, 44, 289.

Huo, Y., Haghighat, F., Zhang, J. S. and Shaw, C. Y. (2000) A systematic approach to describe the air terminal device in CFD simulation for room air distribution analysis. Building and Environment, 35(6), 563-576.

Hyldgaard, C. E. (1994) Humans as a source of heat and air pollution, Proceedings of Roomvent 1994, Krakow, Poland, 413-433.

Johnson Controls (2005) Personal Environments. Retrieved 16 March, 2005 from the World Wide Web: http://www.johnsoncontrols.com/cg/PersEnv/pe_details.htm.

Kaczmarczyk, J., Melikov, A. and Fanger, P. O. (2004) Human response to personalized ventilation and mixing ventilation. Indoor Air, 14 (Suppl 8), 17-29.

Kaczmarczyk, J., Zeng, Q., Melikov, A. and Fanger, P. O. (2002a) The effect of a personalized ventilation system on perceived air quality and SBS symptoms. Proceedings of Indoor Air 2002, Monterey, 4, 1042–1047.

Lee, S.E.. Energy and building performance assessment and classification of commercial buildings in Singapore. (2004) Final report of a collaborative project between National University of Singapore, Building and Construction Authority and PREMAS International.

Matsunawa, K., Iizuka, H. and Tanabe, S. (1995) Development and application of an underfloor air-conditioning system with improved outlets for a "smart" building in Tokyo. ASHRAE Transactions, 101(2), 887-901.

Mayer, E. and Schwab, R. (1988) Direction of low turbulent airflow and thermal comfort. Proceedings of Healthy Buildings '88, Stockholm, Sweden, 2, 577-582.

Melikov AK, Pitchurov G, Naidenov K, and Langkilde G. (2005) Field study of occupants thermal comfort in rooms with displacement ventilation. Indoor Air, 15, (3), 205-214.

Melikov, A. K. (2004) Personalized ventilation. Indoor Air, 14 (Suppl 7), 157-167.

Melikov, A. K., Arakelian, R. S., Halkjaer, L. and Fanger, P. O. (1994b) Spot cooling-part 2: recommendations for design of spot-cooling systems. ASHRAE Transactions, 100 (2), 500-510.

Melikov, A. K., Cermak, R., Kovar, O. and Forejt, L. (2003) Impact of airflow

interaction on inhaled air quality and transport of contaminants in rooms with personalized and total volume ventilation. Proceedings of Healthy Buildings 2003, Singapore, 2, 592-597.

Melikov, A. K., Cermak, R. and Majer, M. (2002) Personalized ventilation: evaluation of different air terminal devices. Energy and buildings, 34, 829-836.

Melikov, A., Kaczmarczyk, J., Silva, D. (2008) Impact of air movement on perceived air quality at different level of relative humidity. Proceedings of the 11th International conference on Indoor Air Quality and Climate - Indoor Air 2008, 17-22 August 2008, Copenhagen, Paper ID: 1037.

Melikov, A. and Kaczmarczyk, J. (2008) Impact of air movement on perceived air quality at different level of air pollution and temperature. Proceedings of the 11th International conference on Indoor Air Quality and Climate - Indoor Air 2008, 17-22 August 2008, Copenhagen, Paper ID: 1033.

Melikov, A. and Kaczmarczyk, J. (2007) Indoor air quality assessment by a breathing thermal manikin. Indoor Air, 17(1), 50-59.

Melikov, A. K., Halkjaer, L., Arakelian, R. S. and Fanger, P. O. (1994a) Spot cooling-part 1: human responses to spot cooling with air jets. ASHRAE Transactions, 100(2), 476-499.

Melikov, A. K. and Zhou, G. (1996) Air movement at the neck of the human body. Proceedings of Indoor Air '96, Nagoya, Japan, 1, 209–214.

Nielsen, P. V. (1992) Development of supply openings in numerical models for room air distribution. ASHRAE Transactions, 98(1), 963-971.

Nilsson, H., Holmér, I., Bohm, M. and Norén, O. (1997) Equivalent temperature and thermal sensation - comparison with subjective responses. Associatione Tecnica Del'Automobile, Bologna.

Niu, J.L. (2003) Potential IAQ and energy benefits achievable with personalized air supply. In Proceedings of Healthy Buildings 2003-7th Intrenational Conference, Singapore, 2, 825-830.

Sekhar, S. C., Gong, N., Maheswaran, C. R. U., Cheong, K. W. D., Tham, K. W., Melikov, A. and Fanger, P. O. (2003a) Preliminary findings of a pilot study of personalized ventilation in a hot and humid climate. Proceedings of Healthy Buildings 2003, Singapore, 2, 825-830.

Sekhar, S. C., Gong, N., Maheswaran, C. R. U., Cheong, K. W. D., Tham, K. W., Melikov, A. and Fanger, P. O. (2003b) Energy efficiency potential of personalized ventilation system in the tropics. Proceedings of Healthy Buildings 2003, Singapore, 2, 686-691.

Sekhar, S. C., Gong, N., Tham, K. W., Cheong, K. W. D., Melikov, A. K., Wyon, D. P. and Fanger, P. O. (2005) Findings of personalized ventilation studies in a hot

and humid climate, International Journal of Heating. Ventilating, Air-Conditioning and Refrigerating Research (HVAC&R), USA (to appear).

Tanabe, S., Arens, E. A., Bauman, F. S., Zhang, H. and Madsen, T. L. (1994) Evaluating thermal environments by using a thermal manikin with controlled skin surface temperature. ASHRAE Transactions, 100 (1), 39 – 48.

Tham, K.W. (2004a) Effects of temperature and outdoor air supply rate on the performance of call center operators in the tropics, Indoor Air; 14(Suppl 7): 119-125.

Tham, K. W., Sekhar, S. C., Cheong, K. W. D. and Gong, N. (2004b) Experimental study of draft perception of tropically acclimatized subjects under personalized ventilation, Proceedings of Roomvent 2004, Coimbra: DEM-FCT, Univ. of Coimbra.

Tham, K. W., Sekhar, S. C., Cheong, K. W. D. and Gong, N. (2004c) Thermal sensation of tropically acclimatized subjects under fixed air flow of personalized ventilation, Proceedings of Roomvent 2004, Coimbra: DEM-FCT, Univ. of Coimbra.

Toftum, J. (1994). Draught complains in the industrial work environment, Ph.D. dissertation. Laboratory of Heating and Air Conditioning, Technical University of Denmark (In Danish).

Toftum, J. (2004). Air movement-good or bad? Indoor Air; 14(Suppl 7): 40-45.

Toftum, J., Melikov, A. K., Tynel, A., Bruzda, M. and Fanger, P. O. (2002) Human preference for air movement. Proceedings of Roomvent 2002, Copenhagen, Denmark, 301-304.

Toftum, J. and Nielsen, R. (1996) Draft sensitivity is influenced by general thermal sensation. International Journal of Industrial Ergonomics, 18, 295-305.

Tsuzuki, K., Arens E. A., Bauman, F. S. and Wyon, D. P. (1999) Individual thermal comfort control with desk-mounted and floor-mounted task/ambient conditioning (TAC) systems. Proceedings of Indoor Air 1999, Edinburgh, Vol. 2, pp 368 – 373.

Wargocki, P, Wyon, D. P., Baik, Y. K., Clausen, G. and Fanger, P. O. (1999) Perceived air quality, Sick Building Syndrome (SBS) symptoms and productivity in an office with two different pollution loads. Indoor Air, 9, 165-179.

Xia, Y.Z., Niu, J.L., Zhao, R.Y. and Burnett, J. (2000) Effects of turbulence air on human thermal sensations in a warm isothermal environment. Indoor Air, 10, 289-296.

Yang, B., Melikov, A.K. and Sekhar, S.C. (2008) Performance evaluation of ceiling mounted personalized ventilation system. ASHRAE Transactions, (Approved).

Yang, B. and Sekhar, S.C. (2007) Three-dimension numerical simulation of a hybrid fresh air and re-circulated air diffuser for decoupled ventilation strategy. Building and Environment, 2007, Vol. 42(5), pp1975-1982.

Zeng, Q., Kaczmarczyk, J., Melikov, A. and Fanger, P.O. (2002) Perceived air quality and thermal sensation with personalized ventilation system, Proceedings of Roomvent 2002, Copenhagen, 61–64.

Zhou, W., Sun, W., Gong, N. and Tham, K.W., (2005) The impact of turbulence intensity on perceived air quality of tropically acclimatized subjects exposed to personalized ventilation operating in isothermal and slightly warmer ambient environments. In Proceedings of Indoor Air 2005, the 10th International Conference on Indoor Air Quality and Climate.

Zuo, H. G., Niu, J. L. and Chan, W. T. (2002) Experimental study of facial air supply method for the reduction of pollutant exposure, Proceedings of Indoor Air 2002, Monterey, CA, 1090-1095.

Appendix 1. Manikin calibration data

The manikin based equivalent temperature can be expressed as a function of the sensible heat loss from each body segment:

$$T_{eq} = 36.4 - C(Q_t) \quad (1)$$

Where t_{eq} is manikin based equivalent temperature, °C,

Q_t is sensible heat loss, W/m^2,

36.4 is deep body temperature, °C,

C is constant dependent on clothing, body posture, chamber characteristics and thermal resistance offset of skin surface temperature control system, K.m^2/W.

In order to obtain exact measurements, manikin must be calibrated frequently by making measurements at known environmental temperatures of the manikin Calibration chamber at ICIEE-DTU is controlled at desired temperature with only $\pm$ 0.1 °C fluctuation. Nude Manikin sitting on metal chair is exposed to unique thermal environment (Figure 1a) under controlled temperature (20 °C and 30 °C). To calibrate manikin temperature, the following steps must be taken:

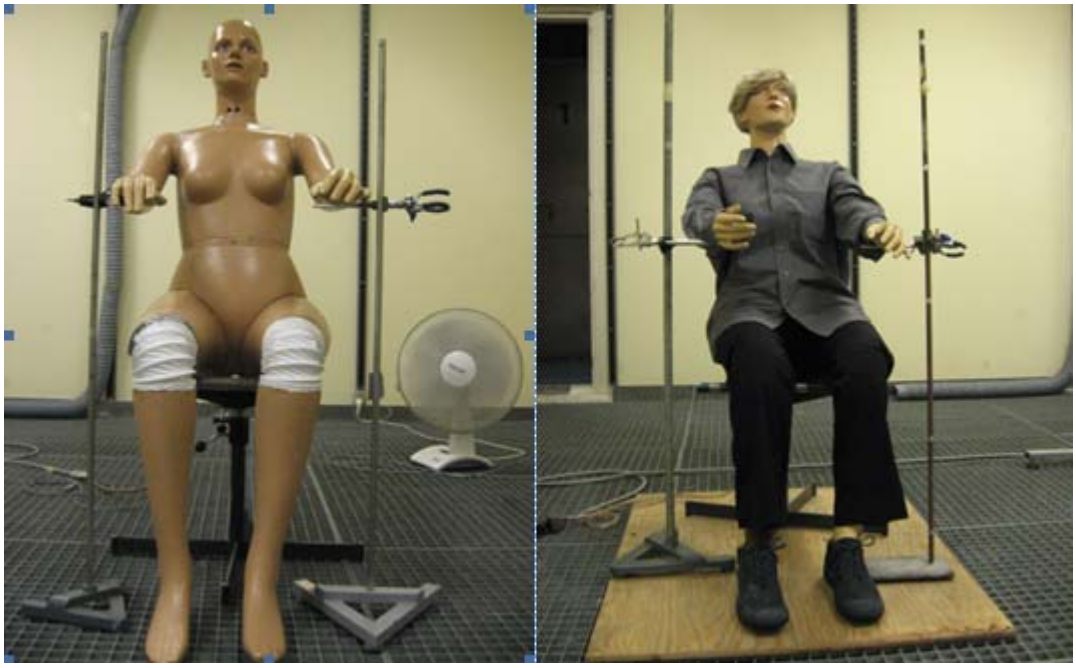

Figure 1 a. Nude manikin for temperature calibration b. Manikin for manikin based equivalent temperature calibration

1. Log a data-record when all parts of the manikin have uniform temperatures (20 °C) by selecting the function Body Segment / Calibrate Temperature A
2. Item 1 is repeated with Calibrate Temperature B at another temperature (30 °C)
3. The new temperature constants are calculated automatically

Make sure that the temperatures of all body parts are the same. Log the data-records with the function Record A or Record B where you will be prompted for the instant temperature of the manikin.

Based on the definition of manikin based equivalent temperature, a uniform enclosure was created, in which a thermal manikin with realistic skin temperatures would lose heat as the same rate as it would in the actual environment (Figure 1b). The

environment was created at different temperature (18 °C, 21 °C, 24 °C and 27 °C), which can cover the temperature range in formal experiments. The C values of each body segments as well as whole body are derived by averaging four values under these four temperatures to offset the small influence of temperature on C values.

No.	Body segments	Constants C values (K.m^2/W)				
		18 °C	21°C	24°C	27°C	Average
1	L.Foot	4.54	4.78	4.61	4.65	4.65
2	R.Foot	4.47	4.68	4.61	4.61	4.59
3	L.Low.Leg	6.54	6.88	6.81	7.02	6.81
4	R.Low.Leg	6.41	6.72	6.74	7.03	6.73
5	L. Front thigh	5.81	6.08	5.9	5.89	5.92
6	L. Back thigh	6.66	6.93	6.92	6.75	6.82
7	R. Front thigh	5.81	6.02	5.89	5.93	5.91
8	R. Back thigh	6.6	6.83	6.52	6.36	6.58
9	Pelvis	3.29	3.4	3.28	3.22	3.30
10	Back side	4.23	4.4	4.27	4.29	4.30
11	Scull	2.92	3.07	3.08	3.2	3.07
12	L. Face	6.69	7.14	7.05	6.97	6.96
13	R. Face	6.56	7.03	7	7.07	6.92
14	Back of neck	5.11	5.23	4.95	4.76	5.01
15	L.Hand	8.89	8.97	9.43	8.56	8.96
16	R.Hand	7.94	8.22	7.84	7.15	7.79
17	L.Forearm	5.31	5.59	5.32	5.25	5.37
18	R.Forearm	5.32	5.61	5.37	5.34	5.41
19	L.Upper Arm	5.09	5.29	5.11	5	5.12
20	R.Upper arm	4.87	5.06	4.84	4.74	4.88
21	L.Chest	3.8	3.97	3.78	3.74	3.82
22	R.Chest	3.73	3.84	3.73	3.71	3.75
23	Back	4.61	4.73	4.69	4.71	4.69
All	Whole body	5.27	5.46	5.36	5.32	5.35

Appendix 2. Theory analysis of circular free jet (isothermal case)

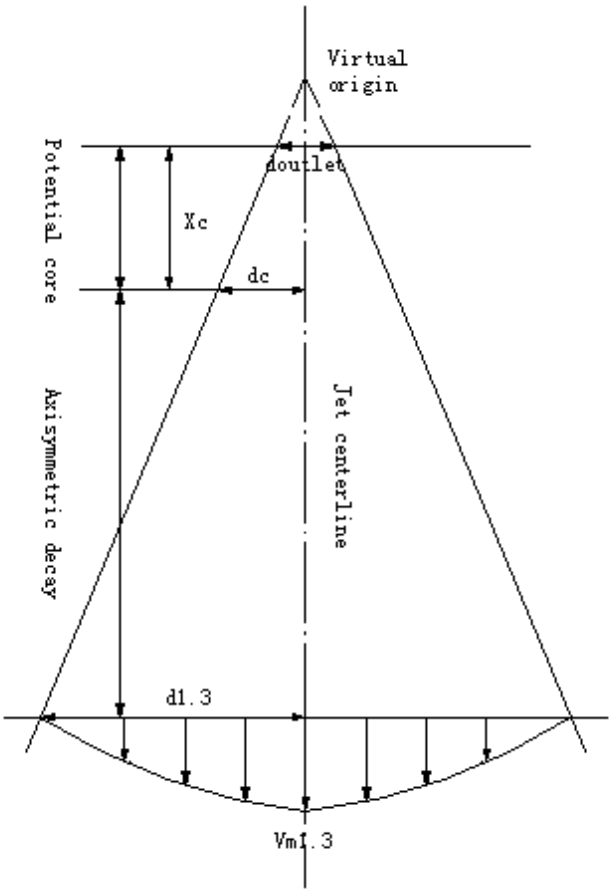

Figure 1. Schematics of circular free jet flow

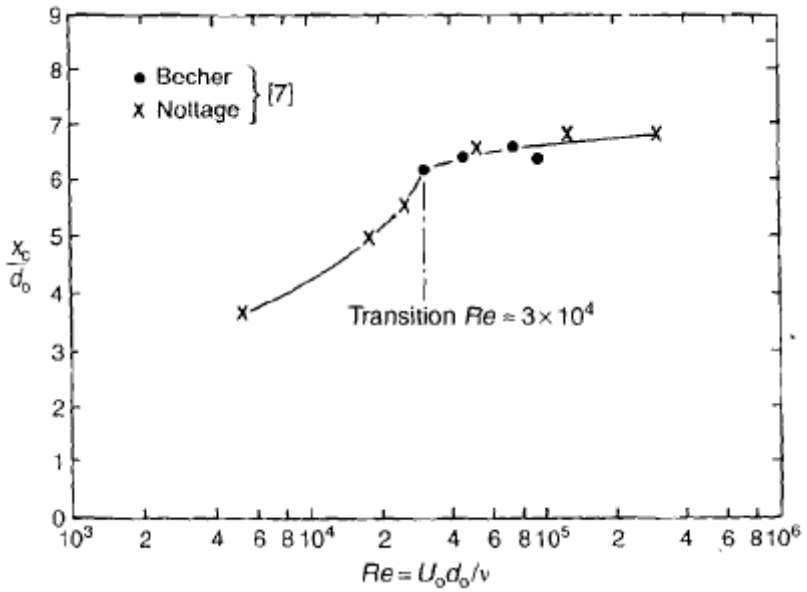

Figure 2. Relationship between Reynolds number and coefficient a

$$v_{outlet} = \frac{Q}{\frac{1}{4}\pi d_{outlet}^2} \quad (1)$$

$$\mathrm{Re} = v_{outlet} \bullet d_{outlet} / \upsilon \quad (\upsilon = 1.5 \times 10^{-5} m^2 / s \text{, t=20° C}) \quad (2)$$

$$\mathrm{Re} = f(a) \quad (3)$$

$$x_c = a \bullet d_{outlet} \quad (4)$$

$$\delta_c = 0.27 \bullet x_c \quad (5)$$

$$\delta_{1.3} = \frac{1.3 \times (\delta_c - 0.0475)}{x_c} + 0.0475 \quad (6)$$

$$v_{1..3} = \frac{0.48 \times v_{outlet}}{0.14 + a \times 1.3 / d_{outlet}} \quad \text{(a=0.068 for this case)} \quad (7)$$

v_{outlet} ----velocity at jet outlet (m/s)

Q ----volumetric flow rate of personalized air (m3/s)

d_{outlet} ----diameter of jet outlet (m)

Re----Reynolds number

υ ----kinetic viscosity (m^2/s)

a ----coefficient

x_c ----length of core region (m)

δ_c ----radius at the end of core region (m)

$\delta_{1.3}$ ---- radius at the 1.3 m vertical distance from jet outlet (m)

$v_{1.3}$ ---- velocity at the 1.3 m vertical distance from jet outlet (m/s)

Appendix 3. Detailed description of measuring instruments

1. Thermo-anemometer measurements system HT400

The thermo-anemometer measurements system HT400 system consists of 8 hot-sphere-type anemometer probes HT-412, transducer units HT-428, connecting cables, multi-channel power supply HT-430, and data acquisition module HT-470 (Figure 4.11). The probe has a short response time which is particularly required when measuring fluctuating velocities. The full standard system comprises 8 measurement channels. The multi-channel power supply creates 8 DC voltage galvanic insulated for supplying the transducer units. It also transforms current output signal from transducer units to voltage signals that are used to connect to data acquisition module HT-470. The data acquisition module HT-470 is connected to a computer via the RS-232 interface. Computer software for the system was used to display real-time measurement data (mean velocity, turbulence intensity, mean temperature, and draft rating) with compensating barometric pressure and export results to Microsoft Excel format for further analysis. The velocity measurement range of the system is 0.05m/s-5m/s, with the accuracy of ±0.02m/s ±1% of readings for velocity range of 0.05m/s to 1m/s and accuracy of ±3% of readings for velocity range of 1m/s to 5m/s. The temperature measurement range of the system is from -10°C to 50°C, with the accuracy of 0.2°C.

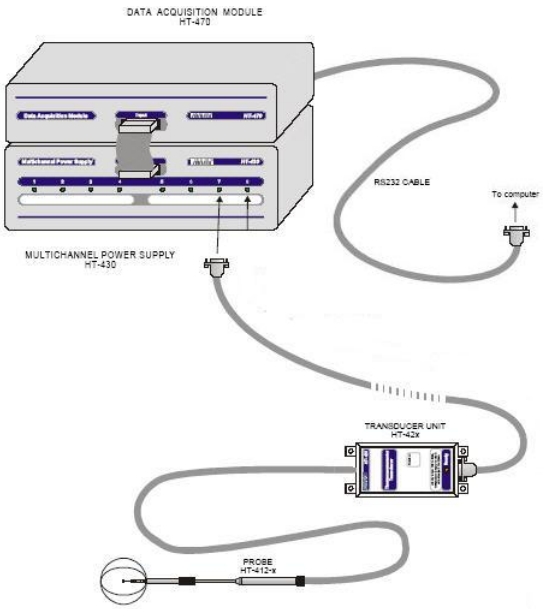

Figure 1. Thermo-anemometer measurements system HT400

2. Thermal manikin

Skin temperatures and heat losses from all 23 body segments of the thermal manikin are measured and recorded. The control method is the comfort control, which is based on Fanger's comfort equation. During the experiment, real-time measurement results are displayed in the manikin program windows (Figure 2). Measurements data logged under steady-state conditions are exported to Microsoft Excel format for further analysis.

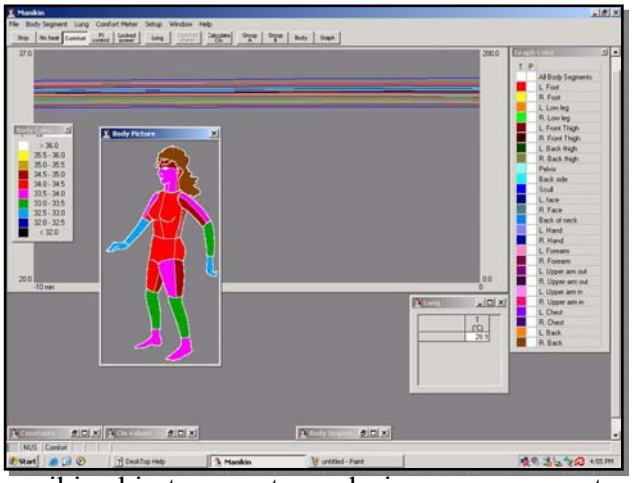

Figure 2. Snapshot of manikin skin temperatures during measurements

3. Thermistor sensor and datalogger

A thermistor probe, Craftemp® from Gambro Crafon AB of Sweden, is utilized to measure the inhaled air temperature of the manikin (Figure 3). This type of probe is very small and light so that it could be mounted in the manikin's mouth and measure the inhaled air temperature with fast response. The probe is connected to Agilent Data Acquisition Unit 34970A through screw-terminal connection (Figure 3). The Agilent 34970A consists of a three-slot mainframe with a built-in 6 ½ digit digital multi-meter and is connected to a computer via the RS-232 interface. Windows-based software named Agilent Benchlink Data Logger II is utilized to control the sampling and record and analyze the data. During the measurements, the analogue signal in ohms from the probe is continuously transformed into the digital signal by the 34970A and then collected by the software at a specified frequency, which in the present study was 2 Hz.

Figure 3. CRAFTEMP thermistor probe and Agilent Data Acquisition Unit 34970A

4. Tracer gas (SF_6) measurement system

Tracer gas (SF_6) measurements are performed to investigate the performance of the CMPV ATD in terms of ability to provide occupants with fresh outdoor air. SF_6 is continuously dosed at a constant rate into the supply duct of mixing ventilation system with a Bronkhorst EL-FLOW® mass flow controller (F-201C-FAC) and FLOW-BUS digital power supply/readout system (E-7100-AAA) (Figure 4). The purpose of doing so is to uniformly mark the ambient air in the personalized ventilation chamber with SF_6, used to simulate indoor pollutant. The 100% outdoor

air supplied by the personalized ventilation system is kept free of SF_6.

Figure 4. Mass flow controller and digital power supply/readout system

The SF_6 is continuously sampled at several locations inside the personalized ventilation chamber by INNOVA Multipoint Sampler 1309 (Figure 5). The 1309 is a multiplexer that has 12 inlet channels, each with a solenoid valve. Each inlet channel has a tube-mounting stub on the front panel of the 1309. The 12 tubes connect each channel to the respective sampling point. The 12 inlet channels converge into one; a three-way valve then directs the gas sample to a gas monitor for analysis, or vents it to the waste-air outlet for purging the sampling lines. While the gas monitor is measuring the sample, the 1309 will purge the next sample line. The speed at which the 1309 transports gas samples from the sampling point is approximately 4 m/s, which, however, is dependent on the type of pump, the diameter of the tubing, and the length of tubing attached to the 1309. For each sampling tube, an air-filter is attached to its end to keep the samples free of particles.

Figure 5. INNOVA Multipoint Sampler 1309 and Multi-gas Monitor 1312

The gas monitor used in conjunction with the 1309 in the present study is INNOVA Photoacoustic Multi-gas Monitor 1312 (Figure 5). It uses a measurement system based on the photoacoustic infra-red detection method and is capable of measuring almost any gas that absorbs infra-red light. Gas selectivity is achieved through the use of appropriate optical filters. By installing up to 5 of these filters in the 1312's filter carousel, it can selectively measure the concentration of up to 5 component gases plus water vapor in any air sample. The accuracy of these measurements is ensured by the 1312's ability to compensate for temperature and pressure fluctuations, water vapor interference, and interference from other gases known to be present.

This sampling and monitoring system is set up and remote-controlled from a personal computer connected to the 1312 via the RS-232 interface. Communication between the 1312 and 1309 is via the IEEE-488 interface. INNOVA application software Win7620 is utilized to operate the communication between the 1312 and 1309 and to store and analyze the measured data.

Appendix 4. Questionnaires

Questionnaire 1 (used to assess the environment under PV)

Group Number: Name: Gender: Age: Height: Weight:

1. Thermal Sensation

Please enter a number in each of the 6 boxes in the diagram below to indicate the thermal sensation of each body section. The 7-value numerical scale to be used appears in the table below:

+3	Hot
+2	Warm
+1	Slightly warm
0	Neutral
-1	Slightly cool
-2	Cool
-3	Cold

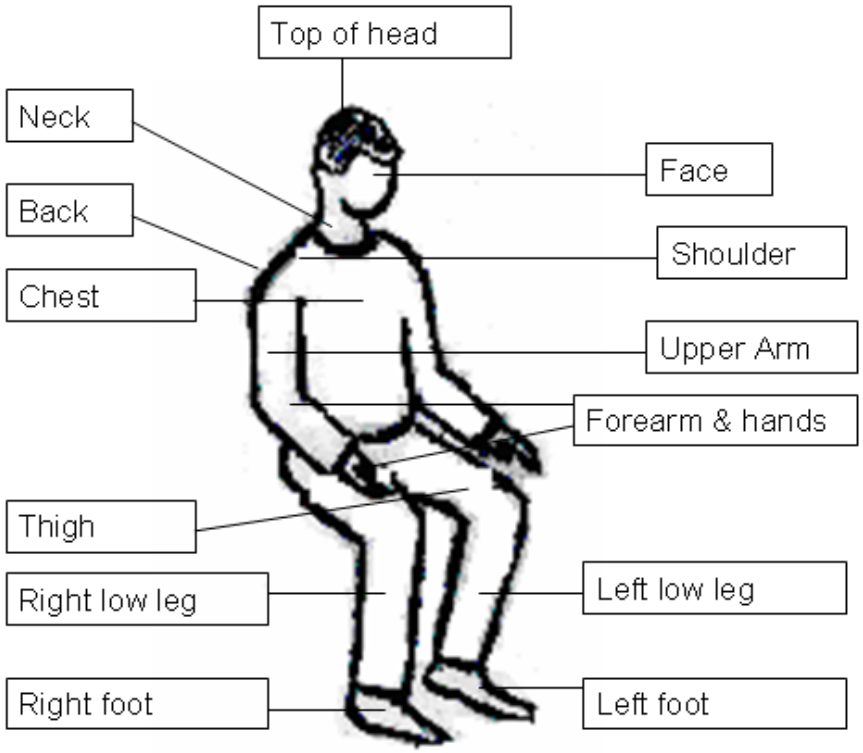

Please also assess your thermal sensation for your whole body:

2. Please assess the acceptability of your thermal comfort condition in the following continuous scale. Please do NOT mark between “Just Unacceptable” and “Just acceptable”:

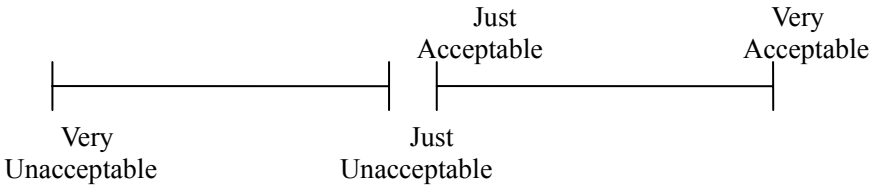

3. Air Movement Perception

Do you feel air movement: yes no

If “yes” please enter a number in each of the 5 boxes in the diagram below to indicate the air movement perception of each body section. The 7-value numerical scale to be used appears in the table below. If you don’t feel any air movement, just choose “No” in the corresponding box.

+3	much too breezy
+2	too breezy
+1	slightly breezy
0	just right
-1	slightly still
-2	too still
-3	much too still

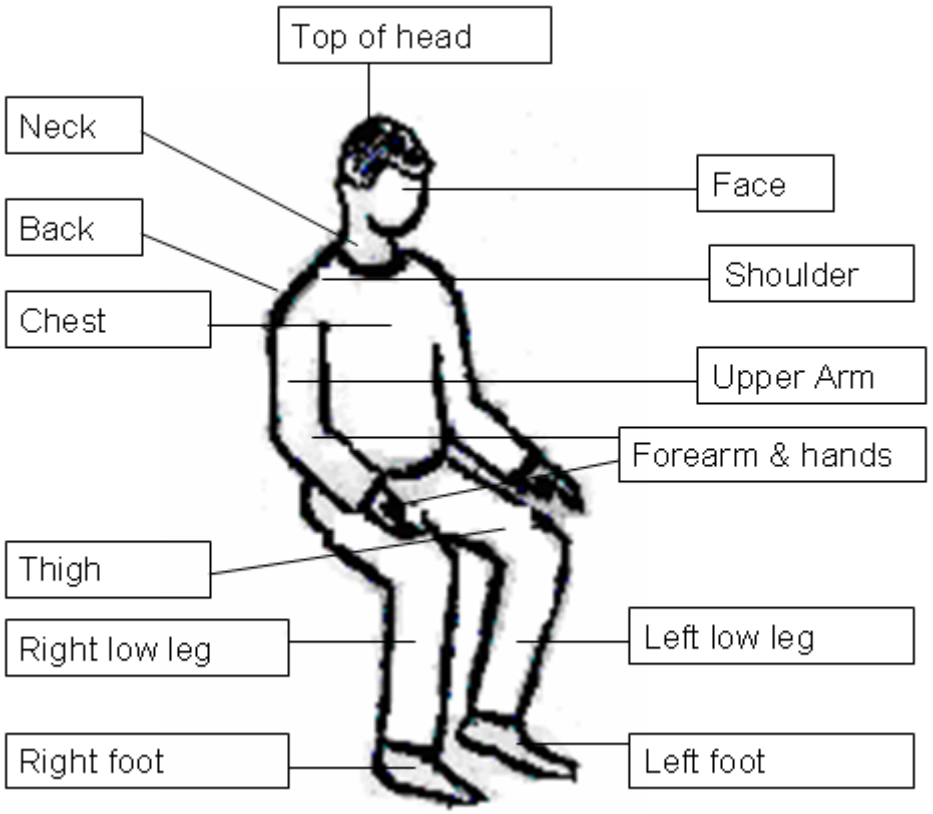

4. Please assess the acceptability of the air movement in the following continuous scale. Please do NOT mark between “Just Unacceptable” and “Just acceptable”:

a1. Please assess the acceptability of the air movement on the top of head

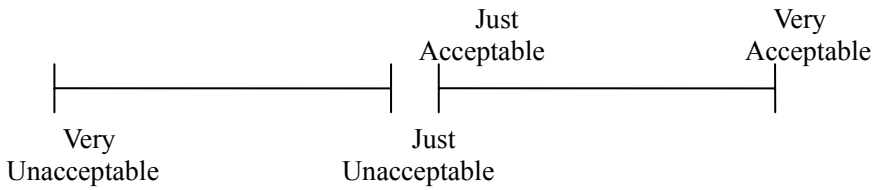

a2. Please indicate the change in the air movement preferred on the top of head?

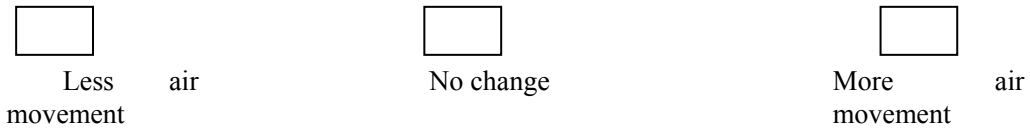

b1. Please assess the acceptability of the air movement on the facial part

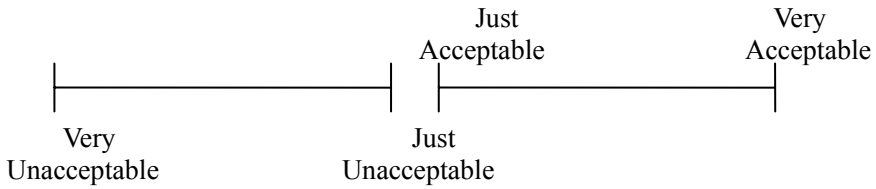

b2. Please indicate the change in the air movement preferred on the facial part?

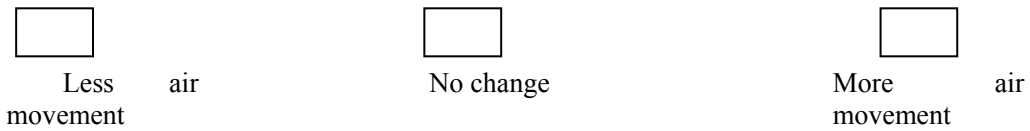

c1. Please assess the acceptability of the air movement on neck

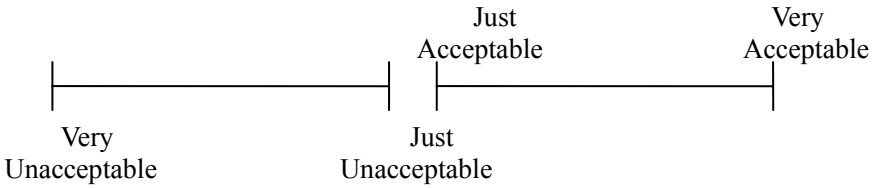

c2. Please indicate the change in the air movement preferred on neck?

☐ Less air movement ☐ No change ☐ More air movement

d1. Please assess the acceptability of the air movement on chest

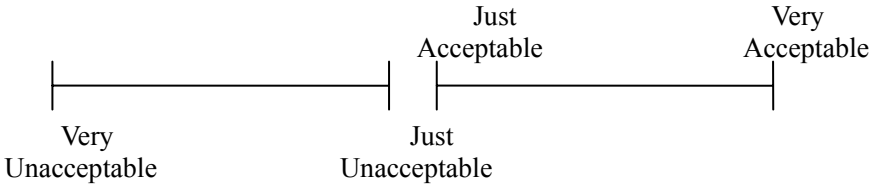

d2. Please indicate the change in the air movement preferred on chest?

☐ Less air movement ☐ No change ☐ More air movement

e1. Please assess the acceptability of the air movement on shoulder

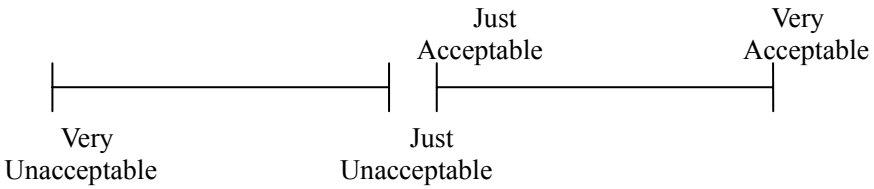

e2. Please indicate the change in the air movement preferred on shoulder?

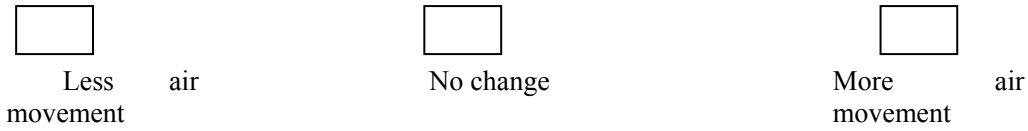

f1. Please assess the acceptability of the air movement on upper arm

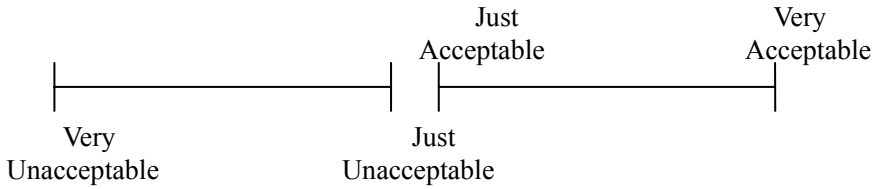

f2. Please indicate the change in the air movement preferred on upper arm?

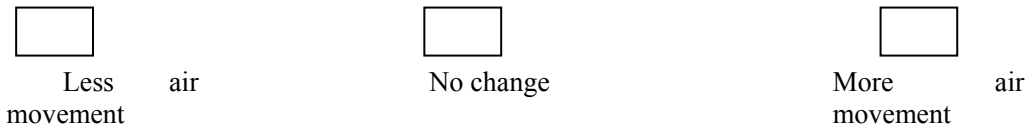

g1. Please assess the acceptability of the air movement on forearm and hands

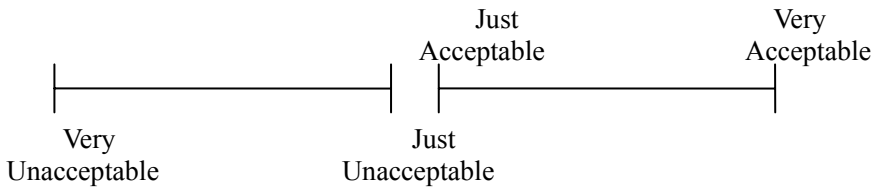

g2. Please indicate the change in the air movement preferred on forearm and hands?

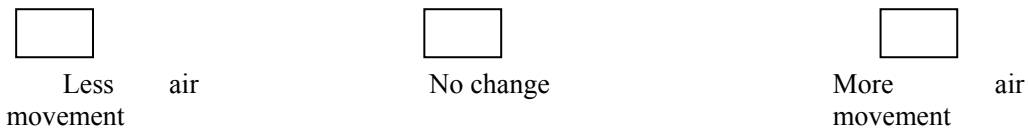

h1. Please assess the acceptability of the air movement on thigh

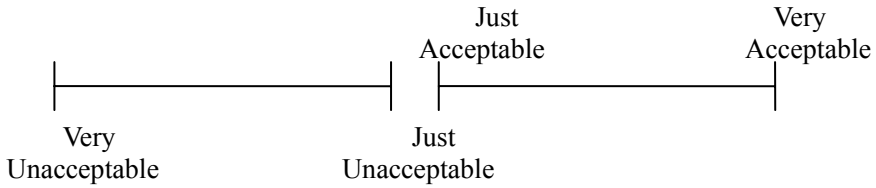

h2. Please indicate the change in the air movement preferred on thigh?

☐ Less air movement ☐ No change ☐ More air movement

i1. Please assess the acceptability of the air movement on left low leg

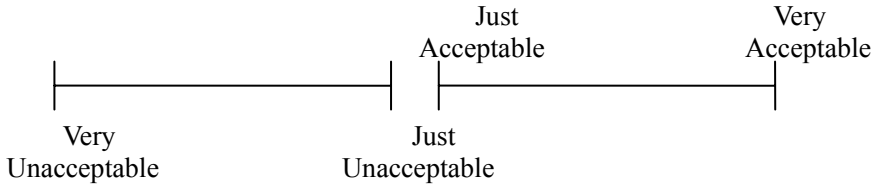

i2. Please indicate the change in the air movement preferred on left low leg?

☐ Less air movement ☐ No change ☐ More air movement

j1. Please assess the acceptability of the air movement on right low leg

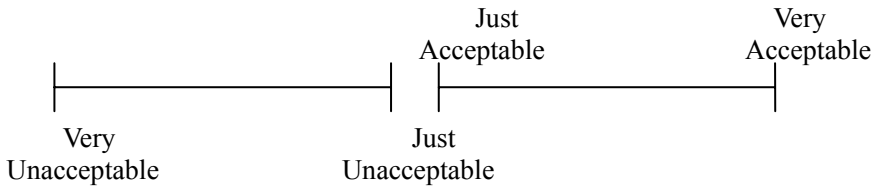

j2. Please indicate the change in the air movement preferred on right low leg?

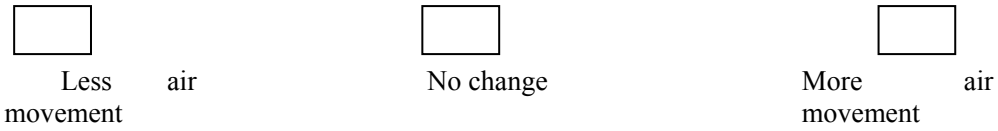

k1. Please assess the acceptability of the air movement on left foot

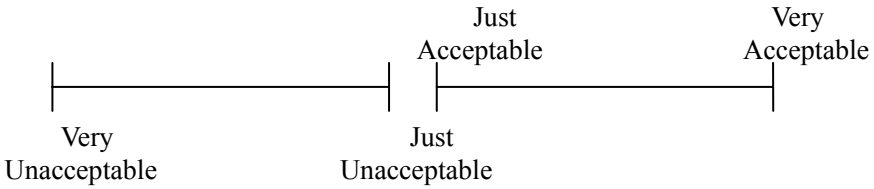

k2. Please indicate the change in the air movement preferred on left foot?

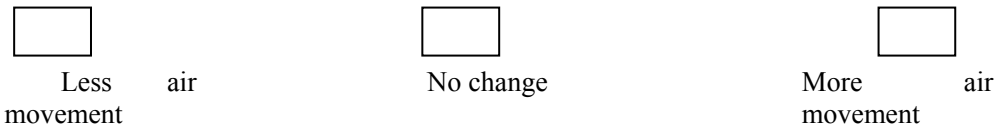

l1. Please assess the acceptability of the air movement on right foot

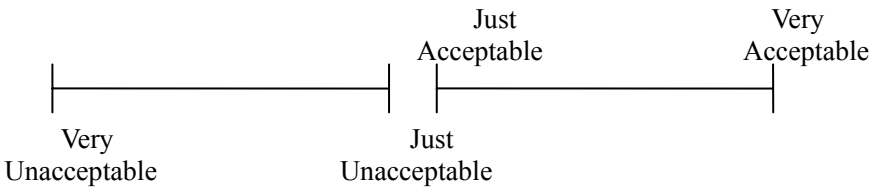

l2. Please indicate the change in the air movement preferred on right foot?

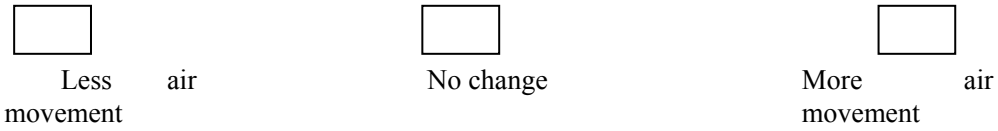

m1. Please assess the acceptability of the air movement on whole body

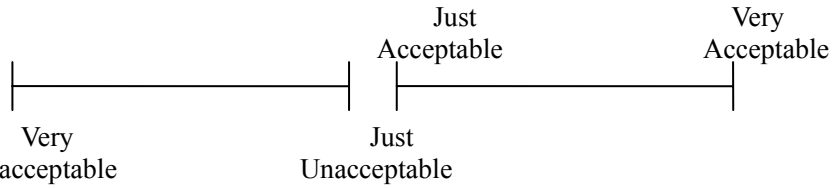

m2. Please indicate the change in the air movement preferred on whole body?

☐ Less air movement ☐ No change ☐ More air movement

Questionnaire 2

1. Please assess the thermal comfort state of your body. Please do NOT mark between "Just Unacceptable" and "Just acceptable":

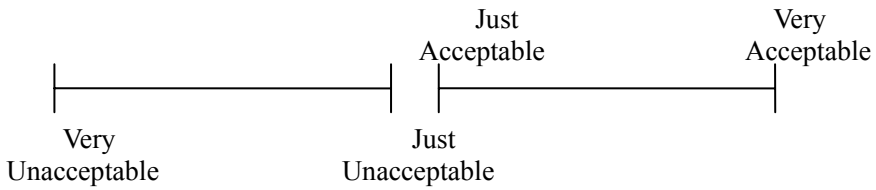

2. Please respond to the following questions:

a. Please assess the inhaled air quality (do not mark between "Just Unacceptable" and "Just acceptable"):

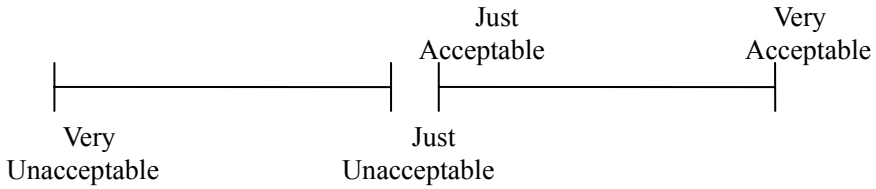

b. Please assess the inhaled air temperature:

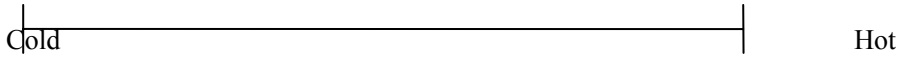

c. Please assess the inhaled air humidity:

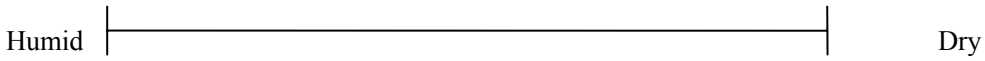

d. Please assess the odour of inhaled air:

e. Please assess the freshness of inhaled air:

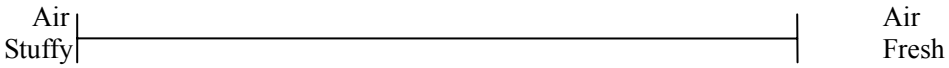

3. Please respond to the following questions:

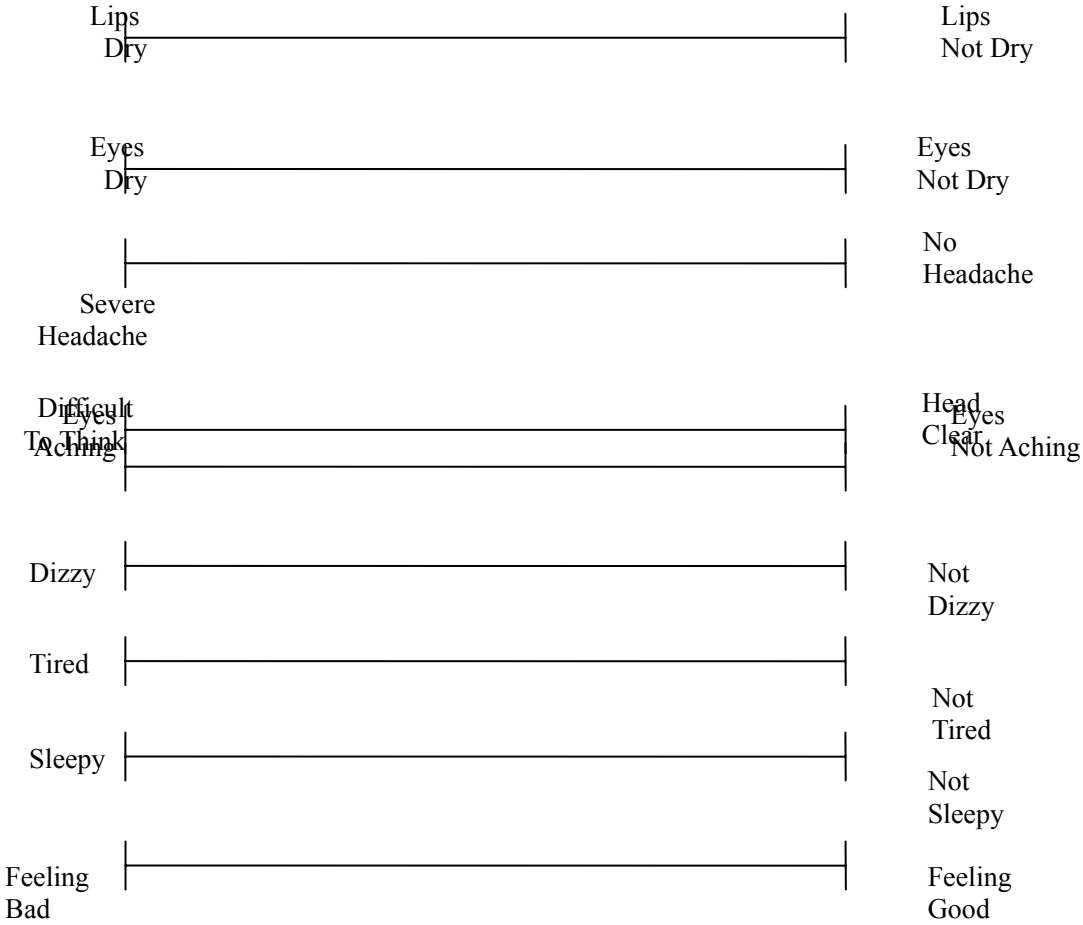

4.Evaluation of noise level:

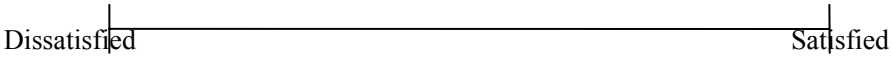

5. Evaluation of lighting level:

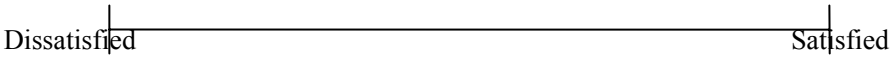

6. Additional info: Do you wear contact lens?

Yes ☐ No ☐

Questionnaire 3

Please tick which of the following dress you are wearing:

Underwear/ Innerwear	☐ Panties ☐ G strings	☐ Singlet ☐ T-shirt	☐ Shirt with long sleeves ☐ Briefs	☐ Stockings ☐ Bra

Shirts/Blouses	☐ short sleeves ☐ Long sleeves light weight shirt	☐ Long sleeves normal shirt ☐ Long sleeves flannel shirt	☐ Tube top ☐ Long sleeves light weight blouse	☐ Long sleeves turtleneck blouse

Trousers	☐ shorts ☐ exercise shorts	☐ Light weight trousers ☐ Normal trousers	☐ Bermudas ☐ Overalls
Skirts, Dresses	☐ Light skirt, 15cm above knees ☐ Knee-length heavy skirt	☐ Light skirt, 15cm below knee ☐ Long sleeves winter dress	☐ Sleeves light dress

Sweaters	☐ Sleeveless Vest ☐ Sweater	☐ Thin Sweater ☐ Thick Sweater	☐ Turtleneck long Sleeves thin sweater ☐ Turtleneck thick sweater

Jacket	☐ Vest	☐ Light summer jacket ☐ Jacket	☐ High insulative fibre-pelt vest ☐ High insulative fibre-pelt jacket

Socks	☐ Socks	☐ Thick ankle socks ☐ Thick long socks	☐ High insulative fibre-pelt vest ☐ High insulative fibre-pelt jacket

Shoes	☐ Sandals, mules	☐ Thin soled shoes ☐ Thick soled shoes	☐ Ankle boot ☐ Boots

If you wear something that you can't find proper description from above, please write here.

_____

Appendix 5. Results of objective measurements

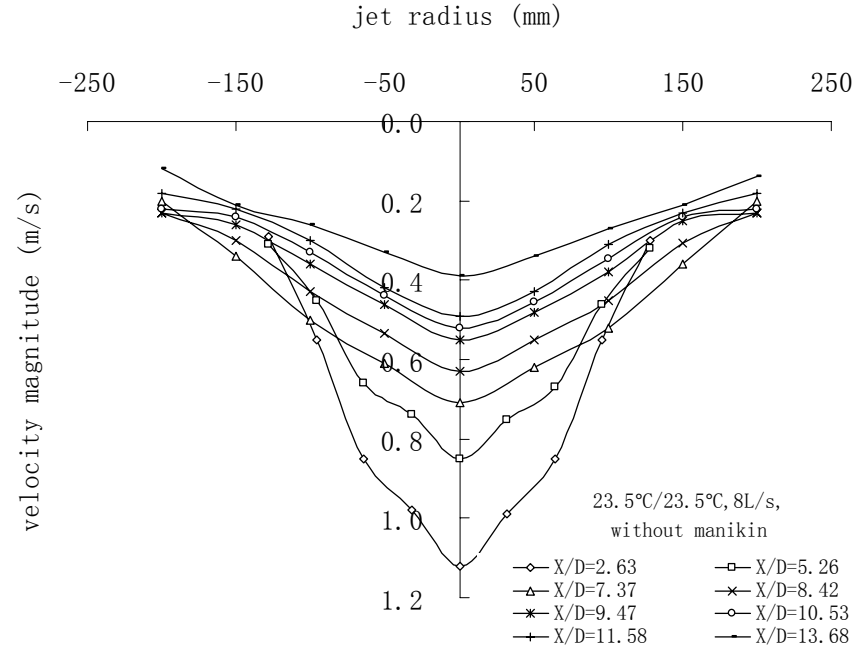

Figure 1 Air velocity profile with 8 L/s personalized airflow rate under 23.5°C/23.5°C isothermal case

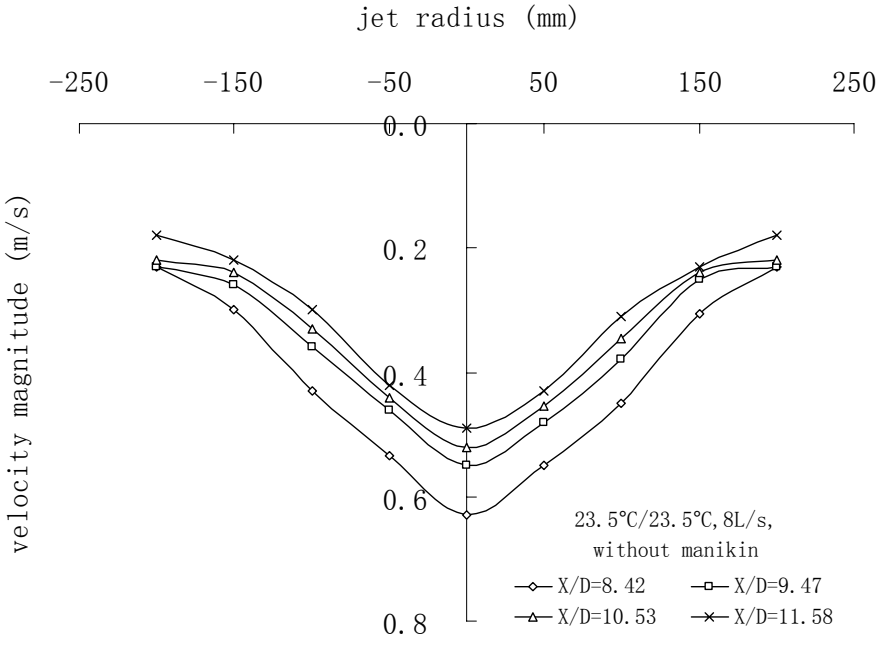

Figure 2a Air velocity profile with 8 L/s personalized airflow rate under 23.5°C/23.5°C isothermal case without manikin

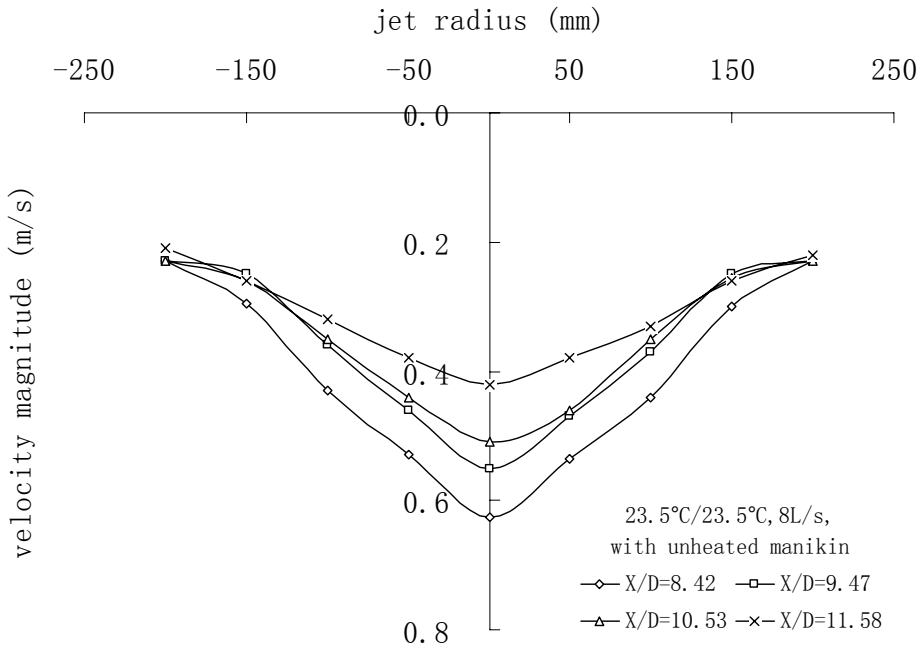

Figure 2b Air velocity profile with 8 L/s personalized airflow rate under 23.5°C/23.5°C isothermal case with unheated manikin

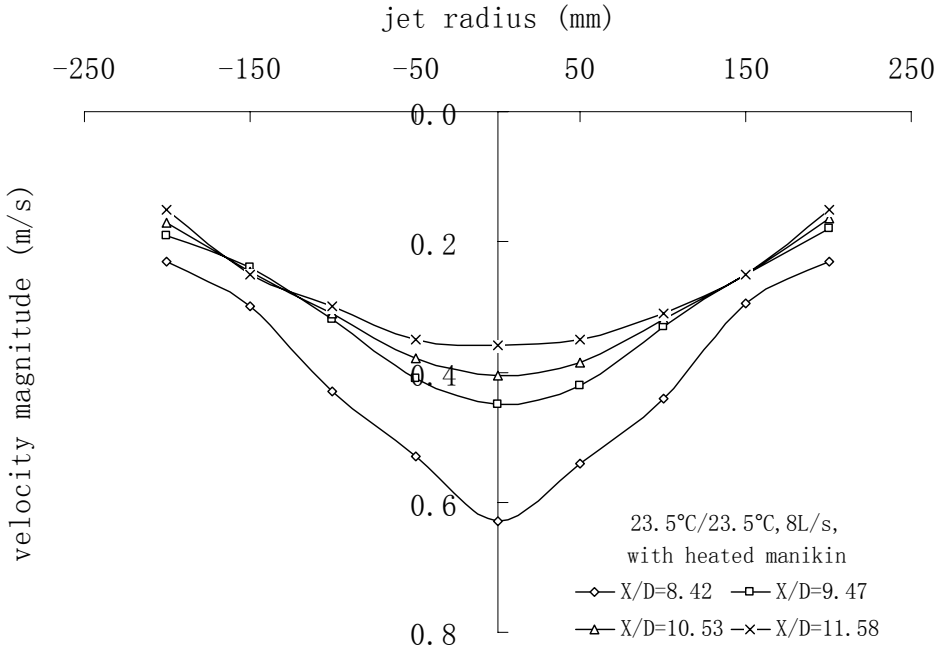

Figure 2c Air velocity profile with 8 L/s personalized airflow rate under 23.5°C/23.5°C isothermal case with heated manikin

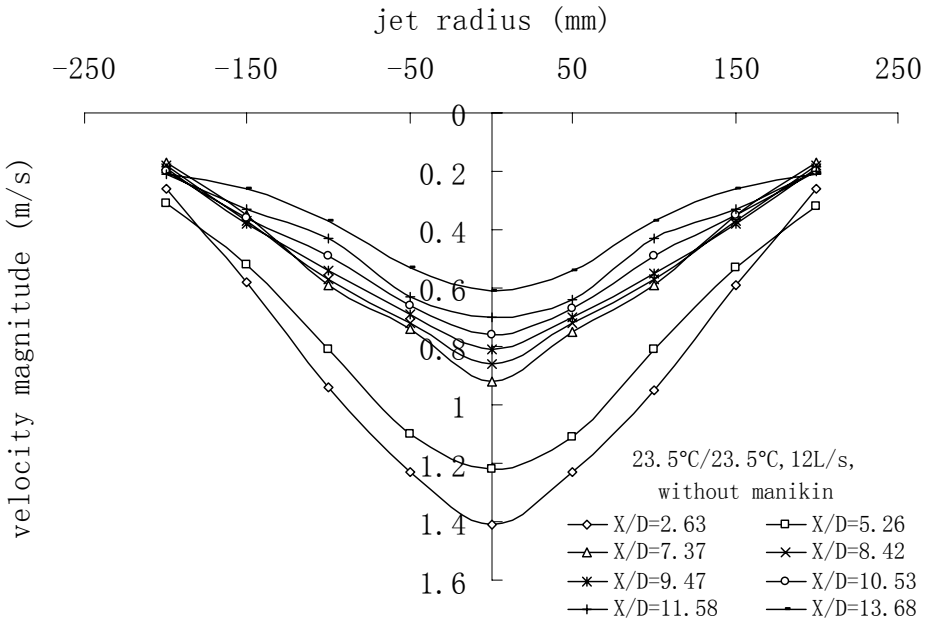

Figure 3 Air velocity profile with 12 L/s personalized airflow rate under 23.5°C/23.5°C isothermal case

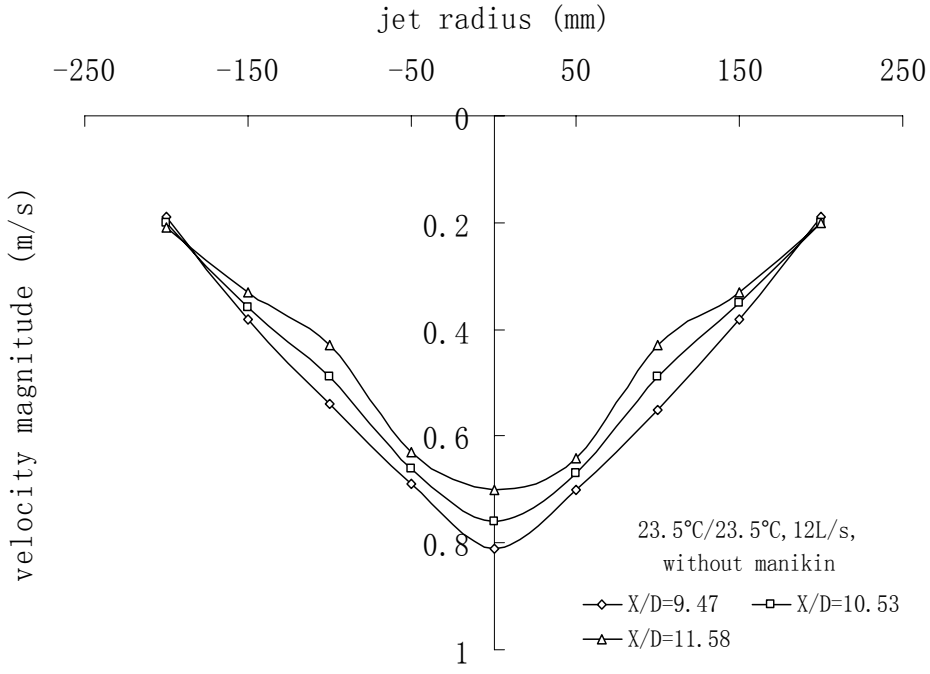

Figure 4a Air velocity profile with 12 L/s personalized airflow rate under 23.5°C/23.5°C isothermal case without manikin

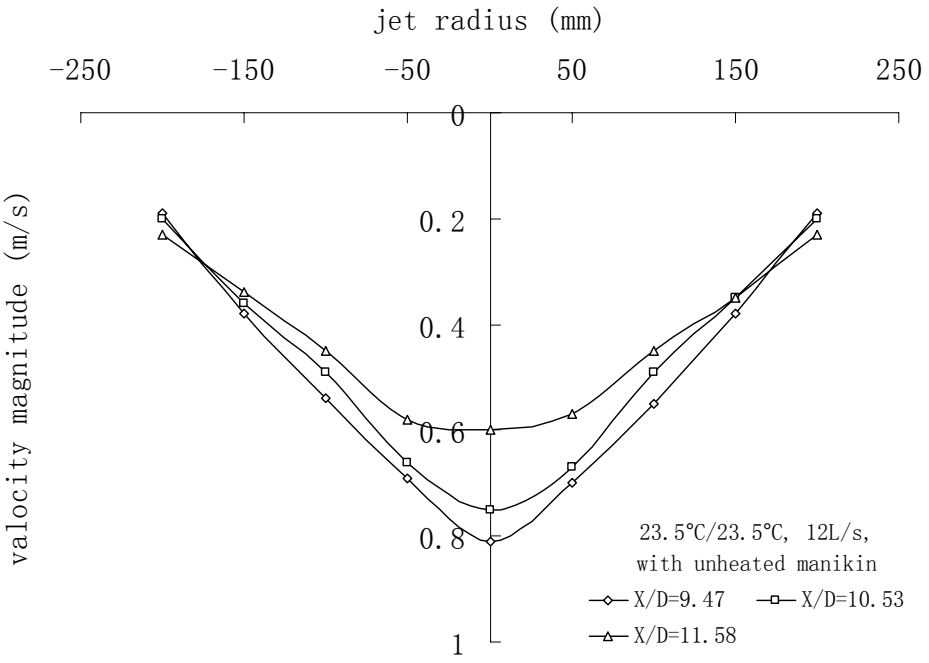

Figure 4b Air velocity profile with 12 L/s personalized airflow rate under 23.5°C/23.5°C isothermal case with unheated manikin

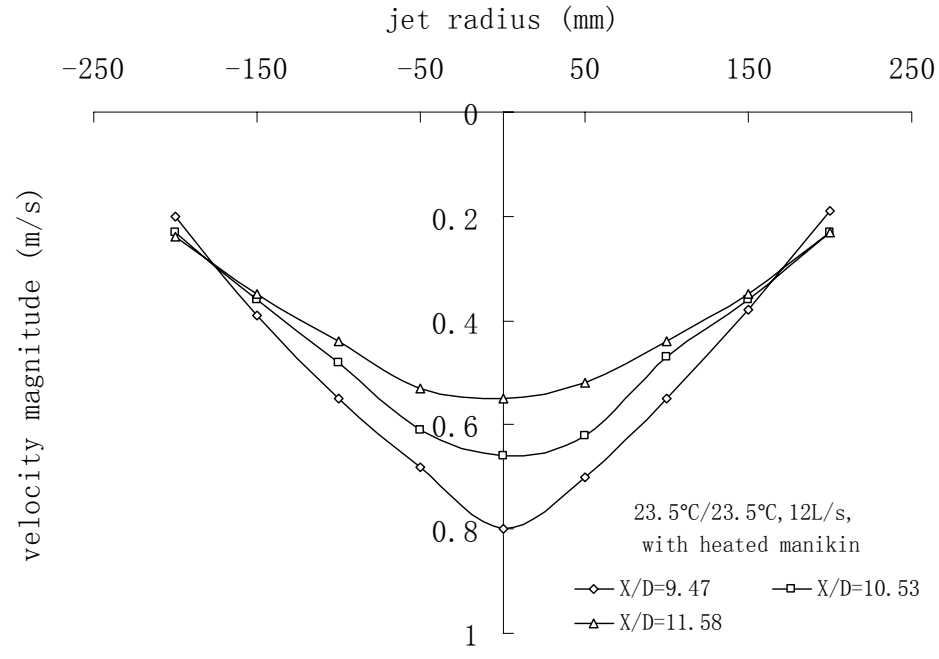

Figure 4c Air velocity profile with 12 L/s personalized airflow rate under 23.5°C/23.5°C isothermal case with heated manikin

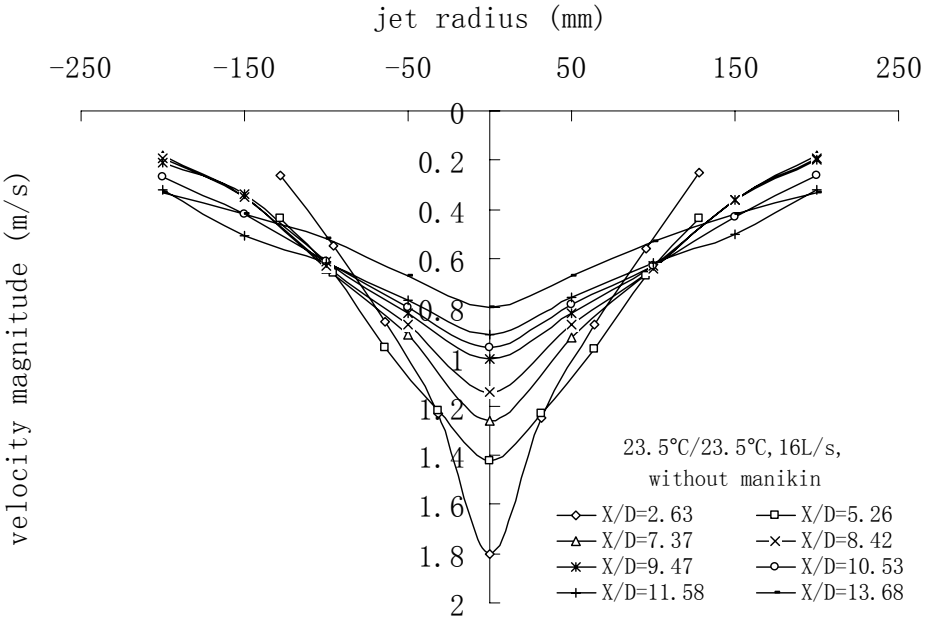

Figure 5 Air velocity profile with 16 L/s personalized airflow rate under 23.5°C/23.5°C isothermal case

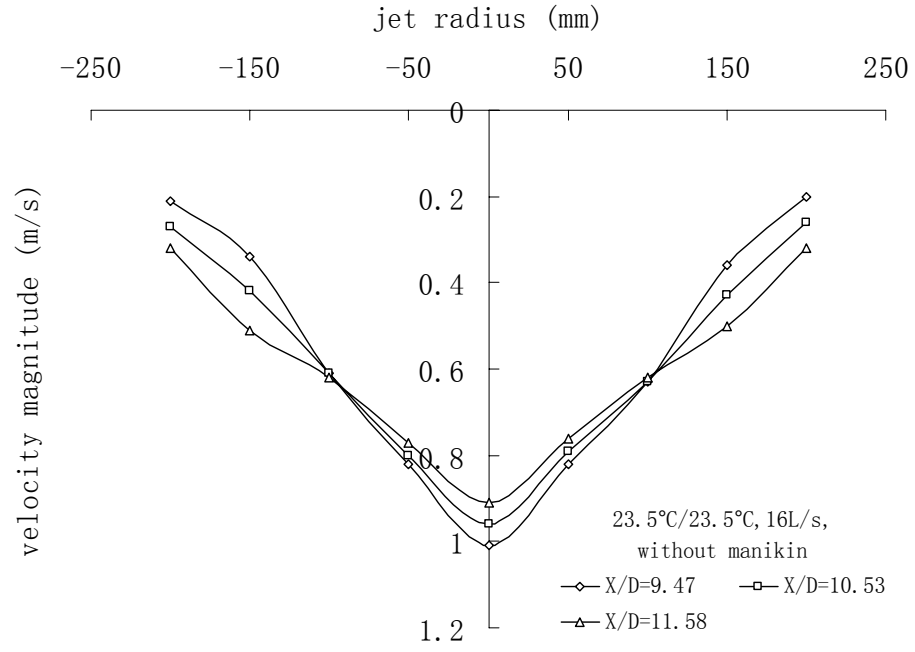

Figure 6a Air velocity profile with 16 L/s personalized airflow rate under 23.5°C/23.5°C isothermal case without manikin

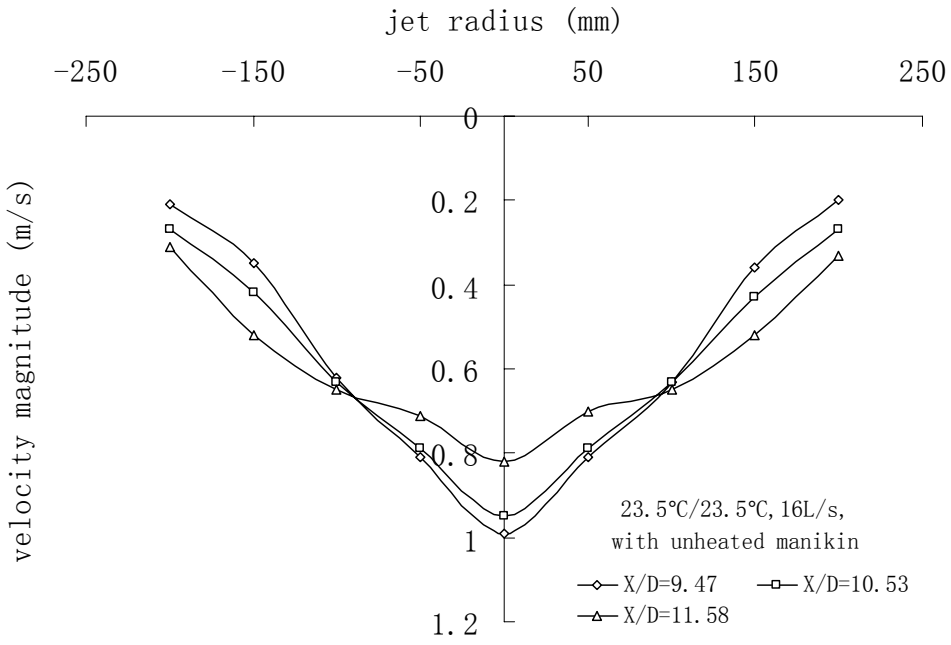

Figure 6b Air velocity profile with 16 L/s personalized airflow rate under 23.5°C/23.5°C isothermal case with unheated manikin

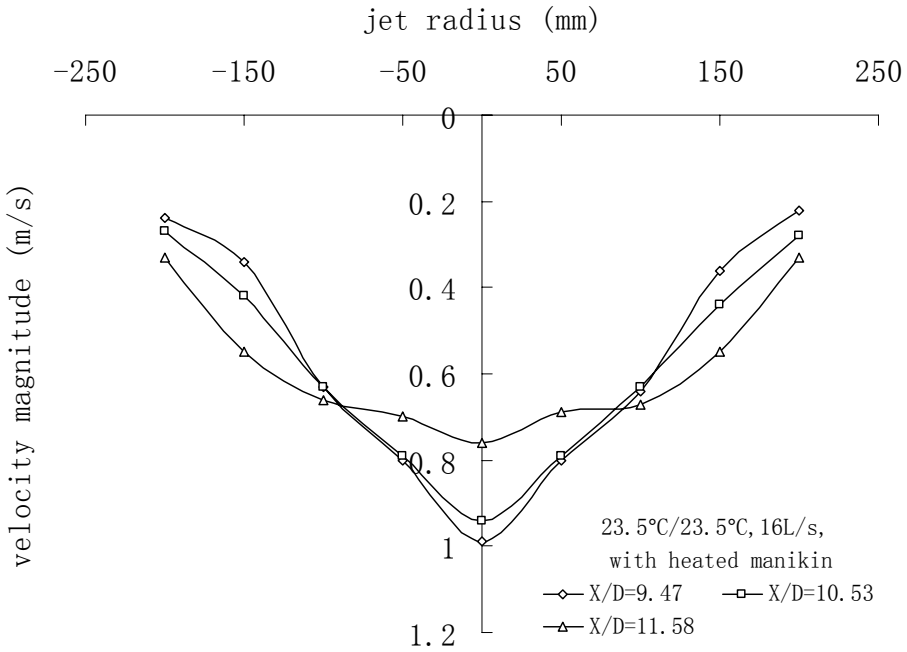

Figure 6c Air velocity profile with 16 L/s personalized airflow rate under 23.5°C/23.5°C isothermal case with heated manikin

Appendix 6. Thermal comfort acceptability

Table 1 Thermal comfort acceptability based on the first choice (after 15 minutes' exposure) of PV airflow rates under different temperature combinations (based on subject number)

Subject No.	23.5°C/21°C				26°C/21°C				23.5°C/23.5°C				26°C/23.5°C				26°C/26°C			
	4	8	12	16	4	8	12	16	4	8	12	16	4	8	12	16	4	8	12	16
11			0.05				0.06				0.06				0.07				0.1	
22		0.29				0.18				0.17				0.45				0.26		
14		0.28				0.17				0.13				0.42				0.22		
29		0.26				0.16				0.06				0.28				0.28		
23		0.26				0.14				0.05				0.32				0.15		
1		0.19				0.1				0.35				0.33				0.3		
6		0.15				0.08				0.4				0.22				0.25		
8		0.18				0.08				0.34				0.22				0.25		
26		0.17				0.07				0.3				0.25				0.26		
18		0.15				0.05				0.28				0.19				0.18		
30		0.15				0				0.26				0.15				0.16		
4		0.14				0.4				0.27				0.12				0.14		
25		0.12				0.35				0.24				0.1				0.1		
21		0.11				0.25				0.25				0.1				0.01		
32		0.09				0.23				0.23				0.12				0.04		
7		0.08				0.22				0.11				0.1				0.01		
20		0.07				0.2				0.1				0.1				0.02		
17		0.55				0.2				0.07				0.11				0.05		
2		0.5				0.15				0.09				0.1				0.04		
5		0.5				0.17				0.1				0.1				0.05		
10		0.45				0.19				0.12				0.03				0.04		
13		0.47				0.1				0.13				0				0.01		
24		0.4				0.22				0.17				0.04				0.02		
28		0.37				0.21				0.16				0.04				0		

19	0.35	0.2	0.15	0.02	0.01
3	0.27	0.19	0.13	0.03	0
15	0.13	0.18	0.12	0.04	0.01
31	0.15	0.13	0.1	0.02	0.05
12	0.14	0.14	0.12	0.01	0.03
16	0.11	0.11	0.11	0.1	0.02
27	0.35	0.33	0.23	0.18	0.04
9	0.28	0.28	0.22	0.16	-0.01

Note: -1=very unacceptable, 0=just unacceptable/acceptable, +1=very acceptable

Table 2 Thermal comfort acceptability based on the second choice (after 30 minutes' exposure) of PV airflow rates under different temperature combinations (based on subject number)

Subject No.	23.5°C/21°C				26°C/21°C				23.5°C/23.5°C				26°C/23.5°C				26°C/26°C			
	4	8	12	16	4	8	12	16	4	8	12	16	4	8	12	16	4	8	12	16
11		0.34				0.18				0.18				0.17				0.2		
22	0.51				0.19				0.19				0.16					0.26		
14	0.46				0.18				0.14					0.43				0.22		
29	0.44				0.17				0.07					0.28					0.43	
23	0.42				0.15				0.06					0.33				0.17		
1	0.39				0.11					0.38					0.38				0.32	
6	0.36				0.09					0.45				0.24					0.34	
8	0.34				0.09					0.34					0.36				0.27	
26	0.33				0.08				0.13						0.66				0.29	
18	0.28				0.06					0.31					0.36				0.26	
30	0.26				0.05					0.3					0.29				0.25	
4	0.24					0.44				0.29					0.28				0.22	
25	0.23				0.04					0.27					0.27				0.13	
21	0.17					0.26				0.25					0.26				0.05	
32	0.15					0.24				0.23					0.25				0.17	
7	0.12					0.23				0.11					0.24				0.15	
20	0.12					0.22				0.09					0.22				0.14	
17		0.55				0.2				0.07					0.21				0.16	
2		0.52				0.13					0.35				0.13				0.18	
5		0.5				0.19					0.38				0.17				0.16	
10		0.48				0.18					0.43				0.18				0.15	
13		0.47				0.08					0.56				0.05				0.14	
24		0.4					0.45				0.33				0.31				0.13	
28		0.39					0.34				0.29				0.27				0.11	
19		0.37					0.31				0.27				0.25				0.09	
3		0.28					0.33				0.3				0.22				0.1	
15		0.13					0.29				0.19				0.21				0.13	

31	0.46		0.28		0.22		0.17		0.08	
12	0.4		0.23		0.18		0.18		0.05	
16	0.37		0.17		0.17		0.17		0.08	
27	0.35			0.56		0.27		0.22		0.07
9	0.28			0.47		0.25		0.21		0.05

Note: -1=very unacceptable, 0=just unacceptable/acceptable, +1=very acceptable

Table 3 Thermal comfort acceptability based on the third choice (after 45 minutes' exposure) of PV airflow rates under different temperature combinations (based on subject number)

Subject No.	23.5°C/21°C				26°C/21°C				23.5°C/23.5°C				26°C/23.5°C				26°C/26°C			
	4	8	12	16	4	8	12	16	4	8	12	16	4	8	12	16	4	8	12	16
11	0.49				0.2				0.22				0.23				0.29			
22	0.51				0.21				0.19					0.46				0.26		
14	0.46				0.18				0.14					0.43				0.22		
29	0.46				0.17				0.07					0.28					0.43	
23	0.43				0.15				0.06					0.33				0.17		
1	0.39				0.12					0.38					0.38				0.32	
6	0.36				0.13					0.45				0.24					0.34	
8	0.35				0.09					0.34					0.36				0.27	
26	0.33				0.13					0.32					0.66				0.29	
18	0.28				0.08					0.31					0.36				0.26	
30	0.26				0.05					0.3					0.29				0.25	
4	0.25					0.45				0.29					0.28				0.22	
25	0.23					0.37				0.27					0.27				0.13	
21	0.17					0.26				0.25					0.26				0.05	
32	0.15					0.24				0.23					0.25					0.31
7	0.12					0.23				0.11					0.24					0.31
20	0.12					0.22				0.09					0.22					0.27
17		0.55				0.2				0.07					0.21					0.24
2		0.52				0.13					0.35				0.13					0.23
5		0.5				0.19					0.38				0.17					0.21
10		0.48				0.18					0.43				0.18					0.29
13		0.47				0.08					0.56				0.05					0.18
24		0.4					0.45				0.33					0.57				0.17
28		0.39					0.34				0.29					0.41				0.16
19		0.37					0.31				0.27					0.39				0.16
3		0.28					0.33				0.3					0.37				0.14
15		0.13					0.29					0.39				0.36				0.15

31	0.46	0.28	0.36	0.31	0.12
12	0.4	0.23	0.31	0.25	0.07
16	0.37	0.17	0.29	0.28	0.09
27	0.35	0.56	0.27	0.22	0.07
9	0.28	0.47	0.25	0.21	0.05

Note: -1=very unacceptable, 0=just unacceptable/acceptable, +1=very acceptable

Table 4 Thermal comfort acceptability based on the fourth choice (after 60 minutes' exposure) of PV airflow rates under different temperature combinations (based on subject number)

Subject No.	23.5°C/21°C				26°C/21°C				23.5°C/23.5°C				26°C/23.5°C				26°C/26°C			
	4	8	12	16	4	8	12	16	4	8	12	16	4	8	12	16	4	8	12	16
11	0.51				0.2				0.25				0.23				0.28			
22	0.51				0.21				0.19					0.47				0.26		
14	0.46				0.18				0.14					0.43				0.22		
29	0.46				0.17				0.07					0.28					0.43	
23	0.43				0.15				0.06					0.33				0.17		
1	0.39				0.12					0.38					0.38				0.32	
6	0.36				0.13					0.45				0.24					0.34	
8	0.35				0.09					0.34					0.36				0.27	
26	0.33				0.13					0.32					0.66				0.29	
18	0.28				0.08					0.31					0.36				0.26	
30	0.26				0.05					0.3					0.29				0.25	
4	0.25					0.45				0.29					0.28				0.22	
25	0.23					0.37				0.27					0.27				0.13	
21	0.17					0.26				0.25					0.26				0.05	
32	0.15					0.24				0.23					0.25					0.31
7	0.12					0.23				0.11					0.24					0.31
20	0.12					0.22				0.09					0.22					0.27
17		0.55				0.2				0.07					0.21					0.24
2		0.52				0.13					0.35				0.13					0.23
5		0.5				0.19					0.38				0.17					0.21
10		0.48				0.18					0.43				0.18					0.29
13		0.47				0.08					0.56				0.05					0.18
24		0.4					0.45				0.33					0.57				0.17
28		0.39					0.34				0.29					0.41				0.16
19		0.37					0.31				0.27					0.39				0.16
3		0.28					0.33				0.3					0.37				0.14
15		0.13					0.29					0.39				0.36				0.15

31	0.46	0.28	0.36	0.31	0.12
12	0.4	0.23	0.31	0.25	0.07
16	0.37	0.17	0.29	0.28	0.09
27	0.35	0.56	0.27	0.22	0.07
9	0.28	0.47	0.25	0.21	0.05

Note: -1=very unacceptable, 0=just unacceptable/acceptable, +1=very acceptable

Table 5 Thermal comfort acceptability based on the make-up choice (after 90 minutes' exposure) of PV airflow rates under different temperature combinations (based on subject number)

Subject No.	23.5°C/21°C				26°C/21°C				23.5°C/23.5°C				26°C/23.5°C				26°C/26°C			
	4	8	12	16	4	8	12	16	4	8	12	16	4	8	12	16	4	8	12	16
11				-0.09				-0.05				-0.03				-0.03				0.03
22			0.15				0.07				0.07				-0.02				0.1	
14			0.14				0.04				0.07				-0.01				0.09	
29			0.14				0.04				0.07				-0.02					0.23
23			0.14				0.04				0.05				0				0.1	
1			0.18				0.08				0.08					-0.04				0
6			0.15				0.04				0.09				-0.03					0.05
8			0.16				0.06				0.07					0				0.02
26			0.17				0.07				0.1					0.05				0.08
18			0.16				0.05				0.08					0				0
30			0.13				0.01				0.1					0.07				0.07
4			0.12				0.09				0.1					0.05				0.04
25			0.14				0.07				0.06					0.05				0.05
21			0.13				0.11				0.07					0.04				0
32			0.12				0.1				0.08					0.07	0.01			
7			0.12				0.11				0.05					0.06	0			
20			0.1				0.09				0.02					0.06	0			
17			0.11				0.05				0					0.05	0.03			
2			0.12				0.09					0.09				0.07	0.03			
5			0.13				0.1					0.1				0.08	0.02			
10			0.13				0.1					0.11				0.07	0.02			
13			0.15				0.05					0.08				0	-0.01			
24			0.19				1.46	-0.03				0.18	0.03				0			
28			0.18					-0.01				0.15	0.01				-0.02			
19			0.17					0.09				0.16	0.01				-0.03			
3			0.15					-0.02				0.18	0				-0.05			
15			0.19					0.08	0.08				0.02				-0.02			

31		0.12		0.04	0.07		0.04		0.03			
12		0.1		0.02	0.09		0.06		0			
16		0.11		-0.1	0.07		0.06		-0.01			
27	0.21		0.23	0.07		0.18		0.11	0	0		
9		0.1	0.17			0.15		0.1		-0.1		

Note: -1=very unacceptable, 0=just unacceptable/acceptable, +1=very acceptable

Appendix 7. Inhaled air quality acceptability

Table 1 Inhaled air quality acceptability based on first choice (after 15 minutes' exposure) of PV airflow rates under different temperature combinations (based on subject number)

Subject No.	23.5°C/21°C				26°C/21°C				23.5°C/23.5°C				26°C/23.5°C				26°C/26°C			
	4	8	12	16	4	8	12	16	4	8	12	16	4	8	12	16	4	8	12	16
11			0.05				0.06				0.06				0.03				0	
22		0.09				0.08				0.09				0.13				0.1		
14		0.11				0.11				0.05				0.12				0.07		
29		0.16				0.1				-0.02				0.08				0.08		
23		0.14				0.1				0.05				0.12				0		
1		0.1				0.07				0.2				0.12				0.06		
6		0.13				0.08				0.24				0.1				0.08		
8		0.1				0.08				0.2				0.1				0.02		
26		0.07				0.04				0.1				0.07				0.02		
18		0.1				0.05				0.1				0.09				0.07		
30		0.05				-0.04				0.13				0.1				0.04		
4		0				0.35				0.11				0.07				0.03		
25		0.02				0.22				0.1				0.07				0		
21		-0.03				0.2				0.1				0.07				-0.01		
32		-0.09				0.14				0.05				0.09				0.02		
7		-0.08				0.2				0.1				0.07				0.02		
20		0.11				0.2				0.1				0.1				0.02		
17		0.25				0.14				0.01				0				-0.05		
2		0.14				0.03				0.09				-0.01				-0.04		
5		0.17				0.07				0.05				0				-0.05		
10		0.22				0.14				0.12				0.03				0.04		
13		0.18				0.09				0.08				0				0.01		
24		0.05				0.05				0.03				0.02				0.02		
28		0.06				0.11				0.1				0.07				0.02		

19	0.06	0.1	0.07	0.07	0.01
3	0.09	0.09	0.07	0.05	0.02
15	0.13	0.11	0.1	0.07	0.01
31	0.14	0.07	0.12	0.07	0
12	0.15	0.11	0.12	0.07	0.03
16	0.16	0.11	0.11	0.08	0.02
27	0.07	0.07	0.15	0.08	-0.01
9	0.14	0.13	0.12	0.1	-0.01

Note: -1=very unacceptable, 0=just unacceptable/acceptable, +1=very acceptable

Table 2 Inhaled air quality acceptability based on second choice (after 30 minutes' exposure) of PV airflow rates under different temperature combinations (based on subject number)

Subject No.	23.5°C/21°C				26°C/21°C				23.5°C/23.5°C				26°C/23.5°C				26°C/26°C			
	4	8	12	16	4	8	12	16	4	8	12	16	4	8	12	16	4	8	12	16
11		0.17				0.18				0.12				0.03				0.02		
22	0.25				0.24				0.25				0.1					0.1		
14	0.21				0.17				0.08					0.12				0.07		
29	0.18				0.13				0					0.08					0.13	
23	0.2				0.15				0.06					0.12				0		
1	0.12				0.1					0.2					0.19				0.12	
6	0.16				0.12					0.24				0.1					0.2	
8	0.13				0.11					0.21					0.23				0.13	
26	0.1				0.05				0.06						0.19				0.1	
18	0.12				0.08					0.11					0.15				0.1	
30	0.06				-0.01					0.13					0.14				0.05	
4	0.05					0.36				0.12					0.12				0.05	
25	0.04				0.1					0.11					0.13				0.04	
21	0.03					0.2				0.11					0.12				0	
32	-0.05					0.14				0.05					0.11				0.08	
7	0.02					0.21				0.1					0.12				0.08	
20	0.12					0.22				0.09					0.22				0.14	
17		0.25				0.14				0.01					0.1				0.06	
2		0.14				0.03					0.15				0.02				0.08	
5		0.17				0.07					0.23				0.04				0.08	
10		0.22				0.14					0.3				0.08				0.08	
13		0.18				0.09					0.24				0.1				0.08	
24		0.05					0.22				0.08				0.13				0.08	
28		0.06					0.27				0.11				0.13				0.07	
19		0.06					0.23				0.09				0.14				0.06	
3		0.09					0.32				0.12				0.14				0.08	
15		0.13					0.18				0.16				0.13				0.05	

31	0.16	0.09	0.16	0.12	0.01
12	0.36	0.19	0.16	0.13	0.05
16	0.32	0.22	0.17	0.13	0.07
27	0.07	0.28	0.17	0.09	0
9	0.14	0.29	0.19	0.11	0.01

Note: -1=very unacceptable, 0=just unacceptable/acceptable, +1=very acceptable

Table 3 Inhaled air quality acceptability based on third choice (after 45 minutes' exposure) of PV airflow rates under different temperature combinations (based on subject number)

Subject No.	23.5°C/21°C				26°C/21°C				23.5°C/23.5°C				26°C/23.5°C				26°C/26°C			
	4	8	12	16	4	8	12	16	4	8	12	16	4	8	12	16	4	8	12	16
11	0.24				0.22				0.13				0.06				0.03			
22	0.25				0.24				0.25					0.13				0.1		
14	0.21				0.16				0.07					0.12				0.07		
29	0.18				0.13				0					0.08					0.13	
23	0.2				0.15				0.06					0.12				0		
1	0.12				0.1					0.2					0.19				0.12	
6	0.16				0.12					0.24				0.1					0.2	
8	0.13				0.11					0.22					0.23				0.13	
26	0.1				0.05					0.13					0.19				0.1	
18	0.11				0.08					0.12					0.15				0.11	
30	0.06				-0.01					0.13					0.14				0.05	
4	0.05					0.36				0.12					0.13				0.05	
25	0.04					0.24				0.11					0.13				0.04	
21	0.03					0.2				0.11					0.12				0	
32	-0.05					0.14				0.05					0.11					0.19
7	0.02					0.21				0.1					0.12					0.21
20	0.12					0.22				0.09					0.22					0.2
17		0.25				0.14				0.01					0.1					0.16
2		0.14				0.03					0.15				0.02					0.11
5		0.17				0.07					0.23				0.04					0.13
10		0.22				0.14					0.3				0.08					0.14
13		0.18				0.08					0.24				0.1					0.15
24		0.05					0.22				0.08					0.19				0.08
28		0.06					0.27				0.11					0.21				0.08
19		0.06					0.23				0.09					0.2				0.08
3		0.09					0.32				0.12					0.23				0.11
15		0.13					0.18					0.22				0.17				0.06

31	0.16	0.09	0.21	0.14	0.02
12	0.36	0.19	0.26	0.19	0.08
16	0.32	0.22	0.33	0.18	0.08
27	0.07	0.28	0.17	0.09	0
9	0.14	0.29	0.19	0.11	0.01

Note: -1=very unacceptable, 0=just unacceptable/acceptable, +1=very acceptable

Table 4 Inhaled air quality acceptability based on fourth choice (after 60 minutes' exposure) of PV airflow rates under different temperature combinations (based on subject number)

Subject No.	23.5°C/21°C				26°C/21°C				23.5°C/23.5°C				26°C/23.5°C				26°C/26°C			
	4	8	12	16	4	8	12	16	4	8	12	16	4	8	12	16	4	8	12	16
11	0.24				0.22				0.13				0.06				0.03			
22	0.25				0.24				0.25					0.13				0.1		
14	0.2				0.16				0.07					0.12				0.07		
29	0.18				0.13				0					0.08					0.13	
23	0.2				0.14				0.06					0.12				0		
1	0.12				0.1					0.2					0.19				0.12	
6	0.16				0.12					0.24				0.1					0.2	
8	0.13				0.11					0.22					0.23				0.13	
26	0.09				0.05					0.13					0.19				0.11	
18	0.11				0.08					0.13					0.15				0.11	
30	0.06				-0.01					0.13					0.14				0.05	
4	0.05					0.36				0.12					0.13				0.05	
25	0.04					0.24				0.11					0.13				0.04	
21	0.03					0.21				0.11					0.12				0	
32	-0.05					0.15				0.05					0.11					0.19
7	0.02					0.21				0.09					0.12					0.21
20	0.12					0.22				0.09					0.22					0.2
17		0.26				0.14				0.01					0.1					0.16
2		0.14				0.03					0.15				0.02					0.11
5		0.17				0.07					0.23				0.04					0.13
10		0.22				0.14					0.3				0.08					0.14
13		0.18				0.09					0.24				0.1					0.15
24		0.05					0.22				0.08					0.19				0.08
28		0.06					0.27				0.11					0.21				0.08
19		0.06					0.23				0.09					0.2				0.08
3		0.09					0.32				0.12					0.23				0.11
15		0.13					0.18					0.22				0.17				0.06

31	0.16	0.09	0.21	0.14	0.02
12	0.36	0.19	0.26	0.19	0.08
16	0.32	0.22	0.33	0.18	0.08
27	0.07	0.28	0.17	0.09	0
9	0.14	0.29	0.19	0.11	0.01

Note: -1=very unacceptable, 0=just unacceptable/acceptable, +1=very acceptable

Table 5 Inhaled air quality acceptability based on make-up choice (after 90 minutes' exposure) of PV airflow rates under different temperature combinations (based on subject number)

Subject No.	23.5°C/21°C				26°C/21°C				23.5°C/23.5°C				26°C/23.5°C				26°C/26°C			
	4	8	12	16	4	8	12	16	4	8	12	16	4	8	12	16	4	8	12	16
11				-0.08				-0.05				-0.04				-0.03				-0.03
22			0.15				0.05				0.05				0.1				0.08	
14			0.19				0.08				0.02				0.05				0.05	
29			0.14				0.08				-0.04				-0.06					0.09
23			0.15				0.04				0				0.03				-0.05	
1			0.18				0.05				0.05					0.12				0.05
6			0.18				0.04				0.17				0.03					0.05
8			0.16				0.06				0.15					0.15				0.08
26			0.15				0				0.1					0.05				0.05
18			0.09				0.05				0.05					0.06				0.02
30			0.13				-0.05				0					0.07				0.03
4			0.05				0.19				0.1					0.05				0.04
25			0.04				0.1				0.06					0.05				0.01
21			-0.03				0.17				0.07					0.08				0
32			-0.08				0.1				0.02					0.07	0.01			
7			-0.08				0.11				0.05					0.06	0			
20			0.1				0.17				0.05					0.15	0			
17			0.18				0.08				0					0.05	-0.13			
2			0.12				0					0.01				-0.07	0.05			
5			0.13				0.05					0				0.02	0.07			
10			0.13				0.1					0.1				0.07	0.02			
13			0.15				0.05					0.02				0	0.01			
24			0.08					-0.03				0.02	0.02				0			
28			0.08					0				0.02	0.06				0.01			
19			0.08					0.09				0.02	0.06				0.03			
3			0.08					0.3				0.02	0.03				0.01			
15			0.1					0	0.08				0.05				-0.02			

31		0.12		0.06	0.1		0.06		0.03			
12		0.21		0.3	0.09		0.06		0			
16		0.2		0.09	0.07		0.06		0.01			
27	0.05		0.06		0.06		0.06		-0.03			
9		0.1	0.11		0.1		0.07		-0.03			

Note: -1=very unacceptable, 0=just unacceptable/acceptable, +1=very acceptable

Appendix 8. Air movement preference

Table 1 Whole body air movement preference based on first choice (after 15 minutes' exposure) of PV airflow rates under different temperature combinations (based on subject number)

Subject No.	23.5°C/21°C				26°C/21°C				23.5°C/23.5°C				26°C/23.5°C				26°C/26°C			
	4	8	12	16	4	8	12	16	4	8	12	16	4	8	12	16	4	8	12	16
11			-1				-1				-1				-1				-1	
22		-1				-1				-1				0				0		
14		-1				-1				-1				0				0		
29		-1				-1				-1				0				1		
23		-1				-1				-1				0				0		
1		-1				-1				-1				0				1		
6		-1				-1				-1				0				1		
8		-1				-1				-1				0				1		
26		-1				-1				-1				0				1		
18		-1				-1				-1				0				0		
30		-1				0				-1				0				0		
4		-1				0				0				0				0		
25		-1				0				0				0				0		
21		0				0				0				0				0		
32		0				0				0				0				0		
7		0				0				0				0				0		
20		0				0				0				0				0		
17		0				0				0				0				0		
2		0				0				0				0				0		
5		0				0				0				0				0		
10		0				0				0				0				0		
13		0				1				0				0				0		
24		0				1				0				0				0		
28		0				1				1				0				0		

19	0	1	1	0	0
3	0	1	1	0	0
15	0	1	1	0	0
31	1	1	1	1	0
12	1	1	1	1	0
16	1	1	1	1	0
27	0	1	1	1	0
9	0	1	1	1	1

Note: -1=less air movement, 0=no change, +1=more air movement

Table 2 Whole body air movement preference based on second choice (after 30 minutes' exposure) of PV airflow rates under different temperature combinations (based on subject number)

Subject No.	23.5°C/21°C				26°C/21°C				23.5°C/23.5°C				26°C/23.5°C				26°C/26°C			
	4	8	12	16	4	8	12	16	4	8	12	16	4	8	12	16	4	8	12	16
11		-1				-1				-1				-1				-1		
22	-1				0				0				0					0		
14	-1				0				0					0				0		
29	0				0				0					0					0	
23	0				0				0					0				0		
1	0				0					0					0				0	
6	0				0					0				0					0	
8	0				1					0					0				0	
26	0				1				0						0				0	
18	0				1					0					-1				0	
30	0				1					0					-1				0	
4	0					0				0					-1				0	
25	0				1					0					0				0	
21	0					0				0					-1				0	
32	0					0				0					0				0	
7	0					0				0					0				0	
20	0					0				0					0				0	
17		0				0				0					-1				0	
2		0				0					0				0				0	
5		0				0					0				0				0	
10		0				0					0				0				0	
13		0				0					0				0				0	
24		0					0				0				1				0	
28		0					0				0				0				0	
19		0					0				0				0				0	
3		0					0				0				0				0	
15		0					0				1				1				1	

31	0	0	1	1	0
12	0	0	1	1	0
16	0	0	1	1	1
27	0	0	0	0	0
9	0	0	0	0	0

Note: -1=less air movement, 0=no change, +1=more air movement

Table 3 Whole body air movement preference based on third choice (after 45 minutes' exposure) of PV airflow rates under different temperature combinations (based on subject number)

Subject No.	23.5°C/21°C				26°C/21°C				23.5°C/23.5°C				26°C/23.5°C				26°C/26°C			
	4	8	12	16	4	8	12	16	4	8	12	16	4	8	12	16	4	8	12	16
11	-1				0				0				-1				0			
22	0				0				0					0				0		
14	0				0				0					0				0		
29	0				0				0					0					0	
23	0				0				0					0				0		
1	0				0					0					0				0	
6	0				0					0				0					0	
8	0				0					0					0				0	
26	0				0					0					0				0	
18	0				0					0					0				0	
30	0				0					0					0				0	
4	0					0				0					0				0	
25	0					0				0					0				0	
21	0					0				0					0				0	
32	0					0				0					0					0
7	0					0				0					0					0
20	0					0				0					0					0
17		0				0				0					0					0
2		0				0					0				-1					0
5		0				0					0				-1					0
10		0				0					0				-1					0
13		0				0					0				0					0
24		0					0				0					0				0
28		0					0				0					0				0
19		0					0				0					0				0
3		0					0				0					0				0
15		0					0					0				0				0

31	0	0	0	0	0
12	0	0	0	0	0
16	0	0	0	0	0
27	0	0	0	0	0
9	0	0	0	0	0

Note: -1=less air movement, 0=no change, +1=more air movement

Table 4 Whole body air movement preference based on fourth choice (after 60 minutes' exposure) of PV airflow rates under different temperature combinations (based on subject number)

Subject No.	23.5°C/21°C				26°C/21°C				23.5°C/23.5°C				26°C/23.5°C				26°C/26°C			
	4	8	12	16	4	8	12	16	4	8	12	16	4	8	12	16	4	8	12	16
11	0				0				0				-1				0			
22	0				0				0					0				0		
14	0				0				0					0				0		
29	0				0				0					0					0	
23	0				0				0					0				0		
1	0				0					0					0				0	
6	0				0					0				0					0	
8	0				0					0					0				0	
26	0				0					0					0				0	
18	0				0					0					0				0	
30	0				0					0					0				0	
4	0					0				0					0				0	
25	0					0				0					0				0	
21	0					0				0					0				0	
32	0					0				0					0					0
7	0					0				0					0					0
20	0					0				0					0					0
17		0				0				0					0					0
2		0				0					0				0					0
5		0				0					0				0					0
10		0				0					0				0					0
13		0				0					0				0					0
24		0					0				0					0				0
28		0					0				0					0				0
19		0					0				0					0				0
3		0					0				0					0				0
15		0					0					0				0				0

31	0	0	0	0	0
12	0	0	0	0	0
16	0	0	0	0	0
27	0	0	0	0	0
9	0	0	0	0	0

Note: -1=less air movement, 0=no change, +1=more air movement

Table 5 Whole body air movement preference based on make-up choice (after 90 minutes' exposure) of PV airflow rates under different temperature combinations (based on subject number)

Subject No.	23.5°C/21°C				26°C/21°C				23.5°C/23.5°C				26°C/23.5°C				26°C/26°C			
	4	8	12	16	4	8	12	16	4	8	12	16	4	8	12	16	4	8	12	16
11				-1				-1				-1				-1				0
22			-1				-1				-1				-1				-1	
14			-1				-1				-1				-1				-1	
29			-1				-1				-1				-1					0
23			-1				-1				-1				-1				-1	
1			-1				-1				-1					-1				0
6			-1				-1				-1				-1					-1
8			-1				-1				-1					-1				0
26			-1				0				-1					0				0
18			-1				0				-1					0				0
30			-1				0				-1					0				0
4			0				0				-1					0				-1
25			0				0				-1					0				-1
21			0				0				-1					0				-1
32			0				0				-1					0	1			
7			0				0				-1					-1	1			
20			0				0				0					0	1			
17			0				0				-1					-1	0			
2			0				0					-1				0	0			
5			0				0					-1				-1	0			
10			0				0					-1				0	0			
13			0				0					-1				0	0			
24			0					-1				-1	1				1			
28			0					-1				0	1				0			
19			0					-1				-1	1				0			
3			0					0				0	0				0			
15			0					0	1				0				0			

31	0	0	0	1	0
12	0	0	1	0	0
16	0	0	0	1	0
27	1	1	1	1	1
9	0	1	1	1	1

Note: -1=less air movement, 0=no change, +1=more air movement

Appendix 9. List of publications

Journal papers

1. **Bin Yang**, S. C. Sekhar. 2007. Three-dimension numerical simulation of a hybrid fresh air and re-circulated air diffuser for decoupled ventilation strategy, *Building and Environment*, 42(5), p1975-1982.

ABSTRACT

In conventional mixing ventilation air conditioning system, fresh air which has been polluted by re-circulated air is supplied to occupied zone. Therefore, more fresh air which results in energy penalty needs to be supplied in order to keep good indoor air quality (IAQ) and thermal comfort. Some alternatives such as personalized ventilation air conditioning system can address this problem effectively by supplying fresh air directly into occupied zone. However, room layouts and visual effects will be influenced deeply because of extended air ducts. A new approach supplying fresh air directly by utilizing high velocity circular air jet without mixing with re-circulated air is introduced. Objective measurements and computational fluid dynamics (CFD) tool are used to evaluate corresponding indoor parameters to verify that it can both supply fresh air into occupied zone effectively and avoid draught rating. It is found that the measured air velocities are within the limits (0.25 m/s) of thermal comfort standards, although they are close to the limits. Higher air change rate can be obtained in breathing zone than that in ambient air in the background area. The predicted results show unique distributions of airflow characteristics and are in fair agreement with empirical measurements. Different angles of re-circulated air diffuser blades, different lengths and directions of protruding fresh air jets and different inlet velocities of fresh air are adopted for comparing the effectiveness and efficiency of this new ventilation

strategy numerically.

KEYWORDS: Air jet, CFD, Draught rating, Air change rate

2. Bin Yang, S. C. Sekhar. 2007. Numerical algorithm studies of CFD modeling for a compartmented cooling coil under dehumidifying conditions, *Numerical Heat Transfer, Applications,* 52(8): 737-755.

ABSTRACT

The compartmented cooling coil is the core component of the newly developed air conditioning and air distributing system called the Single Coil Twin Fan (SCTF) system. In prototype experiments, the SCTF system has clearly demonstrated its ability to provide enhanced indoor air quality and achieve significant energy savings (12%). However, the geometric parameters of the compartmented coil were chosen based on approximate estimates and intuitive reasoning, which makes parametric optimization studies necessary. Computational fluid dynamics (CFD) simulation is more feasible than experimental methods because of its flexibility and economic considerations, especially for the compartmented coil. A newly developed numerical algorithm for simulating latent heat transfer is coupled to the coil model, which is created on the platform of commercial software FLUENT. A simple two-dimensional case which has an analytical solution is utilized to validate the accuracy of the new algorithm. The accuracy of the three-dimensional model based on the prototype of the compartmented coil is validated by experimental data and can be utilized for further parametric optimization studies. This simulation model based on the new algorithm, which was developed particularly for the compartmented coil, can be generalized and paves the way for the development of numerical tools for compact heat exchangers operating under dehumidifying conditions.

3. Bin Yang, S. C. Sekhar. 2008. The influence of evenly distributed ceiling mounted personalized ventilation devices on indoor environment, *International Journal of Ventilation*, 7(2): 99-112.

ABSTRACT

The advantage of conventional PV is to improve the fresh air percentage much higher near PV ATDs. However, the distribution of fresh air percentage is very uneven in the field. Occupants are confined to their working zones in order to obtain good inhaled air quality. Ceiling mounted PV can overcome these disadvantages of conventional PV, although fresh air percentage is lower than that of conventional PV near working zones. A typical office workplace consisting of either ceiling mounted PV ATDs or conventional PV ATDs and ambient air supply diffusers is simulated, based on an indoor air quality chamber at the National University of Singapore. Based on the numerical results, it is concluded that ceiling mounted PV can improve inhaled air quality for both seated occupants and moving occupants over a longer occupied area although conventional PV can improve inhaled air quality much better in the immediate breathing zones at the work stations.

KEYWORDS: Ceiling mounted personalized ventilation (PV), Conventional personalized ventilation, Moving person, Computational fluid dynamics (CFD), Dynamic mesh

4. Bin Yang, Arsen Melikov, Chandra Sekhar. 2008. Performance evaluation of ceiling mounted personalized ventilation system, *ASHRAE Transactions,* (In press).

ABSTRACT

The interaction of the personalized airflow supplied from ceiling mounted nozzle (diameter of 0.095 m) with the thermal plume generated by a seated thermal manikin with the body size of an average Scandinavian woman and its impact on the body cooling was studied. Experiments were performed in a test room with mixing ventilation at numerous conditions comprising four combinations of room air temperature and personalized air temperature (23.5°C/21°C, 23.5°C/23.5°C, 26°C/23.5°C, 26°C/26°C), four airflow rates of the personalized air (4, 8, 12, 16 L/s) and positioning of the manikin directly below the nozzle (1.3 m distance between the top of manikin's head and the nozzle). The asymmetric exposure of the body to the personalized flow was studied by moving the manikin 0.2 m forward, backward and sideward. The blockage effect of the unheated manikin on the personalized airflow distribution, studied at the case 23.5°C/23.5°C, was clearly observed 0.2 m above the top of manikin's head where the centerline velocity was reduced to about 85% under all personalized airflow rates. The neutral level, Xnl, defined as the distance from the nozzle where the impact of the thermal plume on the velocity distribution in the personalized airflow was observed, increased from 0.8 m to 1.1 m with the increase of the airflow rate. Above 16 L/s the personalized airflow was able to completely destroy the thermal plume. In comparison with the reference case without personalized airflow, the manikin based equivalent temperature for the head decreased with the increase of the airflow rate from -1°C to -6°C under 23.5°C/21°C case and from -0.5°C to -4°C under 26°C/26°C case, which are the two extreme cases among the four cases studied. The personalized airflow was least efficient to cool the body when the manikin was moved forward.

KEYWORDS: Ceiling mounted nozzle, Personalized ventilation, Blockage effect, Neutral level, Occupant movement analysis

5. Bin Yang, Chandra Sekhar, Arsen Melikov. 2008. Ceiling mounted personalized ventilation system integrated with a secondary air distribution system – A human response study in hot and humid climate, *Indoor Air,* (Approved).

ABSTRACT

The benefits of thermal comfort and Indoor Air Quality (IAQ) with personalized ventilation (PV) systems have been demonstrated in recent studies. One of the barriers for wide spread acceptance by architects and HVAC designers has been attributed to challenges and constraints faced in the integration of PV systems with the work-station. A newly developed ceiling mounted PV system addresses these challenges and provides a practical solution while retaining much of the apparent benefits of PV systems. Assessments of thermal environment, air movement and air quality for ceiling mounted PV system were performed with tropically acclimatized subjects in a Field Environmental Chamber. 32 subjects performed normal office work and could choose to be exposed to four different PV airflow rates (4, 8, 12 and 16 L /s), thus offering themselves a reasonable degree of individual control. Ambient temperatures of 26°C and 23.5°C and PV air temperatures of 26°C, 23.5°C and 21°C were employed. The local and whole body thermal sensations were reduced when PV airflow rates were increased. Inhaled air temperature was perceived cooler and perceived air quality and air freshness improved when PV airflow rate was increased or temperature was reduced.

KEYWORDS:

Personalised Ventilation, Ceiling mounted air terminal devices, Tropically acclimatized, Thermal comfort, Indoor air quality

International conference papers

1. S. C Sekhar, **Bin Yang**. 2005. CFD modeling of a compartmented coil for demand ventilation to achieve enhanced indoor air quality, Proceedings of the 10th international conference on indoor air quality and climate, September 4-9, Beijing, China.

ABSTRACT

Compartmented cooling coil is a key component of a newly developed air-conditioning and air distribution system at the National University of Singapore called the Single-coil Twin Fan (SCTF) system. In prototype experiments, the SCTF system has clearly demonstrated its ability to provide enhanced indoor air quality (IAQ) and achieve significant energy savings. It has been observed that the unique features of the compartmented cooling coil are fundamental to improving the heat and mass transfer performance of the coil. Whilst empirical measurements have been undertaken to evaluate the performance of such a coil, flow visualization employing CFD modeling techniques are also envisaged to provide a better insight into the fundamental characteristics of a compartmented coil which addresses both indoor air quality and energy issues according to zone-specific demand of ventilation and cooling loads. A highly refined cooling coil model is developed with distinct compartments which has finer meshing at the key surfaces. Boundary conditions obtained from experiments will include bulk air stream conditions upstream of both the compartments of the coil. Three different models (k-ε model, RNG model, Reynolds stress model) are used to compare the simulation results. This paper presents the development of the CFD model of the compartmented coil and an evaluation of the heat transfer characteristics.

KEYWORDS: Demand ventilation, Compartmented coil, IAQ, Energy efficiency, CFD simulation

2. **Bin Yang**, S. C. Sekhar. 2006. An innovative fresh air supply method for decoupled ventilation strategy, Proceedings of the 8th international conference on healthy buildings, June 4-8, Lisbon, Portugal.

ABSTRACT

An innovative approach by utilizing high velocity circular air jet which is located at the center of a normal air diffuser is introduced. Less fresh air is polluted by re-circulated air when compared with mixing ventilation strategy. Room layouts and visual effects will not be affected deeply when compared with personalized ventilation strategy. A computational fluid dynamics (CFD) tool is used to simulate corresponding indoor parameters to verify that it can both supply fresh air into occupied zone effectively and avoid draught rating. Some experiments are conducted in a small chamber to validate the effectiveness of the simulation model.

KEYWORDS: Air jet, CFD, Draught rating, Air change rate

3 **Bin Yang**, S. C. Sekhar. 2006. CFD modeling and experimental validation of a compartmented cooling coil under dehumidifying conditions, Proceedings of the 8th international conference on healthy buildings, June 4-8, Lisbon, Portugal.

ABSTRACT

Compartmented cooling coil is a key component of a newly developed air-conditioning and air distribution system at the National University of Singapore called the Single-coil Twin Fan (SCTF) system. In prototype experiments, the SCTF system has clearly demonstrated its ability to provide enhanced indoor air quality

(IAQ) and achieve significant energy savings (12%). In order to evaluate the unique features of the compartmented cooling coil, one CFD model is created based on a one-row plate-fin compartmented coil which is utilized in a prototype experiment. A newly developed numerical algorithm for simulating latent heat transfer is coupled into the coil model which is created on the platform of commercial software FLUENT. The accuracy of the simulation is validated by experimental data and can be used for further parametric variation studies. This algorithm can also be generalized and open the door to new design procedures for compact heat exchangers operating under dehumidifying conditions.

KEYWORDS: Compartmented coil, CFD simulation, Dehumidifying conditions

4 Bin Yang, S. C. Sekhar. 2007. Numerical study of circular jet diffuser for task ventilation of displacement ventilation system in tropics. Proceedings of the 10th international conference on air distribution in rooms, June 13-15, Helsinki, Finland.

ABSTRACT

Bases on the concept of task/ambient ventilation, fresh air can be decoupled from re-circulated air so as to improving ventilation effectiveness in breathing zone. Ceiling mounted high velocity circular jet diffusers, which are regarded as remote personalized ventilation air terminal devices (PV ATDs) without affecting room aesthetic effects, can be utilized to supply fresh air without causing draft rating because tropically acclimatized occupants prefer slightly higher air movement. Displacement ventilation (DV) cylinders are used to supply re-circulated air. Corresponding mixing ventilation system by only utilizing DV cylinders are compared with this task/ambient ventilation system. Numerical simulation using a validated computational fluid dynamics (CFD) model for circular jet diffusers is

conducted to investigate the difference between task/ambient ventilation systems and mixing ventilation systems. Fresh air with high momentum can penetrate the air plume around human bodies easily. Corresponding areas with negative static pressure appear, which can induce more recirculated air for floor levels, because of the high kinetic pressure. Location weighted personal exposure effectiveness is utilized as an evaluation index for evaluating indoor air quality (IAQ). Air velocity and temperature are utilized as evaluation indices for evaluating thermal comfort level.

KEYWORDS: Task/ambient ventilation, Mixing ventilation, Displacement ventilation, Circular jet diffuser

5 S. C. Sekhar, **Bin Yang,** K. W. Tham and David Cheong. 2007. IAQ and energy performance of the newly developed single coil twin fan air-conditioning and air distribution system – results of a field trial. Proceedings of the 9th REHVA world congress Clima, June 10-14, Helsinki, Finland.

ABSTRACT

The Single Coil Twin Fan (SCTF) system is a newly developed air-conditioning and air distribution system that aims to deliver enhanced IAQ as well as save energy. The fundamental principle of this system is based on “demand ventilation” and “demand cooling”, which is achieved in the individual occupied zones through localized temperature and carbon dioxide sensors positioned in the respective return grilles. The conditioning of the two air streams is achieved by a single compartmented cooling coil, which provides ease of control of the chilled water flow through the coil. Following a successful pilot study on a small-scale laboratory project in 2003 with an estimated energy saving potential of around 12%, a field trial of the SCTF system was embarked upon that involved an office floor area of about 2500 m2 in a newly

constructed office building within the campus of National University of Singapore. This paper presents the IAQ and energy data in this office area served by the SCTF system.

6 **Bin Yang**, S. C. Sekhar. 2007. Numerical study of circular jet diffuser for task ventilation of under-floor air supply system in tropics. Proceedings of the 10th international building performance simulation association conference and exhibition, September 7-8, Beijing, China.

ABSTRACT

Bases on the concept of task/ambient ventilation, fresh air can be decoupled from re-circulated air so as to improving ventilation effectiveness in breathing zone. Ceiling mounted high velocity circular jet diffusers, which are regarded as remote personalized ventilation air terminal devices (PV ATDs) without affecting room aesthetic effects, can be utilized to supply fresh air without causing draft rating because tropically acclimatized occupants prefer slightly higher air movement. Under-floor air diffusers are used to supply re-circulated air. Corresponding mixing ventilation system by only utilizing under-floor air diffusers are compared with this task/ambient ventilation system. Numerical simulation using a validated computational fluid dynamics (CFD) model for circular jet diffusers is conducted to investigate the difference between task/ambient ventilation systems and mixing ventilation systems. Location weighted personal exposure effectiveness is utilized as an evaluation index for evaluating indoor air quality (IAQ). Air velocity and temperature are utilized as evaluation indices for evaluating thermal comfort level.

KEYWORDS: Task/ambient ventilation, Circular jet diffuser, Mixing ventilation, Under-floor air supply

7 Qi Chengying, **Bin Yang**, Yang Hua, Jin Fengyun, Tham Kwok Wai. 2007. Numerical study of personalized ventilation application in tollway charging station. Proceedings of the 5th International Symposium on Heating, Ventilation and Air Conditioning, September 3-6, Beijing, China.

ABSTRACT

Split air conditioning system is commonly utilized in tollway charging station for dealing with thermal load. Outdoor air, without conditioning, is introduced passively through small opening window, which is utilized for charging tools. Because of its highly polluted ambient environment, many kinds of contaminants are introduced simultaneously. In order to improve air quality in breathing zone for the staff in an energy efficient way, personalized air is conditioned and distributed separately. Air conditioning and filtration equipments are installed above the roof of the station. Extended air duct is utilized to distribte personalized air. AIRPAK, commerical software of Computational fluid dynamics (CFD) is utilized to simulate flow fluid, age of air and predicted mean vote (PMV). Corresponding boundary conditions are measured in one tollway charging station of Hebei Province. Location of personalized ventilation air terminal devices (PV ATDs) and personalized air flow rate are utilized as variable parameters. According to the simulation results, personalized air flow rate above 54 m^3/h can restrain outdoor air invasion effectively so as to diluting indoor contaminants.

KEYWORDS: Numerical study, Personalized ventilation (PV), Tollway charging station, Air age, Predicted mean vote (PMV)

8 **Bin Yang**, S. C. Sekhar. 2007. Numerical study of effects of moving person on

personalized ventilation. Proceedings of ASHRAE IAQ 2007: Healthy and Sustainable Buildings, October 15-17, Baltimore, Maryland, U.S.A.

ABSTRACT

Outdoor air, with high temperature and humidity in tropics, is conditioned and distributed into indoors as fresh air to improve indoor air quality (IAQ). In order to save energy, optimizing strategy for supplying fresh air, reasonable locating inlets and exhausts are important. Re-circulated ventilation, which mix fresh air and re-circulated air before supplying, is commonly utilized and simulated as base case in this study. Fresh air, without mixing with re-circulated air, can be distributed into breathing zone directly by extended air duct and corresponding personalized ventilation (PV) air terminal device (ATD) for improving personal exposure effectiveness (PEE). For indoor esthetics, ceiling mounted air jet can be utilized as an alternative device to supply fresh air in a high velocity because of slightly higher air movement preference of tropically acclimatized occupants. Displacement ventilation (DV) cylinder can be utilized to supple fresh air in a relatively low outlet momentum. All of above-mentioned strategies for supplying fresh air are studied numerically based on a private office. Commercial software for computational fluid dynamics (CFD) simulation, FLUENT 6.2, is utilized. Different exhaust locations for different strategies are also taken into consideration for good air organization. Computational based PEE is utilized as IAQ evaluating index. Air velocity and temperature are utilized as thermal comfort evaluating index.

KEYWORDS: Private office, Indoor air quality, Thermal comfort, Fresh air

9 **Bin Yang**. 2007. Numerical study of the influence of moving person on ceiling mounted personalized ventilation performance in tropics. Proceedings of Indoor

Climate of Buildings, November 27-30, Slovakia.

ABSTRACT

The purpose of ceiling mounted personalized ventilation (PV) is to provide clean air into breathing zone of occupants directly without affecting indoor aesthetics. High momentum, at outlet of PV air terminal device (ATD), is utilized in order to avoid inducing more ambient air and let more personalized air come into breathing zone. The feasibility of such a high outlet momentum, which will cause the air velocity above 0.25 m/s (threshold value of thermal comfort), is based on the fact that tropically acclimatized occupants prefer slightly higher air movement. In steady state, its performance depends much on the ceiling mounted ATD because supply air momentum, other than buoyant effects and ambient air flow, is the major driving force in the micro-environment of occupied zone. In dynamic state, person movement near PV ATD causes entrainment or detrainment effect, which can be regarded as another comparable factor influencing ceiling mounted PV performance. A typical office workplace consisting of a ceiling mounted PV ATD and ambient air supply diffuser is simulated based on the chamber. One person is assumed to be seated under the PV ATD and another moving person near the PV ATD is simulated by dynamic meshes in computational fluid dynamics (CFD). Simulations at moving person velocities of 0.5, 1 and 1,5 m/s and distance between seated person and moving person of 0, 0.2, 0.4m are performed. Personalized air flow rate is 13 l/s corresponding to 10% of total air flow rate. A new index, computational personal exposure effectiveness, is utilized to assess the performance of the PV ATD in regard to inhaled air quality under the influence of moving person. According to numerical results, the impact of moving person on ceiling mounted PV performance is addressed in this study.

10 **Bin Yang**, Arsen Melikov, Chandra Sekhar. 2008. Cooling effect of ceiling mounted personalized ventilation system, Proceedings of the 11th international conference on indoor air quality and climate, August 17-22, Copenhagen, Denmark, Paper ID: 852.

ABSTRACT

Ceiling mounted individually controlled personalized ventilation (PV) aims for providing each occupant with thermal comfort and clean air without affecting the indoor aesthetics. The interaction of the personalised flow supplied from ceiling mounted nozzle (diameter of 0.095 m) with the thermal plume generated by a seated thermal manikin and its impact on the body cooling was studied. Experiments were performed at room air temperature equal to the temperature of the personalised air (23.5°C), different flow rate of the personalised air (4, 8, 12, 16 L/s) and positioning of the manikin directly bellow the nozzle. The neutral level increased from 0.8 m to 1.1 m with the increase of the flow rate. Above 16 L/s the personalised flow was able to destroy completely the thermal plume. In comparison with the reference case without personalised flow the manikin based equivalent temperature for the head and the chest decreased from -1°C to -5°C when the flow rate increased.

KEYWORDS: Ceiling mounted nozzle, Personalized ventilation, Neutral level, Cooling effect, Equivalent temperature

11 **Bin Yang,** Arsen Melikov, Chandra Sekhar, Occupant movement analysis of ceiling mounted personalized ventilation system, Proceedings of the 5th International Workshop on Energy and Environment of Residential Buildings and the 3rd International Conference on Built Environment and Public Health.

ABSTRACT

As one kind of newly developed personalized ventilation (PV) system, the performance of ceiling mounted PV system was tested in PV laboratory of Technical University of Denmark. Since the control area of this PV system was just comparable to the size of human body, the asymmetric exposure of the body to the personalized flow was necessary to be studied by moving thermal manikin 0.2 m forward, backward and sideward to simulate occupant movement which happens quite often in the real case. Different PV temperature (26°C, 23.5°C, 21°C), ambient temperature (26°C, 23.5°C) and personalized airflow rates (4, 8, 12, 16 L/s) were utilized to conduct parametric variation studies. The cases with lowest ambient/PV temperature combination (23.5°C /21°C) and highest personalized airflow rates (16 L/s) were utilized to analyze the influence of occupant movement on the cooling effect of ceiling mounted PV system. Asymmetric exposure was explored and personalized airflow was least efficient to cool the body when the manikin was moved forward.

KEYWORDS: Personalized ventilation, Occupant movement, Cooling effect, Asymmetric exposure

12 **Bin Yang,** Chandra Sekhar, Arsen Melikov, Subjective assessments of thermal sensation for ceiling mounted personalized ventilation system, Proceedings of the 5th International Workshop on Energy and Environment of Residential Buildings and the 3rd International Conference on Built Environment and Public Health.

ABSTRACT

As one kind of newly developed personalized ventilation (PV) system, human assessments of thermal sensation for ceiling mounted PV system was tested with tropical subjects, who had become passively acclimatized to hot conditions in the course of their day-to-day life. The tests were conducted in field environmental

chamber (FEC) of National University of Singapore. 32 subjects (16 males and 16 females), performed normal office work, can choose to expose to four different PV airflow rates (4, 8, 12, 16 L/s) so as to simulating individual control. Ambient temperatures of 26°C and 23.5 °C and PV air temperatures of 26 °C, 23.5 °C and 21 °C were utilized to conduct parametric variation studies. Each combination was maintained for 15 minutes during which the subjects responded to computer-administered questionnaires. The influence of PV airflow rates and ambient/PV temperature combinations on subjective thermal sensation was analyzed.

KEYWORDS: Subjective assessment, Thermal sensation, Personalized ventilation

13 **Bin Yang,** Arsen Melikov, Chandra Sekhar, Cooling effect of ceiling mounted personalized ventilation system, Proceedings of the 11th International Conference on Air Distribution in Rooms.

ABSTRACT

As one kind of newly developed personalized ventilation (PV) system, the impact of ceiling mounted PV system on body cooling, especially for upper body segments was tested in PV laboratory. Experiments were performed with mixing ventilation at numerous conditions comprising four combinations of room temperature and personalized air temperature (23.5°C/21°C, 23.5°C/23.5°C, 26°C/23.5°C, 26°C/26°C), four airflow rates of the personalized air (4, 8, 12 and16L/s) and positioning of the manikin directly below the nozzle (1.3 m distance between the top of manikin's head and the nozzle). Upper body segments were further analyzed because of obvious cooling effects. The results revealed that the influence of the PV airflow rate was not striking when it was lower than 8 L/s and became obvious when PV airflow rate was greater than 12 L/s especially at personalized air temperature of 21 °C. The left face

and the right face were the two body segments cooled mostly among upper body segments when the airflow increased from 4 L/s to 16 L/s. The decrease in the equivalent temperature (ET) was largest when the PV airflow rate changed from 12 L/s to 16 L/s, i.e. the penetration effect of the personalized air over thermal plume felt at 8 L/s increased with the increase of the airflow rate and caused more cooling of the upper body.

14 **Bin Yang,** Chandra Sekhar, Arsen Melikov, Subjective assessments of Air movement for ceiling mounted personalized ventilation system, Proceedings of the 11th International Conference on Air Distribution in Rooms.

ABSTRACT

As one kind of newly developed personalized ventilation (PV) system, human assessments of air movement perception and acceptability for ceiling mounted PV system was tested with tropical subjects, who had become passively acclimatized to hot conditions in the course of their day-to-day life. The tests were conducted in field environmental chamber (FEC). Thirty two subjects (16 males and 16 females), performed normal office work, can choose to expose to four different PV airflow rates (4, 8, 12, 16 L/s) so as to simulating individual control. Ambient temperatures of 26°C and 23.5 °C and PV air temperatures of 26 °C, 23.5 °C and 21 °C were utilized to conduct parametric variation studies. Each combination was maintained for 15 minutes during which the subjects responded to computer-administered questionnaires. The influence of PV airflow rates and ambient/PV temperature combinations on subjective air movement perception and acceptability was analyzed. Values of whole body air movement perception are lower than that of facial air movement perception.

15 **Bin Yang,** Chandra Sekhar, Arsen Melikov, Subjective assessments of indoor environmental quality for ceiling mounted personalized ventilation system, Proceedings of Healthy Buildings 2009 Conference and Exhibition.

ABSTRACT

Indoor environmental quality, comprising perceived air quality, inhaled air temperature and freshness perception and noise level, for ceiling mounted PV system was studied in human subject experiments. Thirty-two subjects, acclimatized to hot tropical conditions in the course of their day-to-day life, participated in the experiments conducted in field environmental chamber (FEC). The subjects (16 males and 16 females), performed normal office work and could choose to be exposed to one of four PV airflow rates (4, 8, 12, 16 L/s). Ambient temperatures of 26°C and 23.5 °C and PV air temperatures of 26 °C, 23.5 °C and 21 °C were utilized to conduct parametric variation studies. Each combination was maintained for 15 minutes during which the subjects responded to computer-administered questionnaires. The influence of PV airflow rates and ambient/PV temperature combinations on indoor environmental quality was analyzed. Inhaled air temperature was perceived cooler and the inhaled air quality and air freshness improved when PV airflow rate increased or the room and the personalized air temperature decreased. Subjects' satisfaction with the noise level decreased when PV airflow rate increased.

KEYWORDS: Indoor environmental quality, Subjective assessment, Personalised ventilation

16 **Bin Yang,** Chandra Sekhar, Arsen Melikov, Human perception relation between thermal sensation and air movement for ceiling mounted personalized ventilation

system, Proceedings of Healthy Buildings 2009 Conference and Exhibition.

ABSTRACT

Response of 32 subjects on their local and whole body thermal sensation and air movement perception and preference to ceiling mounted personalized ventilation (PV) system was studied. The experiments were performed in a field environmental chamber with controlled environment. The subjects (16 males and 16 females) were acclimatized to hot tropical conditions in the course of their day-to-day life. During the experiments they performed normal office work and could choose to be exposed to one of four different PV airflow rates (4, 8, 12, 16 L/s). Ambient temperatures of 26°C and 23.5 °C and PV air temperatures of 26 °C, 23.5 °C and 21 °C were utilized to conduct parametric variation studies. The subjects were exposed to each combination for 15 minutes during which time period they responded to computer-administered questionnaires. Relationships between facial/whole body thermal sensation, air movement perception/acceptability/preference were established.

KEYWORDS: Thermal sensation, Air movement perception, Personalised ventilation, subjective assessment.